Development of micellar novel drug carriers utilizing temperature-sensitive block copolymers containing cyclodextrin moieties

Author:
Yhaya, Mohd Firdaus

Publication Date:
2012

DOI:
https://doi.org/10.26190/unsworks/15581

The University of New South Wales

Development of micellar novel drug carriers utilizing temperature-sensitive block copolymers containing cyclodextrin moieties

Mohd Firdaus Yhaya

A thesis submitted in fulfillment of the requirements for the degree of

Doctor of Philosophy

August 2012

PLEASE TYPE **THE UNIVERSITY OF NEW SOUTH WALES**

Thesis/Dissertation Sheet

Surname or Family name: Yhaya
First name: Mohd Firdaus Other name/s: None
Abbreviation for degree as given in the University calendar: PhD
School: Chemical Engineering Faculty: Engineering
Title: Development of micellar novel drug carriers utilizing temperature-sensitive block copolymers containing cyclodextrin moieties

Abstract 350 words maximum: (PLEASE TYPE)

The objective of this thesis is to investigate well-defined nanoparticles as potential drug delivery systems. To achieve this aim, the block copolymers were synthesized using the Reversible Addition Fragmentation Chain Transfer (RAFT) process and conjugated with *β*-cyclodextrin moieties using click chemistry to obtain amphiphilic characteristics. Huisgen azide-alkyne 1,3-dipolar cycloaddition and thiol-ene click reactions were used for post-modification of block copolymers. Upon heating above the lower critical solution temperature (LCST) of the block copolymers, the *β*-cyclodextrin-based block copolymers undergone self-assembly in aqueous environment to form micelles. These nanostructured particles were capable of carrying drugs, both in the hydrophobic core and the *β*-cyclodextrin cavities. The drug loading efficiency was increased by means of acetylation and cross-linking. The conjugation of *β*-cyclodextrin to block copolymers reduced its toxicity and capable of dissolving more hydrophobic drugs, while big enough in size to behave as drug delivery systems.

Declaration relating to disposition of project thesis/dissertation

I hereby grant the University of New South Wales or its agents the right to archive and to make available my thesis or dissertation in whole or part in the University libraries in all forms of media, now or here after known, subject to the provisions of the Copyright Act 1968. I retain all proprietary rights, such as patent rights. I also retain the right to use in future works (such as articles or books) all or part of this thesis or dissertation.
I also authorise University Microfilms to use the 350 word abstract of my thesis in Dissertation Abstract International (this is applicable to doctoral theses only).

……	……	14/08/2012 ……
Signature	Witness	Date

The University recognises that there may be exceptional circumstances requiring restrictions on copying or conditions in use. Requests for restriction for a period of up to 2 years must be made in writing. Requests for a longer period of restriction may be considered in exceptional circumstances and require the approval of the Dean of Graduate Research.

FOR OFFICE USE ONLY Date of completion of requirements for Award:

THIS SHEET IS TO BE GLUED TO THE INSIDE FRONT COVER OF THE THESIS

COPYRIGHT STATEMENT

Signed ……

14/08/2012

Date ……

AUTHENTICITY STATEMENT

‘I certify that the Library deposit digital copy is a direct equivalent of the final officially approved version of my thesis. No emendation of content has occurred and if there are any minor variations in formatting, they are the result of the conversion to digital format.’

Signed ……

14/08/2012

Date ……

ORIGINALITY STATEMENT

‘I hereby declare that this submission is my own work and to the best of my knowledge it contains no materials previously published or written by another person, or substantial proportions of material which have been accepted for the award of any other degree or diploma at UNSW or any other educational institution, except where due acknowledgement is made in the thesis. Any contribution made to the research by others, with whom I have worked at UNSW or elsewhere, is explicitly acknowledged in the thesis. I also declare that the intellectual content of this thesis is the product of my own work, except to the extent that assistance from others in the project’s design and conception or in style, presentation and linguistic expression is acknowledged.’

Signed……..

14/08/2012

Date……..

Abstract

The objective of this thesis is to investigate well-defined nanoparticles as potential drug delivery systems. To achieve this aim, the block copolymers were synthesized using the Reversible Addition Fragmentation Chain Transfer (RAFT) process and conjugated with *β*-cyclodextrin moieties using click chemistry to obtain amphiphilic characteristics. Huisgen azide-alkyne 1,3-dipolar cycloaddition and thiol-ene click reactions were used for post-modification of block copolymers. Upon heating above the lower critical solution temperature (LCST) of the block copolymers, the *β*-cyclodextrin-based block copolymers undergone self-assembly in aqueous environment to form micelles. These nanostructured particles were capable of carrying drugs, both in the hydrophobic core and the *β*-cyclodextrin cavities. The drug loading efficiency was increased by means of acetylation and cross-linking. The conjugation of *β*-cyclodextrin to block copolymers reduced its toxicity and capable of dissolving more hydrophobic drugs, while big enough in size to behave as drug delivery systems.

Acknowledgements

All praise for God who is the most Gracious, most Compassionate. The PhD thesis may never seen the light without the help of many generous people.

My sincerest appreciation must go to my supervisor, Professor Martina Heide Stenzel, who took the risk of supervising me even knowing that I was from different background. Many thanks for her brilliance, guidance, advice, patience, and constant care; which I am grateful to have you as the supervisor and it will be a priceless experience that I will never forget. Thanks to Australia Research Council (ARC) for the funding of the research project.

Thanks to my father Yhaya Hussin and mother Faridah Sulaiman in Malaysia for their constant support and prayers for me. They have sacrificed a lot to make sure I get the best education possible, which I can never ever repay. Thanks to my younger brother Saffuan who is always supporting me from behind. Special thanks go to my dearest wife Nurul Ainun Hamzah for her patience, love, and understanding through the good and bad times. I am sorry for not being able to be next to you when you need me the most. It must be hard to be pregnant while your husband is thousand kilometers away pursuing his doctorate. I am thankful to my father-in-law Hamzah Idris and my mother-in-law Halimah Salleh for taking care of our precious little daughter Ameera Balqis while her parents were away as full-time PhD students. To my wife and daughter, your husband and dad have to struggle for our future and after this, I will never leave both of you again.

I am also thankful for the excellent CAMD management team, lead by Professor Thomas P. Davis, Dr. Michael R. Whittaker, and Dr. Anthony M. Granville. I appreciate Dr. Istvan Jacenyik for his fast response in obtaining the chemicals needed for my research project. I am also indebted to Dr. Andrew M. Gregory, Dr. Sadik Amajjahe, Dr. Sandra Binauld, and Dr. Mingtao Liang for their patience and sharing their knowledge with me. I feel honored working with among the best polymer chemists in the same laboratory.

I am very thankful to Dr Stuart Thickett (UNSW) and Associate Professor Dr. Allan Leslie White (UWS) for proofreading some parts of the thesis. Thanks to Dr. James Hook, Dr. Donald Thomas, Mrs Hilda Stender, and Dr. Adelle Amoore for their help with NMR spectra analyses. Thank you to the ChemStore people: Ian and John Starling for their quick dispense of chemicals, consumables, and solvents. I would like to extend my thanks to my CAMD colleagues: Khairil Juhanni Abdul Karim, who is like my sister in the laboratory, Yoseop Kim for the help with TEM and cell tests, Johnny Lim for his work on reactivity ratios, and Arlingga Sutinah for the syntheses of P(MMA-*b*-VMA) block copolymers. Thanks also to Vien T. Huynh and Dr. Hien Duong for the help in the lab, Manuela Callari for continuing the study of cyclodextrin and cisplatin, Alex Soeriyadi and Bianca Blunden for mass spectrometry, Yusuke Sugihara and Siti Hajjar Che Man for allowing me to use their fume hood and for flame sealing process. My sincere appreciation to all CAMD members, past and present, who did a great job in ensuring the analytical instruments and laboratories run smoothly. Surely, I will miss the moments working in the most advanced polymer laboratories in Australia.

I am thankful for the scholarship given by the Ministry of Higher Education (MOHE) Malaysia and University Sains Malaysia (USM). Without this, I will never be able to set my feet on this top university. To all Malaysians, I am humbled by your money from which the scholarship is originated. I am now just completed the long journey and ready to go back to serve the country. Rest assured your money would not go to waste.

Now it is time for me to leave Australia and Malaysia Hall Sydney for good after 4 years undertaking this PhD research. Thanks to the Education Malaysia Australia (EMAS), Mrs Norhani Yunus, Mr. Samsuddin (Abang Sam), Mr. Ramlee Ismail, and Mrs. Suri Ibrahim. I feel thankful for the support from my fellow post-graduates, with whom we share our struggle stories. Finally yet importantly, to those who have made contributions direct or indirectly and cannot all be named, thank you very much.

Sincerely,

Key to symbols and constants

CH_2Cl_2	Dichloromethane
cm	centimeter
CaF_2	Calcium fluoride
CO_2	Carbon dioxide
Cu(I)Br	Copper (I) bromide
Cu(I)Cl	Copper (I) chloride
$CuSO_4$	Copper (II) sulfate
d-DMSO	Deuterated dimethylsulfoxide
d_h / Dh	Hydrodynamic particle diameter
D_2O	Deuterium oxide
f	Feed ratio
F	Mole fraction
$[FeCp(CO)_2I]$	Cyclopentadienyl iron(II) dicarbonyl dimer
g	gram
h	Hour/Hours
He	Helium
I_S	Intensity of the sample beam
I_R	Intensity of the reference beam
K	Boltzmann's constant
K_2PtCl_4	Potassium tetrachloroplatinate
$K_2S_2O_8$	Potassium persulfate
L	Liter
$LiClO_4$	Lithium perchlorate
LiH	Lithium hydride
m	meter or mili
(m/z)	Mass/charge ratio
M	mol liter^{-1}
min	Minutes

Me_6TREN	Tris((N,N,-dimethylamino)ethyl)amine
M_n	Number average molecular weight
nm	Nanometer
$NaBH_4$	Sodium borohydride
$Na_2S_2O_4$	Sodium hydrosulfite / Sodium dithionite
Ne	Neon
pH	Measure of the acidity or basicity of an aqueous solution
$Pt(COD)Me_2$	Dimethyl(cyclooctadiene)platinum
r.t	Room temperature
r	Reactivity ratio
R_f	Retention factor
R_g	Radius of gyration
R_h	Hydrodynamic radius
T	Absolute temperature
T_c	Critical temperature
T_g	Glass transition temperature
v/v	Volume by volume
w/v	Weight by volume
α	Alfa
β	Beta
β-CD	Beta-cyclodextrin
β-CD-SH	Beta-cyclodextrin monothiol
β-CD-TEMA	Beta-cyclodextrinthio ethyl methacylate
β-CD-Tos	Beta-cyclodextrin monotosylate
^oC	Degrees Celsius
γ	Gamma / Surface tension
γ-BLG-NCA	Gamma-benzyl-L-glutamate *N*-carboxyanhydride
λ_{max}	Maximum absorption
μ	micro
υ	cycles per 3×10^{10} cm
η	Viscosity

Key to abbreviations and acronyms

2-D NMR	2-Dimensional Nuclear Magnetic Resonance
3-BSPA	3-Benzylsulfanylthiocarbonylsulfanyl propionic acid
4-VP	4-Vinylpyridine
A	Absorption
AcOH	Acetic acid
AAS	Atomic Absorption Spectroscopy
AIBN	2, 2’-Azobis(isobutyronitrile)
ABZ	Albendazole
Ada-PEG	Adamantane-monoended poly(ethylene glycol)
AdMA	1-Adamantylmethylacrylate
ATR	Attenuated Total Reflectance
ATRP	Atom Transfer Radical Polymerization
BHT	2,6-di-tert-butyl-4-methylphenol
CD	Cyclodextrin
CDB	Cumyldithiobenzoate
$CDCl_3$	Deuterated chloroform
CDI	1,1’-Carbonyldiimidazole
CMC	Carboxy methyl cellulose
CMC	Critical Micelle Concentration
COSY	Correlation Spectroscopy
CPDA	Cumyl phenyldithiobenzoate
CPDB	Cumyl dithiobenzoate
CTMS	Chlorotrimethylsilane
CuAAC	Cooper Catalyzed Azide Alkyne Click Chemistry
CuBr	Copper bromide
CuCl	Copper chloride
DBU	1,8-Diazabicyclo[5.4.0]undec-7-ene
DCC	*N*,*N*’-Dicyclohexylcarbodiimide

DCM	Dichloromethane
DDP	trans-dichloro(dypyridine) platinum(II)
DLE	Drug Loading Efficiency
DLS	Dynamic Light Scattering
DMA	*N*,*N*-Dimethylacrylamide
DMAc	*N*,*N*-Dimethylacetamide
DMAP	4-Dimethylaminopyridine
DMPP	Dimethylphenylphosphine
DMF	*N*,*N*-Dimethylformamide
DMP	Dess Martin periodinane
DMPA	2,2-Dimethoxy-2-phenylacetophenone
DMS	Dimethylsuberimidate.2HCl
DMSO	Dimethyl sulfoxide
DMSO-d_6	Deuterated dimethyl sulfoxide
DNA	Deoxyribonucleic Acid
DSC	Differential Scanning Calorimetry
EDX	Energy Dispersive X-ray
EPR	Enhanced Permeation and Retention
ESI-MS	Electrospray Ionization Mass Spectometry
ESR	Electron Spin Resonance
FT-IR	Fourier Transform Infra Red
GPE	Gel Polymer Electrolyte
GSH	Gluthathione
HexAm	Hexylamine
HEA	2-Hydroxyethylacrylate
HEPES	2-Hydroxyethylpiperazinesulfonic acid
HIPS	High Impact Polystyrene
HPLC	High Pressure Liquid Chromatography
HPMA	*N*-(2-Hydroxypropyl methcarylamide)
HSQC	Heteronuclear Single Quantum Coherence
Ir	Iridium

ITC	Isothermal Titration Microcalorimetry
kV	kiloVolt
LCST	Lower critical solution temperature
LiBr	Lithium bromide
MHz	MegaHertz
MMA	Methyl methacrylate
MS	Mass spectrometry
MWCO	Molecular weight cut-off
NaCl	Sodium chloride
NaH	Sodium hydride
NaOH	Sodium hydroxide
NIPAAM	*N*-isopropylacrylamide
NCA	*N*-carboxy anhydride
NMP	Nitroxide-mediated Polymerization
NMR	Nuclear Magnetic Resonance
NMeP	*N*-methylpyrrolidone
NOESY	Nuclear Overhauser Effect Spectroscopy
N/P	Nitrogen/Phosphate
OD	Optical density
OEGMEA	Oligo ethylene glycol methyl ether acrylate
OPDA	*o*-phenylenediamine
PAAs	Poly(amido amine)s
PAHy	α,β-Polyaspartylhydrazide
PDI	Polydispersity Index
PEG	Poly(ethylene glycol)
PEGDPS	Poly(ethylene glycol) dipropanoic succinimide
PhD	Doctor of Philosophy
PHEA	Poly(2-hydroxyethyl acrylate)
PLA	Poly(lactide)
PMMA	Poly(methyl methacrylate)
PNIPAAM	Poly(*N*-isopropylacrylamide)

POEGMEA	Poly(oligo ethylene glycol methyl ether acrylate)
POX	Poly(2-ethyl-2-oxaline)
PPA	Poly(propargyl acrylate)
PTMSPA	Poly(trimethylsilylpropargylacrylate)
PTSC	*p*-Toluenesulfonyl chloride
P4VP	Poly(4-vinylpyridine)
PVMA	Poly(vinyl methacrylate)
RAFT	Reversible Addition-Fragmentation Chain Transfer
RES	Reticuloendhothelial system
ROESY	Rotating Frame Overhauser Effect Spectroscopy
SEC	Size Exclusion Chromatography
SEM	Scanning Electron Microscopy
SFRD	Supercritical Fluid Reactive Deposition
SLS	Static Light Scattering
T	Transmittance
TBAF	Tetrabutylammonium fluoride
TEMPO	2,2,6,6,-Tetramethyl-1-piperidinyl-*N*-oxy
TGA	Thermogravimetric Analysis
THF	Tetrahydrofuran
TLC	Thin Layer Chromatography
TMSPA	Trimethylsilylpropargyl acrylate
TMSPMA	Trimethylsilylpropargyl methacrylate
TEM	Transmission Electron Microscopy
TMS	Tetramethylsilane
UV	Ultraviolet
UV-Vis	Ultraviolet-Visible
VMA	Vinyl methacrylate
VP	Vinyl Pivalate
VP	1-Vinyl-2-Pyrrolidone
XRD	X-ray Diffraction

Table of Contents

Chapter 1: Introduction to the Thesis

1.1 Introduction

Most drugs that are commercially available are hydrophobic in nature. As a consequence, they have low solubility in water, which limits their effectiveness in the body. In order to achieve a therapeutic effect, the drugs must be administered frequently and at high doses. Without an effective delivery system, not all drugs may reach their intended target-as they are cleared earlier by the blood circulation system. In addition, they may also affect healthy cells, causing negative side-effects.

In order to increase the delivery efficiency of hydrophobic drugs, polymeric micelles that can incorporate the drugs may be utilized. Using the Reversible Addition Fragmentation Chain Transfer (RAFT) polymerization process, well-defined structures such as block copolymers can be prepared. Considering the activity of various RAFT agents, trithiocarbonates were used in this work when polymerizing acrylates while dithioesters had to be used for methacrylates. A block copolymer consisting of a hydrophilic block coupled to a hydrophobic block can self-assemble into micelles in aqueous media. Additionally, these copolymers are conjugated with *β*-cyclodextrin moieties by click chemistry to obtain amphiphilic characteristics. These bucket-shaped cyclic structures increase the lower critical solution temperature (LCST) of the hydrophilic component of the block copolymer, while their hydrophobic internal part of the micelle forms inclusion complexes with the hydrophobic drugs. Above the LCSTs of the respective block copolymers, they self-assemble in aqueous environment to form nanosized micelles. The micelles' hydrophobic core and the cavity of *β*-cyclodextrin unit serve as the drug carrier platform and protect the drug from degradation until it has reached its intended target. These micelles are nanosized, yet big enough to demonstrate an enhanced permeation and retention (EPR) effect, as they are not capable of being cleared by the lympathic system of the tumour. Cross-linking can be introduced to the micelles for stabilization in aqueous media. Since its discovery as an anticancer drug, albendazole [ABZ, methyl(5-propylthio-1-*H*-benzimidazol-2-yl)carbamate] has been studied together with cyclodextrin-based polymeric

micelles as potential drug delivery systems. The drug loading efficiency of the polymeric micelles has been increased compared to the parent (unmodified) cyclodextrin alone, and can be increased further by means of acetylation of β-cyclodextrin moieties.

1.2 Aim of the Thesis

The main objective of the thesis is to study the RAFT process and click chemistry as valuable tools to develop well-defined amphiphilic block copolymers with β-cyclodextrin moieties. The suitability of these micellar forming block copolymers as potential drug delivery system is also investigated.

Chapter 1 presents an introduction to the arrangement of the thesis. An introduction to the cyclodextrin-based polymers, inclusion complex formation between albendazole and cyclodextrins, RAFT polymerization and the architectures obtained thereof have been detailed in Chapter 2. Chapter 3 gives a brief understanding of the analytical instruments used product determination throughout the PhD study. Chapter 4 describes RAFT (co)polymerization of vinyl methacrylate and subsequent conjugation with thiols including β-cyclodextrin thiol. For the next two chapters, the azide-alkyne ‘click’ chemistry is used to achieve 100% conjugation 6.0

EMBED ChemDraw.Document.6.0

EMBED ChemDraw.Document.6.0

C

B

A

a

A

1.3 Cumulative Publications

1. Yhaya, F.; Gregory, A. M.; Stenzel, M. H. **Polymers with Sugar Buckets-The Attachment of Cyclodextrins onto Polymer Chains**, *Australian Journal of Chemistry*, **2010**, 63 (2), 195-210.
2. Yhaya, F.; Lim, J.; Kim, Y.; Liang, M.; Gregory, A. M.; Stenzel, M.H. **Development of Micellar Novel Drug Carrier Utilizing Temperature-Sensitive Block Copolymers Containing Cyclodextrin Moieties**, *Macromolecules*, **2011**, 44 (21), 8433-8445.
3. Yhaya, F.; Sutinah. A.; Gregory, A. M.; Liang, M.; Stenzel, M.H. **RAFT Polymerization of Vinyl Methacrylate and Subsequent Conjugation via Enzymatic Thiol-Ene Click Chemistry**, *Journal of Polymer Science: Part A: Polymer Chemistry*, **2012**, Accepted.
4. Yhaya, F.; Binauld, S.; Kim, Y.; Stenzel, M.H. **Shell Cross-linking of Cyclodextrin-Based Micelles *via* Supramolecular Chemistry for the Delivery of Drugs**, *Macromolecular Rapid Communications*, **2012**, Accepted.
5. Yhaya, F.; Binauld, S.; Callari, M.; Stenzel, M.H. **One-pot Endgroup Modification of Hydrophobic RAFT Polymers with Cyclodextrin Using Thiol-Ene Chemistry and the Subsequent Formation of Dynamic Core-Shell Nanoparticles Using Supramolecular Host-Guest Chemistry,** *Australian Journal of Chemistry*, **2012**, Accepted.

Chapter 2: Literature Review

2.1 Well-Defined Cyclodextrin Polymers

Introduction

Cyclodextrins are homochiral cyclic oligosaccharides containing multiple α-D-glycopyranose units. The most commonly encountered cyclodextrins consist of 6 (α-cyclodextrin), 7 (β-cyclodextrin), or 8 (γ-cyclodextrin) D-glycopyranose molecules. Of these, the majority of research has focused on β-cyclodextrin. This is due to several reasons, namely: price, availability, approval status, cavity dimensions amongst others.[1] The cyclodextrin molecules are arranged in a torus-like structure and possess a distinct cavity which acts as a carrier for small molecules (**Figure 2.1**); the size of the ring, and therefore, cavity, is dependent on the number of sugar units which are incorporated into the compound. Cyclodextrins are mainly used to help solubilise poorly water soluble species via the formation of "inclusion complexes" or "host-guest" complexes.[2]

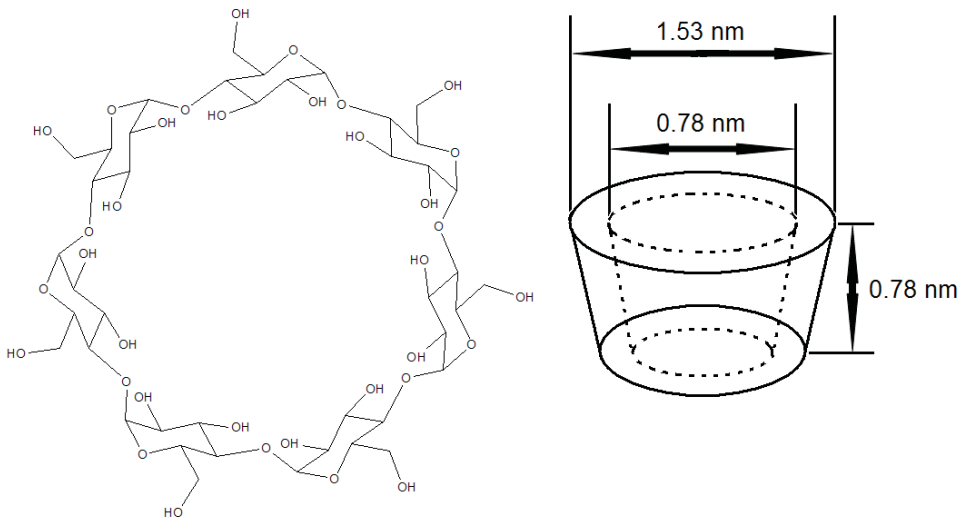

Figure 2.1 *β-cyclodextrin and the generic symbol used to represent cyclodextrins in this thesis.*

With the inclusion complexes the molecule may only be held in place by physical forces, i.e without covalent bonding. The major forces involved in the formation of these complexes are Van der Waals interactions after the release of entalphy-rich water molecules from the cavity.[3] The release of cyclodextrin ring strain after complexation and hydrogen bonding between host and guest are also the driving forces for complexation.The inherent ability of the cyclodextrins to aid in the water solubilisation of molecules has been the driving force for scientific research. The inclusion complexes have been widely utilised in the pharmaceutical industry but they have also found applications in cleaning up toxic materials such as naphtalene[4] and also in science acting as separating materials in chromatography.[5] In aqueous solutions, the slightly apolar cavity is occupied with water, but these are readily replaced with compounds which are of a lesser polarity than water molecules to form the inclusion complexes.[6] In biology, at low concentrations, cyclodextrins generally do not interfere with microbial cells, are biocompatible and show low toxicity in animal and human bodies, an advantage which allows them to be used for a range of medicinal applications.[7-8]

Considering the importance and versatility of cyclodextrins, it is not surprising that these cavities were combined with polymers to create advanced materials. In this review, the term *cyclodextrin polymer* is used for cyclodextrin molecules which are covalently bonded to polymers. Cyclodextrin polymers based on inclusion complexes (e.g. polyrotaxanes) are not discussed here. For these macromolecular systems, comprehensive reviews by Wenz *et al.*[7]. and Harada *et al.*[8] should be consulted.

By combining cyclodextrins and polymers via covalent bonds, the favourable properties of both can be combined.[9] Depending on the nature of the polymers, cyclodextrin polymers can offer advantages compared to the parent cyclodextrins alone, e.g. improved water solubility, higher catalytic effects,[10-14] and improved binding abilities.[15] Cyclodextrin polymers fall into two major groups, namely well-defined and undefined cyclodextrin polymers. In this work undefined polymers are polymers made from cyclodextrin with their multitude of functionalities (up to 21) were reacted with an mostly bifunctional compound leading to polymers with various branching, broad molecular weight distribution, which often includes insoluble products while there is little control over degree of reaction per

cyclodextrin. The type of cyclodextrin polymers commonly described in the literature fall under the category we labelled here as undefined cyclodextrin polymers. The list of references in the literature is endless, reflecting the simplicity of this approach. The most common cyclodextrin polymers are obtained via copolymerisation of cyclodextrin[16] and multifunctional compounds such as epichlorohydrin resulting in branched or even crosslinked polymers. **Figure 2.2.2** is representative of the structure seen with undefined cyclodextrin polymers.[17]

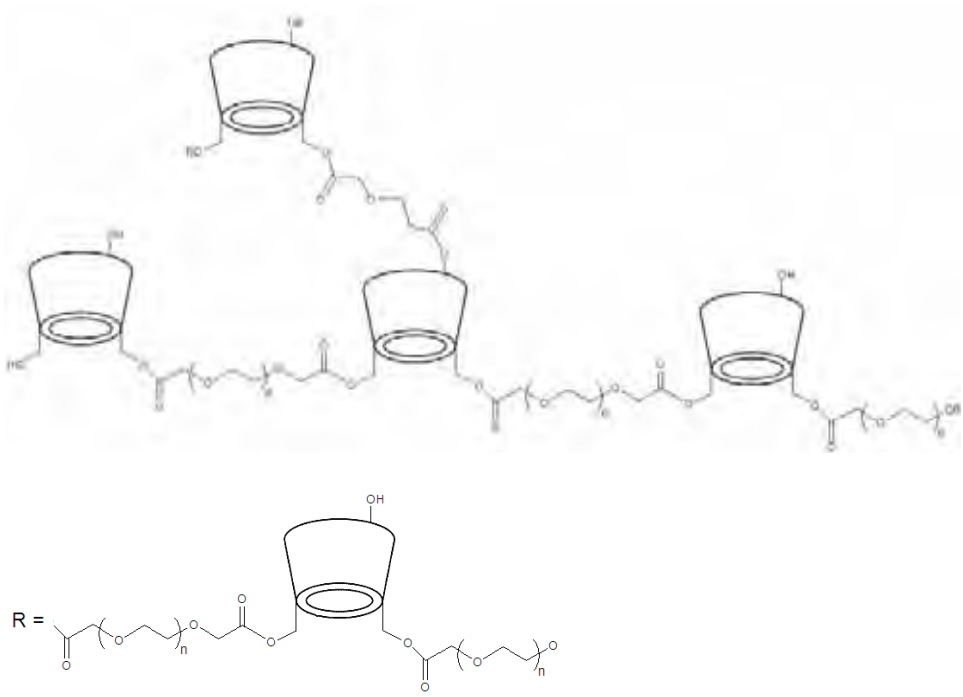

Figure 2.2 *Structure of undefined cyclodextrin polymer (adapted from Nielsen et al.).*[17]

Since most reports in literature use similar techniques, only the basic features are highlighted here. Depending on several parameters, the polymers are either soluble and branched or insoluble and crosslinked. Soluble *β*-cyclodextrin polymers are, depending on the comonomer, often more soluble than their parent *β*-cyclodextrin, hence this property was used to increase the solubility of drugs such as naproxen and ibuprofen.[15] Insoluble *β*-cyclodextrin polymers can still be advantageous. They have been used to remove harmful organic pollutants from wastewater.[18-19] The properties of undefined cyclodextrin polymers are strongly dependant on several parameters: a) initial ratio of multifunctional compound and *β*-cyclodextrin, b) concentration of the reaction medium and c) reaction time.[20] By controlling

these factors, the structure and solubility of the β-cyclodextrin polymers can be tailored to suit the applications.

This review, however, aims to summarise the achievements in the area of cyclodextrin polymers with well-defined structures. Well-defined cyclodextrin polymers are polymers with the degree of functionalization of each cyclodextrin unit is well controlled. The amount of functionalization determines if CD acts as a pendant group of a polymer or maybe as the core of a star. Within these architectures, cyclodextrins were the basis of complex structures such as star polymers or telechelic polymers or they were attached as pendant groups or acted as building blocks for linear polymers, where uncontrolled branching elements were absent.

Well-defined Cyclodextrin Polymers

Four major groups can be indentified in the literature, which are depicted in **Figure 2.3**. These structures range from linear polymers (**Figure 2.3 (a)**) to star polymers with cyclodextrin as core (**Figure 2.3 (b)**), telechelic polymers with cyclodextrin terminal functionalities (**Figure 2.3 (c)**) to star polymers with cyclodextrin as the terminal functionalities (**Figure 2.3 (d)**). Their synthesis will be discussed in detail below.

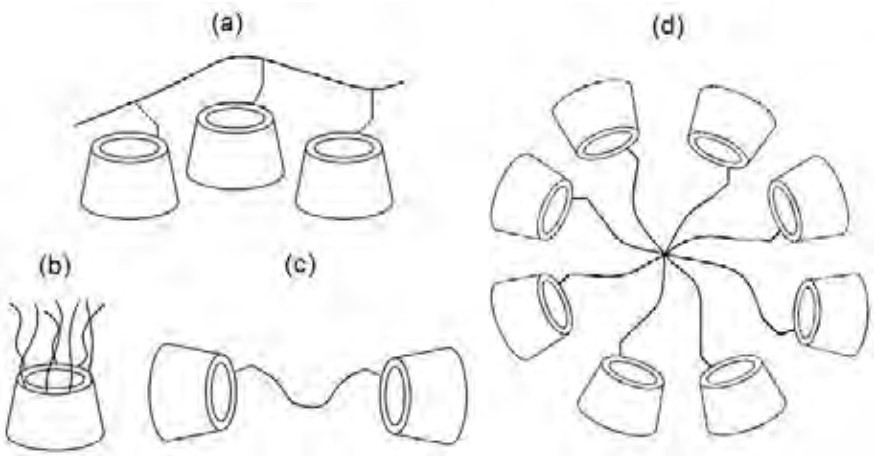

Figure 2.3 *Basic architectures of well-defined cyclodextrin polymers: a) linear cyclodextrin polymer; b) cyclodextrin star polymer; c) linear polymer with cyclodextrin end group(s); d) star-shaped polymer with cyclodextrin end groups.*

2.1.1 Linear Cyclodextrin Polymers

Linear cyclodextrin polymers can be obtained through two pathways, either by polymerisation of cyclodextrin-containing well-defined monomers or by postmodification of the polymer skeleton with monosubstituted cyclodextrins.

2.1.1.1 Synthesis of Linear Polymers Using Cyclodextrin Monomers

A prerequisite for the preparation of linear polymers is the synthesis of well-defined monomers based on cyclodextrin since the use of multifunctional monomers will lead to branched or crosslinked polymers.[20-23] Monofunctional cyclodextrin monomers – frequently methacrylate and acrylate derivatives (**Figure 2.4**) – were prepared for chain polymerisations, but also cyclodextrins with exactly two functionalities for polycondensation reactions were described.

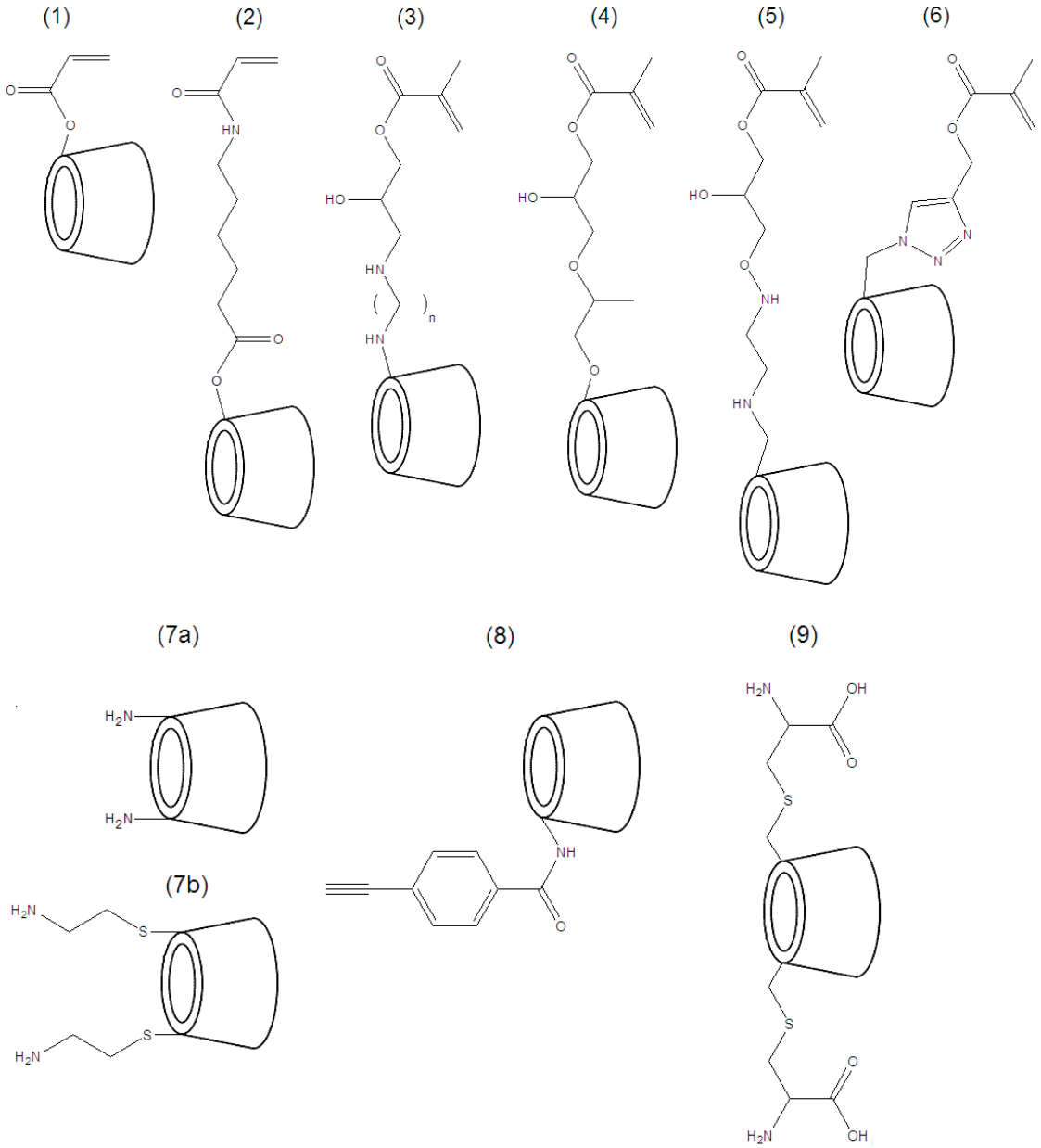

Figure 2.4 *Cyclodextrin monomers used in the syntheses of linear cyclodextrin polymers: acryloyl-β-cyclodextrin* ***(1)****, N-acryloyl-6-aminocaproyl-β-cyclodextrin* ***(2)****, glycidyl methacrylate-ethylenediamine- β-cyclodextrin (****3a****, n=2), glycidyl methacrylate-1,6-hexanediamine-β-cyclodextrin (****3b****, n=6), 2-hydroxy-3-methacryloyloxy propyl-β-cyclodextrin* ***(4),*** *glycidyl methacrylate-β-cyclodextrin* ***(5)****, mono-(1H-1,2,3-triazol-4-yl)(methyl)2-methylacryl-β-cyclodextrin* ***(6)****, $6^A,6^D$ - dideoxy-$6^A,6^D$ - diamino- β-cyclodextrin* ***(7a)****, $6^A,6^D$ - dideoxy-$6^A,6^D$ - di(2-aminoethanethio)- β-cyclodextrin* ***(7b)****, phenylacetylene- β-cyclodextrin* ***(8)****, $6^A,6^D$ -bis-(2-amino-2-carboxylethylthio)- $6^A,6^D$ -dideoxy- β-cyclodextrin* ***(9)****. The polymerisation conditions can be found in* ***Table 2.1****.*

Table 2.1 *Reaction condition and outcome of the polymerisation of cyclodextrin monomers. The structures are displayed in* ***Figure 2.4****.*

Cyclodextrin Monomer	**Polymerisation Conditions**[a)]	**Polymer Type**[b)]	**Molecular Weight Achieved / g mol^{-1}**
Acryloyl-*β*-cyclodextrin (**1**), *N*-Acryloyl-6-aminocaproyl-*β*-cyclodextrin (**2**)[10-12]	AIBN, 60 °C, in water/methanol (1:1, v/v), 48 hrs	Homopolymer	10 000 – 100 000
Glycidyl methacrylate-ethylenediamine- *β*-cyclodextrin (**3a,** n=2), glycidyl methacrylate-1,6-hexanediamine-*β*-cyclodextrin (**3b,** n=6)[9]	AIBN, 70 °C, DMF, 8 hrs	Copolymerised NIPAAM	22 000 (**3a**), 29 000 (**3b**)
-Hydroxy-3-methacryloyloxy propyl-*β*-cyclodextrin (**4**)[24]	$K_2S_2O_8$, 80 °C, deionised water, 24 hrs	Copolymerised with VP	12 000 – 14 000
Glycidyl methacrylate-*β*-cyclodextrin (**5**)[25]	AIBN, 75 °C, DMF, 3 hrs	Homopolymer	10 400[c)]
Mono-(1*H*-1,2,3-triazol-4-yl)(methyl)2-methylacryl-*β*-cyclodextrin (**6**)[26]	AIBN, 65 °C, DMF, overnight	Homopolymer	13 000
$6^A,6^D$ - Dideoxy-$6^A,6^D$ - diamino- *β*-cyclodextrin (**7a**),[27] $6^A,6^D$ - Dideoxy-$6^A,6^D$ - di(2-aminoethanethio)- *β*-cyclodextrin (**7b**)[27]	25 °C, DMF, 15 hrs	Copolymerised with DMS	8 000
Phenylacetylene- *β*-cyclodextrin (**8**)[28]	Rhodium catalyst[d)], 30 °C, triethylamine, 17-160 hrs	Homopolymer	19 000 – 163 000
$6^A,6^D$ -Bis-(2-amino-2-carboxylethylthio)- $6^A,6^D$ - dideoxy- *β*-cyclodextrin (**9**)[29]	Room temperature, DMSO, 120 hrs	Copolymerised with PEGDPS	4 170

a) Abbreviations used: 2,2'-azobis(isobutyronitrile) (AIBN), *N'N'*-dimethylformamide (DMF), dimethyl sulphoxide (DMSO); b) abbreviations used: *N*-isopropylacrylamide (NIPAAM), 1-vinyl-2-pyrrolidone (VP), dimethyl suberimidate (DMS), poly(ethylene glycol) dipropanoic succinimide (PEGDPS); c) value quoted in literature is for weight average molecular weight and not number average molecular weight; d) [norbornadiene)rhodium(I) chloride]$_2$.

The synthesis of cyclodextrin polymers using cyclodextrin monomers was first reported by Furue and co-workers in 1975.[10] The majority of the polymers have been formed

through free radical polymerisation using 2,2'-azobis(isobutyronitrile) (AIBN), with the exceptions of rhodium catalyst[28] and potassium persulfate catalyst.[24] The time for the polymerisation to achieve completion varied from 3 hours to 160 hours. Although most of the polymers produced were homopolymers, in some cases copolymerisations were examined. Copolymerisations were undertaken for several reasons, for example, to test the polymerisation ability for the monovinyl cyclodextrin monomers,[9] to prevent formation of crosslinking,[24] to obtain cationic polymers with block structure,[27] and for antitumour drug conjugation.[29] Copolymerisations have rarely been investigated from a mechanistic point of view. As far as the reactivity ratio for the monomers is concerned, the only values reported were 0.93 and 0.06 for the radical copolymerisation of 2-hydroxy-3-methacryloyloxy propyl-*β*-cyclodextrin and 1-vinyl-2-pyrrolidone, respectively.[24] **Table 2.1** summarises the reaction conditions employed for the polymerisation of the monomers depicted in **Figure 2.4**.

2.1.1.2 Polymer Analogous Reaction

In a two-step polymer analogous reaction, the polymer was synthesised first and then subsequently reacted with a monosubstituted *β*-cyclodextrin, which had been prepared in a separate synthetic procedure. A reported one-step polymer analogous reaction[30-32] utilised lithium hydride for the mono-deprotonation of *β*-cyclodextrin to afford lithium *β*-cyclodextrin-2-ate, which was subsequently reacted with the polymer backbone (without isolation of lithium *β*-cyclodextrin-2-ate).

Linear Polymer Precursors

Seo *et al.*[13] were among the first to use the two-step polymer analogous reaction. They used poly(allyl amine) because of high chemical reactivity of the primary amine groups, the high water-solubility, and the commercially availability at low cost. Most of the polymers used were based on vinylic monomers, with the exceptions of poly(ethylenimine) (**12**) and polysaccharides (**15**) (**Table 2.2** and **Figure 2.5**). For copolymers (**16**)–(**20**), the attachment of the cyclodextrin took place at one component of the copolymer which underwent a facile reaction with monosubstituted *β*-cyclodextrin such as in, for example, poly(*N*-

isopropylacrylamide)-*co*-(glycidyl methacrylate) (**17**), where the cyclodextrin derivative rapidly reacts with the epoxy groups. For copolymers (**18**)–(**20**), the attachment took place by ring-opening of the maleic anhydride moieties using mono-deprotonated *β*-cyclodextrin.

Table 2.2 *Preparation of the linear β-cyclodextrin polymers by analogous reaction using polymers depicted in* ***Figure 2.5****.*

Linear Polymer Precursors	Monosubstituted *β*-Cyclodextrin[b)]	Attachments Procedure[d)]	Degree of Substitution	Molecular Weight/ g mol^{-1}
Poly(allylamine hydrochloride) **(10)**	Mono-6-*p*-toluenesulfonyl-*β*-cyclodextrin **(21)**	Methanol : DMAc, (2:1), 50 °C	0.16-0.52[13]	10 000 and 60 000[e)]
			0.39-0.77[14]	10 000
			0.05-0.23[33-34]	8 500-11 000
Poly(vinylamine) **(11)**	Monoamino-6-deoxy-*β*-cyclodextrin **(22)**	Water : methanol (1:50), 60 °C	0.20-5.00 mol. %[33]	38 000
			0.20-5.90[34]	36 600
Poly(ethylenimine) **(12)**	Mono-6-*p*-toluenesulfonyl-*β*-cyclodextrin **(21)**	DMSO, 60 °C, 6 hrs	0.012[35]	60 000[e)]
			5-16 %[36]	25 000
Poly(acrylic acid) **(13)**	Monoamino-6-deoxy-*β*-cyclodextrin **(22)**	DCC dissolved in NMeP, 60 °C, 48 hrs	2.1-2.5 % [37]	250 000[e)]
	Ethylenediamine-*β*-cyclodextrin **(23)**		2.9 %[38]	250 000[e)]
Poly(propargyl methacrylate) **(14)**	6I-azido-6I-deoxy-*β*-cyclodextrin **(25)**	DMF in either oil bath or microwave heating, 140 °C, 30 mins	Not given[26]	104 000
Polysaccharides (dextran **(15)**[a)], carboxymethylcellulose (CMC), mannan)	Monoamino-6-deoxy-*β*-cyclodextrin **(22)**	$NaBH_4$, 4 hrs	135, 41, and 175 mol per mol of polysaccharide[39]	(Dextran) = 70 000[e)] (CMC) = 30 000[e)] (Mannan) = 270 000[e)]
α, *β*-Polyaspartylhydrazide **(16)**	6-[Aminoethyl(4'-carboxybutanamide)]-*β*-cyclodextrin**(24)**; monoaldehyde-*β*-cyclodextrin **(26)**	Water, pH 5.5, r.t, 2 hrs	4.0-10.7 mol %[40]	37 200
Poly(*N*-isopropylacrylamide)-*co*-(glycidyl methacrylate) **(17)**	Mono-6-*p*-toluenesulfonyl-*β*-cyclodextrin **(21)**	Dioxane : water (4:1)	2.4 mol %[41]	38 600
Poly(*N*-1-vinyl-2-pyrrolidone)-*co*-(maleic anhydride) **(18)**	–[c)]	–	59.2 wt. %[30]	373 00 (including cyclodextrin moieties)[e)]
Poly(maleic anhydride)-*alt*-(isobutene) **(19)**	–[c)]	–	26.76 wt. %[31]	60 000[e)]
Poly[(methyl vinyl ether)-*alt*-(maleic anhydride) **(20)**	–[c)]	–	0.06-0.80 per maleic anhydride unit[32]	80 000

a) Only the structure for dextran is shown in **Figure 2.5**; b) the structures for the functionalised cyclodextrins are shown in **Figure 2.6**; c) unmodified cyclodextrin with LiH for a one-pot synthesis; d) abbreviations used *N*,*N*-dimethylacetamide (DMAc), dimethyl sulfoxide (DMSO), dicyclohexylcarbodiimide (DCC), *N*-methylpyrrolidone (NMeP), *N*,*N*-dimethylformamide (DMF); e) value quoted in literature is for weight average molecular weight and not number average molecular weight.

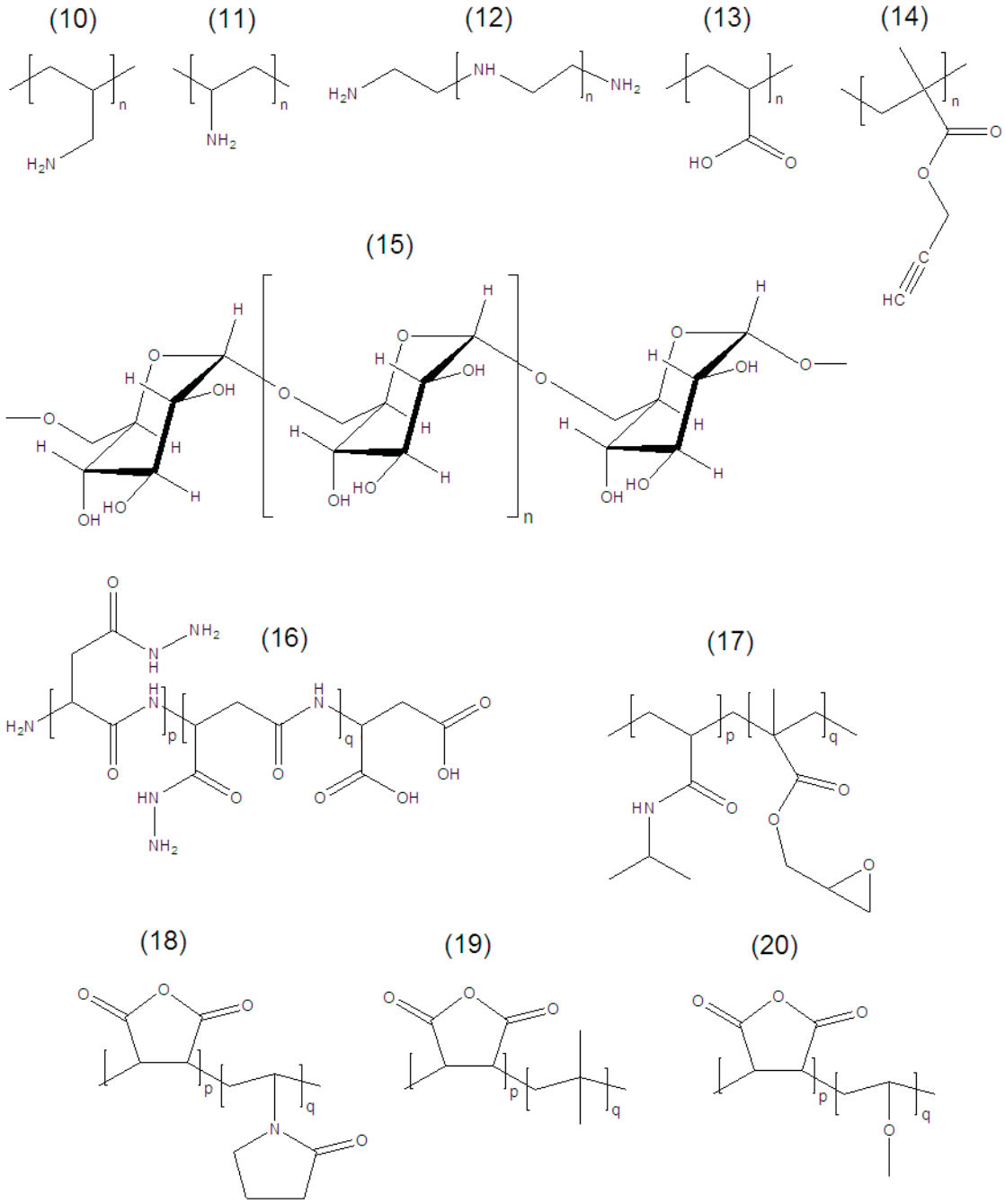

Figure 2.5 *Linear polymer precursors used in the syntheses of linear cyclodextrin polymers. Conditions for the attachment of cyclodextrin groups can be found in* ***Table 2.2****. Polymers: poly(allylamine hydrochloride)* ***(10)****, poly(vinylamine)* ***(11)****, poly(ethylenimine)* ***(12)****, poly(acrylic acid)* ***(13)****, poly(propargyl methacrylate)* ***(14)****, dextran* ***(15)****, α, β-polyaspartylhydrazide* ***(16)****, poly(N-isopropylacrylamide)-co-(glycidyl methacrylate)* ***(17)****, poly(N-1-vinyl-2-pyrrolidone)-co-(maleic anhydride)* ***(18)****, poly(maleic anhydride)-alt-(isobutene)* ***(19)****, poly[(methyl vinyl ether)-alt-(maleic anhydride)* ***(20)****.*

Synthesis of Monosubstituted *β*-Cyclodextrin

Prior to the attachment of *β*-cyclodextrin to the linear polymers, the cavity must be selectively functionalised at one position in order to prevent crosslinking (**Figure 2.6**). The most popular mono-substituted *β*-cyclodextrin is mono-6-*p*-toluenesulfonyl-*β*-cyclodextrin **(21)**,[13-14, 33-36, 42-43] which can easily be obtained using either pyridine[13] or sodium hydroxide solution[44] in the reaction between *β*-cyclodextrin and *p*-toluenesulfonyl chloride. Mono-6-*p*-toluenesulfonyl-*β*-cyclodextrin is typically employed in the polymer analogous reaction with amine containing polymers **(10)**, **(11)**, **(12)**.

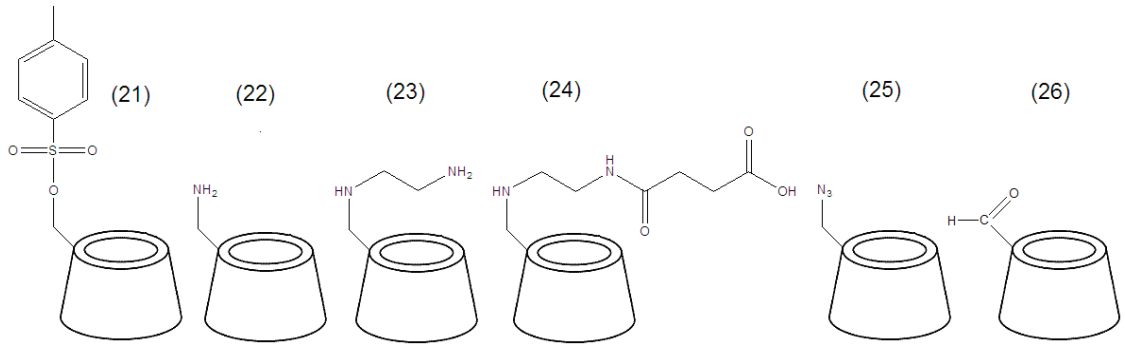

Figure 2.6 *Examples of mono-substituted β-cyclodextrins used in two-step polymer analogous reactions (from left to right): mono-6-p-toluenesulfonyl-β-cyclodextrin* ***(21)****, monoamino-6-deoxy-β-cyclodextrin* ***(22)****, ethylenediamine-β-cyclodextrin* ***(23)****, 6-[aminoethyl(4'-carboxybutanamide)]-β-cyclodextrin* ***(24)****, 6I-azido-6I-deoxy-β-cyclodextrin* ***(25)*** *and monoaldehyde-β-cyclodextrin* ***(26)****. The polymers they are attached to along with the synthetic conditions used are shown in* ***Table 2.2****.*

Alternatively, amino functionalised *β*-cyclodextrins, including **(22)**,[37, 42-43] **(23)**,[38, 41] and **(24)**[42] were frequently used in the reaction with carboxylate containing polymers. These derivatives all originated from **(21)** by using condensed ammonia and *N*,*N*-dimethylformamide.[45] Another product obtained directly from **(21)** is the azide containing **(25)**, which was prepared by the reaction with sodium azide.[46] Azide based cyclodextrin derivatives are employed in a highly efficient 'click' reaction with alkyne containing polymers **(14)**. The aldehyde containing cyclodextrin derivative **(26)**[40, 47] was, in contrast, synthesised directly in high yields from *β*-cyclodextrin by using dimethyl sulfoxide and Dess-Martin periodinane (DMP). DMP is used for direct and mild

oxidation, which is also suitable for protein conjugation. The β-cyclodextrin monoaldehyde was subsequently conjugated to α,β-polyaspartylhydrazide (PAHy) **(16)**.[40]

2.1.1.3 Application of Linear Cyclodextrin Polymers

Since the late seventies, linear cyclodextrin polymers have been used in several applications, including as a catalyst,[10-14] thickener,[31] and artificial enzyme.[35] Three decades later their applications have advanced and broadened to encompass gene delivery and drug carrier agents.

Gene delivery. Polymers used as nonviral gene delivery agents are typically cationic polymers. The polymers **(7a)** and **(7b)** have been used for the delivery of plasmid DNA therapeutic macromolecules[27] with the β-cyclodextrin polymers condensing plasmid DNA leading to a high cell transfection efficiency and low toxicity. Meanwhile, poly(ethyleneimine)-β-cyclodextrin polymers **(12 + 21)** also have been used as *in vitro* and *in vivo* gene delivery agents.[36] This system did not reveal observable toxicities when tested on mice.

Drug carrier. Polysaccharides-β-cyclodextrin **(15 + 22)** have been tested on rats for *in vivo* anti-inflammatory properties of the drug naproxen, which was encapsulated into the cyclodextrin cavity.[39] The solubility of cyclodextrin polymers were higher compared to the native β-cyclodextrin, contributing to higher pharmacological activity. Due to the size of the polymer, the clearance of the drug was reduced, thus improving the pharmacokinetics of naproxen. Copolymer **(9)** was conjugated with the anti-tumour drug camptothecin to be tested on human carcinoma cell lines.[28] The solubility of camptothecin was also increased three times when conjugated to **(9)**. These conjugates were more effective in reducing the tumour compared to the camptothecin alone.

Polymer network. The synthesis of polymer network created by host-guest inclusion complexes between adamantyl and β-cyclodextrin substituents **(22)** on poly(acrylic acid) **(13)** in aqueous solution have also been reported.[37-38] The viscosity was at maximum

when the ratio between two polymers was 1:1, suggesting binary inclusion. By adding native *β*-cyclodextrin to the network, the viscosity was reduced, showing competition between the native *β*-cyclodextrin and *β*-cyclodextrin substituents on the *β*-cyclodextrin poly(acrylic acid).

Self-assembly into micelles. Inclusion complexation was used as driving force to construct polymeric micelles.[25] Micelles were built up between hydrophilic polymer **(5)** and hydrophobic poly(*tert*-butyl acrylate) adamantyl. Due to the inclusion interaction, the former built up the shell of the micelle while the latter formed the core. Crosslinking of the shell and removal of the core resulted in multiscale holes with the large central one containing *β*-cyclodextrin cavities.

Molecular sensor for direct colorimetric detection. A new direct colorimetric detection system was developed for sensing solvent, temperature, and neutral chemical species including enantiomers.[28] Polymers of phenylacetylenes **(8)** with optically active *β*-cyclodextrin residues exhibited an induced circular dichroism in the UV-visible region of the polymer backbones. The inversion of the helicity of the polymer backbones caused a colour change, which was readily observed with the naked eye. Absorption and circular dichroism spectroscopy were used to quantify this phenomenon.

2.1.2 Cyclodextrin Star Polymers

Star-like polymers are formed when a small-molar-mass core links several polymer chains together. The polymers have most of the properties of high molecular weight materials without the penalty of higher viscosities.[48] Star polymers can be obtained by two approaches, the arm-first or core-first approach. The arm-first approach involves the preparation of linear chains with functionalised terminal groups which are attached to a multifunctional core in a subsequent step.[49] The core-first approach utilises a multifunctional initiator or controlling agent with the number of functional end groups being equivalent to the number of arms attached to the core. It was first reported by Topchieva and co-workers in 1997 where one-pot polymerization of ethylene oxide was

initiated by the hydroxyl groups of cyclodextrins.[50] The vast majority of literature uses cyclodextrin in a core-first approach to produce well-defined star polymers with one central cyclodextrin building block[51] usually by employing controlled polymerisation techniques.[52]

2.1.2.1 Core-first Approach

Atom Transfer Radical Polymerisation (ATRP)

ATRP involves halogen transfer from initiating species or dormant polymer chain to a transition metal complex to generate a transient radical. ATRP systems comprise of: initiator, catalyst, ligand, and monomer. Specific details regarding ATRP can be found elsewhere.[53]

Aside from forming inclusion complexes, cyclodextrins are of interest due to their high functionality, which allows the synthesis of ATRP initiators for the synthesis of star polymers with 18 (α–), 21 (β–) and 24 (γ–cyclodextrin) arms, respectively. The idea of using cyclodextrin as a macroinitiator for ATRP was first reported in 2001 by Haddleton and co-workers using β-cyclodextrin.[54] The overview of star cyclodextrin polymers synthesised through ATRP is tabulated in **Table 2.3**.

Table 2.3 *Overview of star cyclodextrin polymers synthesised via ATRP. The initiators, ligands and monomers used can be seen in* ***Figure 2.7***, ***Figure 2.8***, *and* ***Figure 2.9***, *respectively.*

Initiator	Catalyst	Ligand	Monomer	Number of Arms	Ref.
Octadeca-*O*-(2-iodo-2-methylpropionyl)-*α*-cyclodextrin (octadeca-*O*-isobutyryl bromide-*α*-cyclodextrin) **(28)**	$[FeCp(CO)_2I]$	–	Styrene **(39)**	18	55
Heptakis[2,3,6-tri-*O*-(2-bromo-2-methylpropionyl)]-*β*-cyclodextrin **(27)**	Cu(I)Br	*n*-Propyl-2-pyridylmethanimine **(34)**	Methyl methacrylate **(41)**, styrene **(39)**	21	54
		2,2'-Bipyridine **(35)**	[2-(Methacryloyloxy)ethyl] trimethyl ammonium chloride **(43)**	21	48
		N,N,N',N",N"-Pentamethyldiethylenetriamine **(36)**	*tert*-Butyl acrylate **(42)**	21	56
Tetra-*O*-(2-bromo-2-methylpropionyl)-*β*-cyclodextrin **(30)**		Tris[2-(dimethylamino)ethyl]amine **(37)**	*N*-Isopropylacrylamide **(40)**	4	57
		1,1,4,7,10,10-Hexamethyltriethylenetetramine **(38)**	2-(Dimethylamino)ethylmethacrylate **(44)**, poly(ethylene glycol)ethyl ether methacrylate **(45)**	4	58
Octadeca-*O*-(2-bromopropionyl)-*α*-cyclodextrin **(32)**, heptakis[2,3,6-tri-*O*-(2-bromopropionyl)]-*β*-cyclodextrin **(31)**		*N,N,N',N", N"*-Pentamethyldiethylenetriamine **(36)**	*tert*-Butyl acrylate **(42)**	18, 21	51
End functionalised polystyrene with 20 (2-bromoisobutyryl)s *β*-cyclodextrin **(33)**		1,1,4,7,10,10-Hexamethyltriethylenetetramine **(38)**	Methyl methacrylate **(41)**, *tert*-butyl acrylate **(42)**	20	59
Tetradeca-*O*-(2-bromo-2-methylpropionyl)-*α*-cyclodextrin **(29)**		*N,N,N',N", N"*-Pentamethyldiethylenetriamine **(36)**	6-(4-Methoxy-4'-oxy-azobenzene) hexyl methacrylate **(46)**	14	60
Octadeca-*O*-(2-bromo-2-methylpropionyl)-*α*-cyclodextrin **(28)**	Cu(I)Cl	2,2'-Bipyridine **(35)**	Methyl methacrylate **(41)**	18	61

Initiators Initiators were either based on β-cyclodextrin or α-cyclodextrin[55, 59-61] (**Figure 2.7**). γ-Cyclodextrin has not yet been investigated. The macroinitiators were synthesised by reacting cyclodextrin with either 2-bromoisobutyryl bromide/chloride, 2-bromoisobutyric anhydride, or 2-bromopropionyl bromide. By using α-cyclodextrin, 18 arm-stars can be obtained whereas 21 arm-star can be derived from β-cyclodextrin. However, there are exceptions, whereby stars with fewer arms have been produced. Only 4 arms were obtained with β-cyclodextrin when the compound was treated with four equivalents of 2-bromoisobutyryl bromide.[57-58] A 20 arm-star with one nitroxide-capped polystyrene arm was synthesised to obtain a "umbrella-type star polymer" **(33)**.[59] This was accomplished by functionalising the monoamino β-cyclodextrin to obtain one nitroxide-capped polystyrene arm, followed by functionalising another 20 remaining arms with 2-bromoisobutyric anhydride.

Although the majority of the initiators incorporate bromine, exceptions exist. One example is with the iodine based initiator **(28)**, which allows the synthesis of well-defined star polymers in conjunction with $[FeCp(CO)_2I]$.[55]

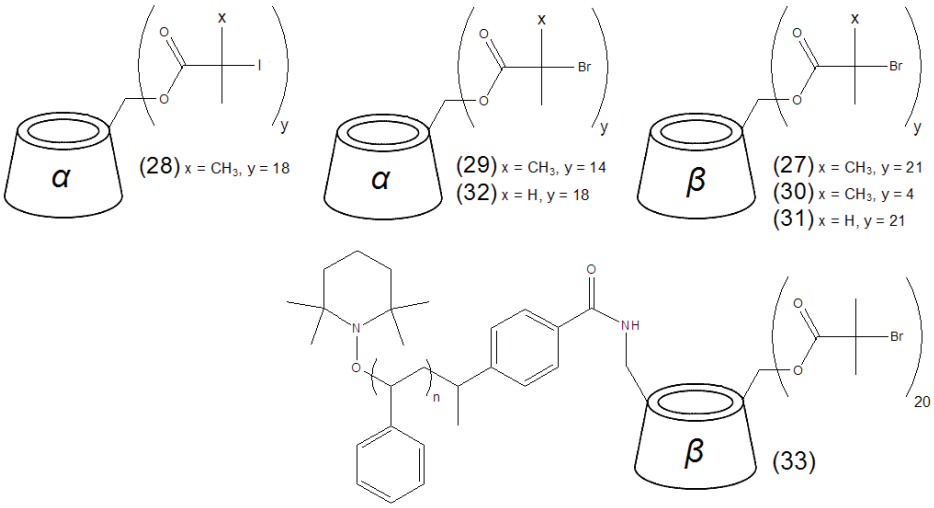

Figure 2.7 *ATRP macroinitiators applied in the synthesis of star cyclodextrin polymers (**Table 2.3**): heptakis[2,3,6-tri-O-(2-bromo-2-methylpropionyl)]-β-cyclodextrin **(27)**, octadeca-O-(2-iodo-2-methylpropionyl)-α-cyclodextrin **(28)**, tetradeca-O-(2-bromo-2-methylpropionyl)-α-cyclodextrin **(29)**, tetra-O-(2-bromo-2-methylpropionyl)-β-cyclodextrin **(30)**, heptakis[2,3,6-tri-O-(2-bromopropionyl)]-β-cyclodextrin **(31)**, octadeca-O-(2-bromopropionyl)-α-cyclodextrin **(32)**, end functionalised polystyrene with 20 (2-bromoisobutyryl)s β-cyclodextrin **(33)**.*

Catalyst system: Copper (I) bromide in combination with various ligands was chosen for almost all the reactions that were reported, with only a few exceptions.[55]

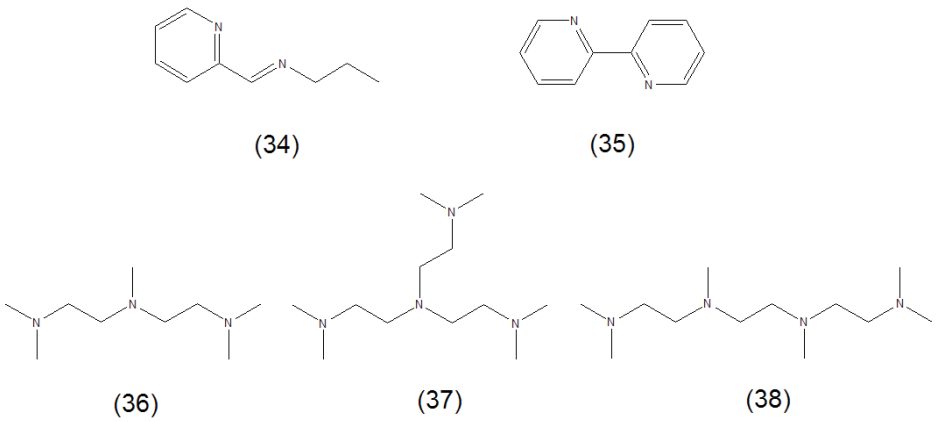

Figure 2.8 *Ligands used in the ATRP of star cyclodextrin polymers (**Table 2.3**): n-propyl-2-pyridylmethanimine **(34)**, 2,2'-bipyridine **(35)**, N,N,N',N",N"-pentamethyldiethylenetriamine **(36)**, tris[2-(dimethylamino)ethyl]amine **(37)**, 1,1,4,7,10,10-hexamethyltriethylenetetramine **(38)**.*

Monomers: So far, for the arms of the star polymers, the monomers polymerised (**Figure 2.9**) have ranged from styrene **(39)** and *N*-isopropylacrylamide **(40)** to (meth)acrylate derivatives **(41-46)**. The growth of chains were living, with the polydispersity indicies reported to be as low as 1.05.

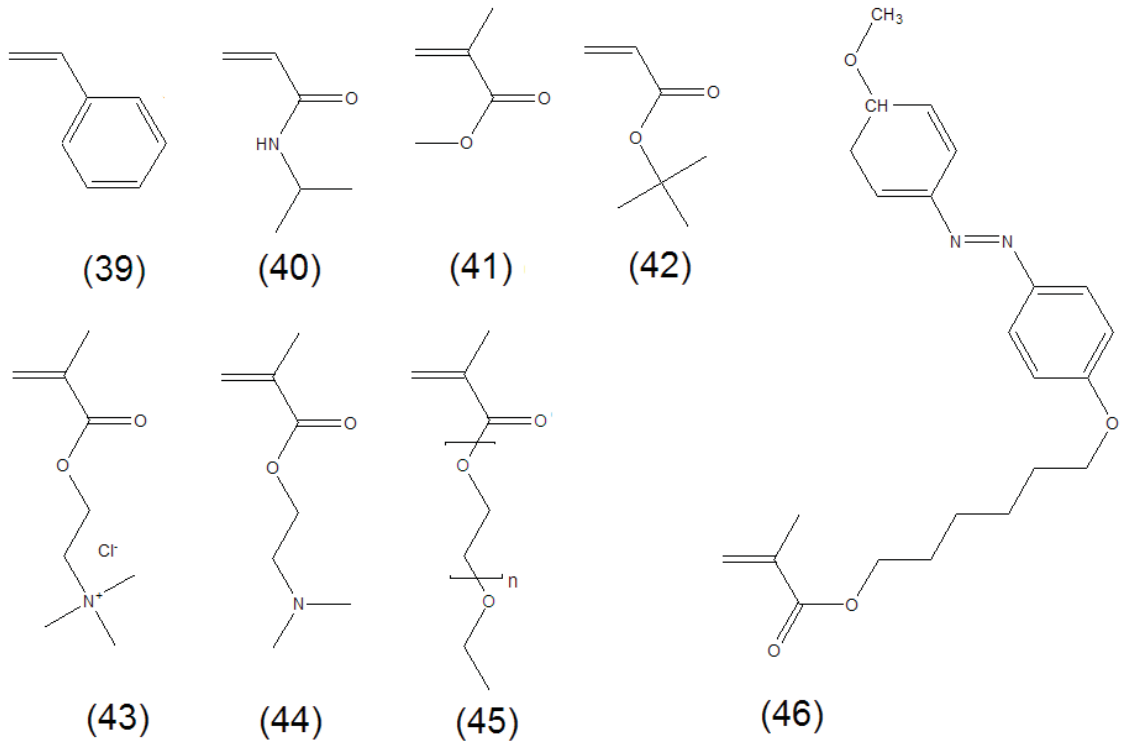

Figure 2.9 *Monomers used in the ATRP of star cyclodextrin polymers (**Table 2.3**): styrene **(39)**, N-isopropylacrylamide **(40)**, methyl methacrylate **(41)**, tert-butyl acrylate **(42)**, [2-(methacryloyloxy)ethyl] trimethyl ammonium chloride **(43)**, 2-(dimethylamino)ethylmethacrylate **(44)**, poly(ethylene glycol)ethyl ether methacrylate **(45)** and 6-(4-Methoxy-4'-oxy-azobenzene) hexyl methacrylate **(46)**.*

Other Polymerisation Techniques

Whilst ATRP dominates the reports on cyclodextrin based star polymers, other polymerisation techniques have also been reported in the literature (**Table 2.4**) and these will be discussed in this section.

Ring-opening Polymerisation. So far, only ethylene oxide,[50, 62] lactide,[63] *ε*-caprolactone,[64-65] and 2-ethyl-2-oxazoline[63] have been utilised in the synthesis of cyclodextrin star polymers by ring-opening polymerisation. Prior to the ring-opening polymerisation, the hydroxyl groups in 2- and 3- position were protected resulting in well-defined 7-arm stars with only the hydroxyl groups in 6-position initiating the polymerisation.[65] Stannous-2-ethylhexanoate ($Sn(Oct)_2$) was used as catalyst for the polymerisation. The use of tin catalyst was usually accompanied by high temperatures exceeding 100 ^{o}C.[63, 65] However due to the biosafety concerns of the authours, sodium hydride was used in an alternative approach using anionic ring-opening polymerisation.[64] Although the sodium hydride method was shown to work, broader PDI values resulted with the ε-caprolactone due to the prevalence of transesterification reactions under the anionic conditions employed.

Ionic Polymerisation. Both anionic[64, 66] and cationic polymerisation[67] have been used in obtaining cyclodextrin star polymers. The anionic polymerisations employed sodium hydride and sodium metal to deprotonate the hydroxyl groups of the *β*-cyclodextrin to generate a *β*-cyclodextrin oxyanions macroinitiator. For cationic polymerisations 1,1'-carbonyldiimidazole (CDI) was used to obtain an activated *β*-cyclodextrin macroinitiator.

Nitroxide-mediated Polymerisation (NMP). 2,2,6,6-tetramethyl-1-piperidinyl-*N*-oxy (TEMPO) modified cyclodextrin was utilised to polymerise styrene in a living radical polymerisation process.[68] Size exclusion chromatography (SEC) traces revealed however, trimodal molecular weight distributions. After fractionation and analyses, the lower molecular weight product was suggested to be TEMPO terminated linear polystyrene chains, whereas the higher fraction was believed to be a star-star coupled polymer hence, revealing an inefficient process.

Reversible Addition-Fragmentation Chain Transfer (RAFT) Polymerisation. Since its inception in 1998, RAFT polymerisation[69] has successfully been utilised to generate complex polymer architectures using thiocarbonyl thio groups as controlling moieties.[70] Stenzel and Davis[71] reported the synthesis of a heptafunctional trithiocarbonate *β*-cyclodextrin-based RAFT agent, which was used to control convey the polymerisation of

styrene. The RAFT agent was anchored to the core via the Z-group approach leading to the absence of star-star coupling products. However, the molecular weight of each arm was observed to slow down in growth at higher conversion, which was assigned to difficulties in accessing the RAFT group by the macroradical due to the shielding effect of the growing arms. The same RAFT agent was used to generate glycopolymer star polymers (**Figure 2.10**). However, to allow the polymerisation of the hydrophilic glycomonomer in water, the RAFT agent had to be converted by adding some 2-hydroxyethyl acrylate units to increase its water solubility.[72]

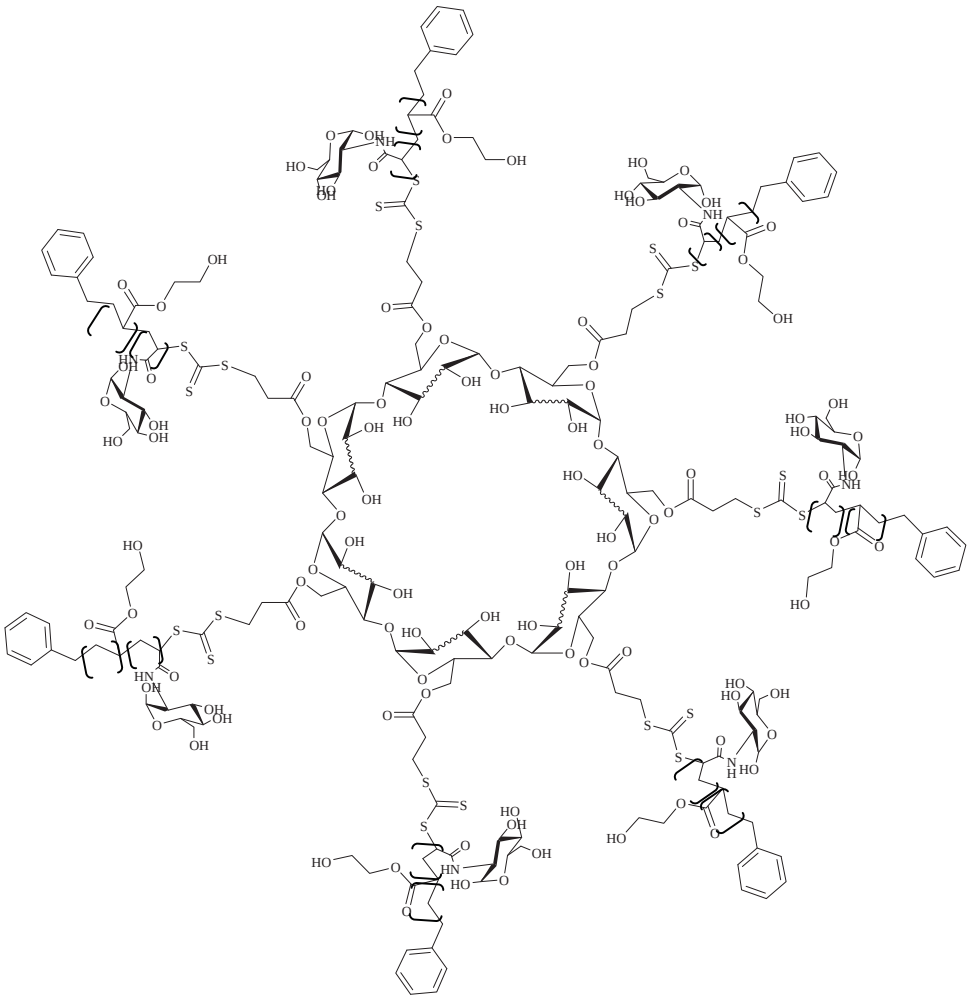

Figure 2.10 *Structure of seven-arm β-CD-(poly(hydroxyethyl acrylate)$_{10}$-b-poly(N-acryloyl glucosamine)$_{7}$)*[72]

Table 2.4 *Overview of star cyclodextrin polymers synthesised through other polymerisation techniques.*

Technique	Conditions[a)]	Monomer	PDI	Number of Arms	Ref.
Ring-opening	$Sn(Oct)_2$ catalyst, 115 ^oC, 8 hrs[b), c)]	Lactide	1.90	14	63
Ring-opening	Acetonitrile, 80 ^oC, 72 hrs[c), d)]	2-Ethyl-2-oxazoline	-	7	63
Ring-opening	Bulk, $Sn(Oct)_2$, 120 ^oC, 3 hrs	ε-Caprolactone	1.00-1.10	7	65
Anionic ring-opening	NaH, room temperature, 12 hrs	ε-Caprolactone	1.14-1.54	6,9,13	64
Anionic	DMF, -5 ^oC, 30 mins	Acrylonitrile	1.08-1.11	7	66
Cationic	DMSO, room temperature, overnight	Oligoethyleneimine	-	multiple arms (3.4-6.8)	67
NMP	Chlorobenzene, 125 ^oC, 2.5 hrs	Styrene	1.03-1.35	7	68
RAFT	Bulk at 100 ^oC or with AIBN at 60 ^oC	Styrene	1.45-1.81	7	71
RAFT	Water, AIBN, 65°C	*N*-Acryloyl glucosamine	1.2-1.8	7	72

a) Abbreviations used: stannous-2-ethylhexanoate ($Sn(Oct)_2$), *N*,*N*-dimethylformamide (DMF), dimethyl sulfoxide (DMSO), 2,2'-azobis(isobutyronitrile) (AIBN); b) in the homopolymer synthesis for lactide, β-cyclodextrin functionalised with seven tosylate units was used as the initiator. The polymerisation occurred at the free hydroxyl sites; c) 21 arm block copolymers were formed from lactide and 2-ethyl-2-oxazoline using a β-cyclodextrin core functionalised with 7 tosylate units; d) in the homopolymer synthesis for 2-ethyl-2-oxazoline, β-cyclodextrin functionalised with seven tosyl units was used as the initiator. The polymerisation was initiated from the tosylate groups.

2.1.2.2 Arm-first Approach

The core-first approach to star polymers is considered to be advantageous over the arm-first approach since difficulties concerning the limitation in the numbers of well-defined arms and the need to remove the linear arms from the product can hamper its effectiveness. Even though the core-first approach was used to synthesise most of the cyclodextrin star polymers seen in the literature, it has its own setbacks such as the, sometimes, tedious procedure to synthesise the appropriate cyclodextrin initiator and the formation of by-products which includes the formation of star-star coupling products. With the renewed interest in the highly efficient copper (I) catalysed azide-alkyne cycloaddition, better known as 'click chemistry', the arm-first approach found a suitable synthesis avenue. Click chemistry was favoured because of high yields, simple reaction conditions, fast reaction times, and high regio-selectivity.[73] The star synthesis can be divided into three major steps: 1) azide-functionalisation of cyclodextrin 2) synthesis of alkyne-terminated polymer arms 3) clicking process. The azido-functionalised *β*-cyclodextrins (**Figure 2.11**) were synthesised by reacting pre-functionalised *β*-cyclodextrin – **(21)** – with sodium azide.[49, 74]

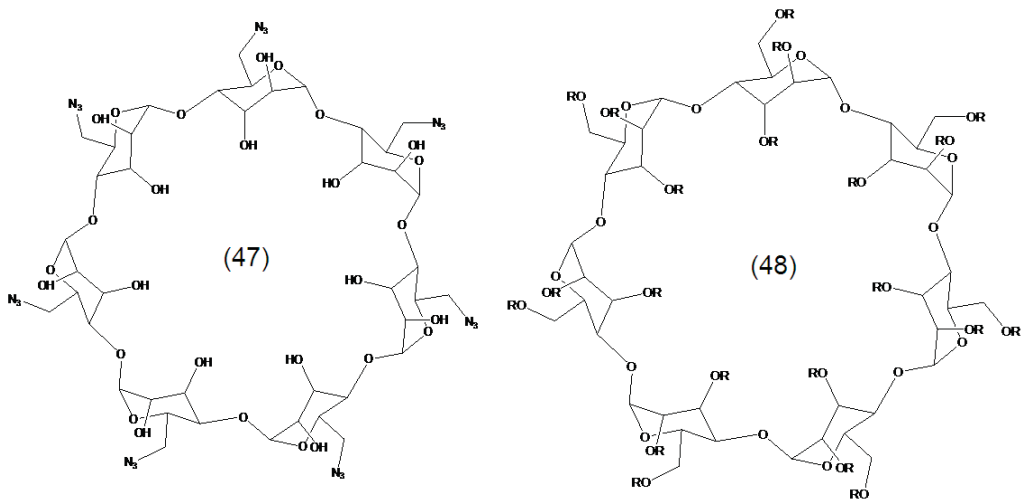

Figure 2.11 *Azido-functionalised β-cyclodextrins: heptakis(6-deoxy-6-azido)-β-cyclodextrin* ***(47)****, heptakis[2,3,6-tri-O-(2-azidopropionyl)]-β-cyclodextrin* ***(48)*** *where R = COCH(CH$_3$)N$_3$.*

In a separate step, alkyne-terminated poly(*N*-isopropylacrylamide) (PNIPAAM) was prepared by ATRP using propargyl 2-bromoisobutyrate as the initiator with the CuCl/Me_6TREN complex at 25 ^oC.[49] For alkyne-terminated poly(*ε*-caprolactone) arms, the ring-opening polymerisation was initiated using 5-hexyn-1-ol together with $Sn(Oct)_2$ at 110 ^oC for 3 hours.[74] Microwave radiation was then used to click poly(*ε*-caprolactone) arms with the addition of $CuSO_4$ and sodium ascorbate at 100 ^oC for 900 seconds.[74]

2.1.2.3 Applications of Cyclodextrin Star Polymers

Gene delivery. Cyclodextrin-cored cationic polymers from poly(2-(dimethylamino)ethyl methacrylate)/poly((polyethylene glycol) ethyl ether methacrylate)[58] and polyethyleneimine[67] stars have been used as non-viral gene delivery vectors. Both systems showed the ability to condense plasmid DNA into 100-200 nm size nanoparticles with positive zeta potentials at nitrogen/phosphate (N/P) ratios of 10 or higher. Interestingly, both cyclodextrin star polymers exhibited much lower cytotoxicity compared to their normal polymers (without cyclodextrin moieties). These stars can be utilised as low cytotoxicity gene delivery vectors with high gene transfection efficiency.

Self-assembled micelles. Depending on the nature of the arms, cyclodextrin star polymers can undergo self-assembly into micelles. Star polymer with seven poly(styrene) arms and the total of 14 unmodified hydroxyl groups at the C-2 and C-3 positions of the *β*-cyclodextrin showed amphiphilic behaviour in toluene.[68] Static light scattering (SLS) was used to estimate the aggregation property. With the poly(*ε*-caprolactone-*b*-ethylene glycol)-*β*-cyclodextrin star, the hydrophobic poly(*ε*-caprolactone) blocks and the hydrophilic poly(ethylene glycol) blocks underwent self-assembly in aqueous solution.[63] Dynamic light scattering (DLS) and transmission electron microscopy (TEM) were used to observe the micellisation.

Thermoresponsivity. Cyclodextrin with grafted PNIPAAM displayed different thermoresponsivity compared to linear PNIPAAM chains[49] or when subjected to host-

guest complexation.[57] The higher the number of PNIPAAM arms on the cyclodextrin, the lower the critical temperature (T_c) compared to linear PNIPAAM. This was explained with the local high chain density resulting in PNIPAAM chains to collapse and aggregate at lower temperatures. When the cyclodextrin star was complexed with adamantyl end-capped poly(ethylene glycol), the T_c shifted to higher temperature. This was suggested due to the increased solubility of the complex by the poly(ethylene glycol).

Polymer-metal complexes. The polymer arms of cyclodextrin star polymers were investigated as ligands for metals such as Cu^{2+}, Zn^{2+}, and Ag^{+} leading to polymer-metal complexes.[66] Infrared and ultraviolet (UV) spectra revealed that complexes were formed between poly(acrylonitrile) arms and metal ions. Differential scanning calorimetry (DSC) curves indicated an increasing glass transition temperatures (T_g) compared to the T_g of the original star polymers. The metal ions restricted the movement of polymer chains and therefore behaved similar to a crosslinker. In addition, star polymer-copper complex exhibited paramagnetism, which was indicated with electron spin resonance (ESR).

Nanocarriers. A cyclodextrin star polymer with amphiphilic block copolymer arms was synthesised from β-cyclodextrin, poly(lactide) (PLA), and poly(2-ethyl-2-oxazoline) (POX) through ring-opening polymerisation.[64] TEM image showed a tube-like self-assembled structure. The suitability as a candidate for host-guest system was tested by loading Congo Red and its release was quantified with a UV spectrophotometer.

Liquid crystalline star polymer. Recently, cyclodextrins were combined with liquid crystalline polymers[60] creating star polymers with poly[6-(4'-methoxy-4-oxy-azobenzene)hexyl methacrylate arms. DSC heating curves showed that the star polymers were thermotropic liquid crystalline polymer with smectic phase and nematic phase transition, similar to linear polymers. As the molecular weight increased, the phase transition temperature for both smectic to nematic and nematic to isotropic phase was also increased. The star polymer showed photoresponsive isomerisation under UV irradiation.

Gel polymer electrolytes. The encapsulation of electrolyte solution of 1 mol.L^{-1} of $LiClO_4$/ethylene carbonate-propylene carbonate (volume 1:1) into the *α*-cyclodextrin star polymer host has created a novel gel polymer electrolytes (GPE).[61] Poly(methyl methacrylate) was selected due to its good compatibility with liquid electrolytes. The GPE system had high ionic conductivity and high electrochemical stability. Even after 20 times of charging-discharging cycles, the system only lost 2% of its initial discharge capacity, showing its potential for application in lithium ion batteries.

Protein conjugates. Polyethylene oxide-cyclodextrin was conjugated with *α*-chymotrypsin protein to form a membranotropic compounds.[75]

Nanopores. Polyethylene oxide-cyclodextrin was able to form channels in lipid bilayers and behaving as biomimetic synthetic nanopores.[62]

2.1.3 Linear Polymers with Cyclodextrin Endgroup/s

2.1.3.1 Synthesis approach

NMP. Mono-6-deoxy-6-amino-*β*-cyclodextrin was reacted with TEMPO in DMF in the presence of *N*-hydroxybenzotriazole and triethylamine to afford an initiator, which was then used in the polymerization of styrene at 120 ^{o}C for 6 hours. As a result, end-functionalised poly(styrene) with an acetylated *β*-cyclodextrin terminal unit was created.[59, 76-77] The yield was 43%, with M_w = 11 400 g mol^{-1} and PDI = 1.13. Deacetylation with sodium methoxide in methanol for 3 days at room temperature led to **(49)** (**Figure 2.12**).

RAFT. Trithiocarbonate-containing *β*-cyclodextrin was reacted with 4-vinylpyridine (4-VP) initiated by AIBN in DMF at 70 ^{o}C for 30 hours under nitrogen. From GPC, the M_n was 4800 g mol^{-1} with a PDI of 1.17. The thiocarbonythio end group was removed by reacting the polymer with $Na_2S_2O_4$ aqueous solution and hexylamine for 24 hours to obtain **(50)**.[78] This polymer, which contained 30 repeating units of 4-VP, was used as the host component, which was complexed with an adamantyl-terminated poly(*N*-isopropylacrylamide) guest.

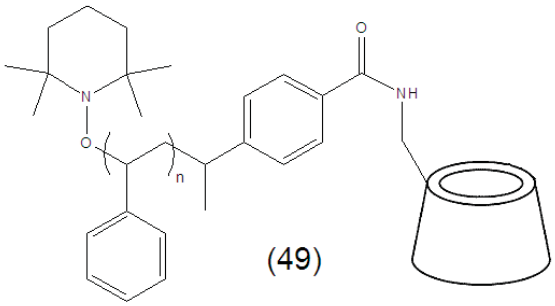

(49)

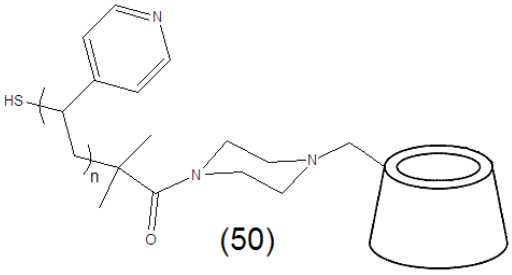

(50)

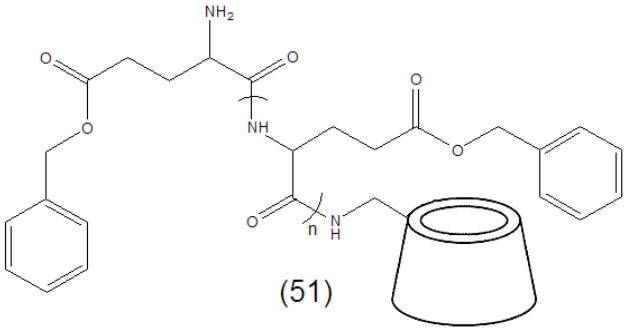

(51)

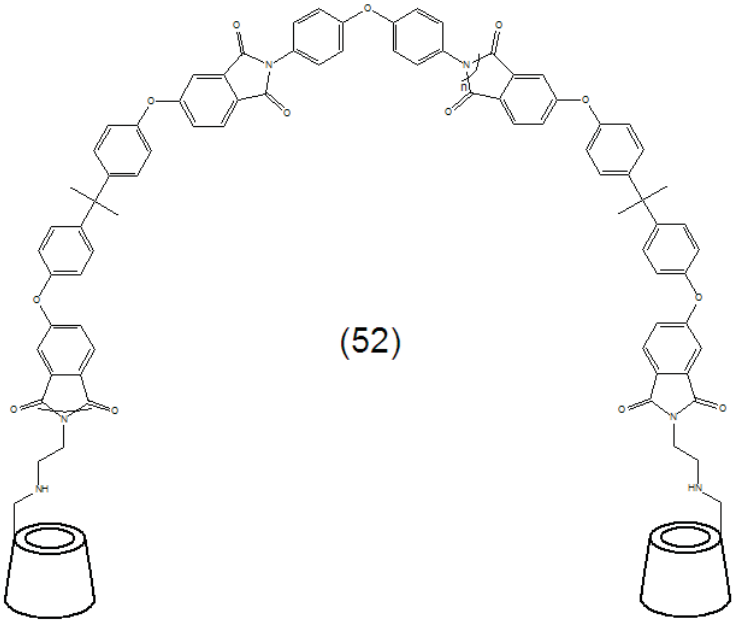

(52)

Figure 2.12 *Linear polymers with cyclodextrin endgroup(s) incorporating: poly(styrene)* ***(49)****, poly(4-vinylpyridine)* ***(50)****, γ-benzyl-L-glutamate N-carboxyanhydride* ***(51)*** *and anhydride-terminated poly(ether imide)* ***(52)****.*

Anionic Ring Opening Polymerisation The polymerisation of γ-benzyl-L-glutamate *N*-carboxyanhydride (γ-BLG-NCA) in dimethylformamide was initiated by 6-monodeoxy-6-monoamino-β-cyclodextrin at 30 ^{o}C.[79] The reaction was stopped when NCA bands disappeared from the FT-IR spectrum. After purification by washing with methanol and diethyl ether, the precipitates were dried under vacuum at 35 ^{o}C for 12 hours to obtain **(51)** (**Figure 2.12**). The weight-average molecular weight M_w for **(51)** was estimated to be about 46 000 g mol^{-1} from intrinsic viscosity measurement in DMF at 25 ^{o}C.

Condensation Polymerisation. The linear polymer **(52)** (**Figure 2.12**) with a terminal cyclodextrin unit at each chain end was prepared by condensation reaction between mono-(6-aminoethylamino-6-deoxy)-β-cyclodextrin and anhydride-terminated poly(ether imide) prepolymer.[80] The reaction proceeded in *N*-methyl pyrrolidone with acetic anhydride and pyridine as imidisation reagents. The M_n and M_w were 10 200 and 18 900 g mol^{-1}, respectively, with a PDI of 1.85.

2.1.3.2 Applications

Self-assembled micelles. All linear polymers with cyclodextrin attached at one or both ends reported in literature have self-assembly properties. The polystyrene cyclodextrin compound **(49)** was found to self-assemble forming nanoparticles in benzene, which was confirmed using dynamic light scattering (DLS) measurement.[59, 76-77] The average diameter ranged from 20-43 nm. The poly(4-vinyl pyridine) cyclodextrin compound **(50)**[78] was complexed with adamantyl-terminated PNIPAAM to form a noncovalent double hydrophilic block copolymer that is responsive to pH and temperature. At pH 4.8 and 25 ^{o}C, the hydrodynamic radius (R_h) and radius of gyration (R_g) of the micelles were 82.4 nm and 87.8 nm, respectively. At pH 2.5 and 60 ^{o}C, the micelles were inverted with a R_h and R_g of 78.4 nm and 63.1 nm, respectively.

The polymer **(51)** underwent self-assembly leading to nanoparticles with diameters between 50-60 nm.[79] In the presence of poloxamer 188, the zeta potential was slightly negative due to the uncharged poly(γ-benzyl-L-glutamate) since the poloxamer added to the suspension medium adsorbed and masked the surface of the particles. FT-IR characterisation suggested that the polymers retained an α-helix conformation even after the nanoparticle formation.

From isothermal titration microcalorimetry (ITC) studies, about 20% of *β*-cyclodextrin was contained within the nanoparticles and able to form inclusion complex with 1-adamantylamine. The rest of *β*-cyclodextrin moieties were either interacting with other chemical moieties within the system or deeply buried inside the nanoparticle. A detailed study was done on **(52)**.[80] It self-assembled easily into nanoparticles after water was added dropwise in its solution in DMF. Because every poly(ether imide) chain end was terminated by *β*-cyclodextrin, the host groups of *β*-cyclodextrin were equally distributed between inside and outside of the vesicles. SLS and DLS measurements gave the value of R_g and R_h to be 77 nm and 70 nm, respectively. The average density was about 1.7 x 10^{-2} g cm^{-3}, supporting the fact that **(52)** self-assembled into vesicles. TEM studies revealed the vesicular shell was about 20 nm in thickness, comparable to the fully extended chain length of poly(ether imide). The M_w of the vesicles was found to be 1.48 x 10^7 g mol^{-1}, while the M_n and M_w of **(52)** was 1.02 x 10^4 and 1.89 x 10^4 g mol^{-1}, respectively. From these, it was estimated that the assembly of 1000 of **(52)** chains built up one vesicle. ITC was used to estimate the degree of inclusion complexation between **(52)** and adamantane-monoended poly(ethylene glycol) (Ada-PEG). It was found that Ada-PEG with M_n of 1100 and 2000 g mol^{-1} were able to fully modify both inner and outer surfaces of **(52)**, whereas Ada-PEG with M_n of 5000 g mol^{-1} was only able to partially modify the inner surfaces.

2.1.4 Star-shaped Polymers with Cyclodextrin Endgroups

2.1.4.1 Synthesis approach

This is the latest architecture for cyclodextrin polymers, developed by van de Manakker *et al.*.[81-82] Instead of having *β*-cyclodextrin as the core with polymer arms dangling from it, this architecture has polymer arms grown from a multifunctional initiator with *β*-cyclodextrin moieties attached at the end of every macromolecular arm (**Figure 2.13**). 6-Monodeoxy-6-monoamino-*β*-cyclodextrin was reacted with succinic acid-end functionalised poly(ethylene glycol) star with M_n of 20 000 g mol^{-1}. The reaction proceeded in the presence of *N*-hydroxysuccinimide and *N*-ethyl-*N'*-(3-(dimethylamino)propyl)-carbodiimide at pH 5.5-6.0 at 25 ^oC to obtain **(53)**.

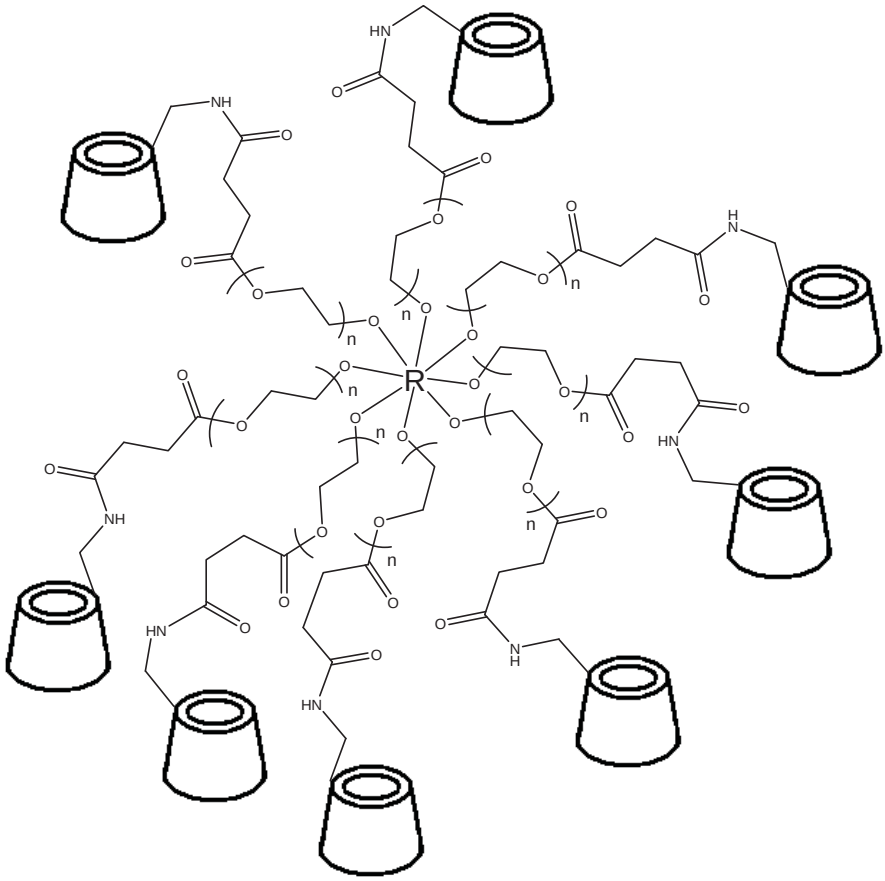

Figure 2.13 *Poly(ethylene) glycol star with β-cyclodextrin end groups* ***(53)*** *with R = hexaglycerine core.*

2.1.4.2 Applications

Hydrogels were obtained after mixing *β*-cyclodextrin endfunctional star polymers and cholesterol-terminated poly(ethylene glycol) stars.[81] Rheological studies showed that the hydrogel was thermoreversible upon repetitive heating and cooling. Rheological studies in combination with 2-D NMR analyses (NOESY ^{1}H) proved that the gels were obtained by inclusion complexation. The properties of the hydrogels were influenced by three factors, namely polymer concentration, the *β*-cyclodextrin/cholesterol stoichiometry, and the molecular weight of the star-shaped poly(ethylene glycol).

2.2 Inclusion Complexes of Cyclodextrins with Albendazole

2.2.1 Introduction

Albendazole (Methyl [6-(propylthio)-1*H*-benzoimidazol-2-yl]carbamate, ABZ) is a low cost antihelminthic drug with a broad spectrum of activity (**Figure 2.14**). However its low water solubility results in low absorption through the gastrointestinal tract and requires a large dose of ABZ for effective treatment. In current practice, the bioavailabity of ABZ is enhanced by means of complexation with cyclodextrins. The complexation between cyclodextrins and ABZ was first studied in early nineties.[83] Most of the published work on cyclodextrins and ABZ complexes concern studies that have attempted to treat human and animal parasites.[84-90] In addition, the cyclodextrin: ABZ complex was also found to be a potential anticancer agent.[91-92] The use of cyclodextrin polymers has been reported to increase the aqueous solubility of ABZ by more than a factor of one thousand.[93] The cyclodextrin/ABZ complex has been shown to be more toxic compared to ABZ alone due to the increased dissolution of ABZ.[86-87, 89, 92] Despite significant progress, the syntheses of well-defined cyclodextrin polymers to act as an ABZ carrier has yet to be reported. Therefore the syntheses of well-defined polymers are necessary to exert enhanced permeation and retention (EPR) effect in solid tumors.

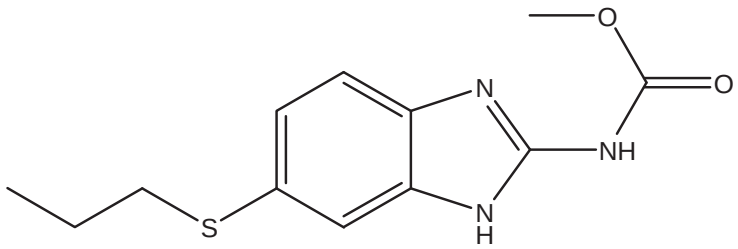

Figure 2.14 *The structure of albendazole (Methyl [6-(propylthio)-1H-benzoimidazol-2-yl]carbamate, ABZ). The propyl end is hydrophobic while the carbamate end is more hydrophilic.*

2.2.2 Types of Cyclodextrins Used for Complexation

From the literature, there are five types of cyclodextrins used for complexation with ABZ (**Figure 2.15**).

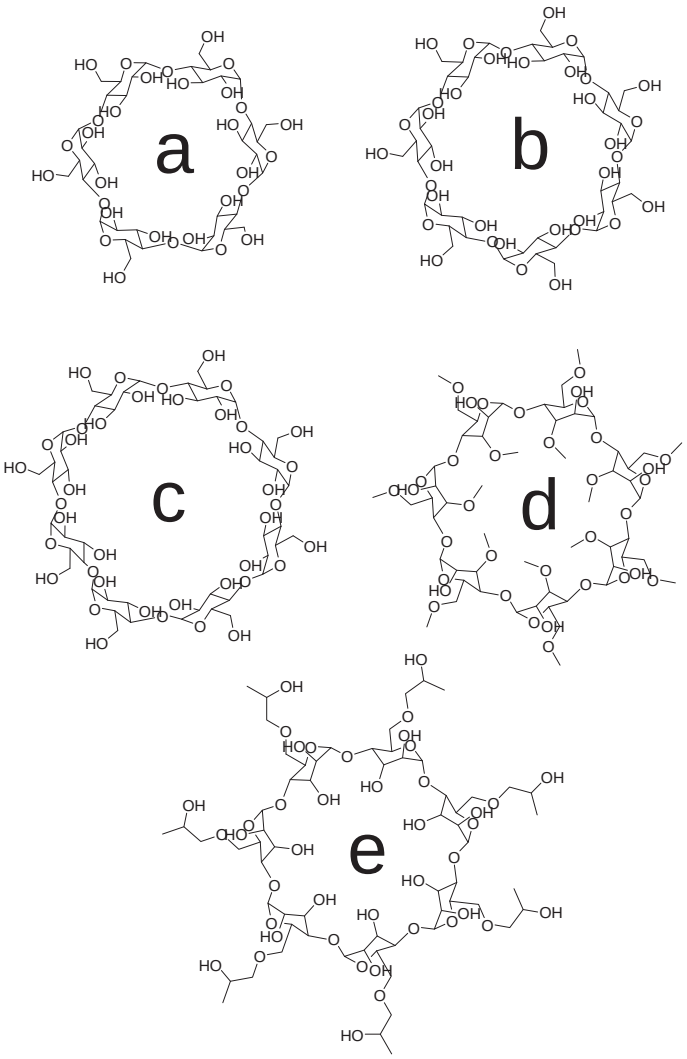

Figure 2.15 *Cyclodextrins used for complexation with albendazole (a) α-cyclodextrin, (b) β-cyclodextrin (c) γ-cyclodextrin, (d) dimethyl-β-cyclodextrin, and (e) 2-hydroxypropyl-β-cyclodextrin.*

Among these, *β*-cyclodextrin and its derivatives are the most widely used because the internal cavities of these cyclodextrins match with the size of ABZ, as demonstrated by higher binding constant values.[85] The *α*-cyclodextrin cavity was smaller while *γ*-cyclodextrin was larger in size to accommodate ABZ. Polycondensation of cyclodextrins

with citric acid leads to the undefined cyclodextrin polymers that are capable of dissolving more ABZ.[92-93]

2.2.3 Preparation of Complexes

Physical mixture 2-hydroxypropyl-β-cyclodextrin was mixed with ABZ for 20 min before filtration through an 80 mesh screen.[94]

Co grinding ABZ and β-cyclodextrin were triturated with methanolic hydrochloric acid, dried, and filtered.[88] ABZ and 2-hydroxypropyl-β-cyclodextrin underwent trituration without any solvent for 20 min before passing through 80-mesh screen.[94]

Kneading ABZ was added into the cyclodextrin paste, triturated, dried at room temperature and passed through 80-mesh screen.[94]

Solvent (Co) evaporation ABZ and 2-hydroxypropyl-β-cyclodextrin were dissolved in ethanol and water respectively before both solutions were mixed together.[86, 89] ABZ and cyclodextrins were dissolved in acetone and water respectively before mixing prior to solvent removal.[93] ABZ solution in methanol and aqueous solution of cyclodextrin were mixed together and stirred before drying.[94]

Solution ABZ was suspended in ten-fold molar excess of 2-hydroxypropyl-β-cyclodextrin solution in water, stirred for 6 days at 55 ^{o}C and freeze-dried.[84] Excess ABZ was added to the cyclodextrins in buffer solution and stirred at 25 ^{o}C. [85] Neutral or acidic 2-hydroxypropyl-β-cyclodextrin solution were used to dissolve excess ABZ, then the solution were shaken at 25 ^{o}C for 48 h before filtration with 0.45 μm filter.[87] An equimolar ratio of ABZ was added to the β-cyclodextrin aqueous solution, agitated at 37 ^{o}C for 3 days.[90] ABZ was shaken in acidic solution of 2-hydroxypropyl-β-cyclodextrin, shaken in water bath at 25 ^{o}C for 48 h before filtration.[92]

Amongst all the protocols used, the kneading method and solvent co-evaporation methods were found to be more effective than others in improving the ABZ aqueous solubility.[94]

2.2.4 Characterization of complexes

Nuclear Magnetic Resonance (NMR): The band broadening and change in peak intensity for the 1H NMR of cyclodextrins/ABZ in deuterated DMSO between 5.6-5.8 ppm were taken as indications for complexation.[90] The greatest, upfield shift of H_1, H_7, H_9, and H_{11} of ABZ/cyclodextrins complex in deuterated DMSO was the characteristic of an inclusion complex.[93]

Fourier Transform-Infra Red (FTIR): Moriwaki and co-workers concluded that the FTIR method cannot be used as an indication of the formation of inclusion complex in their work.[90] The IR bands' significant changes happened only when the mass of guest molecule did not exceed 5-15 % of the total complex mass. The mass of ABZ was 18.9% of the complex mass; therefore the conclusion cannot be made. In contrast, Joudieh and coworkers have reported that the disappearance of the $–CH_3$ absorption band for ABZ at 1442 cm^{-1} in the final product was attributed due to the complex formation.[93] Patel *et al.* have taken the reduction in intensity of transmittance for ABZ bending vibrations (1525-1630 cm^{-1}) was due to the complexation.[94]

Differential Scanning Calorimetry (DSC): The disappearance of an endothermic peak at 200 ^oC and appearance of a new peak between 260-270 ^oC suggested complex formation.[86]

X-ray Diffraction (XRD): Patel and coworkers have stated that the reduced diffraction intensity for the complex compared to the ABZ in crystalline form was an indication for the formation of the inclusion complex.[94]

Ultraviolet Spectra (UV): Bassani *et al.* have reported that strong broad negative peak in circular dichroism at 220 nm was taken as indication for complex formation.[84] They also have indicated the increase in the absorption intensity of complex in UV spectrophotometry as a sign for interaction between cyclodextrins and ABZ. Similar observation was also reported by Diaz and coworkers.[85, 90] The occurrences of bathochromic shift and/or band broadening were used as a sign of complexation.[94]

2.3 RAFT Polymerization and Block Copolymers

2.3.1 Introduction

Since first reported in 1998,[69] Reversible Addition-Fragmentation Chain Transfer (RAFT) polymerization has transformed the way the polymers are synthesized. Previously, complex polymer architectures were made through anionic living polymerization. One of the drawbacks of anionic polymerization, however, is that the system must be totally free from water or alcohol in order to avoid termination. Free radical polymerization was not the preferred method for making complex architectures due to the inherent limitation that it is not a living polymerization. Termination events in conventional free radical polymerization made it difficult to obtain living polymer chains that can be extended further. The breakthrough came when living free radical polymerization was discovered, beginning with Nitroxide-Mediated Polymerization (NMP),[95] Atom Transfer Radical Polymerization (ATRP),[96] and recently RAFT. Since then many publications regarding RAFT polymerization appeared in the literature, as the result of growing interest in this field.[97] RAFT polymerization is a very useful as a tool for constructing star, comb, and block copolymers.

A copolymer is a polymer containing two or more different monomers. There are many types of copolymers, including alternating, periodical, statistic, graft, and block copolymers.[98] Copolymerization has many advantages over homopolymerization. By copolymerization, a combination of properties from both homopolymers can be obtained, which is not possible with single homopolymer. For example, PNIPAAM is well-known for its thermoresponsive properties, whereas poly(acrylic acid) is pH responsive. A copolymer of these two homopolymers gives a double-responsive copolymer, which can be utilized as a drug delivery system in humans.[99] Copolymerization is also used to improve the physical properties of a polymer. For instance, polystyrene is a brittle but hard polymer. When polybutadiene chains are grafted onto the polystyrene backbone, high-impact polystyrene (HIPS) copolymer is produced.

In this subchapter, the basic features of RAFT chemistry and polymerization will be discussed. Utilization of RAFT polymerization to build block copolymers is also explained.

2.3.2 RAFT Polymerization

The key to successful RAFT polymerization can be attributed to the presence of a thiocarbonylthio end group, which regulates the polymerization process. This end group later can be used to extend the polymer chain; hence it is a living polymerization process. With RAFT polymerization, complex polymer architectures with low polydispersity can be realized, a wide variety of monomers can be polymerized, and many kinds of solvent can be tolerated.

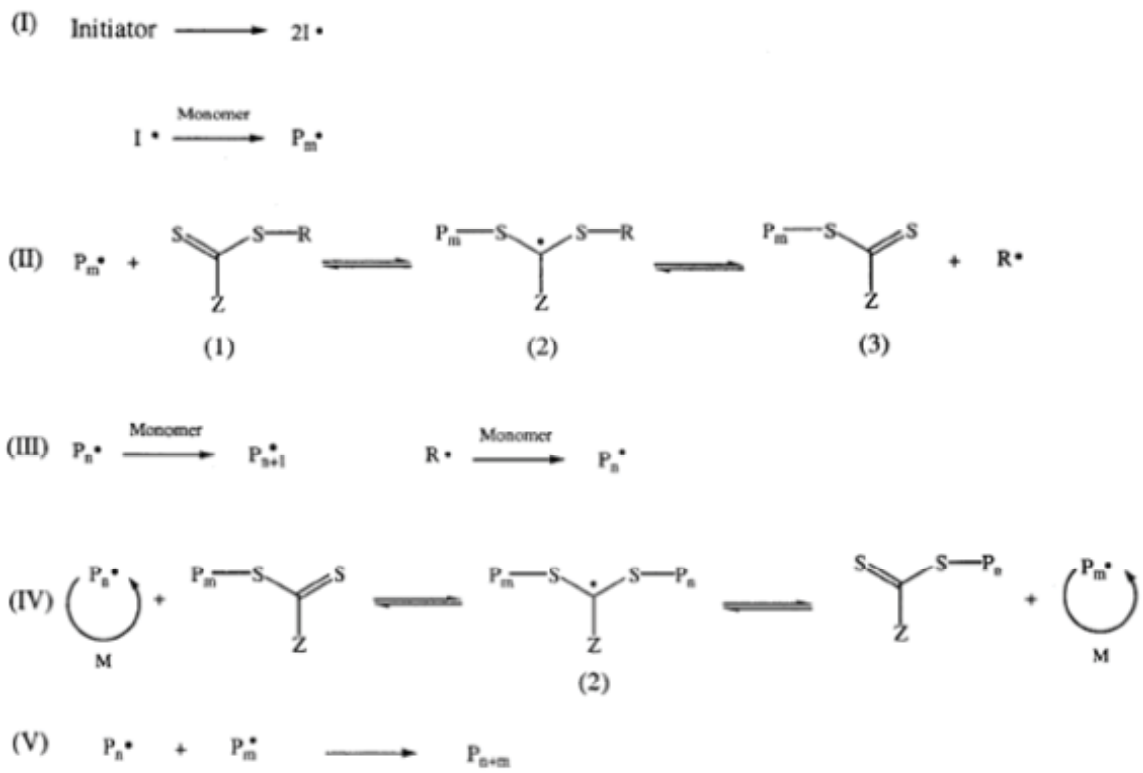

Scheme 2.1 *A set of reactions describing basic RAFT mechanisms.*[100]

The RAFT mechanisms can be described in five major steps (**Scheme 2.1**).

Initiation: The initiator decomposes into primary radicals and reacts with monomer, forming a macro-radical.

Reversible chain transfer: The macro-radical reacts with the RAFT agent. The R group leaves the newly formed macro-RAFT agent as part of a reversible addition-fragmentation process, to become a radical.

Reinitiation: The R radical then reacts with monomer again to form a macro-radical.

Chain equilibrium: This is the main reversible addition-fragmentation step that minimizing termination events between growing chains. Polymer chains convert between propagating radicals and polymeric transfer agents. The living characteristics of this process is proven by linear relationship between molecular weight and conversion, low polydispersity index, and pseudo first-order kinetics.[101]

Termination: Termination by bimolecular termination between two free polymeric radicals, forming 'dead' polymer.

Components of RAFT Polymerization

Initiator: Similar to the free-radical polymerization, RAFT polymerization requires initiators to commence polymerization. The most popular initiator is 2,2-Azobisisobutyronitrile (AIBN). If a narrow molecular weight distribution is desirable, the low concentration of initiator in comparison with RAFT agent concentration shall be used.[102] High initiator concentrations liberate more free radicals which subsequently lead to many termination processes, slowing down the polymerization.[103] The selection of initiator is also important. The initiator must not affect the stability of RAFT agent. Dibenzoyl peroxide and potassium peroxydisulfate may oxidize RAFT agent to sulfine by replacement of sulfur with oxygen atom.[104] In addition, the initiator-derived radical should be a good leaving group with respect to the propagating radical.

Chain transfer agent (RAFT agent): Most RAFT agents can be categorized under two main groups (**Figure 2.16**); dithiocarbonate and trithiocarbonate (thiocarbonylthio).

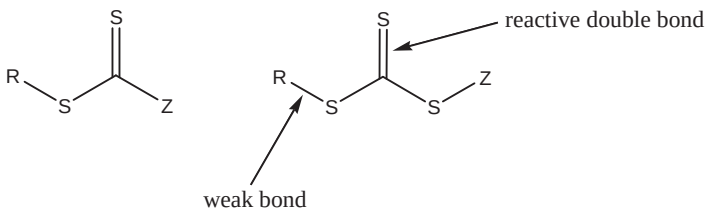

Figure 2.16 *Structure of chain transfer agent; dithiocarbonate (left) and trithiocarbonate (right).*

Not all monomers can be polymerized by the same RAFT agent. This can pose problems when two monomers are to be copolymerized for making block copolymers and will be discussed in Section 2.3.3.4. The structure of the RAFT agent itself plays an important role in RAFT polymerization. The difference between these two RAFT agents is cumyl phenyldithioacetate (CPDA) carries benzyl group as its Z-group, whereas cumyl dithiobenzoate (CDB) contains phenyl group as its Z-group (**Figure 2.17**).

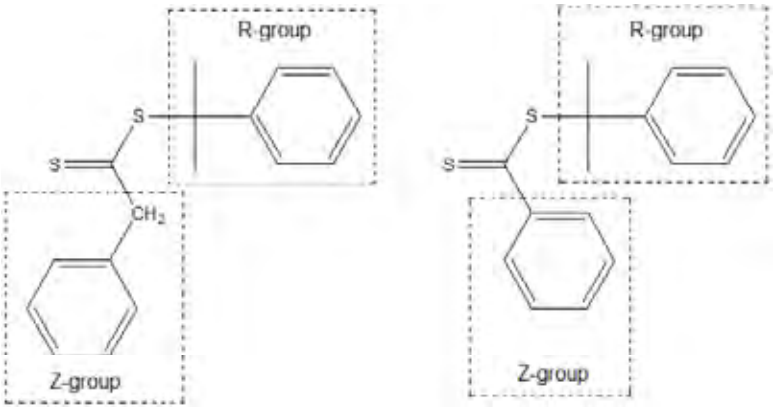

Figure 2.17 *Structure of cumyl phenyldithioacetate (CPDA) on the left side and cumyl dithiobenzoate (CDB) on the right side.*

CDB was found to significantly retard the RAFT polymerization of styrene.[100] CPDA did not show similar behavior, due to benzyl moiety that was not a stabilizing moiety to the macro-RAFT radical.[105]

Monomer: RAFT polymerization has its own advantage because it can control a large scale of monomers, as long as the monomer does not degrade the RAFT agent during polymerization. RAFT polymerization also allows functional monomers to be polymerized without recourse to protective chemistry, while being tolerant to the presence of oxygen and low temperatures.[106]

Solvent: RAFT polymerization can be carried out in bulk, solvent, and heterogeneous (emulsion, suspension) system. However, there are few considerations. Light, alkaline conditions, amine, and oxidizing species (such as dioxane and THF) must be avoided.

Advantages and Disadvantages of RAFT Polymerization

Compared to other polymerization techniques, RAFT polymerization also comes with its own advantages and disadvantages. RAFT polymerization can control a large scale of monomers. It is an inexpensive technique and can be used in many solvent systems. However, RAFT agent is not very stable against hydrolysis, aminolysis, UV, and heat. Due to its chemistry, every polymer chain made by RAFT polymerization carries the RAFT end-group (dithioester) at the end of the polymerization. Since RAFT polymers are finding their way as biomaterials, the toxicity issue is an important consideration. The RAFT polymers are usually colored due to the existence of this end-group. A simple decolorization technique was proposed by using AIBN to remove dithiobenzoate end-group from PMMA.[107] The effectiveness of this technique was proven by elemental analysis, UV-visible spectroscopy, and SEC.

2.3.3 Block Copolymers

Many reports about block copolymers produced through RAFT polymerization (**Scheme 2.2**) emphasized on diblock copolymers, but triblock copolymers were also included. There are four main routes to obtain block copolymers, namely

a) Diblock copolymers via chain extension of macro-RAFT agent
b) Triblock copolymers via chain extension of macro-RAFT agent
c) Block copolymers based on polycondensates and other polymer chains
d) Block copolymers via click chemistry

For a) and b), the formation of a block copolymer was achieved by the addition of the second monomer into the previously made macro-RAFT agent. Beforehand, the macro-RAFT agent was obtained by polymerizing the first monomer with RAFT agent. The

polymer chains produced were capped at the end by RAFT functionalization, e.g. thiocarbonylthio. The macro-RAFT agent behaved similarly as low-molecular weight RAFT agent during copolymerization. Copolymerization was done by adding the second polymer block onto the first one, regulated by RAFT functionalization. For c), the block copolymers are made by combining polycondensation or ring-opening polymers with macro-RAFT agent (polymers with RAFT end group). For d), two or more polymers were combined through click chemistry. The reason for this was that monomers with too dissimilar reactivities would have required different RAFT agents to be polymerized. Each homopolymer was made separately by RAFT polymerization and functionalized before they were joined together.

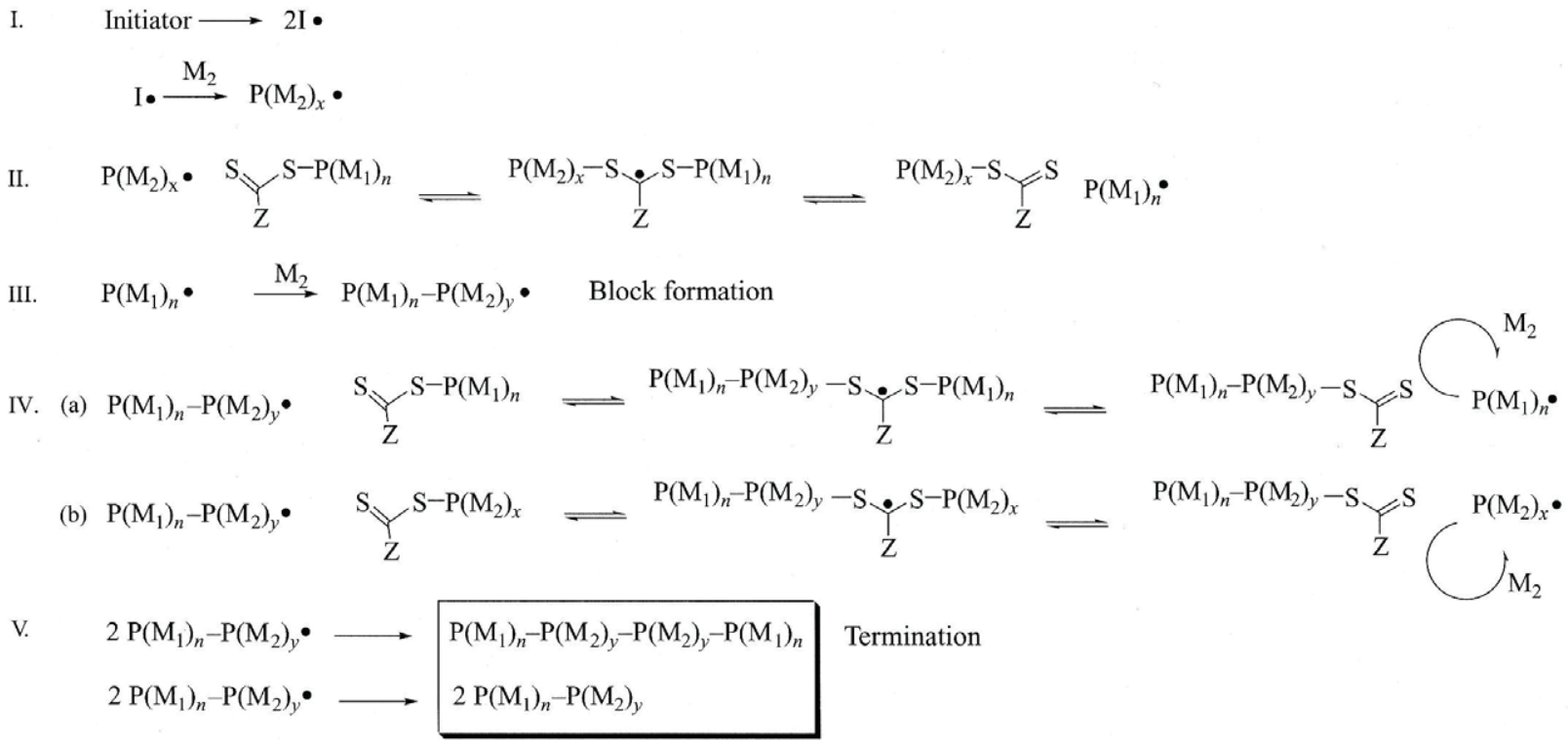

Scheme 2.2 *Detailed mechanisms of chain extension forming block copolymers.*

2.3.3.1 Diblock copolymers via chain extension of macro-RAFT agent

Theoretical Considerations

The chain extension of macro-RAFT agent in making block copolymers is illustrated in **Scheme 2.3**. The polymerization process is similar to the homopolymerization by RAFT agent. The process can be described in five major steps.

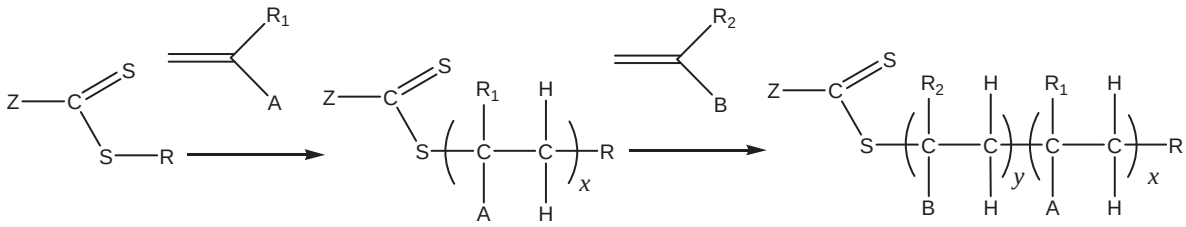

Scheme 2.3 *Chain extension of macro-RAFT agent in making block copolymers.*

Initiation: The initiator breaks up and reacting with second monomer, forming a macroradical containing the second block.

Reversible chain transfer: The second block macroradical reacts with the macro-RAFT agent. The first monomer block behaves as a leaving group and becomes a macro radical of the first block.

Block formation: The macro-radical of the first block reacts with the second monomer to form a block copolymer macro-radical.

Chain equilibrium: The block copolymer macro-radical reacts with macro-RAFT agent to form a new diblock copolymer with a RAFT end group attached. Reaction IV(a) will become less likely, since the macro-RAFT agent shall be consumed during the earlier chain transfer process. Therefore, the macro-radical of the second block cannot form a block copolymer and remains as a homopolymer impurity in the system.

Termination: Termination by hydrogen abstraction and also the formation of triblock.

Practical Considerations

The selection of the Z group and R group in a RAFT agent are both important. The selected Z group should enable both monomers to be able to be polymerized in a controlled manner. The selection of the R leaving group is crucial for the formation of block copolymers. If the leaving group (i.e. the first polymer block) is more stable than the addition of the second polymer block, the second polymer block will preferentially stay with the macro-RAFT agent. As a result, only homopolymers will be produced. It is advisable to synthesize methacrylate-type macro-RAFT agents before performing chain extension with styrene or acrylate-type monomers. However, many block copolymers can be synthesized in either way.[108-110]

Numerous other factors must be considered in a RAFT polymerization. For example, high initiator concentrations will increase the termination process.[102] Hindered monomers will polymerize slowly, causing more polymer chains without RAFT end group contaminating the final block copolymer.[111] The thiocarbonylthio (trithiocarbonate) group stability is influenced by heat,[112] light,[113] pH values,[114-116] solvents[104, 117-118], hydrolysis,[115] and aminolysis.[116, 119] The syntheses of a well-defined macro-RAFT agent pose their own challenges. Termination events are unavoidable but the reaction conditions can be optimized using mass spectroscopy,[116] NMR or UV analysis.[120] The presence of dead polymer can be observed as a second peak or as low-molecular weight tailing in GPC images.[121-123]

The syntheses of block copolymers require special attention with regards to solvent selection. Some amphiphilic blocks are made by protective group chemistry[124-125] while cationic block copolymers can be made by quaternization.[109, 126] A block copolymer has been reported to polymerize in bulk[127] while copolymer of ionic and hydrophobic block has been prepared by suspension polymerization.[128-129] Ideally, the molecular weight shall increase linearly with conversion and can be predicted using this equation:

$$M_{\text{block copolymer}} = \frac{[M]}{[\text{macro}-\text{RAFT}]} \text{ x conversion x } M_{\text{M}} + M_{\text{macro-RAFT}}$$

Scheme 2.4 *Prediction of molecular weight for RAFT-mediated block copolymerization*

where [*M*] and [macro-RAFT] are the monomer and macro-RAFT agent concentrations, and M_{M} and $M_{\text{macro-RAFT}}$ are the molecular weights of the monomer of the second block and the macro-RAFT agent, respectively. The formation of a block copolymer can confirmed by observing the shift of the molecular weight distribution by GPC curves to higher molecular weights (earlier elution times) as a function of conversion while the overall molecular-weight distribution remains narrow. The broadening of the molecular weight distribution can be caused by impurities of dead polymer in the macro-RAFT agent and with increasing initiator concentration. To prevent side reactions, a high ratio of macro-RAFT agent to initiator is required. The percentage of dead chains can be calculated by this formula:[130]

$$\text{\% dead chains} = \frac{2f[\text{I}]_0 \text{ x } (1 - e^{-k_d t})}{[\text{macro}-\text{RAFT}] + 2f[I]_0 \text{ x } (1 - e^{-k_d t})}$$

Scheme 2.5 *Calculating the percentage of dead chains for RAFT-mediated block copolymerization*

where *f* is the initiator efficiency, k_d the initiator decomposition rate coefficient and [*I*] and [macro-RAFT] are the concentrations of initiator and macro-RAFT agent, respectively. Macro-RAFT agent has been shown to have an effect on the block copolymer formation and rate of polymerization. High molecular weight macro-RAFT agent can cause bimodal distributions[131] and reduce the rate of polymerization.[117, 125, 131] Higher amounts of macro-RAFT agent also exert similar effect.

2.3.3.2 Triblock copolymers via chain extension of macro-RAFT agent

There are three routes in obtaining triblock copolymers (**Scheme 2.6**):

a) Chain extension of diblock copolymer
b) Difunctional RAFT agent
c) Trithiocarbonate RAFT agent with two leaving groups

The synthesis of triblock copolymers according to route a) is similar to the synthesis of a diblock copolymer. However, pentablock copolymers with chain morphology A-B-C-B-A are formed during termination reactions. Lokitz *et al.*[132] reported triblock copolymer made of NIPAAM, *N*-acryloylalanine and DMA. Mertoglu *et al.* [133] developed charged stimuli-responsive amphiphilic A-B-C triblock copolymers using similar approach. Yang *et al.*[134] also used a similar pathway to generate pH and stimuli-responsive A-B-A triblock copolymers using poly(methacrylic acid) and NIPAAM.

Route b) utilizes a bifunctional linker to link two RAFT agents, either through the R group or the Z group. The polymerization mechanisms are similar to the star polymer synthesis using RAFT.

Route c) is the most popular way to obtain A-B-A triblock copolymer, by utilizing a trithiocarbonate RAFT agent with two leaving groups. The difference here is that there is no Z group, as both leaving group and later the polymer chain take role as both Z and R group. Styrene is the favorite monomer here, it is copolymerized with *n*-butyl acrylate,[135-136] 4-vinylpyridine,[137] maleic anhydride,[138] poly(ethylene glycol) methacrylate,[139] and dicyclohexyl itaconate.[111]

Application of di/triblock copolymers via chain extension of macro-RAFT agent

The comprehensive list of RAFT agents, first block, second block, and solvents used are already described in significant detail.[97] In terms of applications, the RAFT di/triblock copolymers are mainly synthesized for the pH-responsive, thermoresponsive, or combination of both properties.

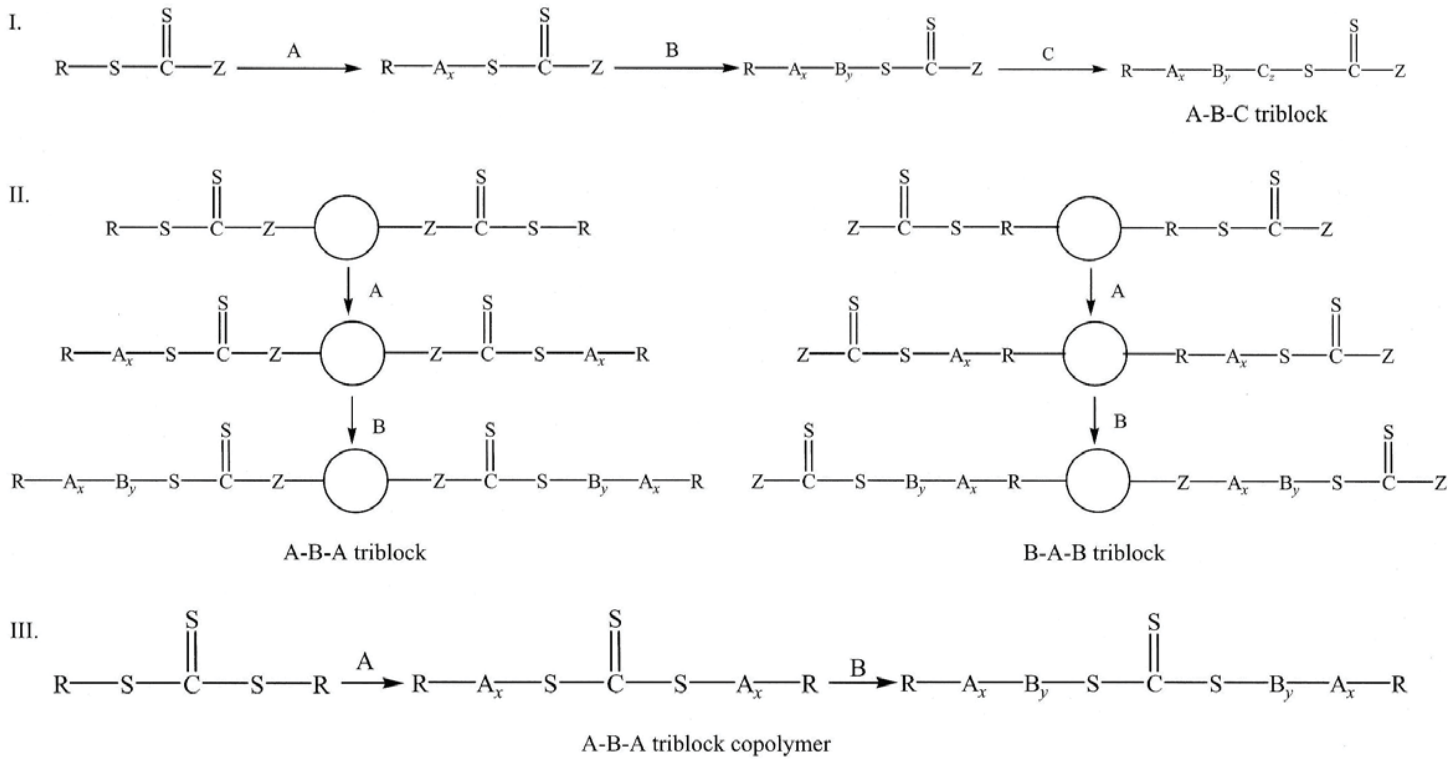

Scheme 2.6 *Three different routes to triblock copolymers.*

2.3.3.3 Block copolymers based on polycondensates and other polymer chains

Theoretical Consideration

Nowadays, combining polymers made by RAFT polymerization with polymers made by other techniques(such as polycondensation and ring opening polymerization) to obtain block copolymers is becoming more popular. There are five possible routes; in each route the end-group functionality is used to link the RAFT agent to another polymer (**Scheme 2.7**).[97] The RAFT agent shall be carefully designed so later it can tolerate polymerizations of non-RAFT monomer or acting as an initiator itself, e.g. in ring-opening polymerization. The placement of functional group either at R-group or Z-group will lead to different types of polymeric RAFT agents and mechanisms.

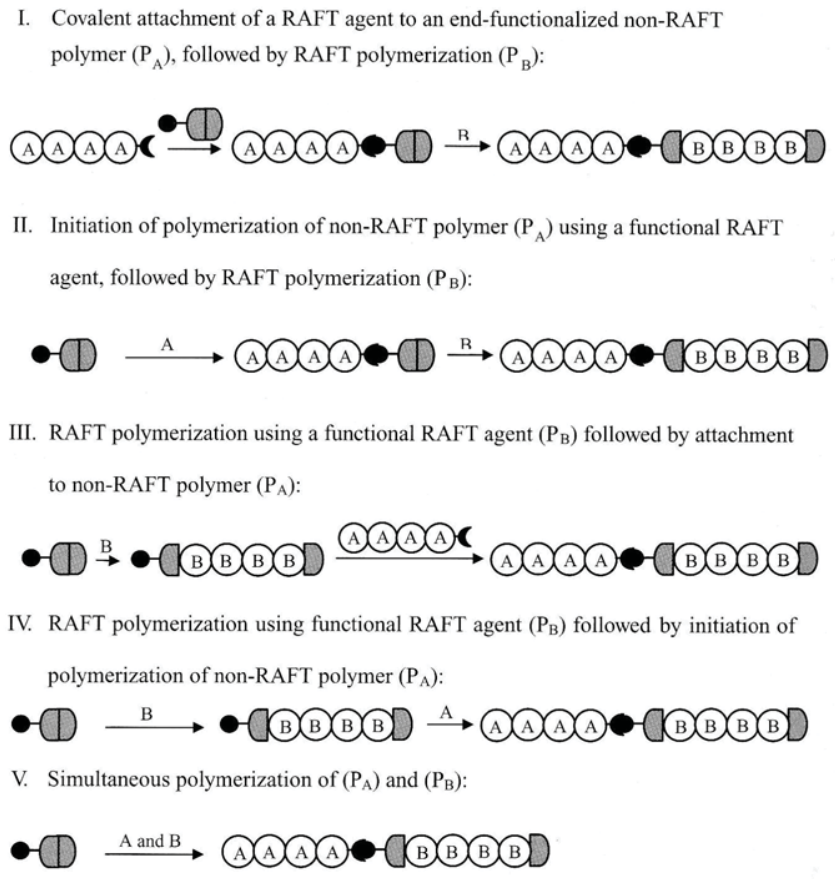

Scheme 2.7 *Five possible routes of obtaining block copolymers based on RAFT-made polymer blocks and non-RAFT polymer blocks.*

Poly-RAFT agent via R-Group Approach

In this approach, the first polymer block is the leaving group (R-group). The two characteristics of this copolymer type is that monomer of the second block can form homopolymer on its own and the triblock copolymers resulting from termination process (**Scheme 2.8**).

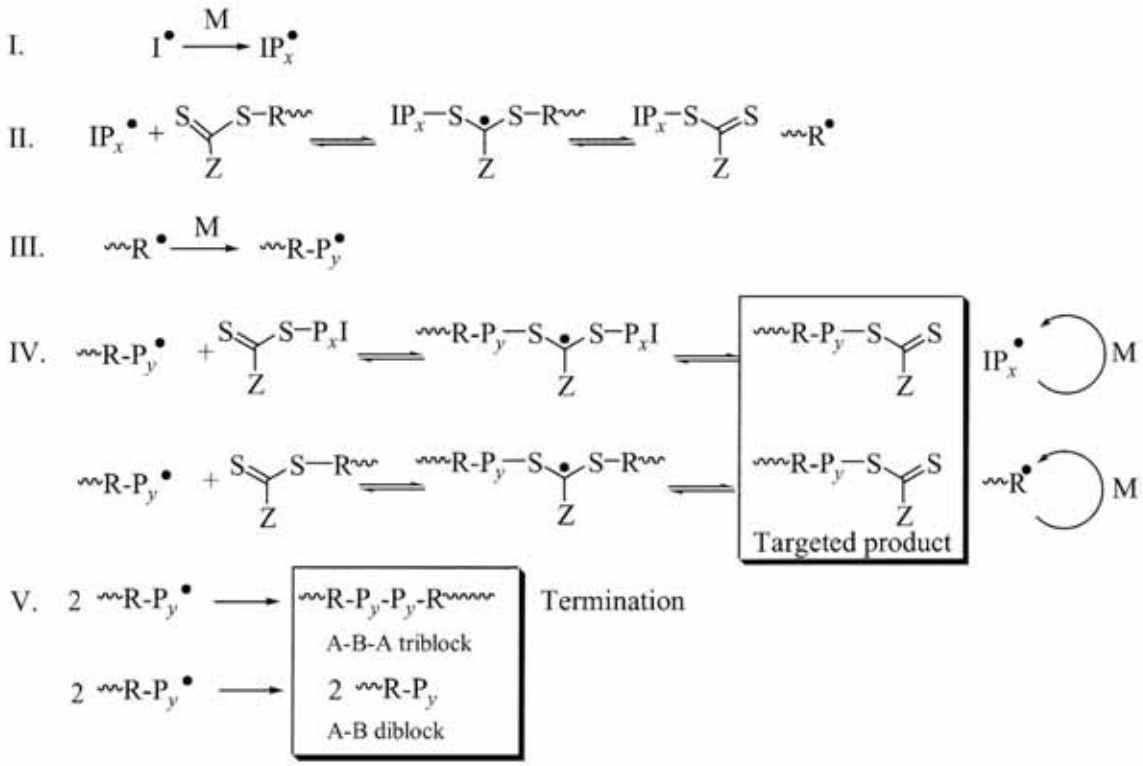

Scheme 2.8 *Block copolymer synthesis using RAFT agent which attached to an end of polymer chain using R-group approach.*

Poly-RAFT agent via Z-Group Approach

Herein, the polymer is attached to the RAFT agent via Z-group and it will bind to the trithiocarbonate group throughout the copolymerization. However, the termination does not produce triblock copolymers (**Scheme 2.9**).

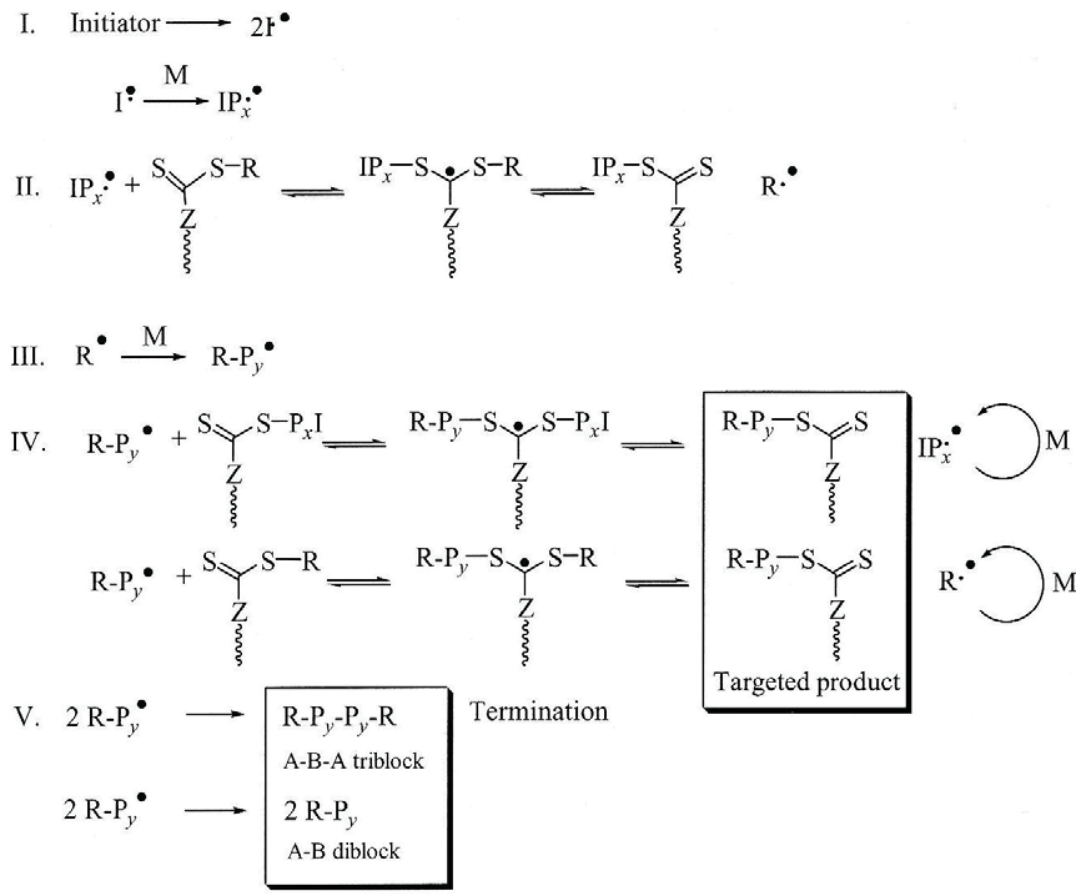

Scheme 2.9 *Block copolymer synthesis using RAFT agent which attached to an end of polymer chain using Z-group approach.*

Practical Consideration

Route 1 is the most popular route, where a preformed polymer is functionalized with RAFT end group by attachment with thiocarbonylthio compound. Primarily the polymers were functionalized with hydroxyl groups, and later esterified with RAFT agents containing carboxy groups. In an alternative route, Grignard reactions were used to synthesized polyethylene based poly-RAFT agents.[140] The extent of this reaction was monitored by NMR analyses. However, there were still remaining unreacted poly-RAFT agents. In order to quantify the amount of RAFT agent left, UV spectroscopy has been

utilized.[141] For absolute quantification, UV spectroscopy was combined with an evaporative light-scattering detector.[142]

Most RAFT agents were attached via the R-group. Hence, it is expected that this approach will result in formation of A-B-A triblock copolymers. Triblock copolymers can also be formed from exposure to UV radiation because the RAFT end group will decompose into radicals, causing more termination reactions. The absence of high-molecular weight shoulders with the Z-group approach confirmed the mechanisms described in **Scheme 2.3**. The polydispersity of the RAFT polymer will be influenced by the polydispersity of the non-RAFT polymer underlying it. Despite of the unavoidable termination reactions, the polydispersity indices of the second copolymer block closely followed the lower polydispersity indices of the first poly(ethylene oxide) blocks.[135, 141, 143-147] Due to the already broad polydispersity index of the underlying polyethylene, the block copolymer of polyethylene and poly(methyl methacrylate) have polydispersity indices above than 2.[148]

The attachment of a polymer chain to the RAFT agent was found to influence the polymerization kinetics due to different steric and polarities. The attachment of polymer chain to a RAFT agent also increased the inhibition time.[149] Poly-RAFT agents will fully involved in the block making as the monomer conversion increases.[142]

In Route 2, block copolymers are generated when RAFT agent initiates the polymerization of non-RAFT polymer, mainly via ring-opening polymerization. Hydroxyl group functionalized RAFT agents were used for lactate ring-opening polymerization.[150-151] However, some RAFT agents remained and were only removed via precipitation.[150] 1,5-cyclobutadiene underwent ring-opening methathesis polymerization with another carboxylic-terminated RAFT agent to obtain poly(butadiene) and poly(*t*-butyl acrylate) triblock copolymers. The triblock had a polydisperse center segment and monodisperse end blocks.[152]

A simultaneous process (Route 5) of RAFT polymerization of styrene and ring-opening of ε-caprolactone was performed in supercritical carbon dioxide.[153] The polymerization of styrene was well controlled but ring-opening polymerization caused formation of block copolymers with broader molecular weight distribution. In a similar way, a bifunctional RAFT agent was polymerized via polycondensation to obtain multifunctional RAFT agent. Poly(ethylene oxide) was polycondensed with diacyloyl chloride RAFT agent to obtain multifunctional poly(ethylene oxide)-based RAFT agent.[154] The polycondensation resulted in broader polydispersity. The RAFT polymerization of styrene that followed was well-controlled. A synthesis of multiblock consisting of alternating RAFT agents and thiourethane blocks was reported. The subsequent RAFT polymerization of styrene created polystyrene spacer between thiourethane blocks, forming a sequentially ordered polymer.[155]

2.3.3.4 Block copolymers via click chemistry

Despite the versatility of RAFT process, it has own limitations. Only monomers with similar reactivities can be copolymerized together using the same RAFT agent. RAFT polymerization of vinyl acetate requires the use of xanthates,[156] while styrene undergoes RAFT polymerization under the presence of dithiobenzoate compounds.[100] However, copolymerizing these two together is not an easy task. A novel fluorinated RAFT agent (benzyl fluoro dithioformate) has been suggested to overcome this problem.[157]

Another strategy is to prepare two homopolymers separately, followed by functionalization and combination. The requirement is the combination reaction must be efficient and unaffected by the presence of other functional groups. Joining two polymers together is thermodynamically and sterically challenged. The efficient way of joining these polymers is through ‘click chemistry’, a term made popular by Sharpless *et al.*[158] The combination of click chemistry and RAFT polymerization pushes the development of advanced polymer architectures much further.

A block copolymer of polystyrene and poly(vinyl acetate) was finally became reality (**Scheme 2.10**), thanks to a combination RAFT polymerization and click chemistry.[159] Styrene was polymerized with RAFT agent containing a trimethylsilyl protective end group. Vinyl acetate was separately polymerized with a RAFT agent containing an azide end group. The polystyrene macro-RAFT agent was deprotected to obtain reactive acetylene end group to be reacted with azide-functionalized poly(vinyl acetate). FTIR spectrum showed the disappearance of azide group, reported as proof of successful click reaction. Similar ratios must be employed between homopolymers to obtain well-defined block copolymer and successful click reaction.[160] Another block copolymer was made from polystyrene and poly(*N*,*N*-dimethylacrylamide). The resulting block copolymer could be clicked with many compounds terminated with acetylene, showing the versatility of click chemistry.[161] O'Reilly *et al.*[162] managed to synthesize block copolymers of poly(acrylic acid-*block*-polystyrene) with acetylene functionalities without resorting to protective chemistry. O'Reilly and co-workers[163] also used clickable monomers to prepare amphiphilic block copolymers with high reactivity. After self-assembly into micelles, the reactive azide functionalities left in the core were available for subsequent reactions.

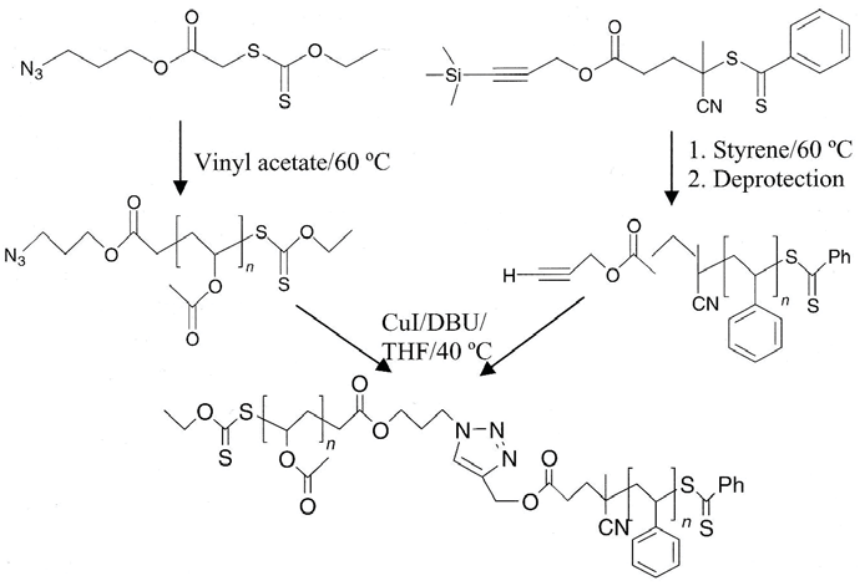

Scheme 2.10 *Combination of RAFT and click chemistry to construct polystyrene-block-poly(vinyl acetate) which was previously difficult to synthesize through normal copolymerization*[159]

Chapter 3: Analytical Instruments

This chapter describes the underlying principles behind instruments used to analyze products as well as general procedures about sample preparation methods. Detailed description can be found in their respective chapter.

3.1 Nuclear Magnetic Resonance (NMR)

NMR is the most valuable spectroscopic technique available to the chemist for determining the structure of both organic and inorganic species. The characteristic that sets NMR apart from ultraviolet, visible, and infrared absorption is that nuclei of atoms rather than outer electrons are involved in the absorption process.[164]

The ^{1}H NMR and ^{13}C NMR studies are the most popular nuclei studied, even though ^{14}N, ^{19}F, ^{29}Si, and ^{31}P NMR are also described. When these nuclei are placed in magnetic field, there are oriented either with or against the field. When irradiated with radiofrequency waves, energy absorption occurs and the nuclear spins flip from the lower-energy state to the higher-energy state. This absorption is detected, amplified, and finally presented as an NMR spectrum. NMR spectrum contains four general features:

Number of peaks Every non-equivalent ^{1}H or ^{13}C nucleus is assigned to a different peak.

Chemical shift Motion of the electrons surrounding the nucleus under applied magnetic field gives rise to the chemical shift. In an NMR spectrum, this is the exact position of each peak. ^{1}H absorptions are usually in the range 0 to 10 δ downfield from the tetramethylsilane (TMS) reference signal.

Integration The number of protons responsible for each peak can be determined by integration of the area under each peak.

Spin-spin splitting Neighbouring hydrogen nuclei can enhance or reduce effective field of each other, splitting an NMR absorption into multiplet. The multiplicity can be determined by adding 1 to the number *n* of magnetically equivalent protons on the neighboring atoms (*n* +1).

Throughout this thesis, all NMR spectra were recorded using a Bruker 300 MHz spectrometer with auto-sampler at 25 ^{o}C. Samples were dissolved in deuterated solvents, mainly deuterated chloroform ($CDCl_3$), deuterated dimethyl sulfoxide (d-DMSO), and deuterium oxide (D_2O). NMR spectra were used mostly to determine chemical structure and also to calculate the conversion of monomer to polymer.

3.2 Fourier Transform Infrared (FTIR)

FTIR, UV, and Visible Spectrometry operate based on interactions between electromagnetic radiation and matter. Selective absorption will happen as an electromagnetic radiation falls upon matter, causing absorption of different amounts of the components of the radiation of different wavelengths. Beer's law describes the basis of quantitative determination:

$$A = \lg \frac{I_o}{I} = \varepsilon \, cl$$

where A is the light absorption (absorbance) of the material being tested, I_o is the light intensity prior to absorption. I is the intensity of light which has passed through and emerges from the solution containing the material to be tested, l is the layer thickness of the solution containing the material to be tested (absorption path length), ε is the molecular absorption coefficient (with the concentration in moles x 1^{-1} and l in cm units), and c is the concentration of the material under test.Transmittance (T) is also used:

$$T = \frac{I_o}{I} \text{ or } T\% = 100\frac{I}{I_o}$$

UV and visible spectroscopic are mainly for quantitative analysis of components present at low concentration levels. Infrared (IR) is more suitable for qualitative analysis. From the electromagnetic spectrum,the infrared region lies between visible and microwave regions, from 14000 cm^{-1} and 4 cm^{-1}. The region of greatest practical use to the chemist lies between 4000 and 400 cm^{-1}. The transitions that generated IR bands are due to molecular vibrations involving bond stretching and bending.[165] Molecular vibrations themselves depend on the nature of the bond. Shorter and stronger bonds (*e.g.* triple and double bonds) stretch at higher energy end (shorter wavelength) of the IR spectrum. No two molecules will have similar molecular vibrations and thus producing same IR spectrum, hence IR spectrum can be said as 'fingerprint' for its own compound. IR is a very useful method to determine the functional group/s available in the sample, including hydroxyl (3600 cm^{-1}), amine (3300-3500 cm^{-1}), nitrile (2250 cm^{-1}), isocyanate (2200-2300 cm^{-1}), and carbonyl group (1630-1850 cm^{-1}).

The IR spectrometer used for IR measurement is the Fourier Transform Infrared (FTIR) Bruker IFS66/S equipped with a tungsten halogen lamp, a CaF_2 beam splitter, liquid nitrogen-cooled InSb detector, and attenuated total reflectance (ATR). Each spectrum in the spectral region of 8000-4000 cm^{-1} was calculated from the coadded interferograms of 12 scans with a resolution of 4 cm^{-1}. For functional group determination, the sample was loaded into the diamond plate of ATR system and the spectrum was recorded. For kinetic studies, ATR was not used. The sample was loaded inside a cuvette (preferably glass) and

capped with rubber septum. The cuvette was then placed inside a heated block and the spectra were recorded continuously. The conversion was determined by following the decrease in the intensity of the vinylic stretching of the monomer at $\upsilon = 6150$.

ATR is a very convenient to use because a) no preparation of potassium or sodium bromide pellet is required b) no preparation of mulls (fine suspension) of solid sample in heavy oil required. The use of potassium bromide pellet is always avoided due to difficulties in obtaining good pellets.[166] In ATR, the IR radiation is passed through an infrared transmitting crystal (diamond) with a high refractive index, causing the radiation to reflect several times within the crystal. During the process, the radiation passes through the material at the depth of few micrometers, producing an absorption spectrum.

3.3 Ultraviolet-Visible (UV-Vis) Spectroscopy

The ultraviolet (UV) and visible spectra are often called ‘electronic spectra’ because the energy absorbed due to electromagnetic radiation causes electronic excitation from low electronic levels to higher ones. UV-Vis spectroscopy is mainly used for quantitative analysis.[167] During the measurement, the light beam is split into half such that one goes through the sample solution and another half goes through the solvent. Thus the absorption from atmosphere in the optical path as well as the solvent is eliminated. Any energy absorption by the sample will cause the intensity of the sample beam (I_S) is lesser than the intensity of the reference beam (I_R) after it has passed through the solvent. Thus, absorption (A) can be derived as:

$$A = \log(I_R / I_S)$$

According to Beer-Lambert’s law, absorbance is proportional to concentration and the path length:

$$A = \varepsilon \times C \times l$$

where ε is molar absorptivity (in M^{-1} cm^{-1}), C is the concentration (in g L^{-1}), and l is the path length through the sample (in cm).[165] There may be one or more absorption peaks in the spectrum but only the maximum absorption (λ_{max}) is reported for the compound.[168] If the values of A and ε are known, the concentration of solvent can be calculated.

Compared to IR, MS, or NMR spectra, UV spectra contains lower information content.[165] Nevertheless, UV-Vis is very useful for analyzing unsaturated compounds. Usually, UV-Vis spectroscopy is used for the determination of solution concentration or structural determination. In this thesis, UV-Vis spectroscopy will be used to determine the cloud point of the polymer solution or its lower critical solution temperature (LCST). The temperature can be plotted against absorption (or transmittance). As the temperature increases, micelles are formed, the solution becomes opaque and therefore causes increase in absorption (or decrease in transmittance). This is plotted in the graph as a sharp drop, taken as the LCST of the polymer.

3.4 Size Exclusion Chromatography (SEC)

Size exclusion chromatography (SEC) is also known as Gel Permeation Chromatography (GPC). It is a powerful technique that is applicable to the analysis of higher-molecular weight species.[164] It is used to measure the average number molecular weight and polydispersity of the polymer in solution. Packing of SEC column consists of small silica or polymer particles with uniformly-sized pores that allow solute and solvent molecules to diffuse through. Molecules larger than the pore size will not be able to reside in the pores and will be eluted out first. Molecules with smaller size than the pore size will permeate in the pore maze and trapped inside for longer periods of time (referred to as the elution time).

SEC columns are made of mobile and stationary phases. The mobile phase is made of a solution consists of polymer solute and a suitable solvent, such as *N,N*-

dimethylacetamide (DMAc), tetrahydrofuran (THF), and water. The selection of the right solvent depends on the types of polymer. The stationary phase must not react with the polymers because this will lead to lower column efficiency. The SEC system is usually calibrated with standards, usually polystyrene of known molecular weight and polydispersity index (PDI).

In this work, an SEC system with *N*,*N*-dimethylacetamide (DMAc) mobile phase was used, unless stated otherwise. A Shimadzu SEC system was used, consisting of an auto-injector, a Polymer Laboratories 5.0 μm bead-size guard column, and a differential refractive index detector. The eluent is DMAc solvent premixed with 0.03 % w/v lithium bromide and 2,6-di-tert-butyl-4-methylphenol (BHT) at 50 ^{o}C with a flow rate of 1 mL min^{-1}. Calibration was done using narrow polystyrene standards ranging from 500 to 10^6 g mol^{-1}. The results are presented as retention time (minutes) versus elution volume (mL). The peak assigned to the shortest retention time represents the highest molecular weight fraction. Computer software is used to analyse the peaks to obtain the number average molecular weight (M_n) and PDI index for the polymer. However, the average molecular weight values obtained are relative values, since the types of polymers tested are different from the polystyrene used for the calibration.

3.5 Dynamic Light Scattering (DLS)

Dynamic light scattering (DLS) is used to study solution dynamics and measuring particle sizes. This technique is capable of measuring particles with diameters of a few nanometers to 5μm.[164] Stokes-Einstein relationship is used to calculate the hydrodynamic particle diameter (d_h) of a spherical particle:

$$d_h = \frac{kT}{3\pi\eta D_T}$$

where

k = Boltzmann's constant

T = absolute temperature
η = viscosity of the medium
D_T = translational diffusion coefficient

In this work, a Malvern Zetasizer Nanoseries Nano ZS particle size analyzer (He-Ne lasers, λ = 632.8 nm, angle = 173°) is used for particle size determination. Samples were removed from dust or foreign particles by means of SEC/GPC micro filter of 0.45μm before analysis and each sample was run at least 3 times. Methanol, deionized water, DMAc, and DMSO were used as solvent and will be mentioned in the respective chapters.

3.6 Mass Spectrometry (MS)

Mass spectroscopy (MS) is very useful to chemists since it can provide information about molecular weight, the presence of specific elements, and the presence of specific functional groups.[168] As an overview, MS involves the ionization of a compound under reduced pressure, the separation of those ions based on their mass/charge ratio (m/z), and the recording of the number of ions as a spectrum.[166]

A compound molecule is bombarded with electrons, causing every molecule to lose an electron to give radical cations called molecular ions (parent ions). These ions are then accelerated through a magnetic field towards a detector. The molecules are separatedut according to their mass and charge. During the bombardment, parent ions also fragmented into smaller ions called daughter ions. A mass spectrum plotted then contains a large number of peaks with varying intensities; the most intense of them all is called the base peak.

In this work, a Thermo Finnigan LCQDECA Ion Trap Mass Spectrometer HPLC system is used. MS is used as support for NMR spectra in confirming the structure of compounds synthesized, such as functionalized β-cyclodextrins. The preparation of sample for MS is

as follows. The compound to be analyzed was dissolved in suitable solvent, such as water : methanol at a 1 : 1 ratio. The concentration used was 1 mg mL^{-1}. The solution was then filtered into SEC glass vial through 0.45 μm filter to remove foreign particles and injected into the mass spectrometer.

3.7 Transmission Electron Microscopy (TEM)

TEM is a microscopy technique whereby an electron beam is firstly illuminated through an ultra thin specimen, followed by interactionwith the specimen and finally scattering. The objective lens will then focus the scattered radiation. The image of convenient size is obtained by changing the aperture. Compared to an optical microscope, TEM has superior resolution due to the usage of electron beam as the light source.[169]

The TEM micrographs were obtained with a JEOL 1400 transmission electron microscope in Chapter 5, 6, and 7. The instrument operates at an accelerating voltage of 100 kV. Samples were negative stained with phosphotungstic acid (2 wt.-%). A Formvar-coated grid was coated by casting a polymer aqueous solution for 1 min. Excess solution was removed using filter paper. For staining, a drop of phosphotungstic acid was gently applied onto the surface of the grid for 30 s. The stained grid was dried under air.

Chapter 4: RAFT Polymerization of Vinyl Methacrylate and Subsequent Conjugation via Enzymatic Thiol-Ene Click Chemistry

Polymerization of vinyl methacrylate (VMA) allows easy access to polymers with pendant double bonds. Polymerization in the presence of 2-cyanopropyl dithiobenzoate as RAFT (reversible addition fragmentation chain transfer) agent led almost exclusively to vinyloxy functional sidegroups, which were available for further reaction. The vinyloxy functionality could not be functionalized using common thiol-ene catalysts, but could be activated using *Candida antarctica* lipase B (CAL-B) (Novozym 435). Reaction between PVMA and various thiols in *N,N*-dimethyl formamide in the presence of CAL-B led exclusively to the formation of the anti-Markovnikov product. The rate of reaction between PVMA and 1-butanethiol was monitored using 1H-NMR. The reaction was complete within 72 hours. Similar results were obtained with other small-sized thiols such as 2-mercaptoethanol, 3-mercaptopropionic acid and 2-(trimethylsilyl)ethanethiol while more bulky thiols such as secondary thiols, thiols with long alkyl chains and sterically demanding thiols such as mono(6-deoxy-6-mercapto)-*β*-cyclodextrin (β-CD-SH) only led to lower conversions.

Note: *The VMA polymerization kinetics study was done by Arlingga Sutinah, an honor student who worked on this for his undergraduate project. Considering the project's integrality, the procedures will still be briefly described as followed.*

4.1 Introduction

Thiol-ene reactions been known for over 100 years and it is simply the hydrothiolation of a carbon double bond with anti-Markovnikov orientation.[170] Compared to the alkyne-azide click reaction, the thiol-ene reaction has the advantages of being metal free, fast and highly efficient.[171] Metal free chemistry simplifies the synthesis (no additional purification steps)[172] and make the process more suitable for biomedical applications due to the absence of a toxic catalyst. Unfortunately, the use of thiol-ene chemistry is often accompanied by thiol odor and thiols can react to multitude of substrates,[173] while the danger of the formation of disulfides is always present.[174] Despite these drawbacks, thiol-ene chemistry has become a valuable tool in macromolecular design, including surface modifications[175] and (bio)organic chemistry.[176]

Thiol-ene chemistry is now a popular tool to build up complex polymer architectures[173, 175-178] or to post-modify polymers with specific functional groups.[179-182] Post modification usually employs polymers with pendant vinyl groups, which are then reacted with various thiols. An alternative strategy was recently reported, which uses polymers with thiolactones as a way to create polymers with a multitude of thiol groups.[183] Postfunctionalization of functional polymers with vinyl groups has the set-back that it introduces an additional, potentially less effective, reaction step.[180, 182] Unfortunately, the direct synthesis of polymers with pendant double bonds using radical polymerization is deemed difficult and crosslinking reactions are common side reactions.[184-186] To suppress cross-linking reactions, two vinyl groups with different reactivities are required, which preferably do not undergo copolymerization. Examples of asymmetric divinyl compounds are 2-vinyloxyethyl methacrylate,[186] allyl methacrylate,[185] 4-(3′-buten-1′-oxy)-2,3,5,6-tetrafluorostyrene,[187-188] and 2-(5-norbornene)methyl methacrylate,[189] which were successfully polymerized via RAFT (reversible addition fragmentation chain transfer) polymerization while gelation was noticeably delayed. A commercially available asymmetric divinyl compound is vinyl methacrylate (VMA). The free radical polymerization of vinyl methacrylate leads to an early onset of gelation

although the reactivity ratio of vinyl acetate (VAc) and methyl methacrylate (MMA) ($r_{MMA} \sim 20$, $r_{VAc} \sim 0.05$) may suggest a high preference for methacrylate during the polymerization.[190] Addition of Lewis acids however was found to suppress crosslinking reactions leading to exclusively linear polymers with vinyl ester side groups.[190] These polymers are usually not the first line of choice as a substrate for thiol-ene reactions. The vinyloxy group is less reactive due to the location of the vinyl group next to oxygen requiring strong catalysts such as boron catalysts to achieve good yields. [191-198] The use of these highly reactive catalysts in a lab environment is undesirable due to the dangers involved.

Enzymes can catalyze a range of reactions. In fact many enzymes show what is called enzymatic promiscuity, which is the ability of enzymes to catalyze many different reactions.[199-202] Especially the synthesis of small molecules has been found to be efficient and often region-selective. Enzymes have also found their way into the synthesis of polymers,[203] but side-group modifications using enzymes have so far only hesitantly been applied.[203-206] Recently, a novel enzymatic thiol-ene click reaction using *Candida antarctica* lipase B (CAL-B) has been reported. The selectivity of the reaction between different thiols and vinyl esters was influenced by the selection of organic media leading to either anti-Markovnikov addition or Markovnikov addition.[207-208]

Encouraged by these findings, post modification of polymers with pendant vinyl esters using enzymes is envisaged. Substrate for the thiol-ene reaction is PVMA. Although the radical polymerization of VMA was reported to be inherently prone to crosslinking, we hypothesized that RAFT polymerization cannot only control the molecular weight, but may also assist in the suppression of crosslinking reactions due to a RAFT agent choice that may preferably undergo addition-fragmentation with the methacrylate group. The ability to undergo enzymatic thiol-ene reaction will be tested using a range of thiols (**Scheme 4.1**).

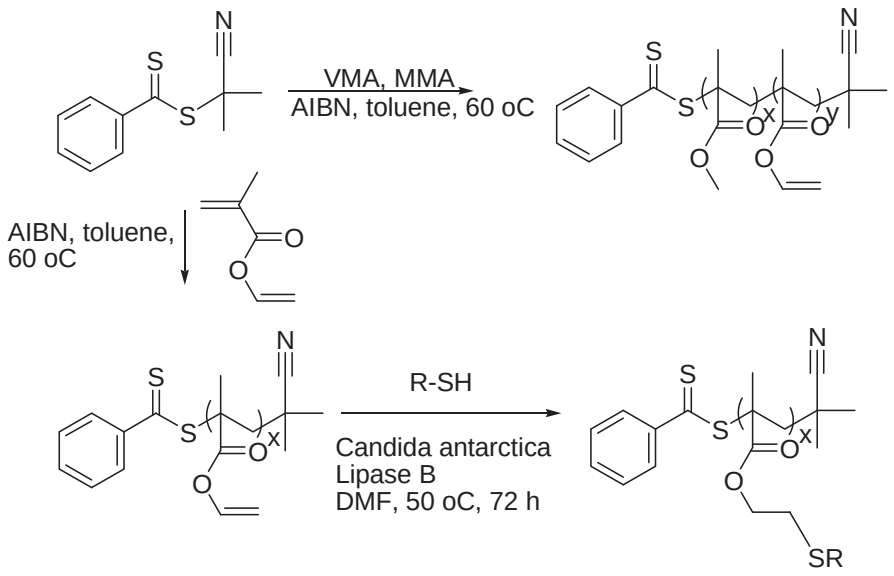

Scheme 4.1 *Syntheses of VMA/MMA copolymer and VMA homopolymer with subsequent enzymatic thiol-ene clicking.*

4.2 Experimental

4.2.1 Materials

The purpled-colored RAFT agent 2-cyanopropyl dithiobenzoate (CPDB) was synthesized according to the procedures described elsewhere.[209] CPDB is a dithiobenzoate which more suitable for polymerizing methacrylates (MMA and VMA). 2,2'-Azobis(2-methylpropionitrile), bis(thiobenzoyl) disulfide, 2,2’-azobisisobutyronitrile (AIBN), methyl methacrylate (MMA), vinyl methacrylate (VMA), 10-undecane-1-ol, 2,2-dimethoxy-2-phenylacetophenone (DMPA), *p*-toluene sulphonyl chloride (PTSC), *β*-cyclodextrin (*β*-CD), trichloroethylene, dimethylphenylphosphine (DMPP), hexylamine (HexAm), were purchased from Sigma-Aldrich. Thiourea, toluene, hydrochloric acid and sodium hydroxide were obtained from Ajax. Novozyme 435 was purchased from Novozymes. Methyl methacrylate (MMA) and vinyl methacrylate (VMA) were diinhibited by passage through basic alumina column prior to polymerization.

Azobisisobutyronitrile (AIBN) was purified by recrystallization twice in methanol while *β*-CD was recrystallized from water. Commercial thiols (1-butanethiol, 1-octanethiol,1-dodecanethiol, 2-aminoethanethiol, 2-mercaptoethanol, 3-mercaptopropionic acid, 11-mercapto-1-undecanol, 2-(trimethylsilyl)ethanethiol, 3,3,4,4,5,5,6,6,7,7,8,8,8-tridecafluorooctane-1-thiol, 2-propanethiol, and 10-undecene-1-ol) were purchased from Sigma-Aldrich. Mono(6-deoxy-6-mercapto)-*β*-cyclodextrin (*β*-CD-SH)[44, 210] were synthesized according to the literature. All solvents used were of analytical grade, except ethyl acetate, *n*-hexane, and methanol. Distilled water from Ultrapure was used throughout this work. All chemicals were used as received unless stated otherwise.

4.2.2 Synthesis of VMA Homopolymer

CPDB (1.98 X 10^{-2} g, 8.95 x 10^{-5} mol) was dissolved in VMA (2.14 mL, 1.996 g, 1.78 x 10^{-2} mol) in a Schlenk tube. The tube was sealed and degassed via four freeze-pump-thawing cycles, and then transferred to the glove box and refilled with nitrogen. Meanwhile, AIBN (2.92 X 10^{-3} g, 1.78 x 10^{-5} mol) was placed in a separate glass vial and transferred into the glove box along with 10 empty glass vials. Toluene (anhydrous, 5.95 mL) was added to solubilize AIBN. The solution was then transferred to the Schlenk tubes containing the mixture of CPDB and VMA. The ratio was [VMA]:[CPDB]:[AIBN] = 1000 : 5 : 1. The solution was distributed amongst the 8 glass vials. The sealed vials were then placed in a preheated oil bath at 60 ^{o}C. Each vial was removed at a pre-set time interval. The polymerizations were stopped by exposing the polymer solution to air and then cooling the solutions. The final polymer was recovered by removing the solvent under vacuum and then purified by redissolving in acetone, followed by precipitation into a cold mixture of methanol and water (80:20). For enzymatic thiol-ene studies, the $PVMA_{62}$ homopolymer was obtained after a polymerization time of 4 h. The polymer for the enzymatic synthesis was thoroughly purified using Soxhlet extraction with methanol.

4.2.3 Synthesis of P(MMA-*s*-VMA) Statistical Copolymers

The statistical copolymers were prepared using a similar procedure as the VMA homopolymerization, but with various ratios between VMA with MMA (total monomer concentration 3M). The molar ratios used for monomers [VMA] : [MMA] were 75 : 25, 50 : 50, 25 : 75, and 10 : 90. The molar ratios between the reaction components: [MMA + VMA]:[CPDB]:[AIBN] = 1000 : 5 : 1.

4.2.4 Synthesis of $PMMA_{70}$ Macro-RAFT Agent

MMA (5.00 mL, 4.67×10^{-2} mol) was placed in a Schlenk tube along with CPDB (1.03×10^{-1} g, 4.68×10^{-4} mol) and AIBN (7.68×10^{-3} g, 4.68×10^{-5} mol) with the ratio used was [MMA]:[CPDB]:[AIBN] = 1000 : 10 : 1. The reagents were dissolved in acetonitrile (9.36 mL) and the Schlenk tube was sealed and subjected to four freeze-pump-thaw cycles. After the last cycle the tube was refilled with dry nitrogen and the Schlenk tube was placed in a preheated oil bath (70 °C) for 16 h. The polymer was collected by precipitation into a cold mixture of methanol and water (75:25) and dried under vacuum. The traces of monomers were removed by Soxhlet extraction for 4 h in methanol to obtain a pink solid of $PMMA_{70}$. (70%, $M_{n(SEC)}$ = 12 000 g mol^{-1}, PDI = 1.09).

4.2.5 Synthesis of $PMMA_{70}$-*b*-P(MMA_{41}-*s*-VMA_{14}) Block Copolymers

The poly$(MMA)_{70}$ macro-RAFT agent (2.00 g, 2.77×10^{-4} mol) was placed in a Schlenk tube along with MMA (5.20 g, 5.55 mL, 5.19×10^{-2} mol), VMA (1.94 g, 2.08 mL, 1.73×10^{-2} mol), and AIBN (4.54×10^{-3} g, 2.77×10^{-5} mol). The ratio used was [MMA + VMA]:[PMMA macro-RAFT]:[AIBN] = 2500 : 10 : 1. The reagents were dissolved in toluene (28.8 mL, for a total concentration of monomer 2.4 M) and subjected to four freeze-pump-thaw cycles. After the last thaw, the flask was refilled with dry nitrogen and the reaction was placed in a pre-heated oil bath at 60 °C. The reaction was allowed to proceed for 15 h before being precipitated into cold methanol. The polymer was collected after centrifugation and drying under vacuum. The traces of monomers were removed by Soxhlet extraction for 4 h in methanol to obtain a pink solid of $PMMA_{70}$-*b*-

P(MMA_{41}-*s*-VMA_{14}). MMA conversion = 22%, VMA conversion = 23%, $M_{n(SEC)}$ = 18 000 g mol^{-1}, PDI = 1.61).

4.2.6 Synthesis of Mono(6-Deoxy-6-Mercapto)-*β*-Cyclodextrin (*β*-CD-SH)

Synthesis of *β*-CD-SH was done in two major steps. For the first step,[211] *β*-CD (30.0 g, 2.65×10^{-2} mol) was suspended in water (200 mL), and sodium hydroxide (3.28 g, 8.20×10^{-2} mol) in water (20 mL) was added drop wise over 6 min. PTSC (5.04 g, 2.65×10^{-2} mol) in acetonitrile (30 mL) was added drop wise over 8 min, causing the immediate formation of a white precipitate. The reaction was stirred for 3 h at room temperature and then filtered to remove the precipitate. The filtrate was put under reduced pressure overnight to remove water slowly, and the resulting colorless precipitate was recovered by filtration and dried in a vacuum oven to yield mono-6-deoxy-6-(*p*-tolylsulfonyl)-*β*-cyclodextrin (*β*-CD-Tos) as a colorless amorphous solid (2.51 g, 1.95×10^{-3} mol, 7.36%). ESI-MS, *m/z* [M+Na] = 1311.42.

For the second step,[210] *β*-CD-Tos (2.00 g, 1.56×10^{-3} mol) and thiourea (2.00 g, 2.64×10^{-2} mol) were dissolved in a mixture of methanol and water (80:20 v/v, 50 mL) and refluxed for 72 h. After this, the solvent was removed under vacuum and the resulting solid was resuspended in methanol (30 mL) and stirred for 1 h at room temperature. The solid was then filtered and dissolved in a sodium hydroxide solution (10 mL, 2.50 M) and stirred for 5 h at 50 °C. The solution was then acidified with hydrochloric acid (1 M) to pH 2, followed by the addition of trichloroethylene (4.8 mL). After stirring overnight, the precipitate was filtered and washed with cold water. Trace trichloroethylene was removed under vacuum and the solid was purified by recrystallization in water yielding an amorphous colorless solid (1.58 g, 1.28×10^{-3} mol, 88.7%). ESI-MS, *m/z* [M+Na] = 1173.69.

4.2.7 Thiol-Ene Click between PMMA-*b*-P(MMA-*s*-VMA) and Mono(6-Deoxy-6-Mercapto)-*β*-Cyclodextrin (*β*-CD-SH) – Michael Addition Approach

In a small glass vial, $PMMA_{70}$-*b*-P(MMA_{41}-*s*-VMA_{14}) (1.00 x 10^{-2} g, 1.09 x 10^{-5} mol) was mixed together with *β*-CD-SH (2.50 x 10^{-2} g, 2.17 x 10^{-5} mol), HexAm (2.86 x 10^{-6} L, 2.17 x 10^{-5} mol), and DMPP (77.0 x 10^{-9} L, 5.43 x 10^{-7} mol) in 40 μL of DMF. The ratio was [VMA in polymer]:[*β*-CD-SH]:[HexAm]:[DMPP] = 1 : 2 : 2 : 0.05. The solution was degassed with nitrogen for 20 min and the highly viscous solution was stirred for 24 h at 20 ^{o}C and the product was dialyzed against water (using a membrane with a 6000-8000 g mol^{-1} cut off) for 5 days with frequent changes of the water. The milky white solution was then freeze-dried for 48 h and subjected for further analysis.

4.2.8 Enzymatic Thiol-Ene Reaction

$PVMA_{62}$ (PDI = 1.36, 10 mg, 2.50 x 10^{-6} mol), Novozyme 435 (20 mg), DMF dried in molecular sieves (0.2 mL), 20 µL of water, and three times mol excess of thiols [1-butanethiol, 1-octanethiol,1-dodecanethiol, 2-aminoethanethiol, 2-mercaptoethanol, 3-mercaptopropionic acid, 11-mercapto-1-undecanol, 2-(trimethylsilyl)ethanethiol, 2-(trimethylsilyl)ethanethiol, (3-mercaptopropyl)triethoxysilane, 2-propanethiol, thiomannose, and mono(6-deoxy-6-mercapto)-*β*-cyclodextrin)] were put in a series of tubes and flame-sealed to prevent the evaporation of low-molecular weight thiols. For 2-aminoetanethiol (cysteamine) and mono(6-deoxy-6-mercapto)-*β*-cyclodextrin), equivalent amount of tris(2-carboxyethyl)phosphine (TCEP) hydrochloride to thiols was added to cleave the disulfide group. The tubes were then immersed in oil bath and shaken at 50 ^{o}C. The samples were taken out after 6, 12, 24, and 72 h. After removal of solvent and volatile reactants under reduced pressure, the obtained solid was redissolved in DMF, filtered to remove Novozyme 435 granules, dialyzed in ethanol for two days, followed by water for another two days. After freeze-drying, the dried solid was dissolved in $CDCl_3$ or DMSO and analyzed using ^{1}H-NMR analyses. Conversion was calculated based on the integration of peaks assigned to the vinylic double bonds at 4.61, 4.90, 7.14 ppm.

4.3 Analysis

4.3.1 NMR Spectroscopy

NMR spectra were recorded using a Bruker 300 MHz spectrometer; samples were analyzed in $CDCl_3$ (1-butanethiol, 1-octanethiol, 1-dodecanethiol, 11-mercapto-1-undecanol, 2-propanethiol, 2-(trimethylsilyl)ethanethiol), C_6D_6 (3,3,4,4,5,5,6,6,7,7,8,8,8-tridecafluorooctane-1-thiol) and d-DMSO (2-mercaptoethanol, 3-mercaptopropionic acid, mono(6-deoxy-6-mercapto)-β-cyclodextrin) at 25 ^{o}C.

4.3.2 Size Exclusion Chromatography (SEC)

Molecular weight distributions of the copolymer systems were determined by means of SEC using a Shimadzu modular system, comprising an auto injector , a Polymer Laboratories (PL) 5.0 μm bead-size guard column (50 x7.5 mm^2), followed by three linear PL columns (10^5, 10^4, 10^3) and a differential-refractive-index detector. The eluent was DMAc (0.05% w/v LiBr, 0.05% 2,6-di-butyl-4-methylphenol) at 50 ^{o}C with a flow rate of 1 mL min^{-1}. The system was calibrated using narrowly dispersed polystyrene standards ranging from 500 to 10^6 g mol^{-1}. The polymer (5 mg) was dissolved in 2 mL DMAc, followed by filtration using a filter with a pore size of 0.45 μm. Poly(2-(3,3,4,4,5,5,6,6,7,7,8,8,8-tridecafluorooctylthio)ethyl methacrylate) synthesized from the reaction between PVMA and 3,3,4,4,5,5,6,6,7,7,8,8,8-tridecafluorooctane-1-thiol was run in THF SEC. For polymer with cyclodextrin pendant groups, the SEC was run in DMac using UV detector.

4.3.3 Electrospray Ionisation Mass Spectrometry (ESI-MS)

Samples were analyzed using a Thermo Finnigan LCQ Deca quadruple ion trap mass spectrometer (Thermo Finnigan, San Jose, CA), equipped with an atmospheric pressure ionisation source operating in the nebuliser assisted electrospray mode and was used in positive ion mode. Mass calibration was performed using caffeine, MRFA and Ultramark

1621 (Aldrich) in the m/z range of 195-1822 Da. All spectra was acquired within the m/z range of 150-2000 Da, and typical instrumental parameters were a spray voltage of 4.5 kV, a capillary voltage of 44 V, a capillary temperature of 275 ^{o}C and flow rate of 5 μL/min. Nitrogen was used as sheath gas (flow: 50% maximum) and helium was used as auxiliary gas (flow: 5% maximum). 30 microscans, with maximum inject time of 10 ms per microscan. For each respective scan, approximately 35 scans were averaged to obtain the final spectrum. The solvent used was a 3:1 mixture of DCM: methanol with sodium acetate concentration of 0.3 μM. Sodium acetate was added to the solvent prior to analyses to ensure ionisation and to suppress potassium salt peaks. All theoretical molecular weights were calculated using the exact mass for the first peak in any given isotopic pattern. The molecular weights of the most abundant isotopes were calculated using the following values: c^{12} = 12.000000; H^{1} = 1.007825; O^{16} = 15.994915; Na^{23} = 22.989768.

4.4 Results and Discussion

4.4.1 VMA Homopolymerisation

Aim of this project was the generation of polymers with vinyloxy functional groups, which are available for subsequent thiol-ene reaction. Vinyloxy pendant groups can be obtained by direct polymerization of VMA, a member of the family of asymmetric diene monomers. Asymmetric diene monomers have generated some interest due to their ability to form networks, but also because of the possibility of ring-formation during the process. Kawai investigated already in the 60’s different asymmetric monomers and found that while many of these monomers crosslink at very low conversions, VMA does not show any noticeable signs of crosslinking up to around 25% conversion (depending on reaction conditions). Reason was the high prevalence of cycle formation that engaged the second vinyl groups (**Scheme 4.2**).[212-213] The amount of pendant vinyl groups in PVMA, which can be used for further reaction, is therefore not only limited by crosslinking, but also by the formation of cycles (**Scheme 4.2**). **Scheme 4.2** summarizes the potential reactions

taking place during the polymerization of VMA. The reactivity ratios of both vinyl groups in VMA were found to be similar to the reactivity ratios of MMA and VAc (r_{MMA} ~ 20, r_{VAc} ~ 0.05).[213] The polymerization of VMA will therefore most likely proceed via the methacrylate group. Free radical polymerization of VMA can lead to crosslinked products at an early stage of the polymerization. In order to achieve control over crosslinking, but also over the molecular weight, VMA was polymerized using RAFT polymerization. The addition of a RAFT agent introduces another step next to the crosslinking and the cyclization reaction as displayed in **Scheme 4.2**.

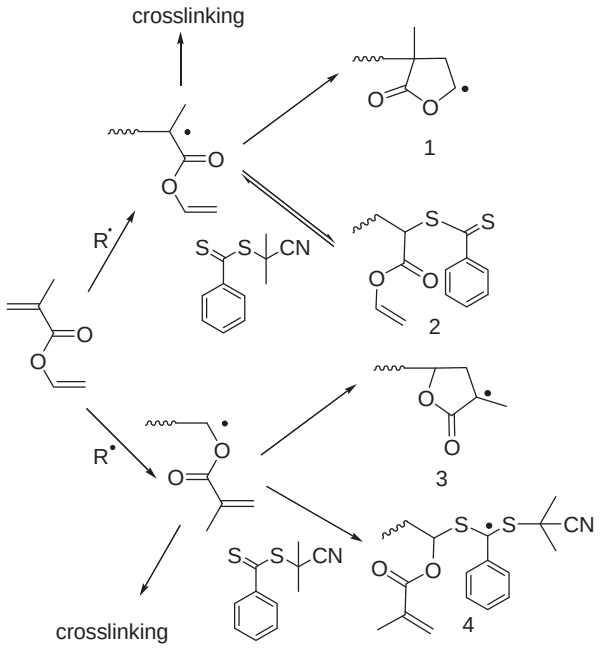

Scheme 4.2 *Formation of cycles during the polymerization of VMA.*

The polymerization of VMA was carried out in toluene at a concentration of 3 mol L^{-1} in the presence of 2-cyanopropyl dithiobenzoate as the controlling agent ([VMA]:[RAFT]= 200:1). Below 20% monomer conversion, the molecular weight distributions were found to monomodal and the PDI ranged well below 2 (**Figure 4.1** and **4.2**). However, once the conversion passed 25%, the formation of high molecular weight products were observed, which became more and more pronounced with increasing conversion (**Figure 4.2**). After 40 hours reaction time at around 40% conversion, the formation of insoluble products was observed. The structure changed from linear polymers to branched or network

polymers, similar to observation by Kamigaito and co-workers.[190] In contrast to free radical polymerization, where gel formation was obtained at 25% conversion, this process was now slightly delayed to conversions of up to 40%. However, the formation of branching was visible already at lower conversions, which was reflected by the PDI exceeding values of well more than 2. Despite the formation of branches, the molecular weight increased with conversion indicating a controlled process (**Figure 4.2**). Even it was a controlled process**;** the branching was well-controlled at lower conversion only. As the conversion increased, the degree of branching started to increase, proven by the multimodal peaks in GPC/SEC results (**Figure 4.2**).

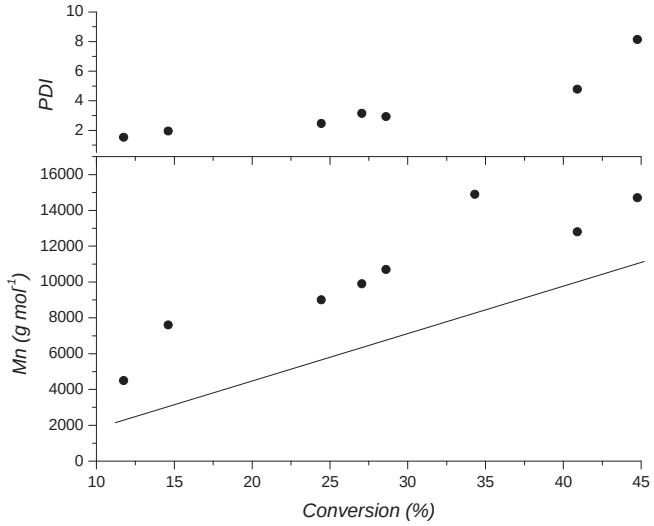

Figure 4.1 *Evolution of M_n vs. the conversion (%) as obtained by SEC of the homopolymerisation of VMA at 60 ^oC in toluene in the presence of RAFT agent CPDB . ([M]= 3 mol L^{-1}, [RAFT groups] = 1.50 x 10^{-2} mol L^{-1},[AIBN] = 2.96 x 10^{-3} mol L^{-1} in toluene. In molecular weight versus conversion graph, the scattered plots correspond to the best fit of the molecular weight evolution, whereas the straight line indicates the theoretical molecular weight development.*

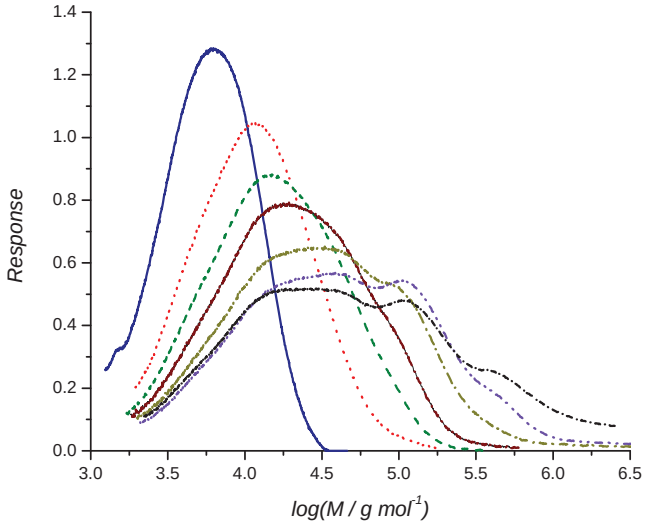

Figure 4.2 *Molecular weight distribution obtained from SEC of the homopolymerisation of VMA at 60 ^{O}C with CPDB RAFT agent. ([M]= 3 mol L^{-1}, [RAFT groups] = 1.50 x 10^{-2} mol L^{-1},[AIBN] = 2.96 x 10^{-3} mol L^{-1} in toluene. The polymerization times of the curves shown are 6, 15, 18, 24, 27, 30, and 45 h, which equates to 12, 15, 27, 28, 34, 41 and 45% monomer conversion.*

$PVMA_{62}$ was thoroughly purified using Soxhlet extraction with methanol. ^{1}H NMR analysis of the product confirmed the presence of the RAFT end group and the vinyl oxy pendant groups at 7.1, 4.9 and 4.6 ppm (**Figure 4.3**). Two very small signals at 5.6 and 6.1 (<2%) revealed the presence of a small amount of methacrylate pendant groups, which are the result of radical addition via the vinyloxy double bond. Comparison of the signal intensity of the methacrylate methyl functionality at around 2 ppm to the vinyl groups does not suggest any ring-formation. The use of ^{13}C NMR, however, was tricky because the signals were too weak and could not be distinguished from the noise. A well adjusted NMR experiments is necessary with sufficient amount of material to make this possible.

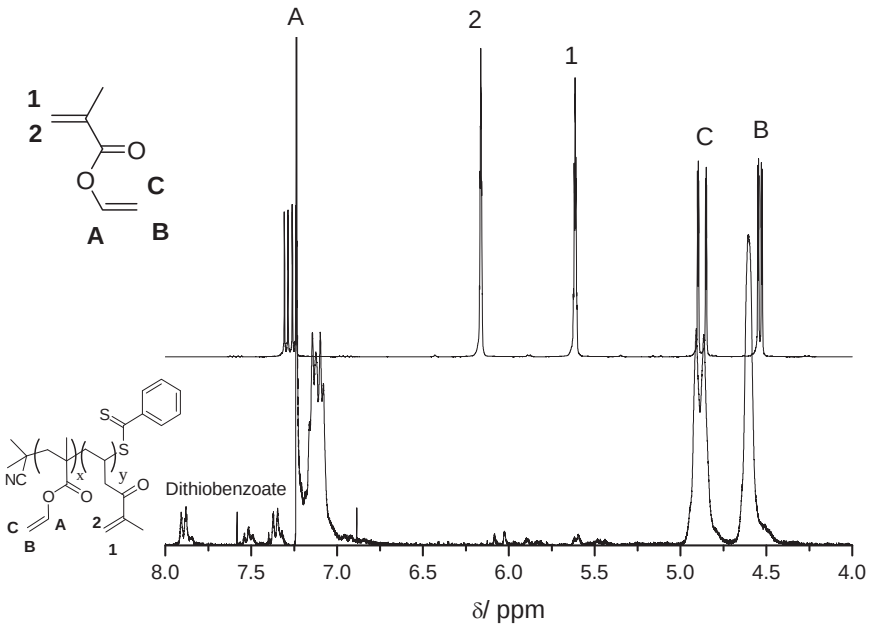

Figure 4.3 *1H-NMR in $CDCl_3$ of the monomer VMA and the polymer PVMA confirms the RAFT end functionality and the presence of vinyloxy groups or more than 98 mol%.*

4.4.2 P(MMA-*s*-VMA) Statistical Copolymerization

In order to delay the onset of gelation, VMA was copolymerized with MMA. Displayed in **Figure 4.4**, the polymerization accelerates with increasing ratio of MMA. This is in contrast to earlier work, where these two monomers were copolymerized via group transfer polymerization,[214] and an increasing rate of polymerization with increasing VMA ratio was measured. The rate retarding effect of VMA may be the result of the presence of the RAFT agent. Although not a frequent event, the polymerization via the vinyloxy group and the subsequent reaction with the RAFT agent will form a stable radical intermediate (Structure 4, **Scheme 4.1**). Fragmentation of this radical may be very slow leading to retardation of the rate of polymerization.[215]

The presence of MMA had in addition a significant effect on viscosity and molecular weight distribution. The viscosity of the solution was in general higher as the amount of VMA increased suggesting a delay in gelation with MMA-rich solutions. Similar to the SEC curves for PVMA, a bimodal molecular weight distribution is clearly visible for longer polymerization times (**Figures 4.5 and 4.6**). Although RAFT polymerization succeeded in preventing cross-linking or branching in the early part of the polymerisations,[185-187, 216] cross-linking or branching still occurred with an increased polymerization time.

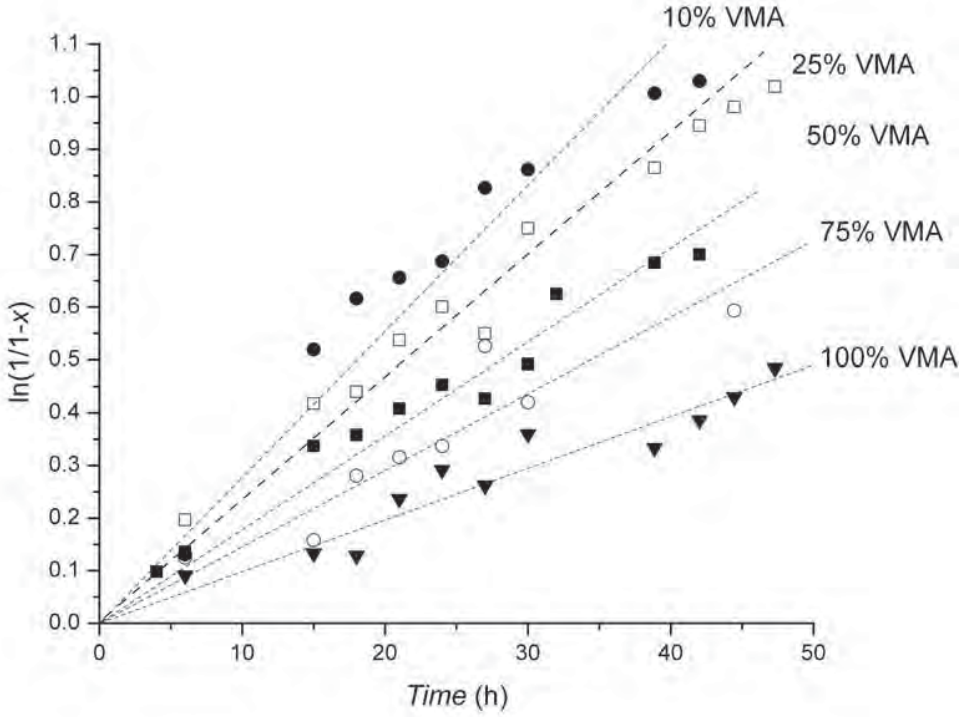

Figure 4.4 *The pseudo first order kinetics of copolymerization with different amount of VMA monomer used; [M]=[VMA+MMA]= 3 mol* L^{-1}

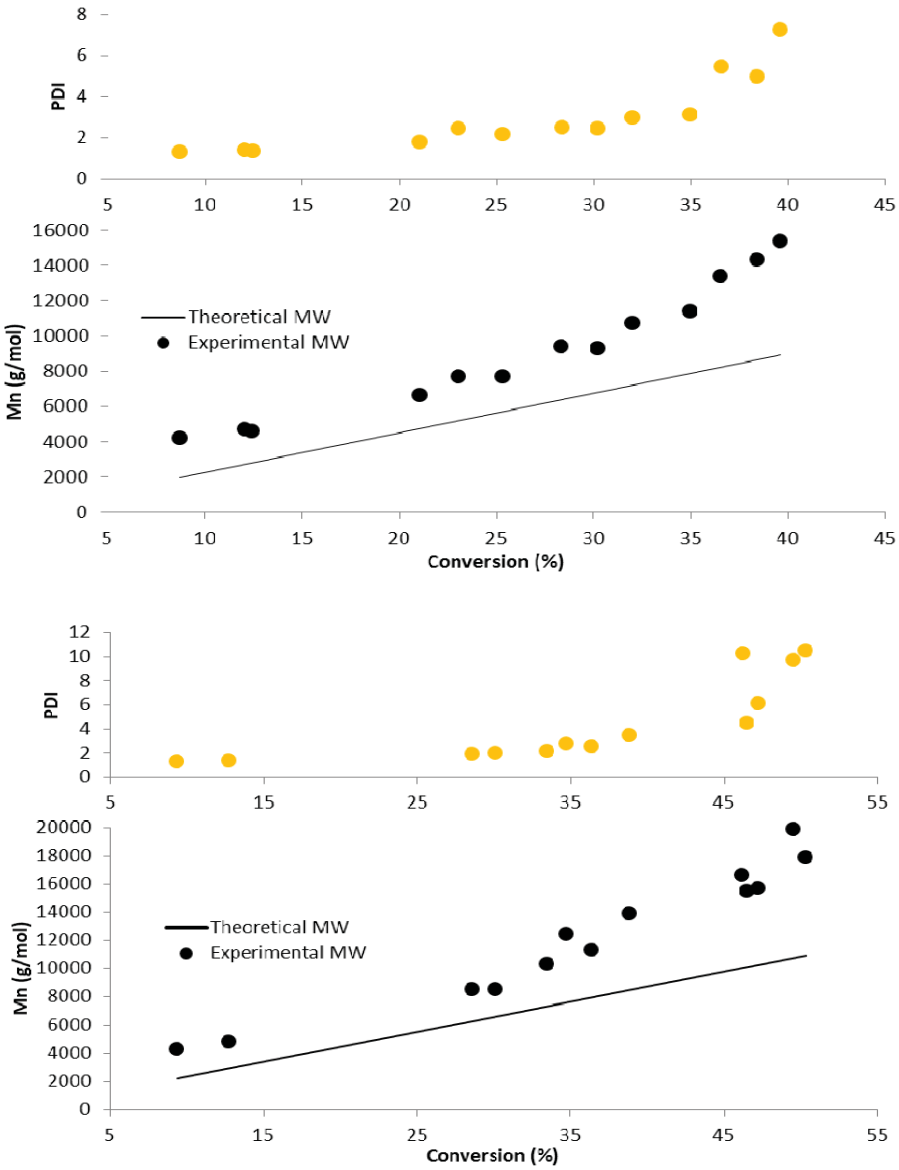

Figure 4.5 (a) *Molecular weight (Mn) and polydispersity indices (PDI) of copolymers [VMA] : [MMA] are (from top to bottom): 75:25 and 50:50.*

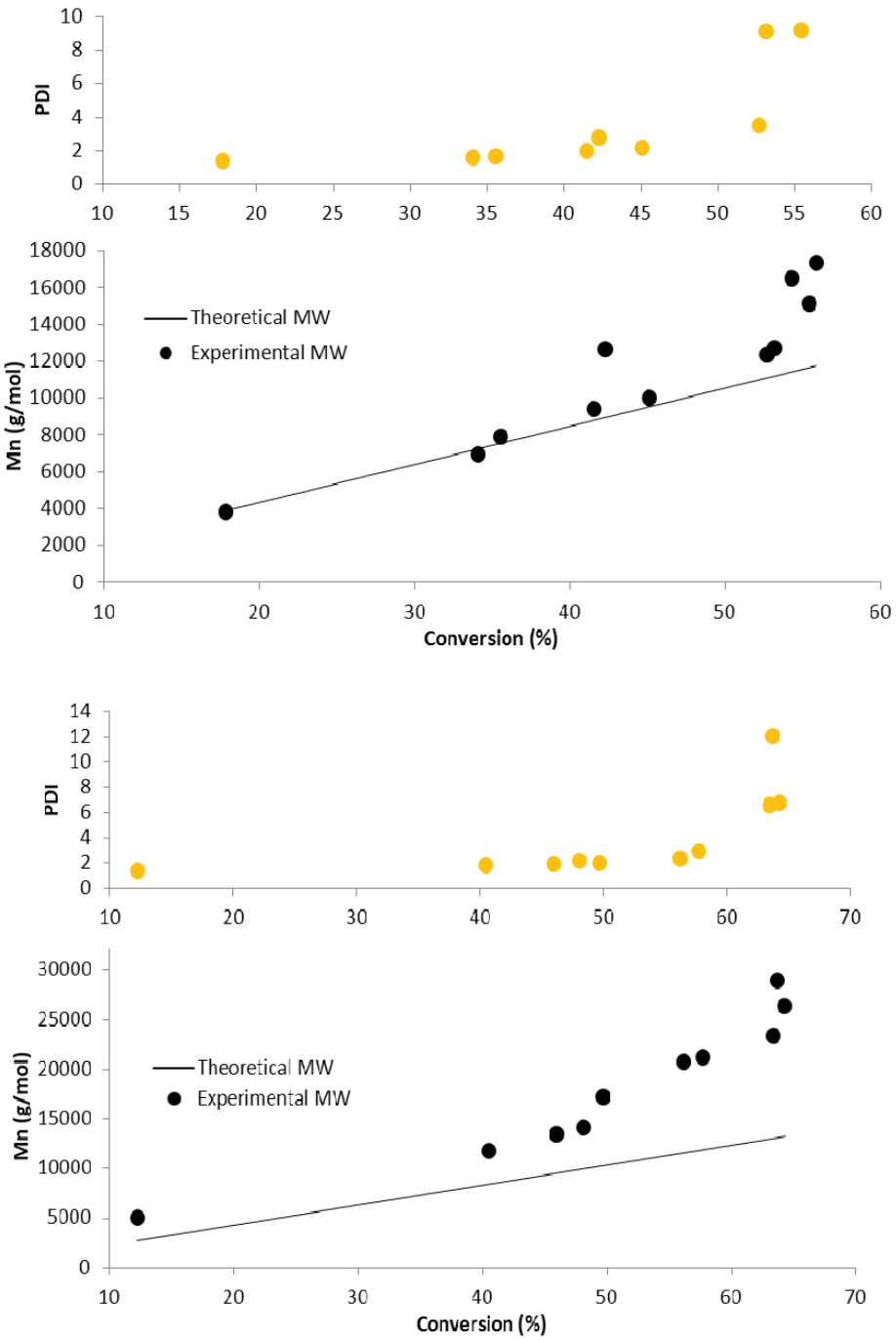

Figure 4.5 (b) *Molecular weight (Mn) and polydispersity indices (PDI) of copolymers [VMA] : [MMA] are (from top to bottom): 25:75 and 10:90.*

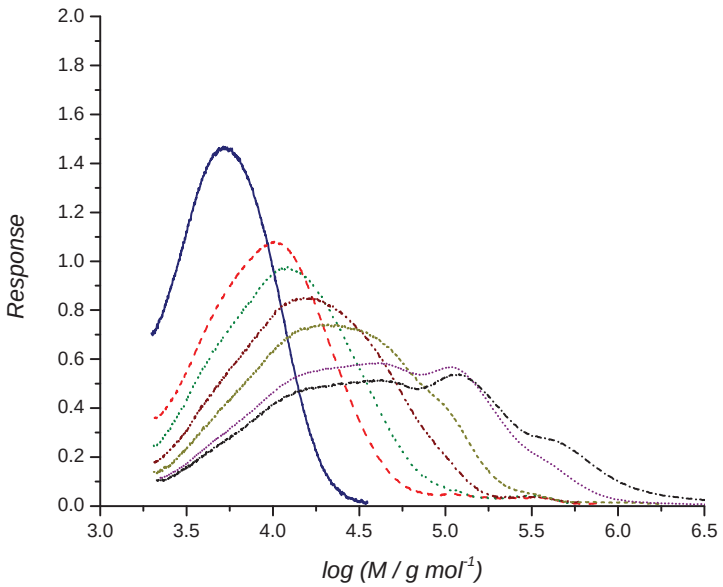

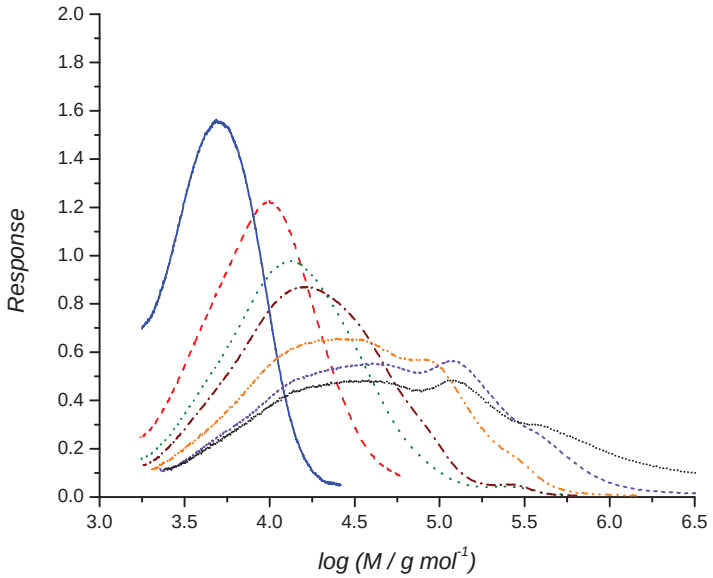

Figure 4.6 (a) *Molecular weight distribution obtained from SEC of the statistical copolymerisation of MMA and VMA at 60 ^{O}C in toluene in the presence of RAFT agent CPDB. ([M]= 3 mol L^{-1}, [RAFT groups] = 1.50 x 10^{-2} mol L^{-1},[AIBN] = 2.96 x 10^{-3} mol L^{-1} in toluene. The mol ratios between [VMA] : [MMA] are (from top to bottom): 75:25 and 50:50. As polymerisation times increased, the cross-linking and branching occurs, shown by bimodal distribution of curves.*

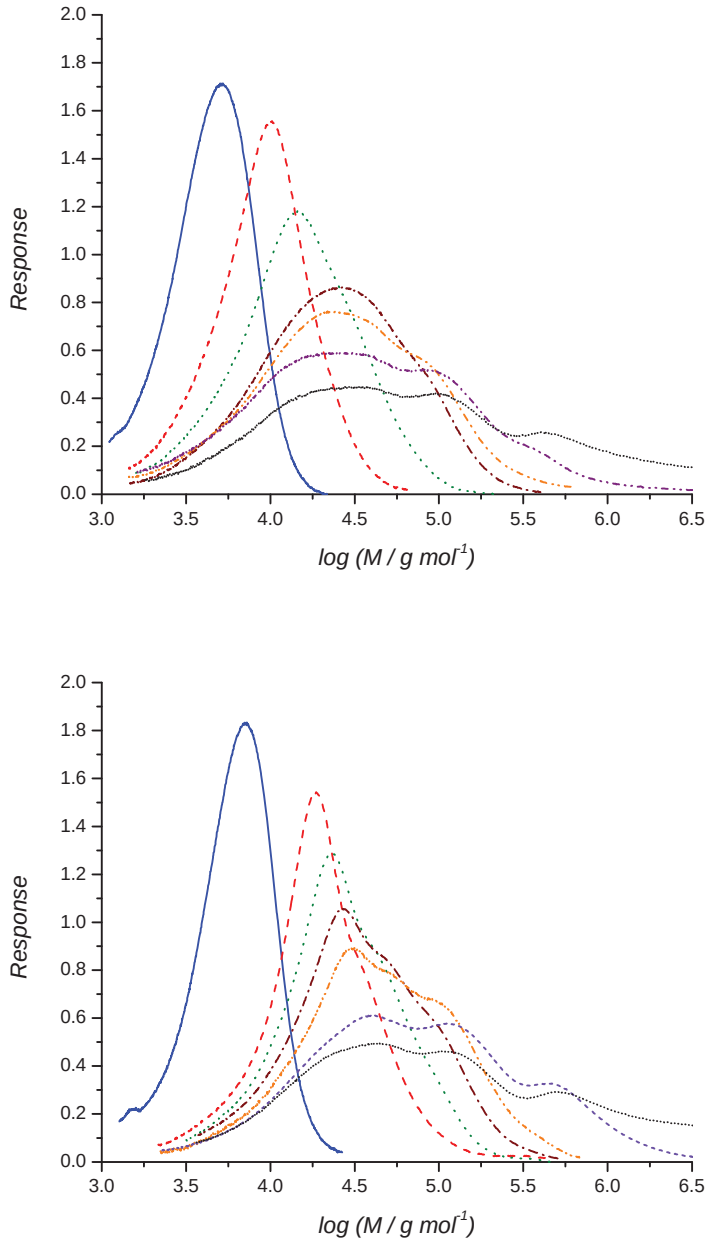

Figure 4.6 (b) *Molecular weight distribution obtained from SEC of the statistical copolymerisation of MMA and VMA at 60 ^{O}C in toluene in the presence of RAFT agent CPDB. ([M]= 3 mol L^{-1}, [RAFT groups] = 1.50 x 10^{-2} mol L^{-1},[AIBN] = 2.96 x 10^{-3} mol L^{-1} in toluene. The mol ratios between [VMA] : [MMA] are (from top to bottom): 25:75 and 10:90. As polymerisation times increased, the cross-linking and branching occurs, shown by bimodal distribution of curves.*

4.4.3 Enzymatic thiol-ene reaction

Conjugation of thiols to the PVMA homo/block polymers by nucleophilic Michael Addition did not work while any attempt to use radical approach to click *β*-CD-SH onto PVMA polymers led to crosslinking (**Figure 4.7**). Recently, it was reported that *Candida antarctica* Lipase B (CAL-B) enzyme was capable of catalyzing the addition of thiols to vinyl esters.[207-208] Depending on the solvent the Markovnikoff (isopropanol) or the anti-Markovnikoff (DMF) products were observed. The yield of the reaction was found to be strongly dependent on the type of solvent and many solvents did promote the reaction at all. Control tests showed that it is indeed the enzyme that is responsible for the selective bond formation between S and C. The rate of reaction was found to have a maximum at 50°C.[207]

Encouraged by these results, a range of thiols were reacted with PVMA in DMF using CAL-B as catalyst. An initial test with1-butylthiol and $PVMA_{62}$ (mol ratio of VMA:1-butylthiol = 1:3) using unpurified DMF directly out of an already opened solvent bottle lead to a yield of 100% after a reaction time of 72 hours. However, the success of this reaction was irreproducible. It was initially thought that the traces of water in DMF/polymer/thiols hampered the enzymatic activity. Dry DMF did not improve the outcome, in contrast, yields as low as 50% were observed. Enzymes require organic solvents to undergo their various catalytic activities, but it has been suggested that a small amount of water is required to keep the enzymes, which are immobilized on beads, active.[217] Addition of a small controlled amount of water to the dry solvent did indeed result again in a high yield.

The rate of the reaction was monitored over a period of 72 hours. Samples were taken different time intervals and the polymers were purified to remove unreacted thiol. The disappearance of the vinyloxy groups in ^{1}H-NMR was clearly visible. Simultaneously, a signal at 4.1 ppm appeared corresponding to methylene group adjacent to the ester functionality. In addition the two methylene groups from the newly formed thioether group emerged (**Figure 4.8**).

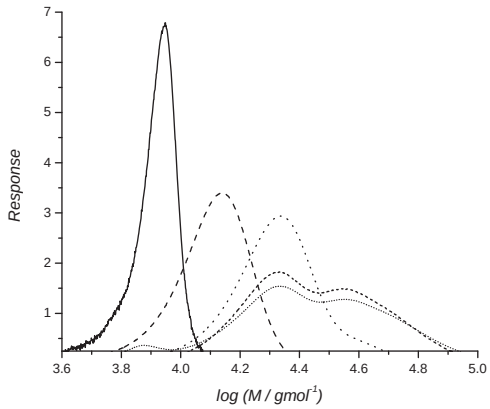

Figure 4.7 *Molecular weight distribution obtained from SEC for (from left to right) β-CD-SH, $PMMA_{70}$ macro-RAFT agent, $PMMA_{70}$-b-P(MMA_{41}-s-VMA_{14}) block copolymer, $PMMA_{70}$-b-P(MMA_{41}-s-VMA_{14}) after thiol-ene click with the presence of AIBN for 48 h, and $PMMA_{70}$-b-P(MMA_{41}-s-VMA_{14}) after thiol-ene click with the presence of 5 times AIBN for 48 h. Bimodal distribution in the curves indicates the formation of cross-linking.*

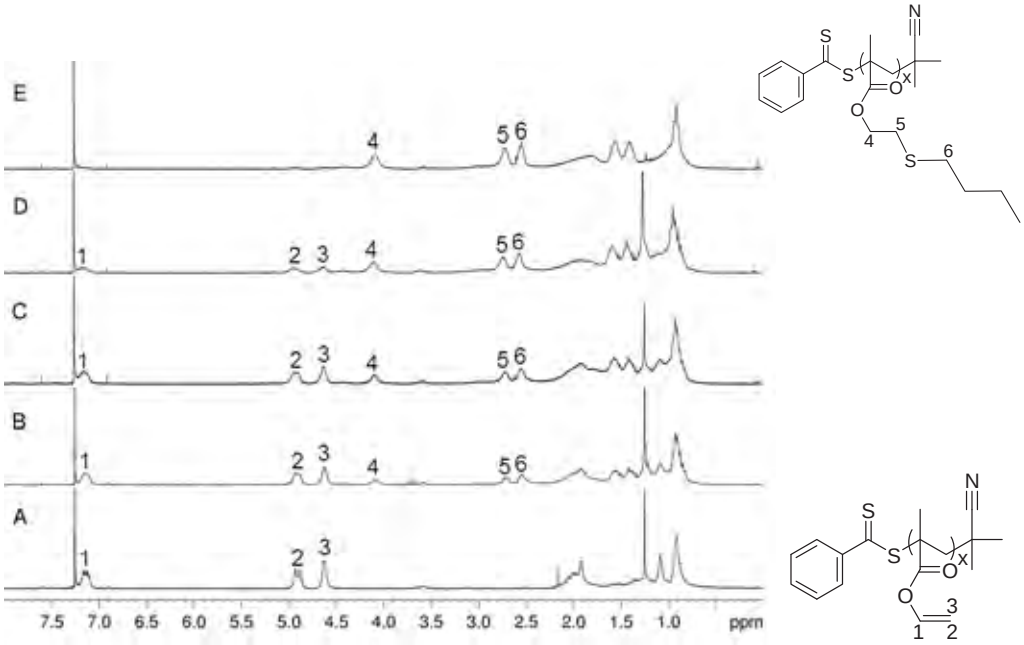

Figure 4.8 *^{1}H-NMR spectra of enzymatic thiol-ene clicking between $PVMA_{62}$ and 1-butanethiol, recorded in $CDCl_3$ after dialysis and freeze-drying. (A) = 0 h, (B) = 6 h, (C) = 12 h, (D) = 24 h, (E) = 72 h. (N.B. – y scale ranges are identical).*

The NMR spectra were integrated and the rate of reaction was quantified. **Figure 4.9** displays the conversion of vinyl oxy groups *vs* time. The SEC traces in addition showed the shift in molecular weight (**Figure 4.10**). What is more important here is that no obvious cross-linking reactions took place. In contrast the molecular weight distribution decreased from a PDI of 1.97 for PVMA to a PDI of 1.57 after the thiol-ene reaction.

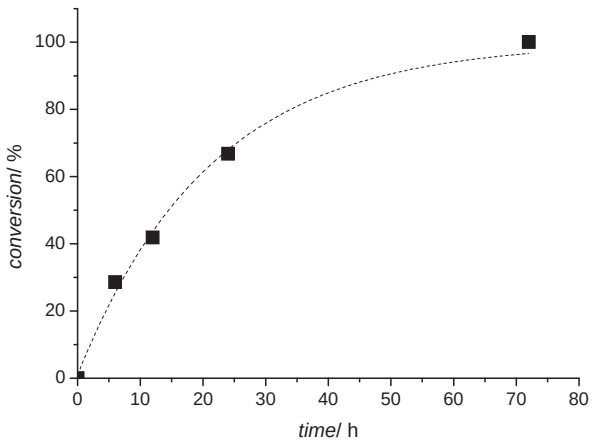

Figure 4.9 *Conversion vs time for the reaction between* $PVMA_{62}$ *and 1-butanethiol in DMF using CAL-B as catalyst.*

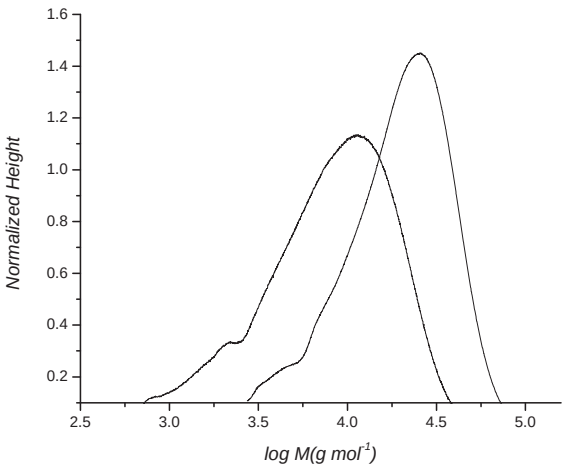

Figure 4.10 *SEC traces of the* $PVMA_{62}$ *before (left) and after (right) enzymatic thiol-ene reaction with 1-butanethiol for 72 h (right).*

A range of other thiols were tested to evaluate the versatility of this approach. In order to comprehend the effect of steric hindrance, a series of thiols were tested ranging from secondary thiols to primary thiols with longer alkane chains. It showed that the steric hindrance played an important role in the clicking efficiency confirming earlier observation.[218] The thiol-ene reaction was completed within 72 hours for 1-butanethiol, a primary thiol (**Figure 4.9**). However, for 2-propanethiol, a secondary thiol, the clicking efficiency dropped below 20% after 72 hours (**Table 4.1**). Also, the conversion is affected by the length of the alkyl chain with the conversion decreasing significantly when the 1-butanethiol is replaced by 1-octanethiol or 1-dodecanethiol (**Figure 4.11**). DMF is a good solvent for both thiol end and the aliphatic end, hence the self-assembly of thiol derivatives can be prevented. However, two polymers, the one with CD and the one with OH, are bigger than expected, which could be the result of aggregation. Potential aggregation of the products can lead to higher than expected molecular weights (**Table 4.1**). A longer reaction time can only improve the conversion to a limited extend since the enzyme will slowly lose its effectiveness. The low activity of the secondary or bulky thiol allows the conclusion that the PVMA as a thiol itself is inactive. Although the RAFT endgroup is present during the reaction, the loss of the RAFT endgroup and the subsequent formation of a thiol as an endfunctionality may be possible. This resulting tertiary thiol is very unlikely to be reactive in such a scenario.

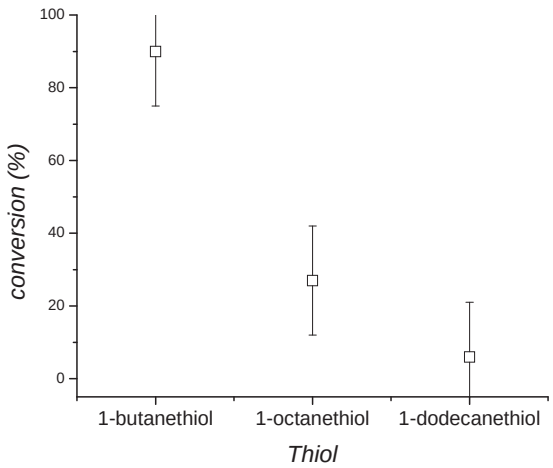

Figure 4.11 *Effect of length of alkyl group of the thiols on the efficiency of the enzymatic thiol-ene reaction.*

Table 4.1 *Summary of reaction between PVMA$_{62}$ and various thiols using CAL-B in DMF for 72 hours at 50°C.*

Thiol	Structure of thiol	conversion (%) ±15%	$M_{n,SEC}$ ($M_{n,theo}$)[a]/ g mol^{-1} After thiol-ene	PDI After thiol-ene
PVMA$_{62}$ before reaction			5800 (6900)	1.97
1.	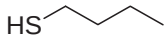	100	15800 (12500)	1.57
2.	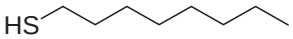	25	7500 (9200)	1.52
3.	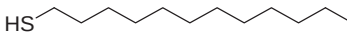	6	5000 (7700)	1.33
4.	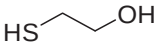	100	21500 (11800)	1.31
5.	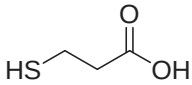	100	11800 (13500)	1.28
6.		5	8437 (7500)	1.25
7.	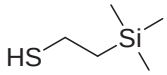	100	12000 (15250)	1.35
8.	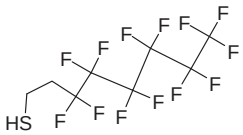	37	59100 (15660)	1.26
9.	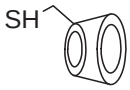	35	18100 (34800)	1.27
10.		19	8000 (7800)	1.50

Thiols: (1) 1-butanethiol, (2) 1-octanethiol, (3) 1-dodecanethiol, (4) 2-mercaptoethanol, (5) 3-mercaptopropionic acid, (6) 11-mercapto-1-undecanol, (7) 2-(trimethylsilyl)ethanethiol, (8) 3,3,4,4,5,5,6,6,7,7,8,8,8-tridecafluorooctane-1-thiol, (9) mono(6-deoxy-6-mercapto)-*β*-cyclodextrin) (*β*-CD-SH), and (10) 2-propanethiol.

[a]The theoretical molecular weight was calculated using $M_{n,theo}$= 62*M_{VMA}+ 61*conversion*M_{thiol}

A range of other thiols was investigated (**Table 4.1**). High conversions were immediately noticeable when the solubilities of the products were tested. Introduction of carboxyl or hydroxyl groups (thiol 4, 5 and 9 in **Table 4.1**) led to polymers that were now soluble in water or ethanol, while the presence of fluorinated side chains or silyl groups (thiol 7 and 8 in **Table 4.1**) led to polymers that are only soluble in chloroform or benzene for NMR analysis. The overall conclusion is that the enzymatic approach is suitable for small molecules while with increasing size of the thiol the conversion of the thiol-ene reaction drops. Small molecules such as 2-mercaptoethanol, 3-mercaptopropionic acid and 2-(trimethylsilyl)ethanethiol can be efficiently reacted while other sterically demanding thiols led only to incomplete reactions. Analysis via ^{1}H-NMR confirmed that only the anti-Markovnikoff product has been formed in all cases evidenced by the presence of the signal of the methyl group adjacent to the ester functionality at around 4 ppm (4 in **Figure 4.12**). The methylene group adjacent to the thiol ether is equivalent in intensity (5 in **Figure 4.12**) indicating that the anti-Markovnikoff was indeed the only product. Depending on the success of the reaction, the molecular weight shifted according to SEC analysis to higher values accompanied by a narrower molecular weight distribution. The polymer with cyclodextrin pendant groups was not visible using a RI-detector and had to be modified with a dye (fluorescein) to be able to carry out the analysis using SEC coupled to an UV/Vis detector. The resulting peak had a bimodal distribution of unknown origin (**Figure 4.13**), which was in contrast to the other products, which had typically monomodal distributions. The measured molecular weights *via* SEC deviate typically from the expected value since the calibration was carried out using polystyrene standards.

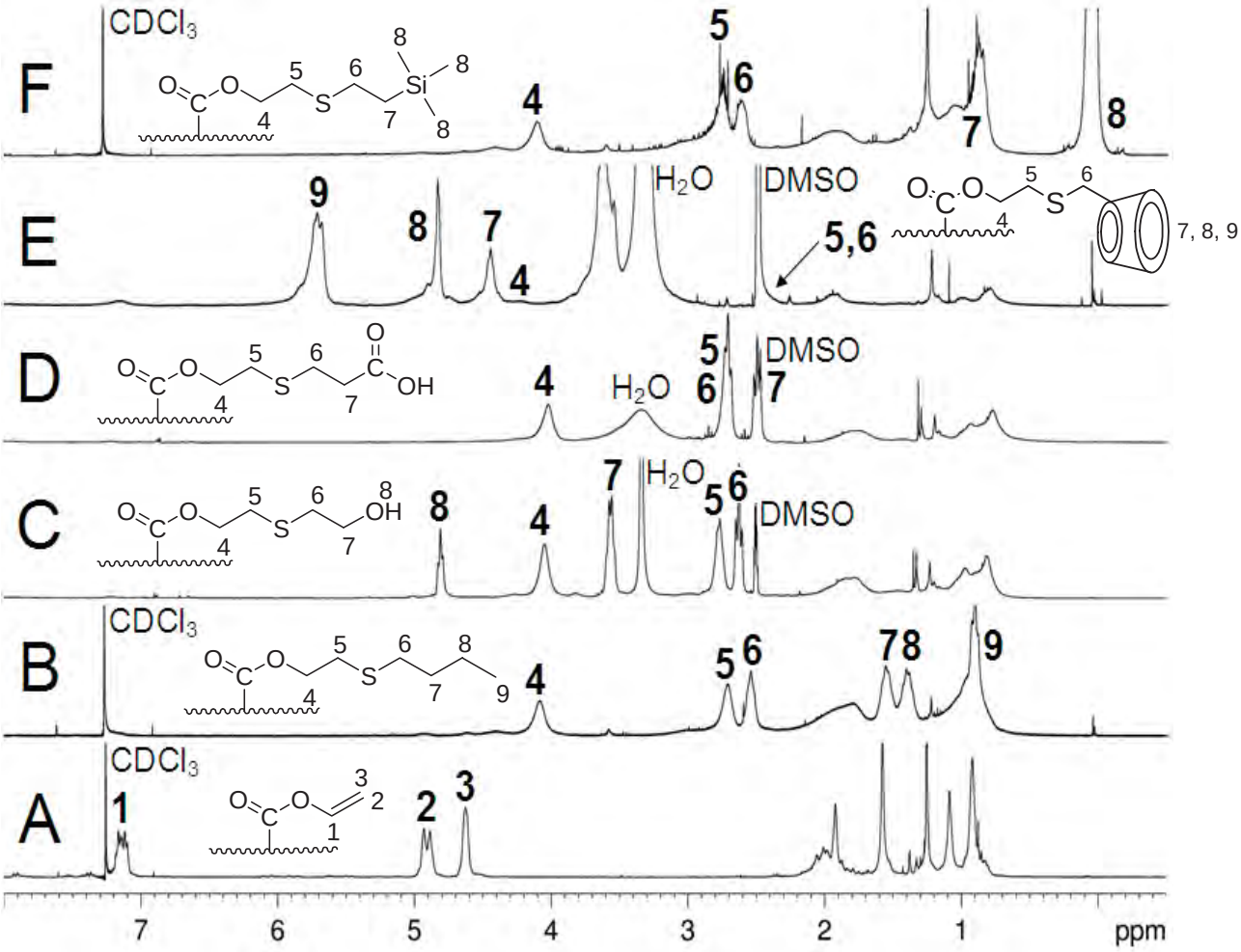

Figure 4.12 *^{1}H NMR spectra for (A) PVMA$_{62}$, (B) PVMA$_{62}$ + 1-butanethiol, (C) PVMA$_{62}$ + 2-mercaptoethanol, (D) PVMA$_{62}$ + 3-mercaptopropionic acid, (E) PVMA$_{62}$ + CD-SH, (F) PVMA$_{62}$ + 2-(trimethylsilyl)ethanethiol. (A), (B), and (F) were run in CDCl$_3$ while (C), (D), and (E) were run in DMSO-d$_6$.*

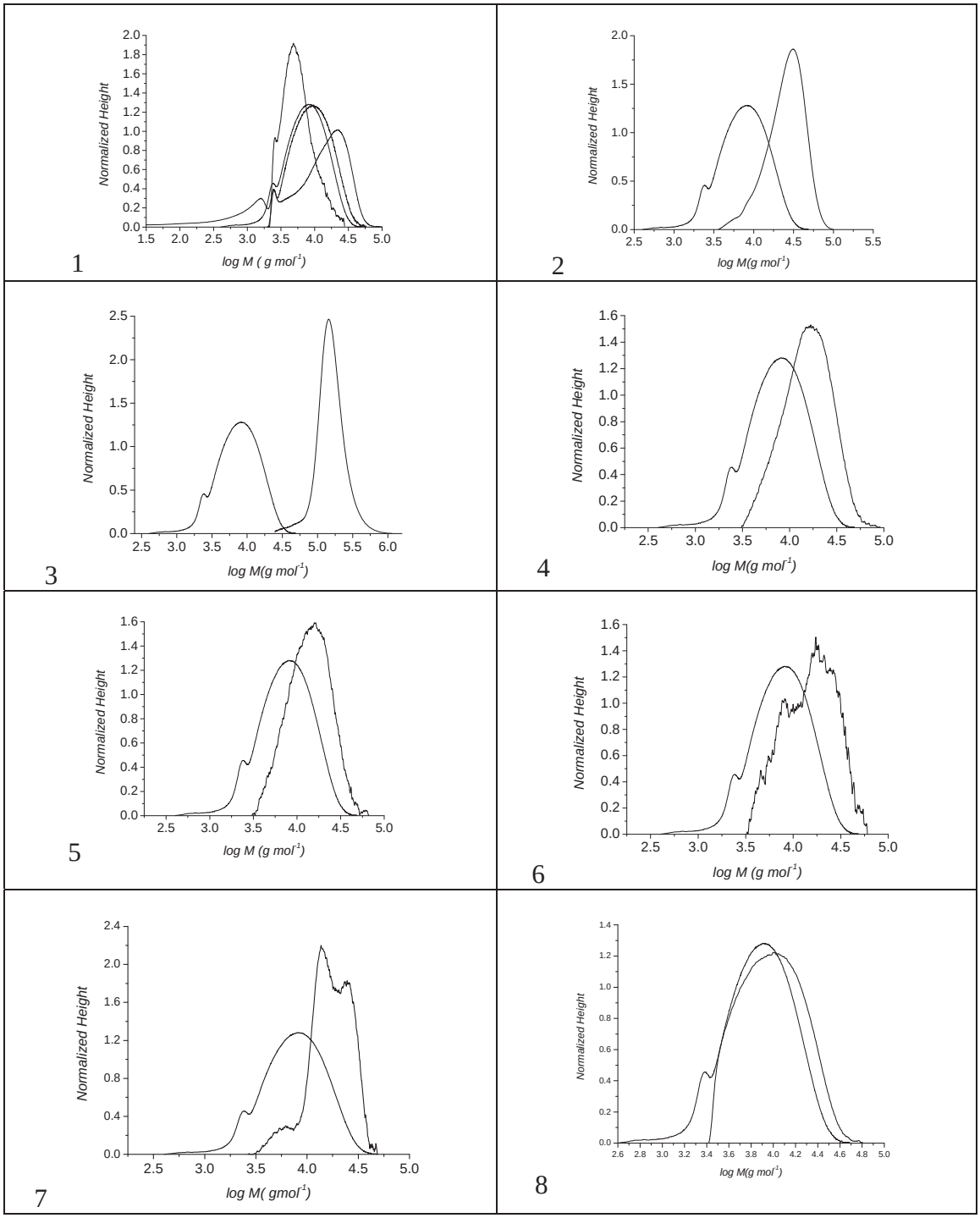

Figure 4.13 *(1) $PVMA_{62}$ and $PVMA_{62}$ after clicking with 1-butanethiol, 1-octanethiol, and 1-dodecanethiol (2) $PVMA_{62}$ + 2-mercaptoethanol, (3) $PVMA_{62}$ + 3-mercaptopropionic acid, (4) $PVMA_{62}$ + 11-mercapto-1-undecanol, (5) $PVMA_{62}$ + 2-(trimethylsilyl)ethanethiol, (6) $PVMA_{62}$ + 3,3,4,4,5,5,6,6,7,7,8,8,8-tridecafluorooctane-1-thiol, (7) $PVMA_{62}$ + β-CD-SH, (8) $PVMA_{62}$ + 2-propanethiol.*

4.5 Conclusion

Polymerization of VMA using the RAFT process led to polymers with vinyloxy pendant groups. The polymerization underwent some crosslinking, which became more pronounced at higher conversions. The vinyloxy pendant groups cannot react via thiol-ene reaction using common catalysts. However, the enzymatic pathway using *Candida antarctica* lipase B as the catalyst allows the reaction between the vinyloxygroup and various thiols at 50 °C. With small primary thiols the reaction is complete after 72 hours while bulky and secondary thiols only lead to very small conversions. The bulkiness of these thiols such as the synthesized β-cyclodextrin thiol restricts the enzyme access to the thiol group, thus rendering it less active for thiol-ene reactions. However, for small thiols enzymatic thiol-ene click chemistry provides a simple and metal-free pathway in constructing novel macromolecular systems. For the next two chapters, azide-alkyne click chemistry is applied for higher clicking efficiency of β-cyclodextrin onto polymers.

Chapter 5: Development of Micellar Novel Drug Carrier Utilizing Temperature-Sensitive Block Copolymers Containing Cyclodextrin Moieties

A drug-delivery system for albendazole (ABZ) based on *β*-cyclodextrin has been synthesized. Well-defined statistical copolymers, composed of *N*-isopropyl acrylamide (NIPAAM) and trimethylsilylpropargyl acrylate (TMSPA), have been prepared by Reversible Addition-Fragmentation Chain Transfer (RAFT) polymerization. The reactivity ratios were determined to be r_{TMSPA}=1.12 and r_{NIPAAM}=0.49, in the absence of RAFT agent, and r_{TMSPA}=1.35 and r_{NIPAAM}=0.35, in the presence of RAFT agent using the average of different techniques. Block copolymers were prepared using $POEGMEA_{40}$ macro-RAFT agent chain extended with NIPAAM and TMSPA of various feed ratios. After deprotection, the polymers were reacted with 6I-azido-6I-deoxy-*β*-cyclodextrin via Huisgen azide-alkyne 1,3-dipolar cycloaddition, resulting in thermo-responsive block copolymers with pendant *β*-cyclodextrin groups, which were then acetylated to modify the polarity and inclusion-complex formation of *β*-cyclodextrin with the drug albendazole (ABZ). Only block copolymers with small amounts of cyclodextrin were observed to have an LCST whilst the copolymers containing higher *β*-cyclodextrin fractions increased the LCST of PNIPAAM beyond measurable temperature ranges. Encapsulation of ABZ increased the LCST. The loading efficiency increased in the polymer *β*-cyclodextrin conjugate compared to native *β*-cyclodextrin with the highest loading observed in the block copolymer after all remaining cyclodextrin hydroxyl groups had been acetylated. While *β*-cyclodextrin is toxic under specific circumstances (e.g. intravenous (IV) injection in large amounts), attachment of a polymer lowered the toxicity to non-toxic levels. The ABZ loaded polymers were all observed to be highly toxic to OVCAR-3 ovarian cancer cell lines with the acetylated polymer showing the highest toxicity.

Note: *The reactivity ratio study was done by Johnny Lim, an honor student who worked on this for his undergraduate project. Considering the project's integrality, the procedures will still be briefly described as followed.*

5.1 Introduction

In order to enhance the aqueous solubility of ABZ and its bioavailability, several strategies have been proposed in the literature. Cylodextrins can be used to help solubilize poorly water soluble species by the formation of 'inclusion complexes' or 'host-guest complexes' **(Figure 5.1)**.[2, 93] Amongst several types of cyclodextrins, used to form inclusion complexes with ABZ, 2-hydroxypropyl-*β*-cyclodextrin was found to be useful in terms of bioavailability and complexation potential.[87, 219] The solubilization of ABZ in cyclodextrin polymers has been found to enhance antiproliferative activity compared to native cyclodextrins alone.[92] Despite the increase in solubility, this technique still required huge amount of cyclodextrins and the inclusion complexes were too small in size for drug delivery systems.

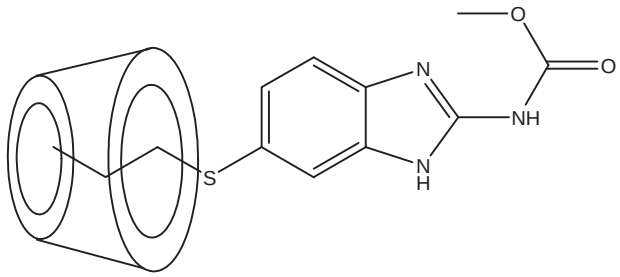

Figure 5.1 *Inclusion complex of ABZ in cyclodextrin. The aliphatic part of ABZ was suggested to be responsible for the formation of the inclusion complex.*[93]

Nanoparticles based on cyclodextrin are widely investigated in order to combine the features of solubility enhancer with the enhanced permeation-retention effect (EPR) of nanoparticles.[36, 39, 220-223] The EPR of nanoparticles allows passive targeting of drugs via the preferred lodgment of nanoparticles in the tumor while the lymphatic system of the

tumor is not capable of clearing the polymer therefore, the drug carrier remains trapped. However, many of these “cyclodextrin polymers” are undefined since they were made by polycondensation of the native cyclodextrins leading to branching and often insoluble networks.[224]

Well-defined polymers with pendant cyclodextrin groups are rarely discussed in the literature, compare to the branched “cyclodextrin polymers”.[224] The synthesis of cyclodextrin polymers using cyclodextrin monomers was first reported by Furue and co-workers in 1975.[10] Although most of the polymers produced were homopolymers,[224] in some cases copolymerisations were examined.[9, 24, 27, 29, 224-226] Alternatively, postfunctionalization of a reactive linear polymer with monofunctional cyclodextrin was investigated.[224] Seo *et al*.[13] were among the first to use the two-step polymer analogous reaction. An efficient route to polymers with pendant cyclodextrin has been developed by Ritter and co-workers using efficient Cu(I) catalyzed alkyne azide Huisgen cycloaddition (click reaction).[223] Despite all the recent advancements in this area, the polymers were typically prepared via free radical polymerization and more complex architectures such as block copolymers are noticeably absent.

RAFT polymerization allows the precise control over the macromolecular architecture with structures such as block copolymers and other complex and elaborate architectures easily accessible through facile reactions.[227-230] Especially the effortless design of amphiphilic block copolymers via RAFT opens the door to new self-assembled structures including micelles, which are attractive nanomaterials for drug delivery.[231-233] Poly(ethylene glycol) (PEG) is the polymer of choice to create the corona of the micelle to enhance circulation time of the drug carrier, although there are some indications that PEG might interact with proteins.[234] The design of the core of the micelle is inspired by the work of Ritter and-coworkers who showed that the LCST of NIPAAM can be influenced by having cyclodextrin as a polymer building block. The changes in the LCST behavior are intrinsically linked to the type of guest.[223, 225] Upon loading of ABZ into β-cyclodextrin and heating of the block copolymer above the LCST of the block copolymer, micelles are expected to form.

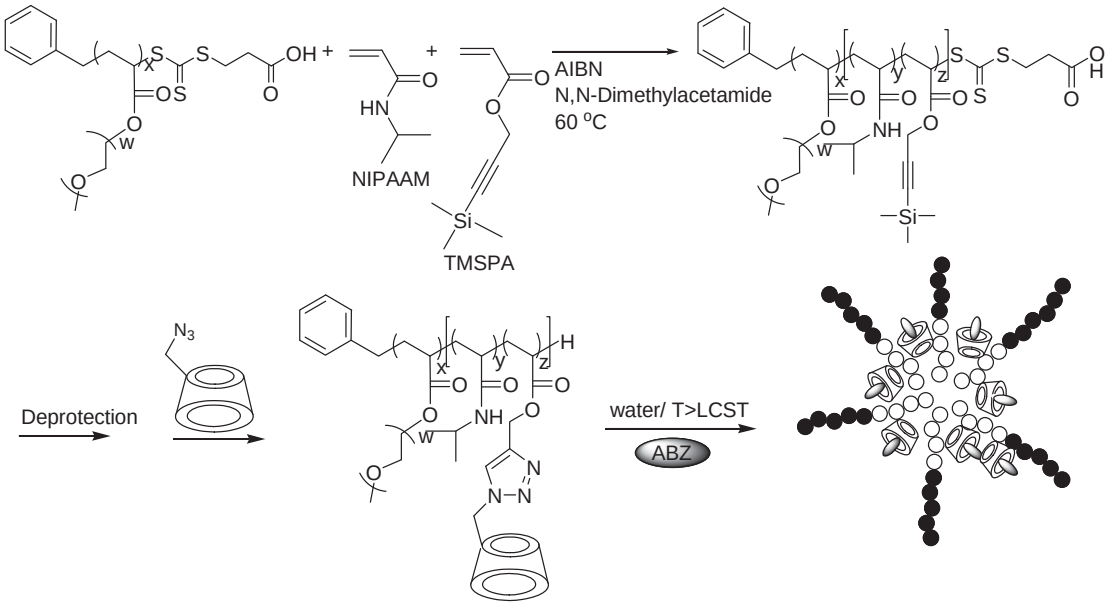

Scheme 5.1 *Schematic approach to thermo-responsive micelles based on block copolymers with pendant β-cyclodextrin.*

5.2 Experimental

5.2.1 Materials

The synthesis of RAFT agent, 3-benzylsulfanylthiocarbonylsulfanyl propionic acid (3-BSPA), is described elsewhere.[235-236] 3-BSPA is a trithiocarbonate more suitable for polymerizing acrylate (TMSPA, OEGMEA) and acrylamide (NIPAAM) respectively. 3-Mercaptopropionic acid, carbon disulphide, benzyl bromide, *N*-isopropyl acrylamide (NIPAAM), propargyl alcohol, acryloyl chloride, oligo(ethylene glycol) methyl ether acrylate (OEGMEA) of M_n ~ 480 g mol^{-1}, chlorotrimethylsilane (CTMS), silver chloride, anhydrous magnesium sulfate, 1,8-diazabicyclo[5.4.0]undec-7-ene (DBU), *p*-toluenesulfonyl chloride (PTSC), sodium azide, tetrabutylammonium fluoride (TBAF), silica gel, sodium azide, ascorbic acid, albendazole, acetic anhydride, pyridine, 4-dimethylaminopyridine (DMAP), *N*,*N'*-dicyclohexylcarbodiimide (DCC), *o*-phenylenediamine (OPDA) and *cis*-diamminedichloroplatinum (II) (cisplatin) were

purchased from Sigma-Aldrich and used as received. 2,2'-azobisisobutyronitrile (AIBN) was purified by recrystallization twice in methanol. Triethylamine was dried using molecular sieves overnight prior to use and *β*-cyclodextrin was recrystallized from water. Only copper sulphate was purchased from BDH. All solvents used were of analytical grade, except acetone and ethanol. Distilled water from Ultrapure was used throughout this work. All chemicals were used as received unless stated otherwise.

5.2.2 Synthesis of the trimethylsilylpropargy acrylate (TMSPA)

The synthesis of TMSPA was done in two-stage process. Propargyl acrylate (2-propynyl propenoate)[237] was synthesized first and later reacted with chlorotrimethylsilane to obtain TMSPA.[238] In the first stage, (8.4217 mL, 0.1032 mol) of acryloyl chloride was added drop wise to a stirred solution of propargyl alcohol (5 mL, 0.0860 mol) and triethylamine (14.38 mL, 0.1032 mol) in dichloromethane (403 mL) at 0 °C. Triethylamine was kept with molecular sieves overnight before being used. The clear solution was then turned yellow. The reaction mixture was allowed to reach room temperature while the color slowly turned to dark. After an overnight, the mixture was quenched with saturated sodium hydrogen carbonate solution. The organic layer was extracted with 10% hydrochloric acid (3 x 30 mL), saturated sodium hydrogen carbonate solution (1 x 30 mL), and water (1 x 30 mL), dried over magnesium sulfate, filtered through neutral alumina, concentrated *in vacuo* to obtain greenish yellow propargyl acrylate (87% yield). In the second stage, (1.5622 g, 0.0109 mol) of silver chloride was suspended in 154 mL of dry dichloromethane. (12.35 mL, 0.1120 mol) of propargyl acrylate and (21.43 mL, 0.1433 mol) of DBU was added to this suspension. A dark red color was observed. The reaction mixture was then heated to 40 °C and chlorotrimethylsilane (21.15 mL, 0.1588 mol) was added drop wise and continued to be stirred for the next 24 hrs. The dark solution obtained was diluted with 400 mL *n*-hexane and the organic phase was washed successively with saturated aqueous sodium hydrogen carbonate, hydrochloric acid (1%) and water, dried over magnesium sulfate, filtered, and concentrated *in vacuo*. The crude product obtained was purified by column chromatography eluting with a 25:1 mixture of

n-hexane and diethyl ether to obtain a colorless trimethylsilylpropargyl acrylate liquid (36.7% yield). R_f = 0.71.

5.2.3 Synthesis of the PNIPAAM and PTMSPA homopolymers

NIPAAM was recrystallized from *n*-hexane and 2,2'-azobisisobutyronitrile (AIBN) was recrystallized twice from methanol. NIPAAM (3.39 g, 3.00×10^{-2} mol) was mixed with RAFT agent (3-BSPA) (32.6 mg, 1.20×10^{-3} mol) inside a Schlenk tube. A stock solution of 1.20×10^{-3} mol L^{-1} of AIBN with *N*,*N*-dimethylacetamide (DMAc) was prepared and 10 mL of this solution was added to the Schlenk tube. The tube was sealed and degassed using 5 freeze-pump-thaw cycle. The polymerization mixture was immersed in an oil bath at 60 ^{o}C for different time intervals. The polymers were analyzed using NMR and SEC analyses to determine monomer conversion and molecular weight, respectively. For the synthesis of PTMSPA homopolymer, TMSPA (5.46 g, 3.00×10^{-2} mol) of was used, but other parameters and conditions were similar as of synthesis of PNIPAAM homopolymer.

5.2.4 Synthesis of the P(NIPAAM-*s*-PTMSPA) statistical copolymers

Statistical copolymers P(NIPAAM-*s*-TMSPA) were prepared similar to the procedures above by varying the feed ratios between NIPAAM and TMSPA monomers. The molar ratios were [NIPAAM]:[TMSPA] = 80:20, [NIPAAM]:[TMSPA] = 90:10, and [NIPAAM]:[SA 95:5]. The total monomer concentration for each copolymer system was kept at 3 mol L^{-1}. For the synthesis of the copolymer with the feed ratio of [NIPAAM]:[TMSPA] = 80:20, NIPAAM (2.71 g, 2.40×10^{-2} mol), TMSPA (1.09 g, 6.00×10^{-3} mol), 3-BSPA RAFT agent (32.0 mg, 1.20×10^{-4} mol), and AIBN (1.97 mg, 1.20×10^{-5} mol) were added to 10 mL of DMAc. After the monomer conversion and molecular weight have been determined, the polymer were purified by dialysis using tubular membranes with a molecular weight cut-off (MWCO) of 3 500 Dalton for 2 days in ethanol to remove TMSPA and 2 days in water to remove NIPAAM. The copolymers were then freeze-dried.

5.2.5 Measuring reactivity ratios of NIPAAM and TMSPA

Two methods were applied to calculate the monomer compositions, using either the unpurified or the purified polymer. Monomer mole fraction was calculated from the undialysed ^{1}H-NMR spectrum of both non-RAFT and RAFT polymerizations by computing the peaks at δ (ppm) -0.5 (s, 9H, C**H**$_3$) and 0.5 (d, 6H, C**H**$_3$) referring to TMSPA and NIPAAM respectively, using the equations

$$f_{TMSPA} = \frac{\frac{I(-0.5)}{9}}{\frac{I(-0.5)}{9} + \frac{I(0.5)}{6}}$$
$$f_{NIPAAM} = 1 - f_{TMSPA}$$

Although the feed ratios should have been known, calculation from the NMR eliminate uncertainties, which are derived from errors occurring during sample preparation. Conversion was obtained by comparing the monomer peak with a corresponding polymer signal according to the equations

$$x_{TMSPA} = 1 - \frac{I(5.1)}{\frac{I(-0.5)}{9}}$$
$$x_{NIPAAM} = 1 - \frac{I(4.7)}{\frac{I(0.5)}{6}}$$

Mole fraction of the polymer could then be determined from the formulae

$$F_{TMSPA} = \frac{f_{TMSPA} \times x_{TMSPA}}{f_{TMSPA}x_{TMSPA} + f_{NIPAAm}x_{NIPAAM}}$$
$$F_{NiPAAm} = \frac{f_{NIPAAM} \times x_{NIPAAM}}{f_{NIPAAM}x_{NIPAAM} + f_{TMSPA}x_{TMSPA}}$$

Results extracted from the unpurified ^{1}H-NMR spectrum were scattered and lacked credibility. However, the polymer mole fractions determined from the dialyzed spectrum assembled into very sensible curves, using the equations

$$F_{TMSPA} = \frac{\frac{I(4.65)}{2}}{\frac{I(4.65)}{2} + I(4)}$$

$$F_{NIPAAM} = 1 - F_{TMSPA}$$

5.2.6 Synthesis of the POEGMEA macro-RAFT agent

In a 100 mL round-bottomed flask, OEGMEA (3.46 g, 7.20 × 10^{-3} mol) was polymerized in toluene (2.4 mL) at 60 ^{o}C in the presence of the RAFT agent 3-BSPA (32.6 mg, 1.20 × 10^{-4} mol) and AIBN (1.97 mg, 1.20 × 10^{-5} mol). The molar ratio used was [OEGMEA]:[RAFT agent 3-BSPA]:[AIBN] = 60:1:0.1. The solution was purged with nitrogen for 45 min. and the polymerization was carried out for 3 h to obtain 44% conversion by NMR. The POEGMEA macro-RAFT agent was purified by dialysis against methanol to obtain a yellow viscous liquid. Theoretical number-average molecular weight calculated using conversion $M_{n\ (theo)}$= 19 200 g mol^{-1}. Size exclusion chromatography (SEC) determined number-average molecular weight $M_{n\ (SEC)}$= 20 600 g $mol^{-1,}$ PDI: 1.23 (polystyrene standards).

5.2.7 Synthesis of POEGMEA-*b*-P(NIPAAM-*s*-TMSPA)] block copolymer

The chain extension was carried out according to the method described for P(NIPAAM-*s*-TMSPA) by replacing 3-BSPA with POEGMEA macro-RAFT agent. The molar ratios [NIPAAM]:[TMSPA] = 80:20, [NIPAAM]:[TMSPA] = 90:10, and [NIPAAM]:[TMSPA]= 95:5 were employed. For ratio of [NIPAAM]:[TMSPA] = 80:20, NIPAAM (2.71 g, 2.40 × 10^{-3} mol), TMSPA (1.09 g, 6.00 × 10^{-3} mol), POEGMEA macro-RAFT agent (2.30 g, 1.20 × 10^{-4} mol), and AIBN (1.97 mg, 1.20 × 10^{-5} mol) were added to 10 mL of DMAc. The samples were then treated as described above. The block copolymers were purified by dialysis in ethanol and then water followed by freeze-drying.

5.2.8 Deprotection of copolymers

The cleavage of the trimethyl silyl protecting group was carried out according to the method by Ladmiral *et. al.*[239] with modifications to the amount of acetic acid and TBAF used and the time taken to complete the reaction. The trimethylsilyl protected polymer (150 mg) and acetic acid (2.0 equiv. mol/mol with respect to the alkyne-trimethylsilyl groups) were dissolved in THF (10 mL). Nitrogen was purged through the solution (*ca.* 20 min) and then cooled to 0 °C. A 1 M solution of tetrabutylammonium fluoride ($TBAF{\cdot}3H_2O$) in THF (2.0 equiv. mol/mol with respect to the alkyne-trimethylsilyl groups) was added slowly via syringe (*ca.* 2-3 min). The resulting turbid mixture was stirred at this temperature for 30 min and then warmed to ambient temperature. The deprotection was complete after 48 h, and the reaction solution was passed through a short silica pad in order to remove excess TBAF and the pad was subsequently washed with additional THF. The resulting solution was then concentrated under reduced pressure, diluted in chloroform, and the polymer was precipitated in petroleum ether 40-60 °C before centrifugation. The copolymer was dissolved in DMAc and dialyzed in dialysis tube 3500 MWCO for 4 days against water, followed by freeze-drying.

5.2.9 Synthesis of 6I-azido-6I-deoxy-*β*-cyclodextrin

β-cyclodextrin was monotosylated before azidification to obtain 6I-azido-6I-deoxy-*β*-cyclodextrin (*β*-CD azide).[240] Recrystallized *β*-cyclodextrin (63.3 g, 5.00×10^{-2} mol) was suspended in 500 mL water and stirred. 5.65 g NaOH was dissolved in 20 mL water and added drop wise into the *β*-cyclodextrin solution. Meanwhile, *p*-toluenesulphonyl chloride (PTSC) (9.50 g, 6.00×10^{-2} mol) was dissolved in 30 mL acetonitrile, and later also added drop wise into the *β*-cyclodextrin solution. A white precipitate was observed immediately. The reaction was run overnight and the white solid was filtered and dried in the vacuum oven at 30 ^{o}C overnight. 4.43 g of mono-6-*p*-toluenesulfonyl-*β*-cyclodextrin was obtained. For the azide formation, dried mono-6-*p*-toluenesulfonyl-*β*-cyclodextrin (4.21 g, 3.26×10^{-3} mol) was reacted with 5 equivalents of sodium azide in 20 mL of anhydrous DMF at 80 ^{o}C overnight. The solution was precipitated in acetone and dried

under vacuum at 30 ^{o}C to obtain 6I-azido-6I-deoxy-*β*-cyclodextrin (*β*-cyclodextrin azide). ^{1}H NMR (d_6-DMSO): δ 6.0-5.90 (14H, OH-2, OH-3), 4.97 (d, 1H, $H1_{I}$), 4.95-4.88 (m, 6H, $H1_{II-VI}$), 4.67-4.53 (m, 6H, OH-6)), 3.90-3.60 (m, 28H, H3, H5, H6), 3.5-3.35 (m, 14H, H4, H2). Yield: 81.0%

5.2.10 Synthesis of adamantyl-terminated RAFT agent

This synthesis was done inside a glove box. Adamantane methanol (1.1 mol) was added together with 4-dimethylaminopyridine (DMAP) (0.2 mol) and RAFT agent 3-BSPA (1 mol) inside a 100 mL round-bottomed flask, before all material was dissolved with 20 mL of anhydrous DCM. 1.2 mol of *N,N'*-dicyclohexylcarbodiimide (DCC) was dissolved in 20 mL of anhydrous DCM in another 50 mL round-bottomed flask and slowly this solution was added into the 100 mL round-bottomed flask. The reaction was stirred for an overnight before the solution was filtered, dried on rotary evaporator, and finally purified by silica column with *n*-hexane : ethyl acetate = 7 : 3 (v/v) to obtain yellow powder of adamantyl-terminated RAFT agent.

5.2.11 Huisgen azide-alkyne 1,3-dipolar cycloaddition model reaction between *β*-cyclodextrin azide and propargyl alcohol

In order to study the feasibility of the reaction of *β*-cyclodextrin azide onto the copolymer, a model reaction was carried out. Propargyl alcohol was reacted with *β*-cyclodextrin azide in DMF. 1.00×10^{-3} mol (5.61 g) of propargyl alcohol and 1.00×10^{-3} mol (1.16 g) of *β*-cyclodextrin azide were dissolved together in 10 mL DMF. The reaction flask was sealed with a rubber septum and the solution was stirred under a nitrogen atmosphere for 24 h at 100 ^{o}C. The product was collected after precipitating the solution into 100 mL of acetone followed by filtration. The liquid phase was dialyzed for 4 days in water and freeze-dried. The dried product was analyzed by ^{1}H-NMR in DMSO-d_6.

5.2.12 Huisgen azide-alkyne 1,3-dipolar cycloaddition reaction between *β*-cyclodextrin azide and polymer

For the reaction of *β*-cyclodextrin azide with various copolymers, two systems were tested: the traditional Huisgen azide-alkyne 1,3-dipolar cycloaddition without catalyst and the Cu(I) catalyzed approach (*click chemistry*), which was carried out according to the method described by Munteanu *et al*.[26] The non-copper system employed similar conditions as the model reaction.

^{1}H NMR (d_6-DMSO): δ 5.73 (OH-3, OH-4), 4.84 (H1), 4.5 (OH-6)), 4.1 (CH_2-N, CO-O-CH_2), 3.8 (CH(CH_3)$_2$,H5, H6), 3.5 (-O-CH_2-CH_2-O, H4, H2), 1.5-2.3 (CH backbone), 1.0 (CH(CH_3)$_2$).

5.2.13 Lower Critical Solution Temperature (LCST) determination

Solution of both albendazole loaded and unloaded copolymers were prepared at the concentration of 1 mg mL^{-1} in water. The solution was filled in a quartz cuvette after passed through 0.45 μm filter to remove the particle impurities. The temperature was increased slowly from 20 to 90 ^{o}C while the change of the average particles diameters vs. temperature was observed. The temperature where particles diameter was drastically increased (cloud point) was taken as the LCST of the copolymers being tested.

5.2.14 Acetylation of copolymer

20 mg of copolymer was mixed together with 1 mL of acetic anhydride, 2 mL of pyridine in a round-bottomed flask and 1 mg of DMAP was added as catalyst. The solution was stirred at 50 ^{o}C for 24 h and dialyzed in dialysis tube 6000-8000 MWCO for 4 days with frequent water changes, followed by freeze-drying for 48 h. ^{1}H NMR (d_6-DMSO): δ 4.8 (H1), 4.1 (CH_2-N, CO-O-CH_2), 3.8 (CH(CH_3)$_2$,H5, H6), 3.5 (-O-CH_2-CH_2-O, H4, H2), 2.1 (CH_3-C=O), 1.5-2.3 (CH backbone), 1.0 (CH(CH_3)$_2$)

5.2.15 Measurement of drug loading efficiency on polymeric micelles

Initially, 20 mg of the *β*-cyclodextrin/copolymer and ABZ (mol ratio of *β*-cyclodextrin moieties:ABZ = 1:1) were dissolved in 4 mL of water and 4 mL of THF (or acetone) separately. Both solutions were then mixed. Water was added slowly and stopped as soon as precipitate started forming. The water addition step is crucial in creating aqueous environment for ABZ, by doing so the ABZ is pushed into the *β*-cyclodextrin cavities, forming the inclusion complexes. Omitting this step would result in zero loading, as proven by ^{1}H-NMR (result not shown). After 24 h of stirring at room temperature, THF was removed by vacuum. The unloaded drug was removed by means of passing the solution through 0.45 μm filter and subsequently the sample was freeze-dried for 48 h. For loading analysis via ^{1}H-NMR, equimolar ratio of adamantane methanol to *β*-cyclodextrin moieties was added, and whole system was dissolved in deuterated DMSO (d-DMSO) with 0.5 microlitre of styrene added as an internal standard. The loading was determined from the vinylic peak of styrene (-C=CH_2, δ = 5.7-6.0) and the ABZ -CH_2-CH_2 peak (δ = 2.8-3.2). The drug loading efficiency (DLE) was calculated according to

$$\text{DLE (\%)} = \frac{\text{amount of ABZ in micelle}}{\text{amount of ABZ added initially}} \times 100$$

5.2.16 In vitro cytotoxicity tests

Human ovarian cancer OVCAR-3 cells were seeded in 96-well plates (3 000 cells per well) with culture medium 10% RPMI-1640 [2 x 10^{-3} M L-glutamine, 1.5 g L^{-1} sodium bicarbonate, 0.010 M of 2-hydroxyethylpiperazinesulfonic acid (HEPES), 4.5 g L^{-1} glucose, 1.00 × 10^{-3} M sodium pyruvate at 37 ^{o}C in 5% CO_2 environment for 24 h. The medium was refreshed with 0.2 mL of a solution consisting of 0.1 mL medium and 0.1 mL of micelle solution of P(NIPAAM$_{116}$-*s*-PA-*β*-cyclodextrin$_{43}$), POEGMEA$_{40}$-*b*-P(NIPAAM$_{150}$-*s*-PA-*β*-cyclodextrin$_{11}$) and acetylated POEGMEA$_{40}$-*b*-P(NIPAAM$_{150}$-*s*-PA-*β*-cyclodextrin$_{11}$) micelles with and without ABZ loading to reach a final micelle concentration of 62.5, 125, 250, and 500 μg ml^{-1}, respectively, followed by incubation at 37 ^{o}C in the incubator for 72 h. Subsequently, the medium was removed and washed 5

times with tap water and 5 times with 1% acetic acid. After drying overnight, 100 μg of 0.010 M Tris (pH = 10.5) was added to solubilize the dye. Absorbance was measured at 570 nm using Σ960 plate reader (Metertech, Taiwan). Non-treated cells were used as controls. The absorbance was measured at 570 nm and the optical density (OD) was used to calculate cell viability [cell viability = (test – blank) / (control – blank) x 100]:

Cell viability (%) = $[(OD_{570,sample} - OD_{570,blank}) / OD_{570,control} - OD_{570,blank})] \times 100$

5.2.17 Self-assembly and thermal properties of micelles

Solution of both ABZ loaded and unloaded copolymers were prepared at the concentration of 1 mg mL^{-1} in water. The solution was filled in a quartz cuvette after passed through 0.45 μm filter to remove the particle impurities. The cuvette was placed in a dynamic light scattering (DLS) particle size analyzer. The temperature was increased slowly from 20 to 80 ^{o}C, with 5 min stabilization period before measurement at each temperature. The change of the average particles diameters or mean count rate vs. temperature was then observed. The temperature where scattering intensity drastically increased (cloud point) was taken as the LCST of the copolymers being tested. Transmission electron microscopy (TEM) was also used to observe the formation of micelles.

5.3 Results and Discussion

5.3.1 NIPAAM and TMSPA (co)homopolymerization

RAFT polymerization was chosen to construct the copolymers due its simplicity and easy control of polymer architecture **(Figure 5.2 and 5.3)**. Concerns about the toxicity of thiocarbonylthio RAFT end group should be dismissed as the deprotection stage and dialysis remove this group irreversibly. Before any block copolymer synthesis as outlined in **Scheme 5.1** was attempted, a detailed study on the RAFT polymerization for the homopolymerization of PNIPAAM and TMSPA and their respective copolymerization

was carried out. *N,N*-dimethylacetamide (DMAc) was chosen as the solvent for the polymerization. It was found that the DMAc dried in magnesium sulphate gave better reproducibility as compared to the DMAc dried in molecular sieves. The polymerization of NIPAAM using 3-BSPA was reported earlier.[241] The co monomer, TMSPA, was homopolymerized using the same RAFT agent resulting in polymers with reasonably low molecular weight distribution, although a hybrid behavior between RAFT and free radical polymerization is observed indicating a sluggish addition of the macro radical too the RAFT agent **(Figure 5.3)**. The copolymerization of NIPAAM and TMSPA was subsequently investigated in detail at various feed ratios (f_{TMSPA}= 5, 10 and 20 %) to establish the distribution of both monomers along the polymer chain **(Scheme 5.2).** In general, the rate of polymerization declined with increasing amounts of TMSPA **(Figure 5.7 and 5.8**). The consumption of both monomers was monitored independently *via* NMR showing a preference for TMSPA in all cases with a typical example displayed in **Figure 5.4** (see as **Table 5.1, Figure 5.5, 5.6, 5.7, and 5.8** for details).

The polymers obtained as a result of the copolymerization were all observed to have PDIs of approximately 1.3. The difference between predicted and experimental molecular weights was very likely due to the SEC calibration using polystyrene standards **(Figure 5.9, Table 5.1). Figure 5.9** display typical molecular weight distributions obtained from statistical polymers P(NIPAAM$_{116}$-*s*-TMSPA$_{43}$), P(NIPAAM$_{84}$-*s*-TMSPA$_{31}$), and P(NIPAAM$_{54}$-*s*-TMSPA$_{19}$), which were generated after a polymerization time of 20 h with molar feed ratios of f_{TMSPA}=0.05, 0.1 and 0.2, respectively **(Table 5.1)**.

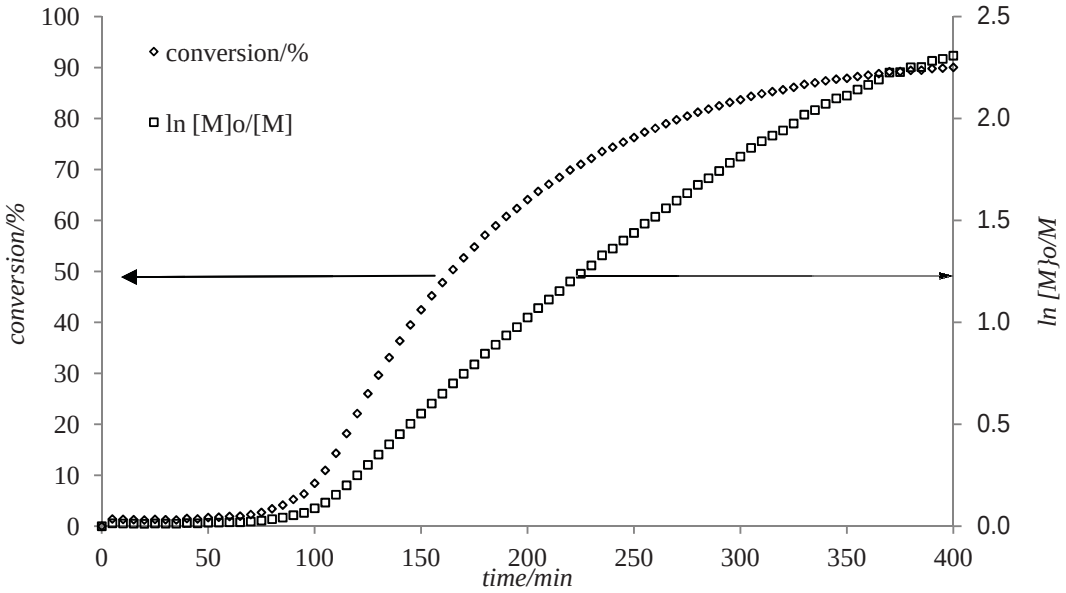

Figure 5.2 *Pseudo-first order kinetic plot and conversion of the homopolymerization of NIPAAM (3.0 mol L^{-1}) in DMAc at 60 ^{o}C vs. time as obtained by real-time FT-NIR. ([AIBN] = 1.2 x 10^{-3} mol L^{-1}, [RAFT agent 3-BSPA] = 1.2 x 10^{-2} mol L^{-1}). Polymerization of TMSPA in similar conditions also shown similar trend; a proof that these 2 monomers undergone living polymerization.*

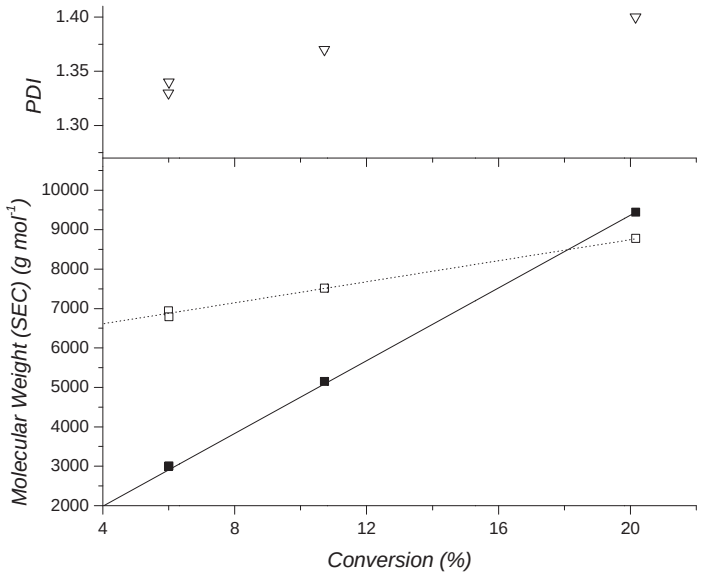

Figure 5.3 *Evolution of M_n vs. the conversion (%) as obtained by SEC of the homopolymerization of TMSPA at 60 ^{o}C in DMAc in the presence of RAFT agent 3-BSPA ([M]= 3 mol L^{-1}, [AIBN] = 1.2 x 10^{-3} mol L^{-1}, [RAFT agent 3-BSPA] = 1.2 x 10^{-2} mol L^{-1}.*

The dotted lines correspond to the best fit of the molecular weight evolution, whereas the straight line indicates the theoretical molecular weight development.

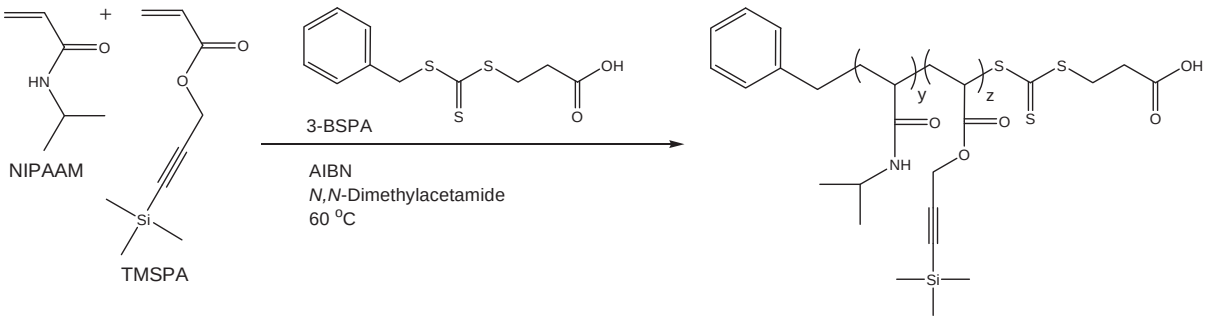

Scheme 5.2 *Reaction scheme of the copolymerization of N-isopropylacrylamide (NIPAAM) and trimethylsilylpropargyl acrylate (TMSPA) at 60 °C in DMAc in the presence of RAFT agent 3-benzylsulfanylthiocarbonylsulfanylpropionic acid (3-BSPA) to obtain [P(NIPAAM-s-TMSPA)].*

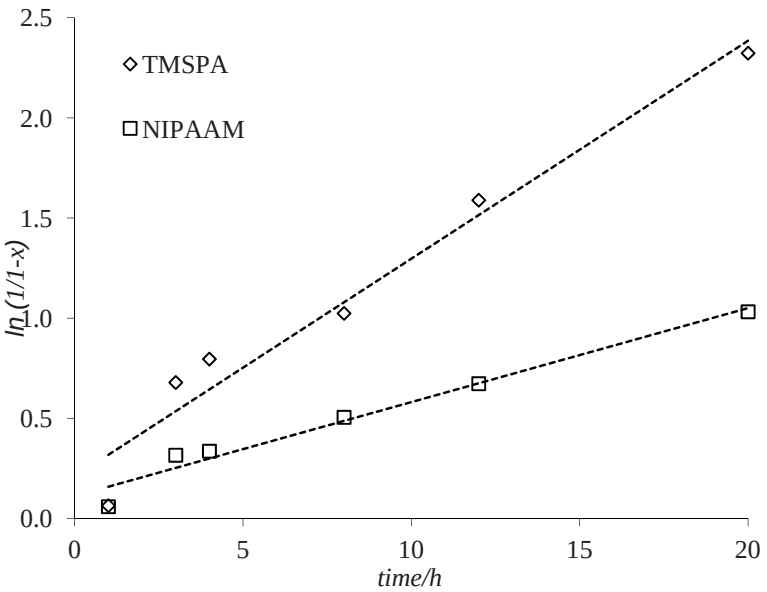

Figure 5.4 *Pseudo-first order kinetic plot of the polymerization of TMSPA and NIPAAM of P(NIPAAM-s-TMSPA) at 60 °C in DMAc in the presence of RAFT agent 3-BSPA ([AIBN] = 1.2 x 10^{-3} mol L^{-1}, [RAFT agent 3-BSPA] = 1.2 x 10^{-2} mol L^{-1}) vs. time for ratio of TMSPA/NIPAAM 5/95. TMSPA and NIPAAM with different ratios (10/90 and 20/80) also behaved similarly in similar polymerization conditions.*

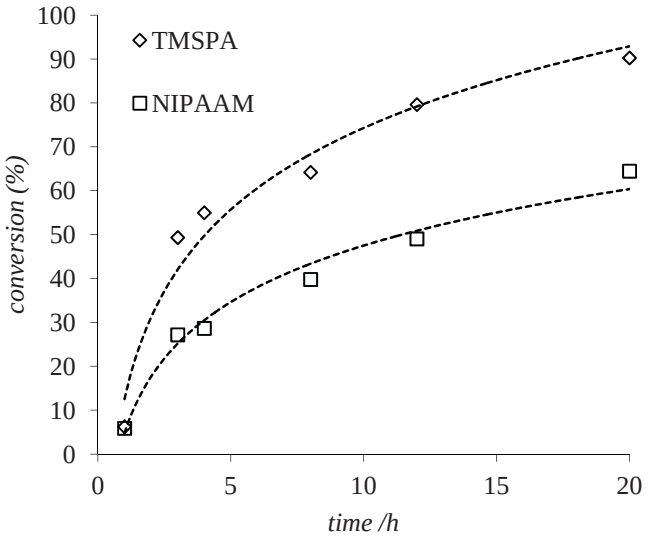

Figure 5.5 *Conversion of the polymerization of TMSPA and NIPAAM of P(NIPAAM-s-TMSPA) at 60 ^{o}C in DMAc in the presence of RAFT agent 3-BSPA ([AIBN] = 1.2 x 10^{-3} mol L^{-1}, [RAFT agent 3-BSPA] = 1.2 x 10^{-2} mol L^{-1}) vs. time for ratio of TMSPA/NIPAAM 5/95.*

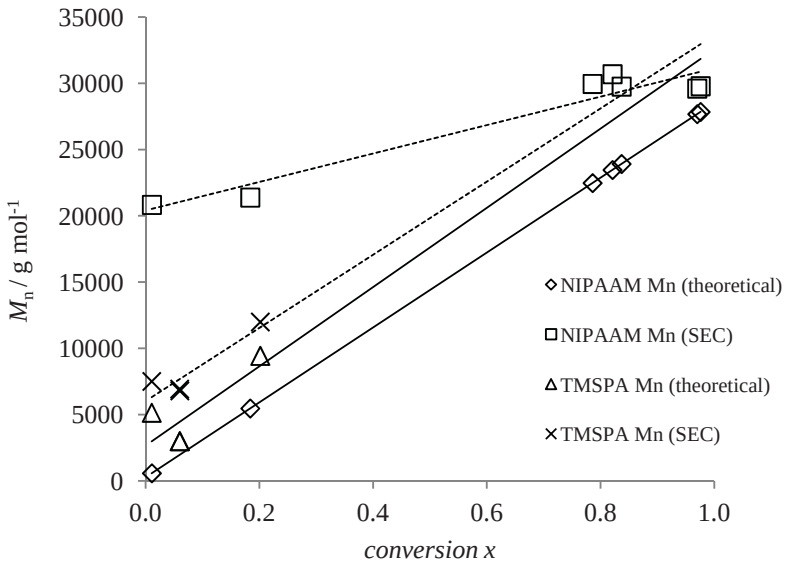

Figure 5.6 *Evolution of M_n vs. the conversion (x) as obtained by SEC of the homopolymerization of NIPAAM and TMSPA in the presence of RAFT agent at 60 ^{o}C in DMAc in the presence of RAFT agent 3-BSPA ([AIBN] = 1.2 x 10^{-3} mol L^{-1}, [RAFT agent 3-BSPA] = 1.2 x 10^{-2} mol L^{-1}. The dotted lines correspond to the best fit of the molecular weight evolution, whereas the straight line indicates the theoretical molecular weight development.*

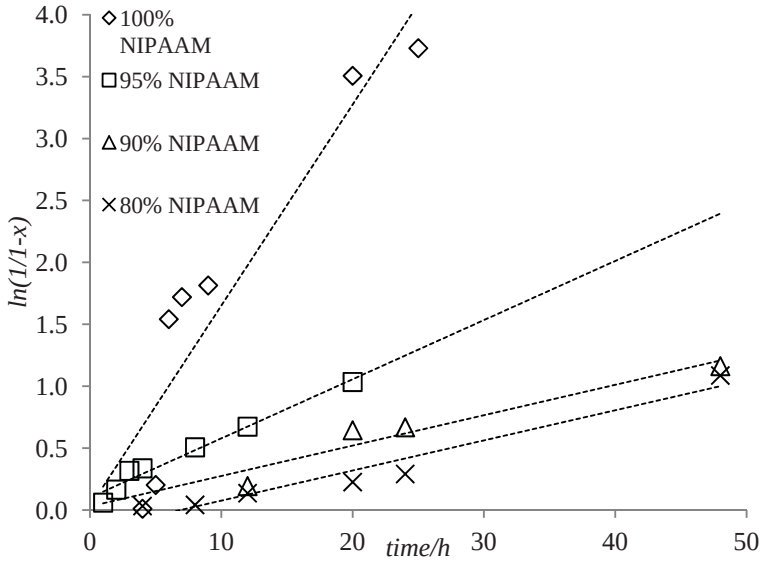

Figure 5.7 *Pseudo-first order kinetic plot of the polymerization of NIPAAM in the P(NIPAAM-s-TMSPA) at 60 ^{o}C in DMAc in the presence of RAFT agent 3-BSPA ([AIBN] = 1.2 x 10^{-3} mol L^{-1}, [RAFT agent 3-BSPA] = 1.2 x 10^{-2} mol L^{-1}). The increase of the amount of TMSPA in the formulation was found to slow down the polymerization.*

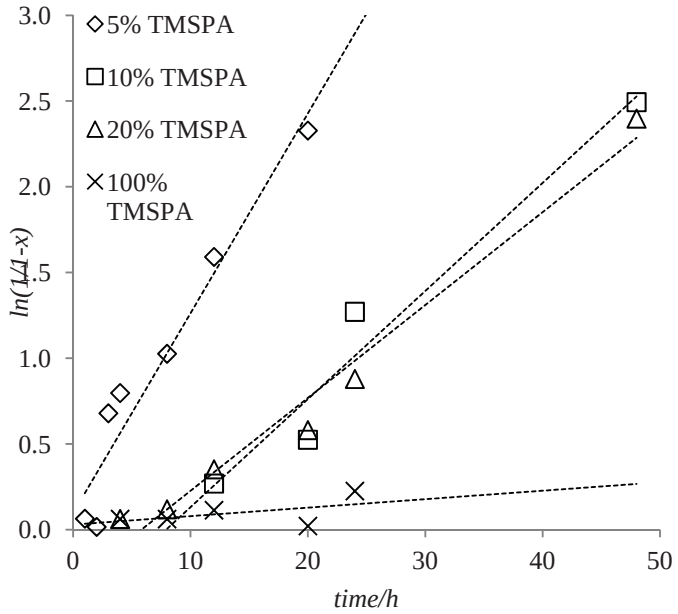

Figure 5.8 *Pseudo-first order kinetic plot of the polymerization of TMSPA in the P(NIPAAM-s-TMSPA) at 60 ^{o}C in DMAc in the presence of RAFT agent 3-BSPA ([AIBN] = 1.2 x 10^{-3} mol L^{-1}, [RAFT agent 3-BSPA] = 1.2 x 10^{-2} mol L^{-1}). The increase of the amount of TMSPA in the formulation was found to slow down the polymerization.*

Table 5.1 *Characteristics of homopolymers and random copolymers, after 20 hrs of reaction.*

Homopolymer/ Random copolymer	Conversion (%)		Molecular weight		PDI	Physical condition
	NIPAAM	SA	$M_{n\ (theo)}$	$M_{n\ (exp)}$		
NIPAAM/TMSPA 0/100	–	16.18	7634	8700	1.44	Viscous liquid
NIPAAM/TMSPA 80/20	27.62	38.46	10014	16000	1.31	Solid
NIPAAM/TMSPA 90/10	42.68	62.50	13967	21000	1.28	Solid
NIPAAM/TMSPA 95/05	58.36	86.21	17794	28000	1.28	Solid
NIPAAM/TMSPA 100/0	97.00	–	27674	29600	1.35	Solid

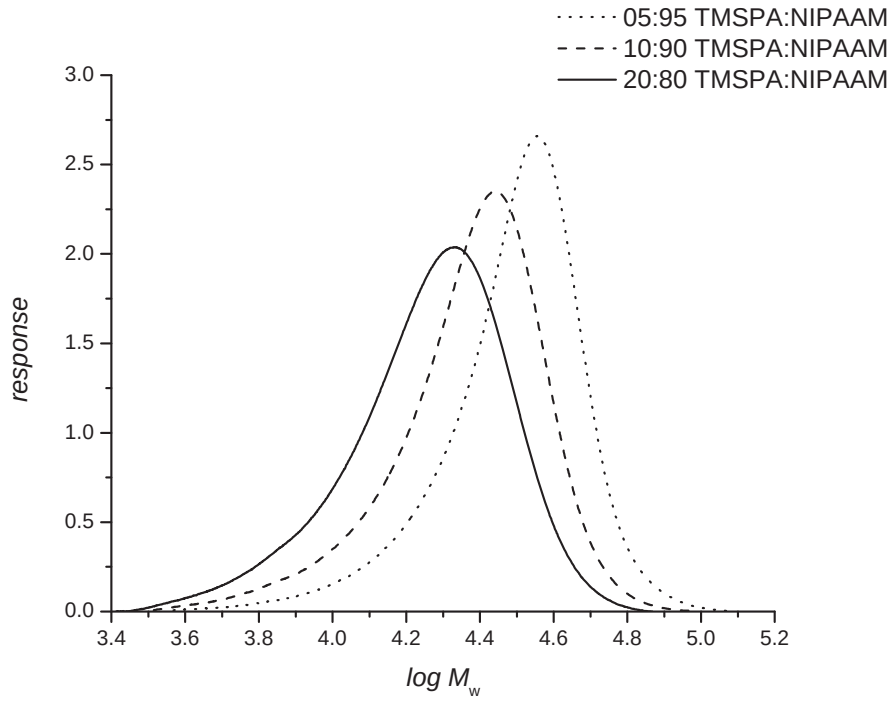

Figure 5.9 *SEC traces of RAFT copolymerization of NIPAAM and TMSPA at 60 ^{O}C. ([RAFT groups]) = 1.20 x 10^{-2} mol L^{-1},[AIBN] = 1.20 x10^{-3} mol L^{-1} in DMAc. As the TMSPA continuously replaced by NIPAAM, the peak shifted to the higher molecular weight (to the right).*

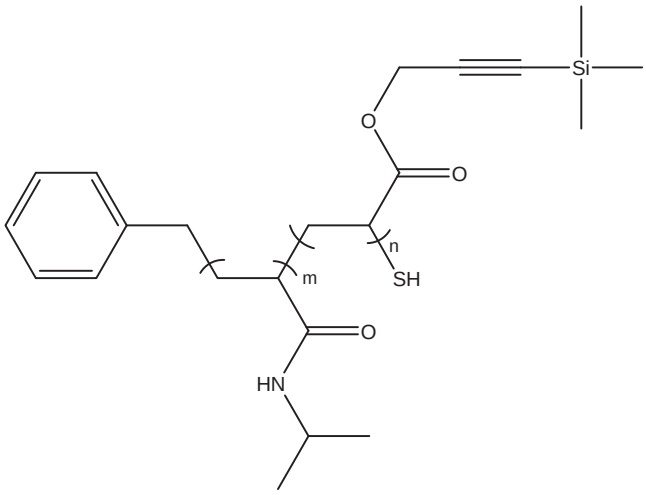

P(NIPAAM-*s*-TMSPA)

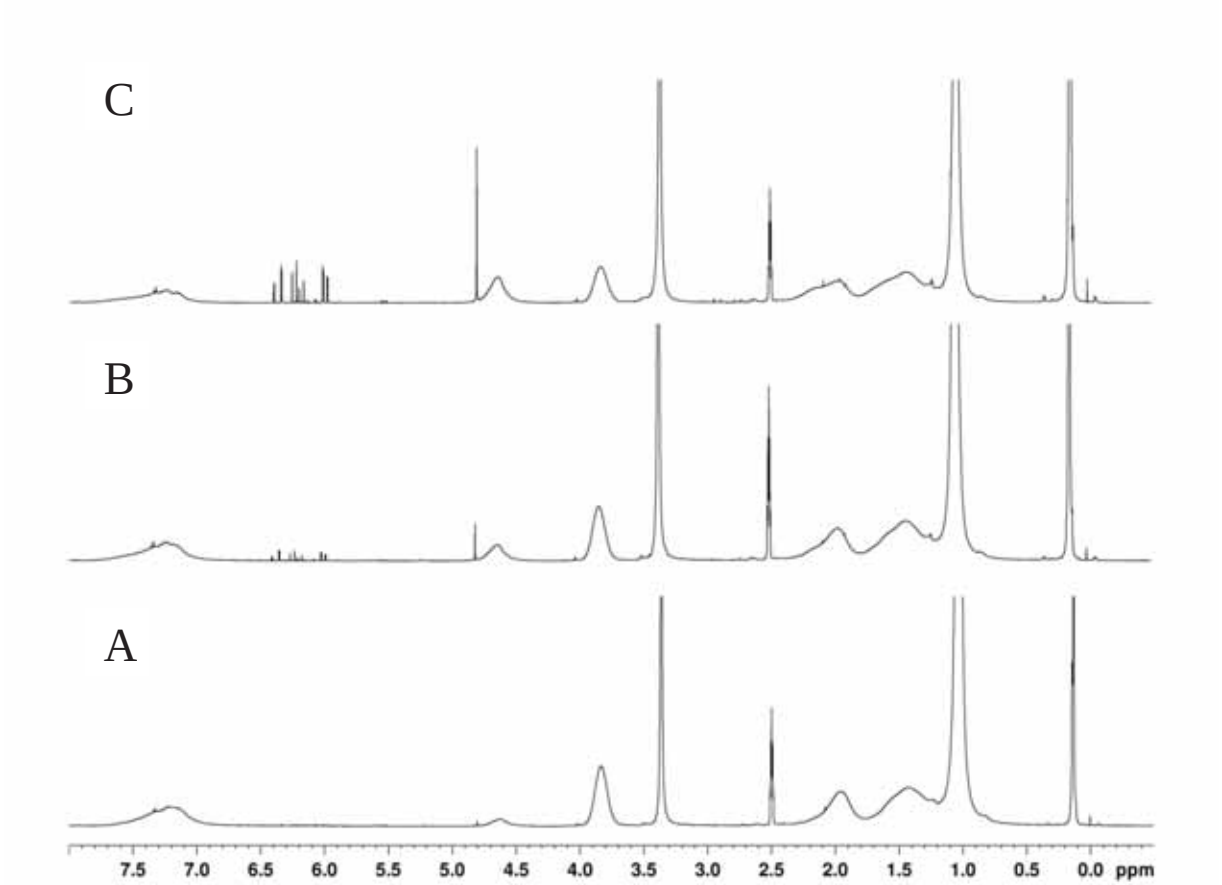

Figure 5.10 *^{1}H-NMR spectra in d_6-DMSO of P(NIPAAM-s-TMSPA) (illustrated) with different feed ratios of TMSPA:NIPAAM; 5:95* ***(A)****, 10:90* ***(B)****, and 20:80* ***(C)****, after been put through dialysis and freeze-drying. Peaks assigned to monomers at 4.0, 4.8, and 5.9-6.5 ppm were still visible even after dialysis.*

According to these initial results, the copolymer should have a gradient structure with the enrichment of TMSPA in the beginning of the polymerization. To quantify this observation, the reactivity ratios of this copolymerization in the presence and absence of the RAFT agent were determined. The monomer feed ratios were varied from f_{NIPAAM}= 0.1 to f_{NIPAAM}= 0.9 in 0.1 increments, hence, resulting in a set of nine samples. To achieve a monomer conversion below 5%, imperative for a reactivity ratio study, the free radical polymerization was stopped at 1 h or less while the presence of the RAFT agent required a reaction time of 3 h due to an inhibition period **(Figure 5.7 and 5.8)**. The composition of the polymers after purification was determined using ^{1}H-NMR spectrum as outlined in **Figure 5.10**. The mole fractions gathered from the NMR spectrum was used to calculate reactivity ratios. Of the four salient methods, Fineman Ross, Kelen Tüdös, Mayo Lewis and the program CONTOUR,[242-243] the latter three methods yielded harmonious results, despite having incomparable calculation approaches **(Table 5.2)**. The program CONTOUR, implemented by van Herk, is generally recommended by IUPAC.[244]

Table 5.2 *Reactivity ratios obtained by different approaches.*

	Free radical polymerization		**RAFT polymerization**	
Reactivity Ratio	$\mathbf{r_1}$	$\mathbf{r_2}$	$\mathbf{r_1}$	$\mathbf{r_2}$
Fineman Ross	1.22	0.56	1.48	0.41
Kelen Tüdös	0.95	0.45	1.22	0.31
Mayo Lewis	1.19	0.51	1.30	0.31
CONTOUR	1.12	0.46	1.40	0.36
Average	1.12	0.47	1.35	0.35

The reactivity ratios suggest that in both polymerization systems, free radical and RAFT, TMSPA (r_1) chain ends have a slight tendency to homopropagation ($r_1 \geq 1$). NIPAAM (r_2) is slightly inclined to cross propagate in RAFT, thus, the slight gradient structure of the polymer. The differences between free radical polymerization and RAFT polymerization are not significant, but visible. Similar to the finding by Barner-Kowollik

and co-workers, the polymer mole fraction of the monomer with the larger reactivity ratio is increased in RAFT polymerization compared to the conventional copolymerization.[244] In summary, as observed by the consumption of the individual monomers, the initial stages of the polymerization consume more TMSPA, therefore an enrichment of TMSPA can be found at the α-terminal of the polymer chain, where the R-group is positioned. The composition drift can be visualized by calculating cumulative *F* using the measured reactivity ratios **(Figure 5.11).**

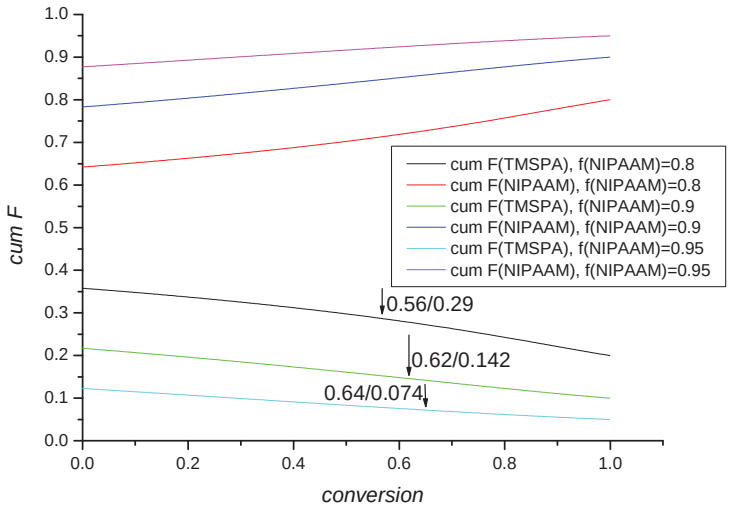

Fig. 5.11 *Calculated cumulative polymer composition of both monomers at different conversions showing the composition drift during the polymerization in dependency of the monomer feed ratio. The value were calculated using the obtained reactivity ratios for RAFT polymerization of* r_1*= 1.35 and* r_2*= 0.35.*

Subsequently, block copolymers were prepared using OEGMA as the building block due to the biocompatible properties of the resulting polymer **(Scheme 5.3)**. Before chain extension of P(OEGMEA) macro-RAFT agent with NIPAAM and TMSPA, POEGMEA homopolymer synthesis was achieved using 3-BSPA at 60 ^{o}C in DMAc as a solvent **(Figure 5.12)**. After 3 h of reaction time, $P(OEGMEA)_{40}$ homopolymer with a theoretical molecular weight of 19 200 g mol^{-1} and a narrow molecular weight distribution with polydispersity index (PDI) of 1.23 was achieved, again suggesting a controlled living system. Purification was carried out via dialysis against methanol as the trial precipitation with *n*-hexane failed.

As outlined in **Scheme 5.3**, $POEGMEA_{40}$ macro-RAFT was utilized in a mixture with NIPAAM and TMSPA, using similar reaction conditions as employed in the copolymerization, to generate block copolymers **(Figure 5.13 and 5.14)**. From the SEC curves in **Figure 5.15**, the absence of by-product and narrow PDI between 1.16-1.36 suggested the polymerization proceeded in a living manner. The purification processes used for these block copolymers were similar to the statistical copolymers. Akin to the copolymerizations, the three mol ratios of f_{NIPAAM}= 95, 90 and 80 % were employed leading after a reaction time of 20 h to the block copolymers $POEGMEA_{40}$-*b*-P($NIPAAM_{150}$-*s*-$TMSPA_{11}$)], $POEGMEA_{40}$-*b*-($NIPAAM_{137}$-*s*-$TMSPA_{18}$)], and $POEGMEA_{40}$-*b*-($NIPAAM_{115}$-*s*-$TMSPA_{24}$)], respectively. The molecular weights were in good agreement with the theoretical value while the SEC curves showed monomodal distributions. In contrast to the copolymerization using a low molecular weight RAFT agent, the rate of polymerization of TMSPA and NIPAAM in the presence of the macro-RAFT agent was less affected by the monomer composition **(Table 5.2)**. With increasing amount of TMSPA only a slight drop in the rate of polymerization has been observed. The reason is the lowered consumption of TMSPA, compared to the copolymerization. The influence of the macro-RAFT agent on the reactivity ratio of the subsequent copolymerization has been described earlier as “bootstrap” effect.[245] The hydrophilic macro-RAFT agent has a preferred accumulation of hydrophilic NIPAAM around the active RAFT end-group leading to the increased consumption of the faster propagating NIPAAM. Comparison of actual compositions of the polymer with the calculated composition using the reactivity ratios in **Table 5.2 (Figure 5.11)** show the incorporation of TMSPA has been delayed in the block copolymerization.

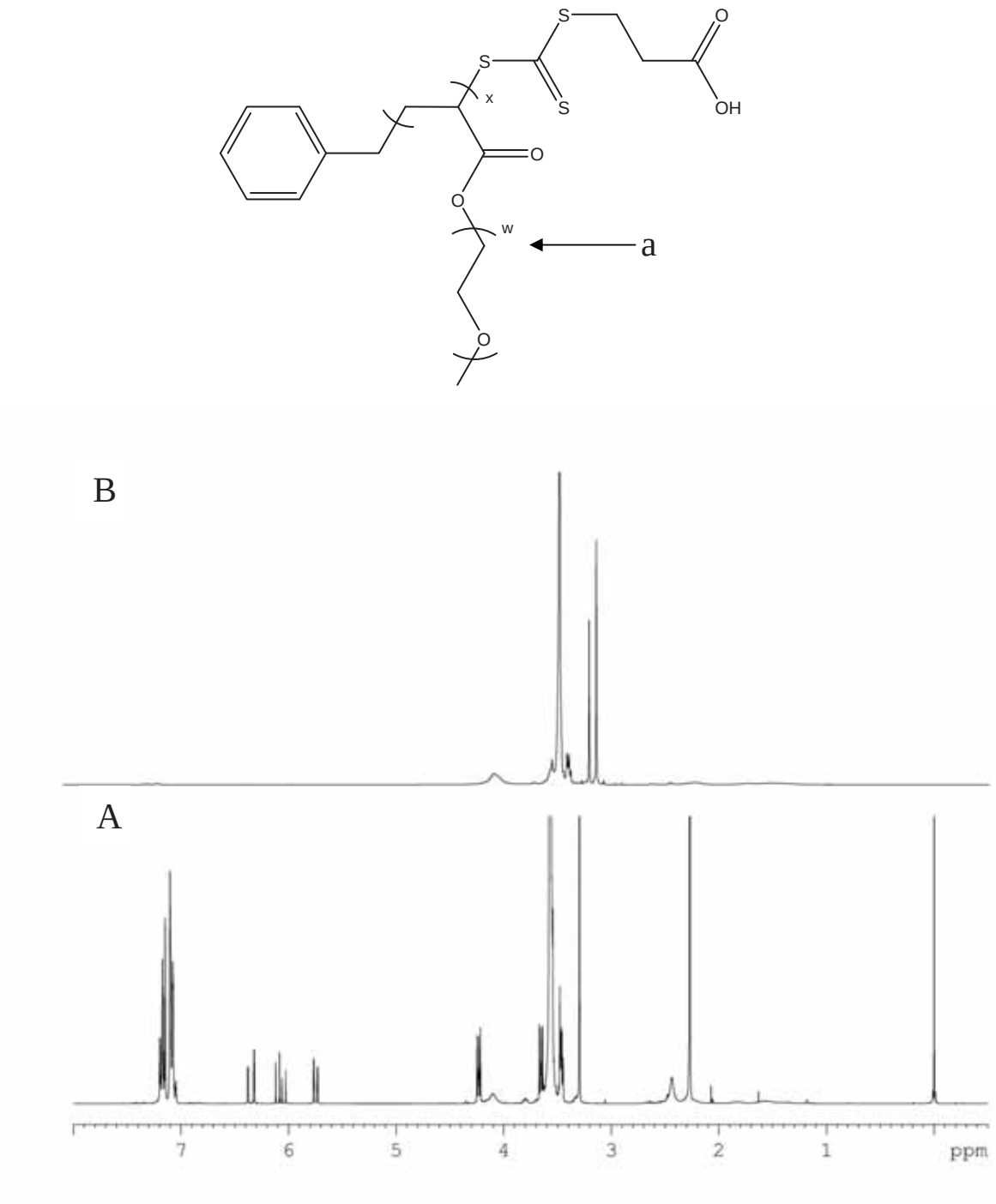

Figure 5.12 *^{1}H-NMR spectra of PEGMEA macro-RAFT agent after reaction/before dialysis* ***(A)*** *and after dialysis against methanol* ***(B)****. The disappearance of peak assigned to monomers at 4.3 and multiplets at 5.7-6.4 ppm in* ***(B)*** *proved a successful purification. Peak at 4.1 ppm was assigned for –CH_2 at* ***(a)****. Peak at 2.3 ppm and multiplets at 7.0-7.3 ppm were assigned to toluene used in polymerization.*

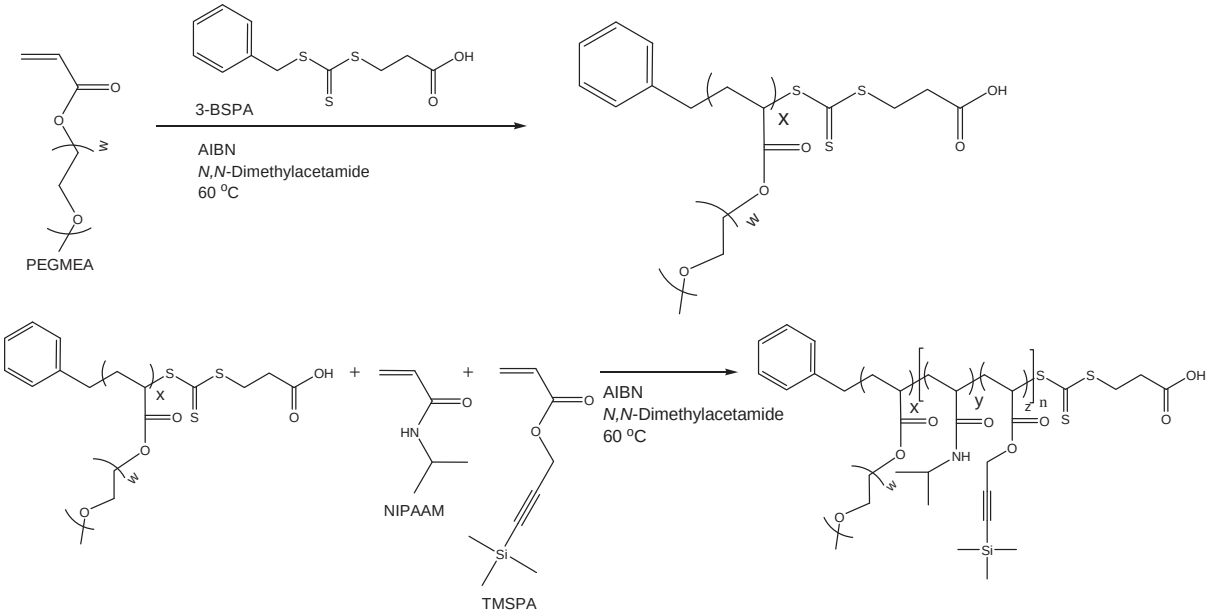

Scheme 5.3 *Reaction scheme of (A) Synthesis of macro-RAFT agent based on poly [poly(ethylene glycol methyl ether acrylate)][P(PEGMEA)]at 60 °C in DMAc;(B) Chain extension of PEGMEA macro-RAFT agent with N-isopropylacrylamide (NIPAAM) and trimethylsilylpropargyl acrylate (TMSPA) at 60 °C in DMAc to form P[PEGMEA-b-P(NIPAAM-s-TMSPA)]block copolymers.*

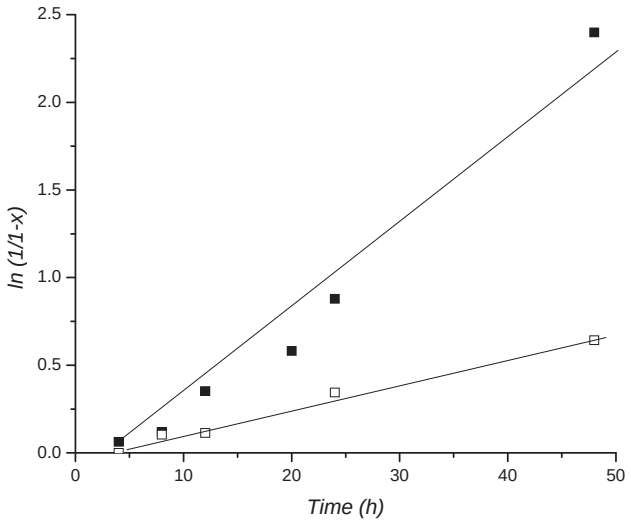

Figure 5.13 *Reaction kinetics of TMSPA in RAFT copolymerization of NIPAAM and TMSPA (■) and PEGMEA chain extended with NIPAAM and TMSPA (□). Both copolymers were obtained through RAFT polymerization at 60 °C for 20 hours with ratio of NIPAAM: TMSPA = 80:20.*

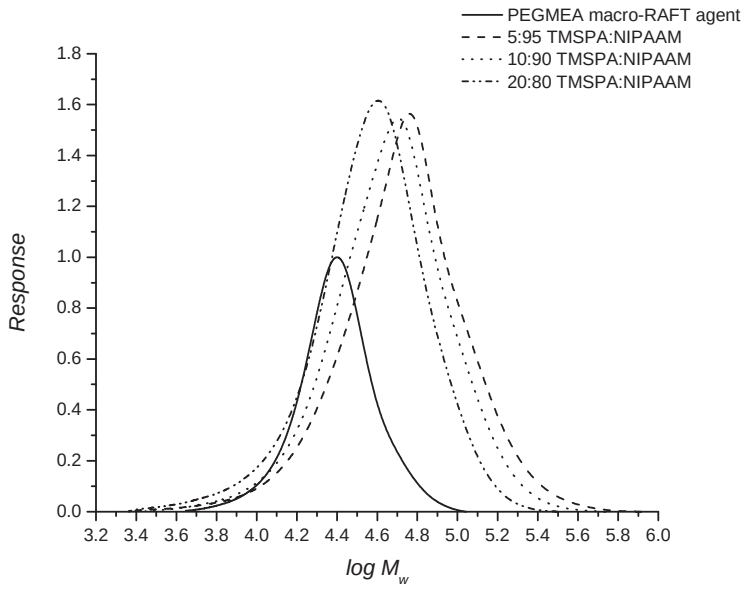

Figure 5.14 *SEC traces of PEGMEA macro-RAFT agent ($M_{n\ (theo)}$ = 20 600 g mol^{-1})(solid line). As the TMSPA continuously replaced by NIPAAM, the peak shifted to the higher molecular weight (to the right). The trend was similar as the copolymerization of TMSPA and NIPAAM without macro-RAFT agent.*

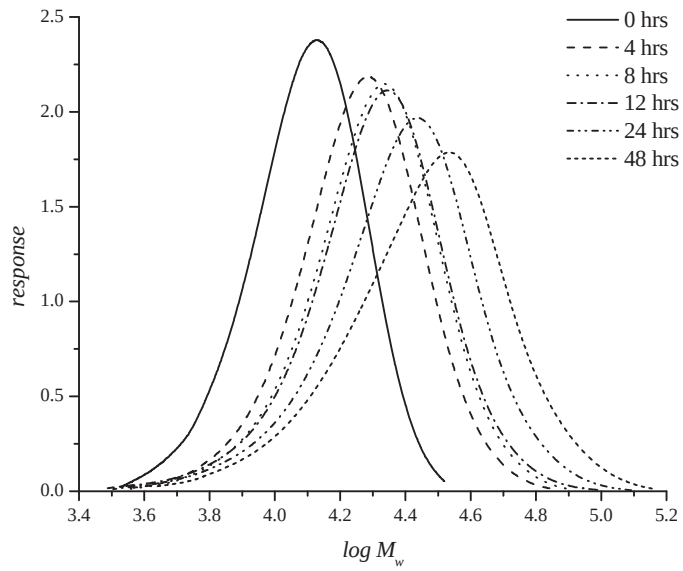

Figure 5.15 *SEC traces of RAFT polymerization of NIPAAM and TMSPA at 60 ^{O}C in the presence of PEGMEA macro-RAFT agent ($M_{n\ (theo)}$ = 13 000 g mol^{-1}) ([RAFT groups]) = 1.20 x 10^{-2} mol L^{-1},[AIBN] = 1.20 x10^{-3} mol L^{-1} in DMAc.*

5.3.2 Huisgen azide-alkyne 1,3-dipolar cycloaddition with 6I-azido-6I-deoxy-*β*-cyclodextrin

Prior to reaction of 6I-azido-6I-deoxy-*β*-cyclodextrin, the polymers were deprotected using tetrabutylammonium fluoride **(Figure 5.16, 5.17, and 5.18)**. The polymer lost its color due to the cleavage of the RAFT group during the procedure, probably replaced by a hydrogen as earlier mass spectroscopy analysis indicated.[246] NMR analysis confirmed the efficient removal of the protective group and the loss of the RAFT end group yielding POEGMEA-*b*-P(NIPAAM-*s*-PA) **(Figure 5.21)**. A procedure has been adopted for the Huisgen azide-alkyne 1,3-dipolar cycloaddition **(Scheme 5.4)** using a copper-catalyzed *click* system using copper(II) sulfate pentahydrate/ascorbic acid at 140 °C.[26] However, full copper removal was deemed impossible. Several procedures were attempted from removal via silica gel, extensive dialysis, to using a thiol complex and to washing with EDTA. After significant product loss, the seemingly colorless product was found to have still traces of Cu(I) ions, which were observed to be cytotoxic. Therefore, the traditional Huisgen azide-alkyne 1,3-dipolar cycloaddition in the absence of any catalyst was employed. A model reaction between 6I-azido-6I-deoxy-*β*-cyclodextrin **(Figure 5.19 and 5.20)** and propargyl alcohol at 100 °C resulted in complete reaction after 24 h with, as expected, the formation of two stereoisomers as evidenced *via* NMR **(Figure 5.20)**.

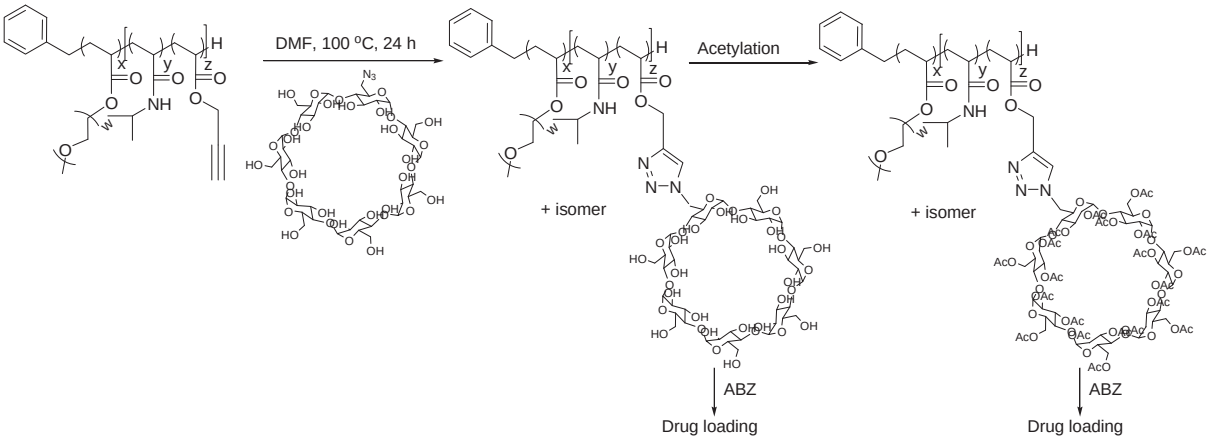

Scheme 5.4 *Huisgen azide-alkyne 1,3-dipolar cycloaddition with 6I-azido-6I-deoxy-β-cyclodextrin and subsequent acetylation.*

***Table 5.3**. Summary of block copolymers obtained using POEGMEA$_{40}$-macro-RAFT with different ratios of TMSPA and NIPAAM after polymerizing for 20 h.*

Feed ratio	**conv.**[a]	**Calculated composition from conversion**	**cum F_{TMSPA} (theo. cum F_{TMSPA})**[b]	Before deprotection POEGMEA-*b*-P(NIPAAM-*s*-TMSPA)		After deprotection and CD modification POEGMEA-*b*-P(NIPAAM-*s*-PA-*β*-cyclodextrin)	
				$M_{n,theo}$/ g mol^{-1}	**$M_{n,GPC}$/ g mol-1 (PDI)**[c]	**$M_{n,theo}$/ g mol^{-1}**	**$M_{n,GPC}$/ g mol^{-1} (PDI)**[c]
f_{TMSPA}= 0.05	64%	POEGMEA$_{40}$-*b*-P(NIPAAM$_{150}$-*s*-TMSPA$_{11}$)	7% (7.4%)	38150	35500 (1.65)	50150	57500 (1.56)
f_{TMSPA}= 0.1	62%	POEGMEA$_{40}$-*b*-P(NIPAAM$_{137}$-*s*-TMSPA$_{18}$)	11% (14.2%)	38000	33000 (1.55)	57550	65000 (1.51)
f_{TMSPA}= 0.2	56%	POEGMEA$_{40}$-*b*-P(NIPAAM$_{115}$-*s*-TMSPA$_{24}$)	17% (29%)	36570	27000 (1.51)	62700	54000 (1.59)

a) overall conversion of both monomers
b) Cumulative composition of the P(TMSPA-*s*-NIPAAM) block at the listed conversion calculated using the reactivity ratios in Table 1 (CONTOUR) for RAFT (Fig. S6 for graph)
c) DMAc, measured against PS standards

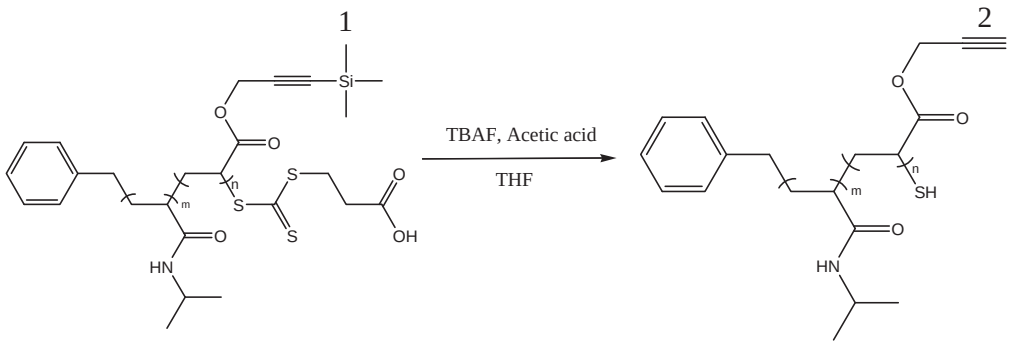

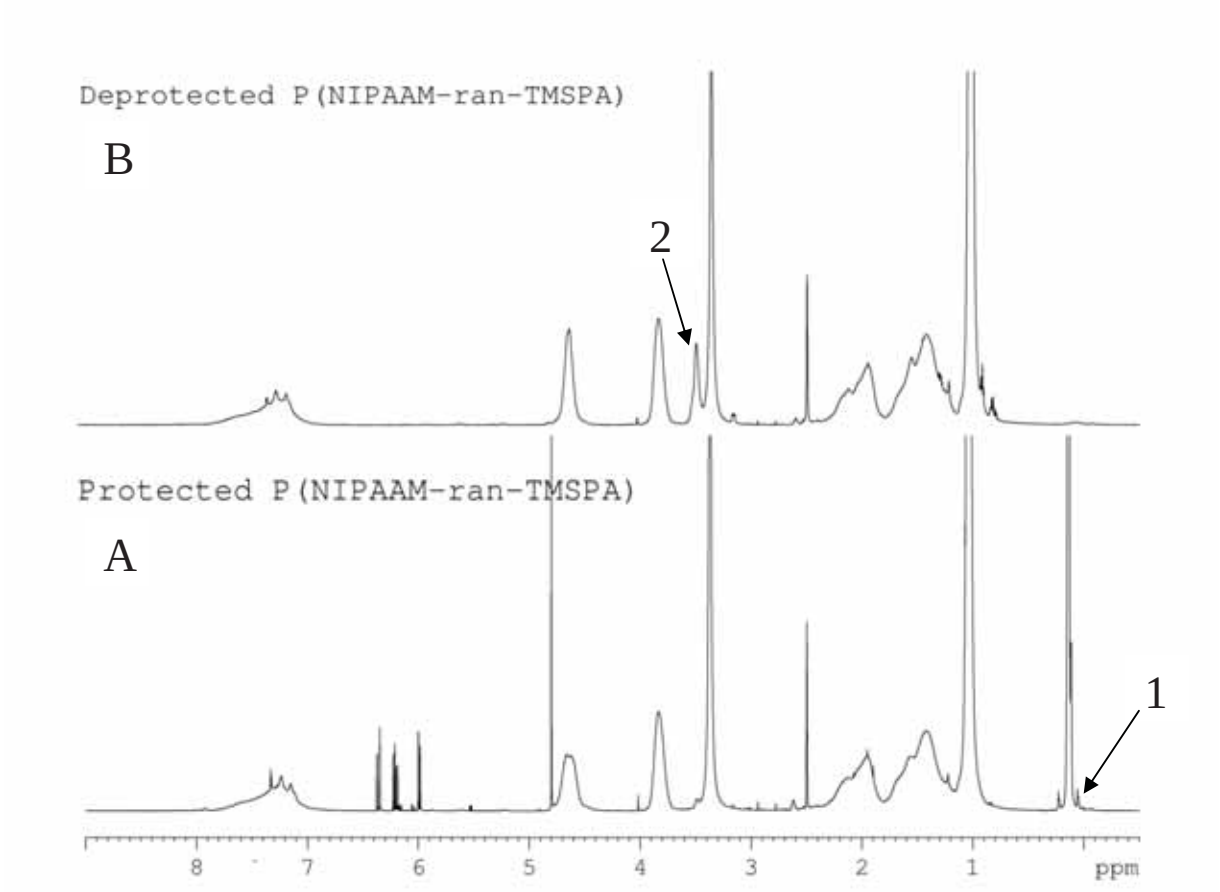

Figure 5.16 *P(NIPAAM-s-TMSPA)before deprotection of trimethylsilyl group* ***(A)*** *and after deprotection* ***(B)****. Deprotection removed the trimethylsilyl peak at 0.1 ppm* ***(1)****, producing terminal acetylene peak at 3.5 ppm* ***(2)****. Peaks assigned to monomers (4.0, 4.8, 6.0-6.4 ppm) were also disappeared after the deprotection and subsequent dialysis. The deprotection step also damaged the RAFT end-group.*

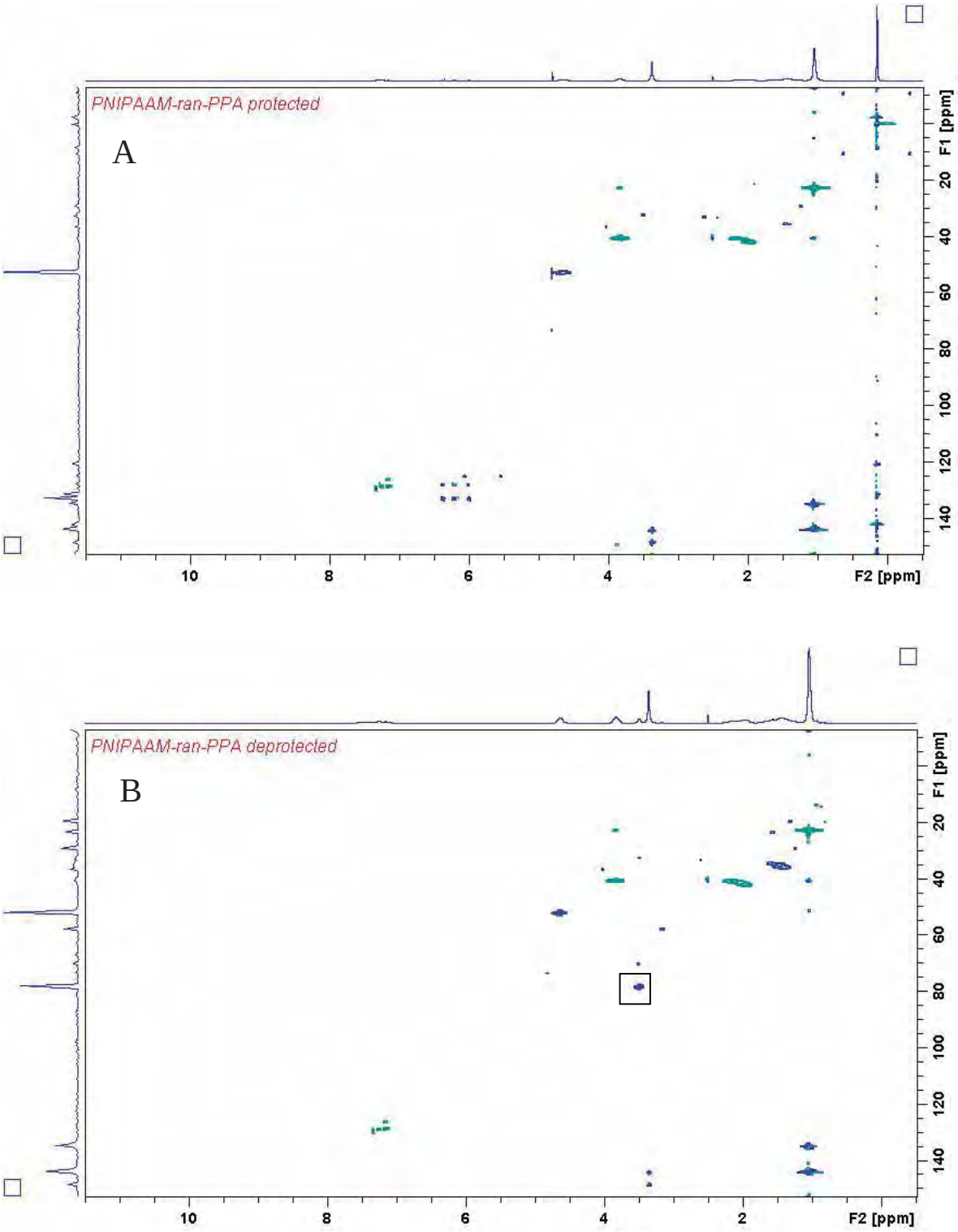

Figure 5.17 *HSQC-NMR of both protected* ***(A)*** *and deprotected* ***(B)*** *copolymer. An intersection point in* ***(B)*** *between 80 ppm and 3.5 ppm (inset box) proved the existence of acetylene group on deprotected copolymer that did not exist before.*

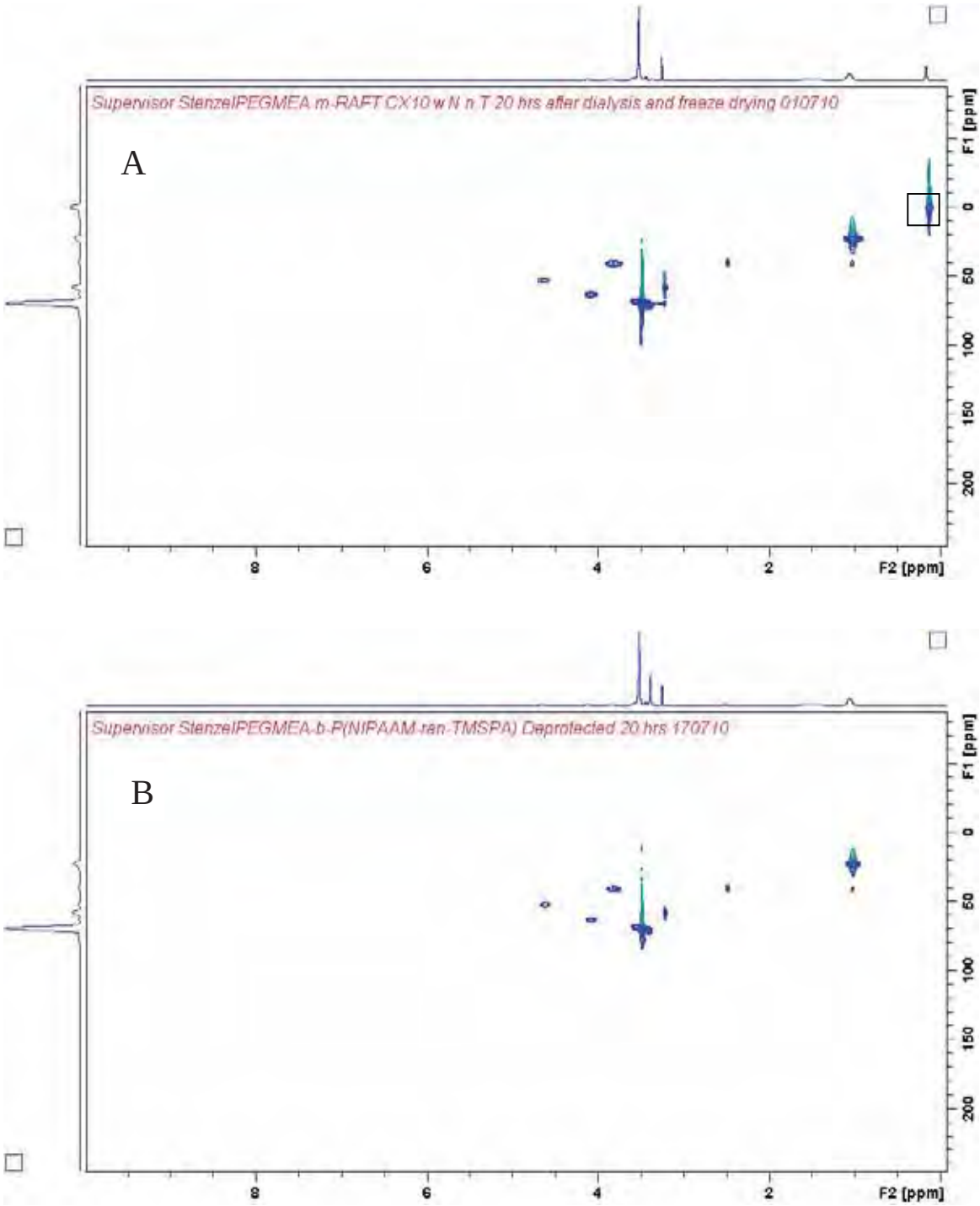

Figure 5.18 *HSQC-NMR of both protected* ***(A)*** *and deprotected* ***(B)*** *POEGMEA-b-P(NIPAAM-s-TMSPA) copolymer. However, the peak for acetylene peak at 80 ppm and 3.5 ppm that should exist in* ***(A)*** *was obscured by polymer peak. An intersection point in* ***(B)*** *between 0 ppm and 0.2 ppm (inset box) that was not observed in* ***(A)*** *proved the successful removal or trimethylsilyl protection group.*

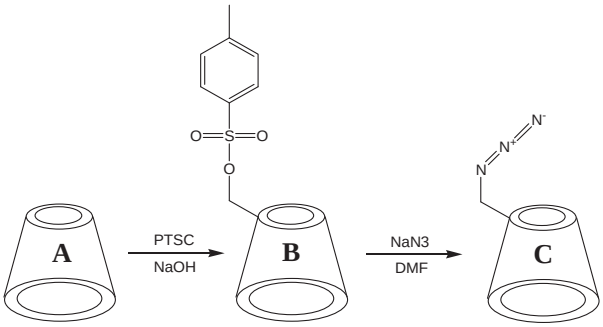

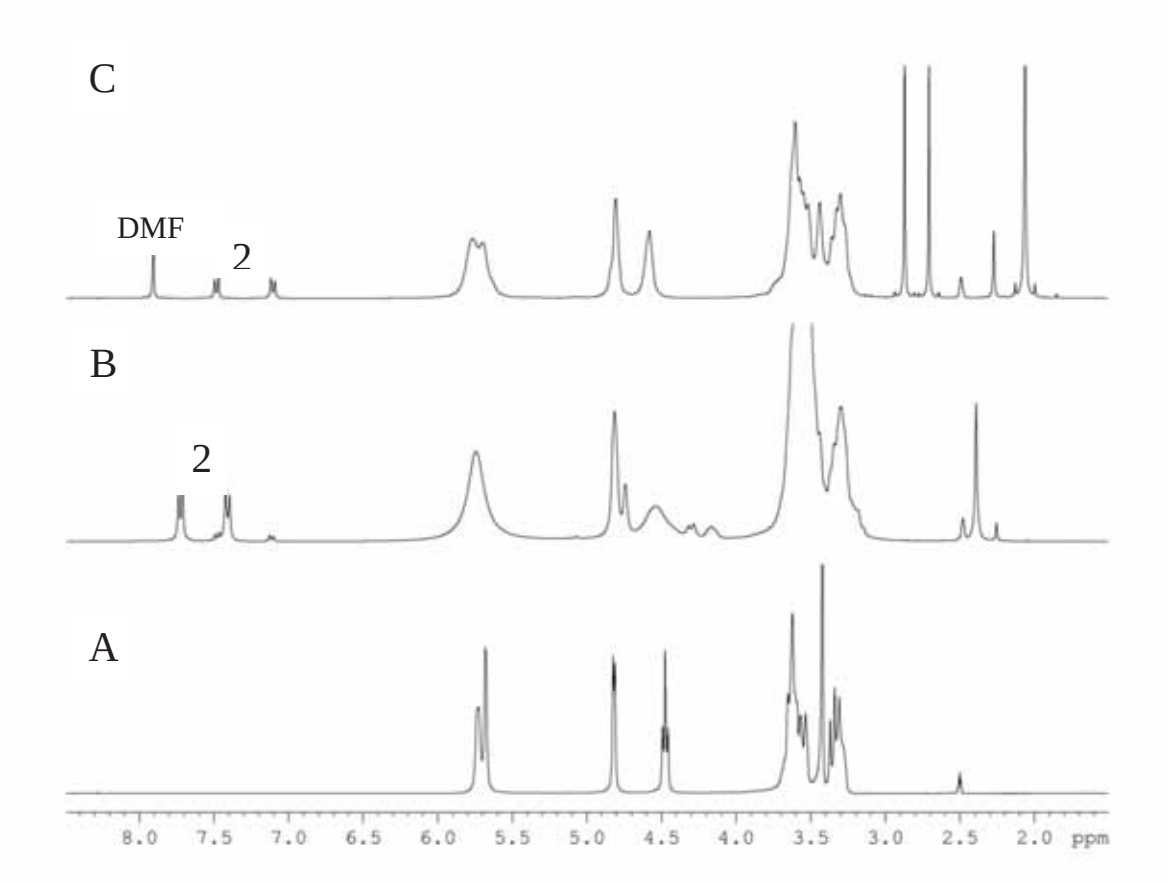

Figure 5.19 *^{1}H-NMR spectra of β-cyclodextrin* ***(A)****, β-cyclodextrin tosylate* ***(B)****, and 6I-azido-6I-deoxy-β-cyclodextrin (β-cyclodextrin azide)* ***(C)****. The signals at 7.3 ppm and 7.7 ppm* ***(2)*** *in* ***(C)*** *are traces of the tosylate, which is an intermediate in the preparation of 6I-azido-6I-deoxy-β-cyclodextrin.7.9 ppm signal is from DMF.*

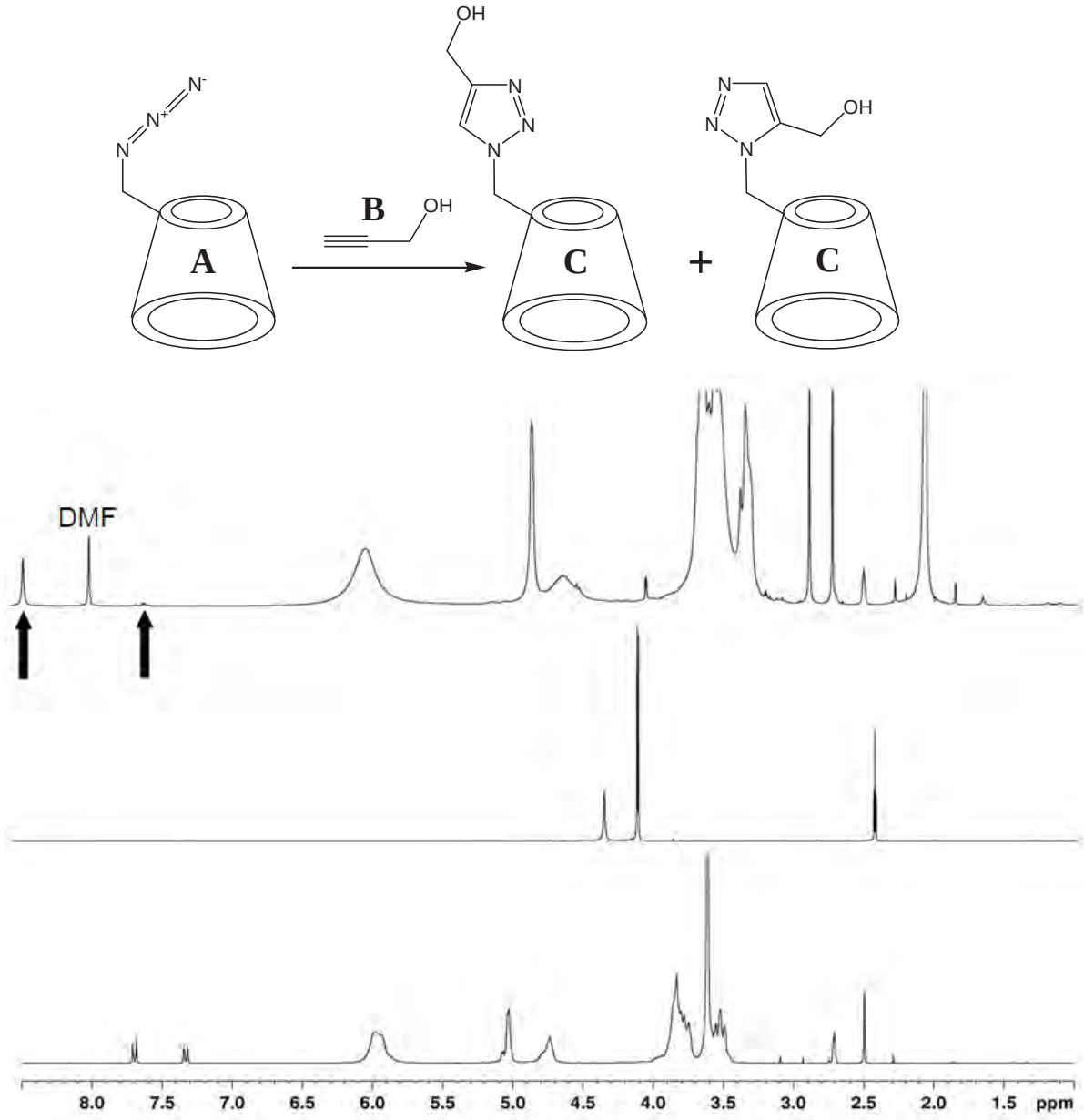

Figure 5.20 *^{1}H-NMR spectra of β-cyclodextrin azide* ***(A)****, propargyl alcohol* ***(B)****, and the clicked product* ***(C)****. Other sample was run in d-DMSO, while sample* ***(B)*** *was run in $CDCl_3$ to avoid peak from d-DMSO obscuring the alkyne peak. The peaks at 7.93 and 8.38 ppm in* ***(C)*** *were assigned to isomers 1,4 and 1,5 respectively, as a proof of the formation of the triazole ring. >95% of 1,4 isomer (8.39 ppm) and a small amount of 1,5 isomer (7.55 ppm) was obtained after click reaction in DMF at 100 ^{o}C for 24 hrs.*

After the successful model reaction, four polymers - one statistical polymer, P(NIPAAM$_{116}$-*s*-PA$_{43}$) and the three block copolymers listed in **Table 5.3** - were reacted with 6I-azido-6I-deoxy-*β*-cyclodextrin. The modification process was confirmed by ^{1}H-NMR **(Figure 5.21)**, FT-IR **(Figure 5.22),** and SEC **(Figure 5.23)**. From ^{1}H-NMR analysis, the modification process with 6I-azido-6I-deoxy-*β*-cyclodextrin was observed to be complete. The -CH_2- signal of the propargyl ester before modification (4.7 ppm) shifted to 4.2 ppm after reaction **(Figure 5.21)**. Even though the peaks assigned to the proton in the triazole ring (7.9-8.4 ppm) appeared in the spectrum of model reaction, these peaks were not detected in the polymer peaks, possibly due to increased relaxation times. In order to confirm that the cyclodextrin peaks were not from free (unreacted) *β*-cyclodextrin azide, the polymer was dialyzed for 7 days in water using a tubular dialysis membrane with a molecular weight cut-off of 6000-8000 Dalton. FT-IR analysis of 6I-azido-6I-deoxy-*β*-cyclodextrin exhibited a sharp peak at 2000 cm^{-1} assigned to the azide functional group, which disappeared after reaction. The broad peak at 3000-3500 cm^{-1} is indicative for the hydroxyl groups of cyclodextrin, which were absent before reaction **(Figure 5.22)**. SEC traces from **Figure 5.23** shows that the SEC curves are monomodal and high molecular weight shoulders are absent suggesting that no linkages formed between polymer chains. This reinforces the purity of 6I-azido-6I-deoxy-*β*-cyclodextrin and the presence of bifunctional cyclodextrin can be assumed absent. It should be noted here that the results for both block copolymers and statistical polymers are similar, unless stated otherwise. The SEC confirmed the increase of the molecular weight of monomodal peak of POEGMEA-*b*-(NIPAAM-*s*-PA) to the higher molecular weight of POEGMEA-*b*-P(NIPAAM-*s*-PA-*β*-cyclodextrin) **(Figure 5.23)**. Interestingly, the are no significant weight differences between the product obtained via Huisgen azide-alkyne 1,3-dipolar cycloaddition with and without Cu(I) catalyst. The non-copper method was preferable since it eliminated the need for copper trace removal and the product was more suitable for biomedical applications. The clicked copolymer also formed inclusion complex with adamantyl-terminated RAFT agent **(Figure 5.24)**. A mixture of 1:1 mol ratio based on *β*-cyclodextrin moieties of clicked copolymer and adamantyl-terminated RAFT agent was stirred overnight in DMF, then dialyzed with water and dried to obtain a water insoluble inclusion complex **(Table 5.4).**

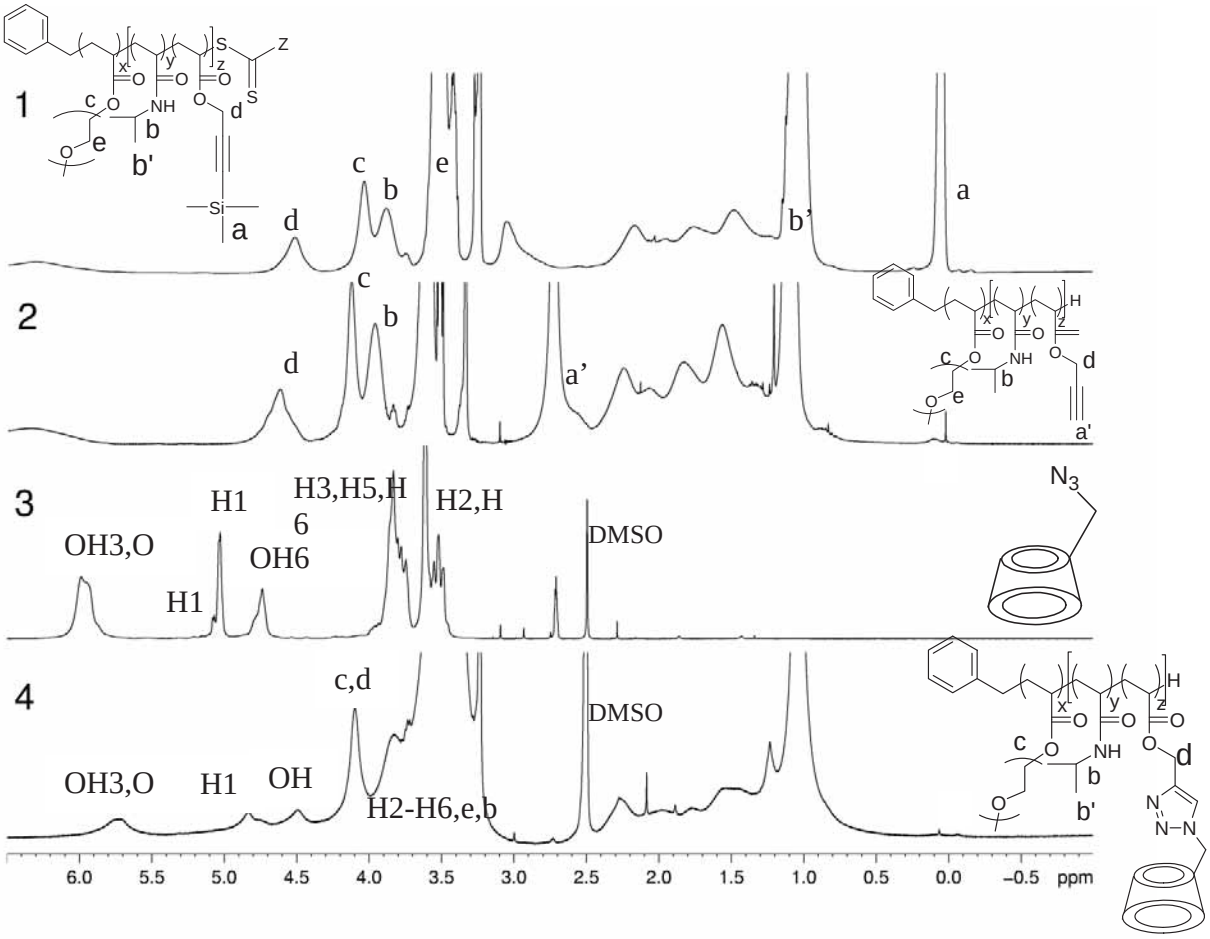

Figure 5.21 *^{1}H-NMR analysis of POEGMEA$_{40}$-b-P(NIPAAM$_{115}$-s-TMSPA$_{24}$) before deprotection (A) and after deprotection (B), 6I-azido-6I-deoxy-β-cyclodextrin (C), and POEGMEA$_{40}$-b-P(NIPAAM$_{115}$-s-PA-β-cyclodextrin$_{24}$) (D). ^{1}H-NMR spectra for (1) and (2) were obtained in CDCl$_{3}$, while spectra for (3) and (4) were obtained in deuterated DMSO.*

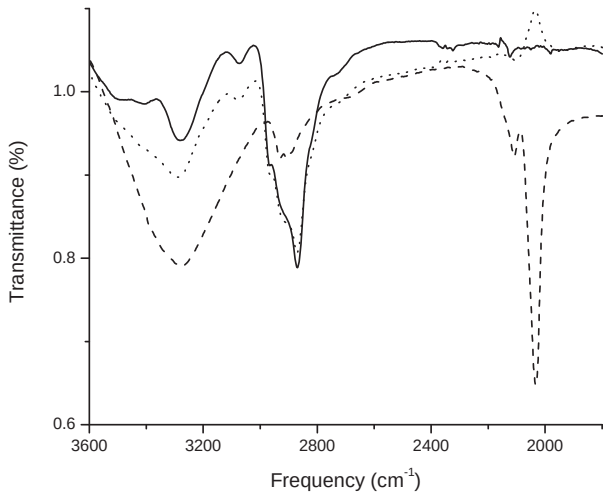

Figure 5.22 *FTIR spectra of P[POEGMEA-b-P(NIPAAM-s-PA)] before clicking (—), β-cyclodextrin azide (----), and P[POEGMEA-b-P(NIPAAM-s-PA)] clicked with β-cyclodextrin azide (·····). A strong, narrow band at 3270-3330 cm^{-1} assigned to terminal alkyne can be observed in (—). The absence of azide peak at 2000 cm^{-1} and appearance of broad hydroxyl peak around 3100-3800 cm^{-1} in (·····) proved a successful click reaction.*

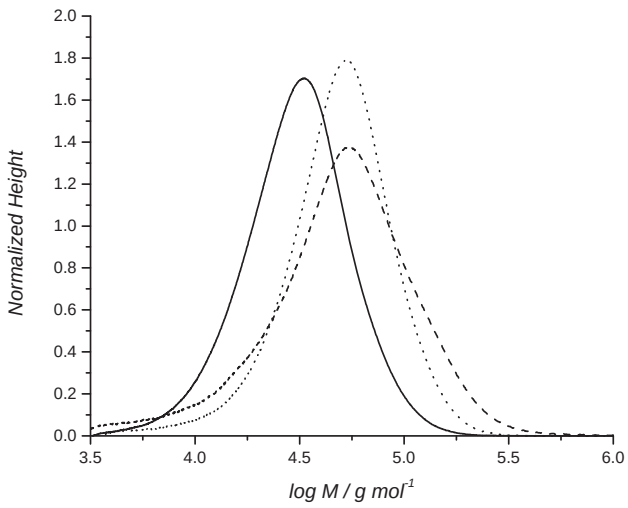

Figure 5.23 *SEC traces of POEGMEA-b-P(NIPAAM-s-PA) before reaction (—), POEGMEA-b-P(NIPAAM-s-PA) clicked with 6I-azido-6I-deoxy-β-cyclodextrin using copper catalyst at 140 ^{o}C for 30 min (·····), and POEGMEA-b-P(NIPAAM-s-PA)] modified with β-cyclodextrin azide at 100 ^{o}C for 24 h (----).*

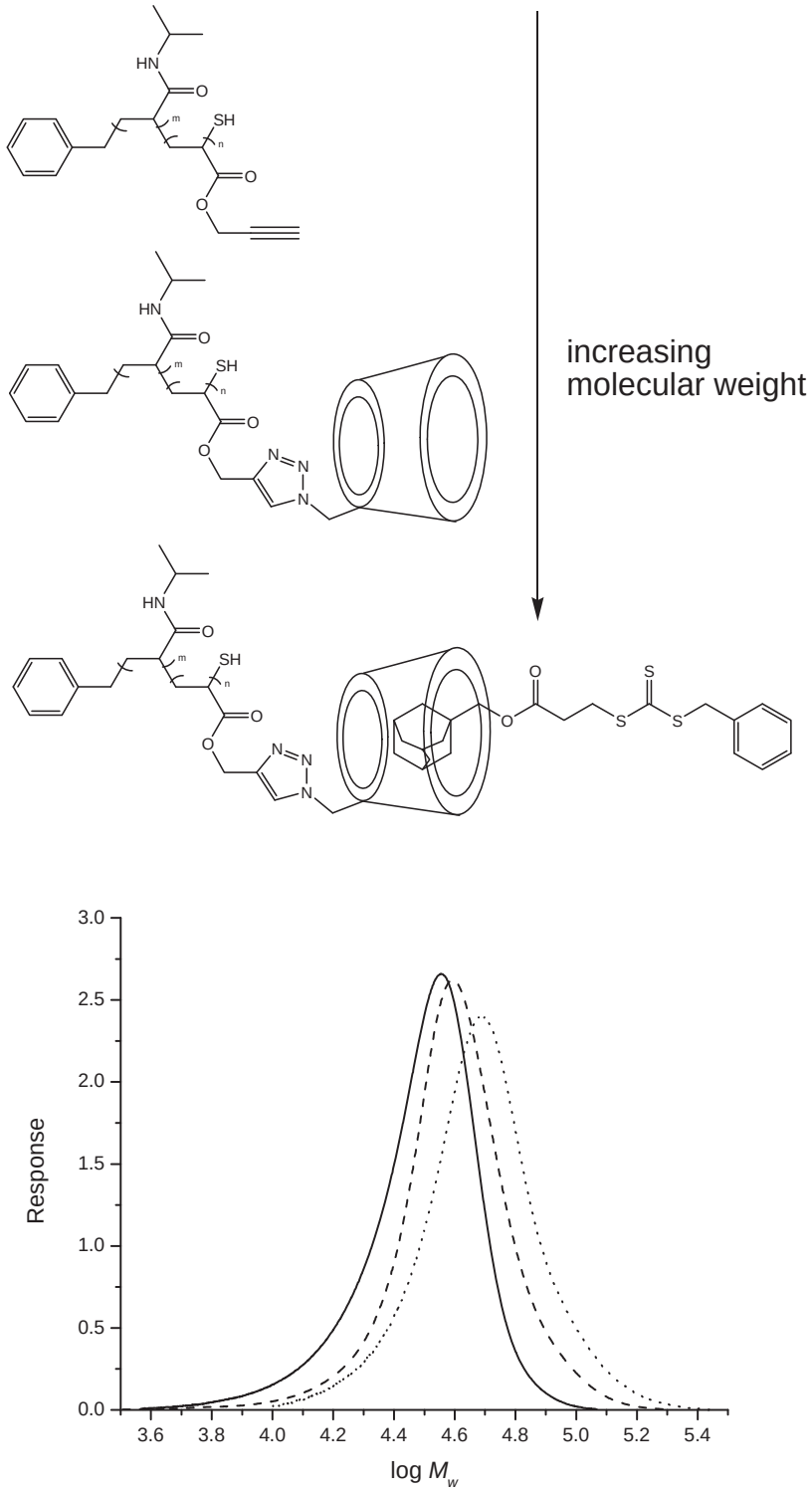

Figure 5.24 *SEC traces of P(NIPAAM-s-PA) (──), after clicked with β-cyclodextrin (----), and after formation of inclusion complex with adamantyl-terminated RAFT agent (·····). As with every progression the molecular weight also increases.*

The changes in water solubility, color, and molecular weight were summarized in **Table 5.4**.

Table 5.4 *Properties of precursors to the adamantyl-cyclodextrin inclusion complex and the complex itself.*

	Structure	Water solubility	Color	Molecular weight M_n (SEC)	PDI
1.	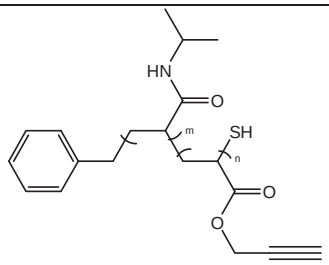	No	Greenish yellow solid	26000	1.22
2.	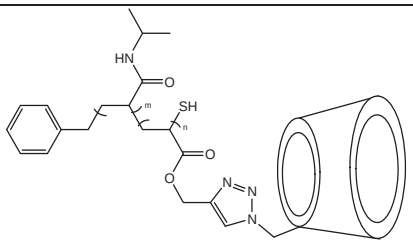	Yes	Brown solid	33000	1.22
3.	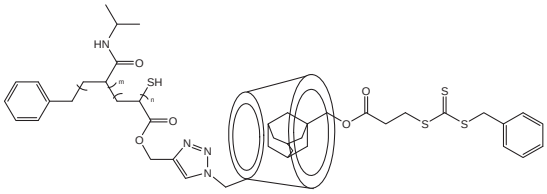	No	Yellow solid	40800	1.22
4.	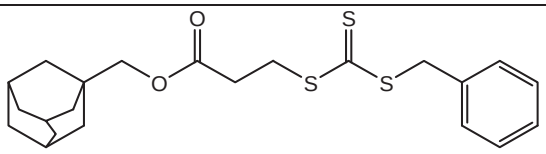	No	Yellow solid	600	1.00

The P(NIPAAM-*s*-PA) (Structure 1) was greenish yellow while the adamantyl-terminated RAFT agent (Structure 4) was yellow. Both are water insoluble. The P(NIPAAM-*s*-PA-*β*-cyclodextrin) (Structure 2) was brown colored and water soluble. After forming the inclusion complex (Structure 3) it was insoluble again in water, yellow in color with huge increase in molecular weight but maintaining the PDI of Structure 2.

This has proven that the click/conjugation between cyclodextrin azide-polymer really took place. Therefore, it can be concluded that the cyclodextrin moieties are readily accessible for the for host-guest interaction.

The statistical polymers prior to β-cyclodextrin modification are insoluble in water while the block copolymers have clearly amphiphilic properties. The presence of TMSPA or, after deprotection, propargyl acrylate clearly lowers the water solubility of PNIPAAM. With conjugation of the hydrophilic β-cyclodextrin, the polymers become fully water-soluble. The presence of a comonomer will ultimately affect the lower critical solution temperature (LCST) of PNIPAAM.[247] The LCST of all polymers was determined via dynamic light scattering (DLS) using the scattering intensity as a means of determining the temperature. The onset of the increase coincides with the formation of more and bigger particle due to precipitation or micelle formation **(Figure 5.25)**. The hydrophobic comonomer TMSPA lowered the LCST in all cases to such an extent that these polymers are insoluble in water at room temperature. In contrast, after reaction with 6I-azido-6I-deoxy-β-cyclodextrin, the LCST increased to temperatures of well above the LCST of PNIPAAM. The LCST of the statistical copolymer increases with increasing fraction of β-cyclodextrin in agreement with earlier studies.[225-226, 248] Interesting is the behavior of the prepared block copolymers. Block copolymers with a low content of β-cyclodextrin still show similar curves to the statistical block copolymer as depicted in **Figure 5.23**. The LCST is slightly lower than the statistical block copolymer owing to the reduced presence of TMSPA, hence, subsequently, yielding lower β-cyclodextrin content. Block copolymers prepared with a higher TMSPA feed radio, however, did not possess a visible LCST and the scattering intensity remain unaffected over the range of temperatures measured. This may be explained by the absence of phase separation between both blocks. While it is expected that above the LCST, POEGMA and PNIPAAM form two immiscible blocks, it also needs to be considered that cyclodextrin undergo inclusion complex formation with many polymers including polyethylene oxide (PEO), although α-cyclodextrin is more suitable for the inclusion complex formation with PEO.[249-252] A range of hydrogels have been generated using this approach,[252-253] although hydrogels from PEO and cyclodextrin only are not very stable in the presence of high amount of

water.[252] This host-guest formation could force the hydrophilic PEO into the PNIPAAM environment shifting the LCST to values above the measured range. Evidence can be found in the aggregate formation below the LCST. Theoretically, below the LCST, aggregate formation should be absent due to the water-solubility of both blocks. However, all block copolymers listed in **Table 5.5** show small round particles of diameters of 10-15 nm under the TEM accompanied with a large fraction of undefined large particles with 100-500 nm **(Figure 5.26)**. Above the LCST and the dehydration of PNIPAAM, the formation of micelles with sizes of around 40 nm (TEM) or 50 nm (DLS) takes place. Aggregate formation below the LCST may not only be caused by inclusion complex formation, but also by the formation of strong hydrogen bonding between two cyclodextrin molecules, a process that is especially prevalent with polymers that contain higher concentrations of cyclodextrin moieties.[248] For further variation of the LCST, the hydroxyl groups of *β*-cyclodextrin were acetylated using a standard procedure. As a result, the hydrophilicity of the building block was lowered, which is reflected by a LCST of 34 °C but also by a strong tendency to form a high fraction of micelles with a hydrodynamic diameter of 100 nm even at room temperature. At the LCST, the core of the micelles collapses forming particles of 30 nm.

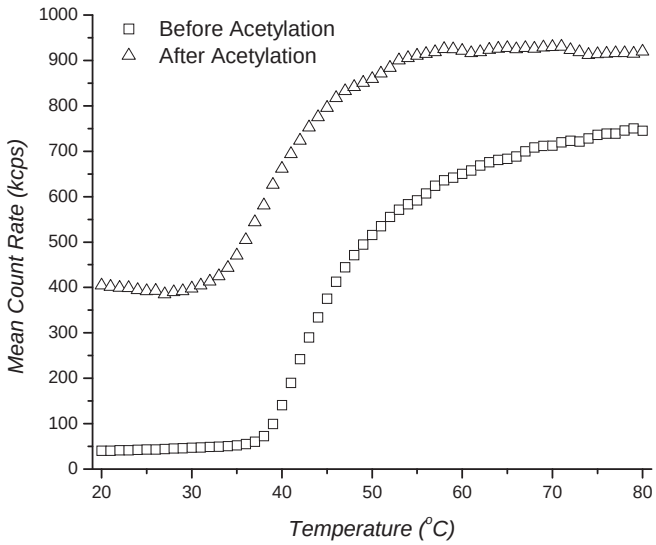

Figure 5.25 *Scattering intensity vs temperature of POEGMEA$_{40}$-b-P(NIPAAM$_{150}$-s-PA-β-cyclodextrin$_{11}$)], before and after acetylation, in water.*

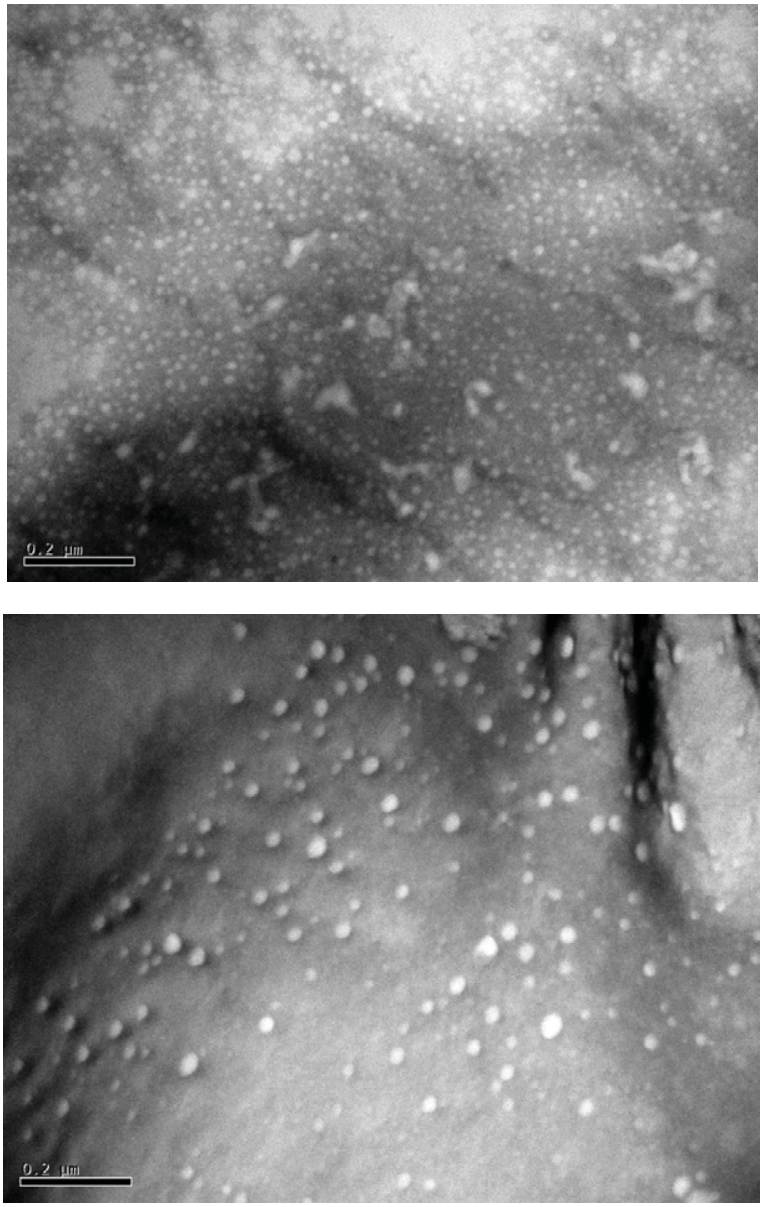

Figure 5.26 *TEM images of block copolymer POEGMEA$_{40}$-b-P(NIPAAM$_{150}$-s-PA-β-cyclodextrin$_{11}$)] particles using phosphotungstic acid negative staining at 25 ^{o}C (top) and 55 ^{o}C (bottom).*

5.3.3 Albendazole drug loading, release and cell toxicity tests

Recently, ABZ has been identified as a potential systemic anticancer agent besides its normal use as an anthelmintic drug against human and animal parasites.[91-92, 254-259] ABZ also has low aqueous solubility, which limits its use for the treatment of cancer.

The insolubility of albendazole in water (2.00×10^{-4} g L^{-1} or 7.57×10^{-6} mol L^{-1})[260] requires the consumption of vast amounts of drug to treat any diseases in a meaningful way. Cyclodextrins have been chosen earlier to address the low water-solubility.[93, 261-262] Phase diagrams have been studied in detail confirming the formation of 1:1 complexes between β-cyclodextrin[93, 262] while NMR analysis suggest inclusion via the butyl group as depicted in **Figure 5.1.**[93] Although the ABZ-CD complex has been thoroughly studied in literature with a range of techniques, NMR studies are limited. In most cases, the shift of β-cyclodextrin signals have been monitored, but also the ABZ signals underwent some changes. As seen in **Figure 5.27**, confirming various studies in literature, the ^{1}H NMR signals corresponding to cyclodextrin is dependent on the amount of albendazole added with the largest changes occurring at a 1:1 molar ratio between β-CD and ABZ **(Figure 5.27)**. The structure of the complex as shown in **Figure 5.1** has been derived from the shift of the propyl signals of ABZ.[93] The aliphatic protons were shielded in the presence of β-CD, but it is not clear to what extend the aromatic group may be involved. However, so far no two-dimensional rotating frame NOE spectroscopy (ROESY)[263] has been carried out to elucidate the structure of the host-guest complex. However, even after many attempts, we failed to obtain suitable cross peaks and the formation of the complex was only characterized by establishing the phase-solubility diagram. The apparent binding constant between ABZ and β-cyclodextrin was calculated using a method developed by Higushi and Connors.[93] The apparent binding constant $K_{1:1}$ = slope/S_o(1−slope) was obtained from the slope of the linear relationship between cyclodextrin concentration and the amount of encapsulated ABZ and the initial solubility of ABZ in the absence of cyclodextrin S_0. Values of $K_{1:1}$ for this inclusion complex formation was reported as 1382 L mol^{-1} [262] and 965 L mol^{-1} (3.643 mL mg^{-1})[93]. Loading was usually achieved by mixing an aqueous cyclodextrin solution with ABZ, which is

dissolved in an organic solvent such as THF or acetone. After incubation, the organic solvent was removed under vacuum and excess ABZ was filtered off. Using this approach, we obtained a slightly higher value for the inclusion complex formation with $K_{1:1}$ 1600 L mol^{-1} **(Table 5.5)**. The loading capacity was not affected when the statistical copolymers P(NIPAAM-*s*-PA-*β*-cyclodextrin) were tested. The apparent binding constant of 1600 L mol^{-1} was obtained with the polymer listed in **Table 5.5**, but also with other copolymers prepared with different feed ratios **(Figure 5.9)**, therefore loading was not affected by the cyclodextrin content in the polymer, in contrast to other work where the interaction was reduced when CD was conjugated to a polymer.[264] In contrast, the block copolymers with POEGMA lead to double the ABZ loading. This can be understood by the role of PEG chains to contribute to the overall enhancement of the solubility of ABZ delaying precipitation of ABZ when the organic solvent is removed from aqueous system. A significant jump in the complex formation can be observed after acetylation **(Table 5.5)**. The effect of the modification of hydroxyl groups on the complex formation has been discussed earlier.[265-266] Acetylation will affect the size of the cavity and also the type of forces between CD and drug.[267]

The drug is encapsulated via the hydrophobic tail while the more hydrophilic part is exposed to the outside. This exposed part of the drug molecule can now manipulate the overall hydrophilicity of the PNIPAAM copolymer influencing the LCST.[223, 225] The measured LCST values were observed to be slightly increased owing to the presence of the hydrophilic carbamate part of the drug ABZ **(Table 5.5)**. The drug molecule also imparts now stimuli-responsive properties to the block copolymers with higher *β*-cyclodextrin content while a visible LCST was absent in the absence of ABZ. Drug loading obviously facilitates phase separation between PNIPAAM and the POEGMEA block. The changes in the LCST in the acetylated polymer were much more pronounced due to the much higher loading of ABZ.

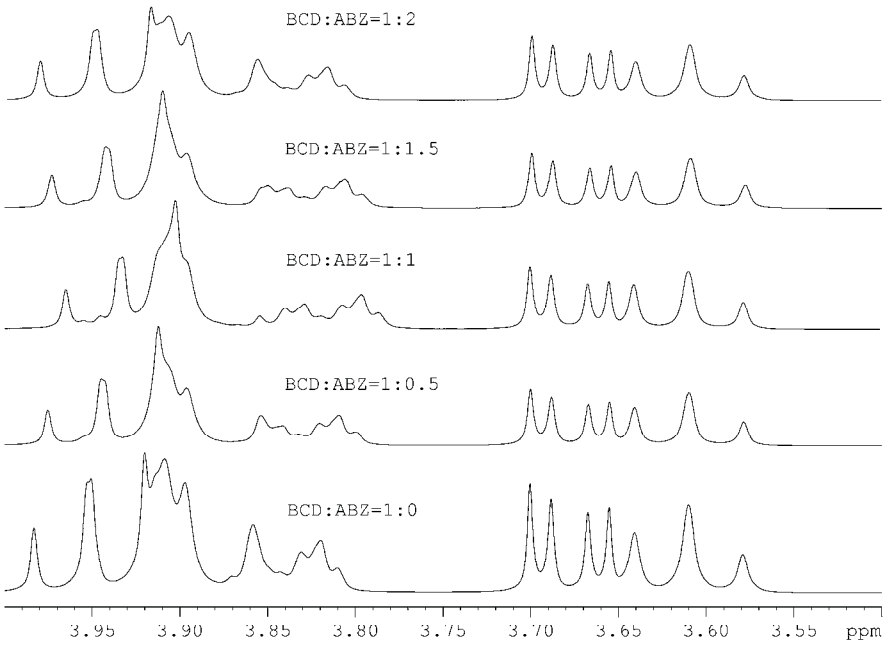

Figure 5.27 *^{1}H-NMR spectra in D_2O of β-CD (BCD) and albendazole (ABZ) at different molar ratios.*

Table 5.5 *LCST values determined using DLS (scattering intensity) before and after ABZ loading.*

Sample	Polymer composition	F	LCST/ °C	LCST (after ABZ loading)/ °C	$K_{1:1}$/ L mol^{-1}
1	*β*-cyclodextrin	-	-	-	1600±5%
2	P(NIPAAM$_{116}$-*s*-PA-*β*-cyclodextrin$_{43}$)	27%	42	46	1600±5%
3	POEGMEA$_{40}$-*b*-P(NIPAAM$_{150}$-*s*-PA-*β*-cyclodextrin$_{11}$)]	7%	38	42	3950±5%
4	POEGMEA$_{40}$-*b*-P(NIPAAM$_{137}$-*s*-PA-*β*-cyclodextrin$_{18}$)]	11%	-	> 55	3950±5%
5	POEGMEA$_{40}$-*b*-P(NIPAAM$_{115}$-*s*-PA-*β*-cyclodextrin$_{24}$)]	17%	-	> 55	4200±5%
6	POEGMEA$_{40}$-*b*-P(NIPAAM$_{150}$-*s*-PA-*β*-acetyl-cyclodextrin$_{11}$)]	7%	34	48	37000±5%

The ABZ loaded polymers were tested as drug delivery carriers. The statistical copolymer and the block copolymer are tested against *β*-cyclodextrin in their performance. Aim is to have a non-toxic carrier while the drug-carrier system should show high cytotoxicity. It should be noted here that the block copolymer is not expected to form micelles under these conditions. LCST values seem to suggest that the polymers are water-soluble at the cell test temperature of 37 °C. In addition, the stability of block copolymer micelles is highly challenged in cell growth media resulting often in disaggregation.[234] However, the presence of PEG can increase biocompatibility and possibly enhance cellular uptake of the drug carrier. Results from preliminary studies have suggested that ABZ is an efficient anti-cancer drug against ovarian cancer.[259] OVCAR-3 cell lines were chosen to test the activity of the ABZ loaded systems. Parent (unmodified) *β*-cyclodextrin, statistical copolymer, and block copolymer were tested for toxicity against cell lines before and after ABZ loading. Initially, the biocompatibility of *β*-cyclodextrin and its polymers were tested on viable OVCAR-3 cells. **Figure 5.28** shows the percentage viability of OVCAR-3 cell relative to the control sample after 72 h incubation at 37 ^{o}C with four different vectors concentration of 62.5, 125, 250, and 500 μg mL^{-1}, which is equivalent to different amounts of cyclodextrin. Therefore the cell viability was recorded against the concentration of cyclodextrin **(Figure 5.28)**. *β*-cyclodextrin alone was found to be toxic to cells, even when unloaded with drug. This has been observed earlier [268-271] and the toxicity of *β*-cyclodextrin may be attributed to its uptake by cells, leading to the disruption of intracellular function or the extraction of lipid membrane components such as cholesterol and phospholipids.[269] The statistical copolymer also showed its toxicity as the concentration increased while the block copolymer, with its PEG chains counterbalanced the toxicity of *β*-cyclodextrin.

The polymers were subsequently loaded with ABZ. Vectors concentration, incubation time, and temperature were the same as before. Even after ABZ loading, the statistical copolymer was more toxic than the block copolymer. ABZ loaded *β*-cyclodextrin is as cytotoxic as *β*-cyclodextrin alone resulting in more than 90% cell death. An interesting result was obtained when comparing two polymers. Although the complex formation constant between ABZ and *β*-cyclodextrin in the block copolymer is slightly higher, the

overall amount of cyclodextrin is lower in this system. As a consequence, the amount of ABZ encapsulated by the same vector concentration is lower in POEGMEA$_{40}$-*b*-P(NIPAAM$_{150}$-*s*-PA-*β*-cyclodextrin$_{11}$). However, the cytotoxicity of the block copolymer is significantly higher leading to more than 90 % cell death even at low concentration.

A remarkable effect is observed using the acetylated polymer. Even very small concentrations lead to more than 90% of cell death. This drug carrier is therefore highly effective owing to the higher ABZ loading, but could also have other origins. To understand these effects further studies are warranted. The increased toxicity may be the preferred cellular uptake of carriers carrying PEG moieties by the cell, but further studies, including drug-release rates, are needed to understand this effect.

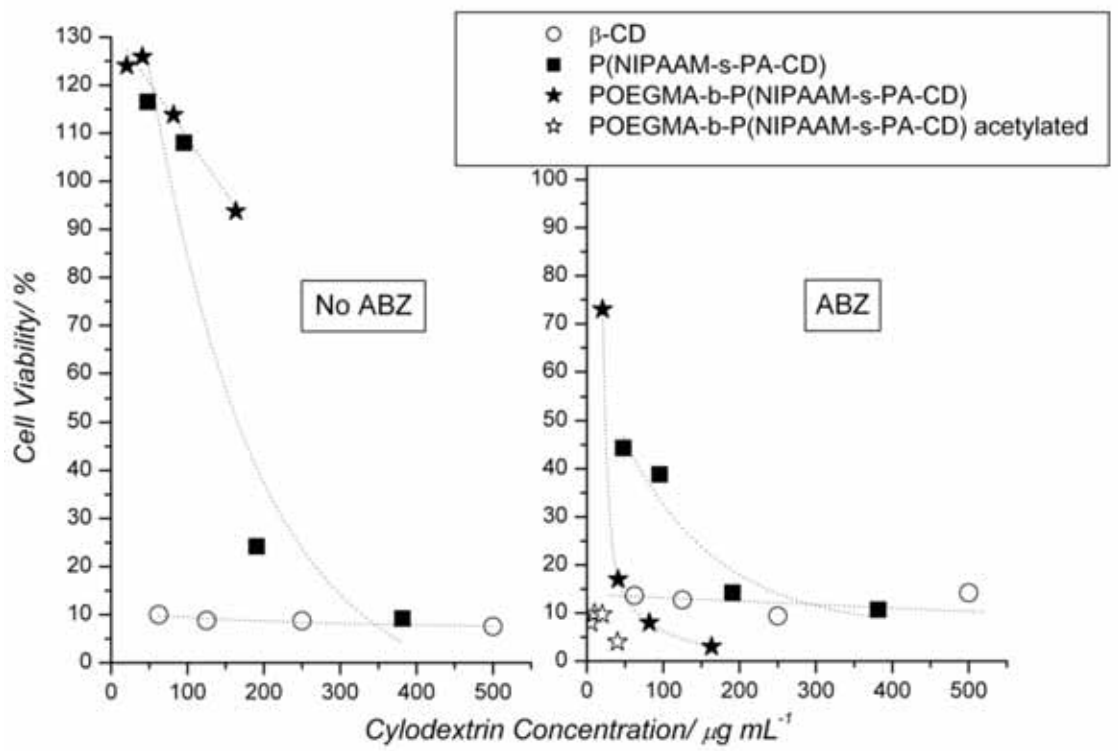

Figure 5.28 *Cell viability test using OVCAR-3 ovarian cancer cell lines with β-cyclodextrin, statistical copolymer P(NIPAAM$_{116}$-s-PA-β-cyclodextrin$_{43}$), and the block copolymer POEGMEA$_{40}$-b-P(NIPAAM$_{150}$-s-PA-β-cyclodextrin$_{11}$) and the acetylated block copolymer before ABZ loading (left) and after ABZ loading (right).*

5.4 Conclusion

A biocompatible drug delivery system has been created which combines the host-guest complexation of β-cyclodextrin with the possibility of targeting a tumor passively by employing polymers. The host-guest complexation between the drug albendazole and the cyclodextrin carrying polymer was highly dependent on the fine-structure of the polymer. Loading efficiencies affected the performance of the drug carrier but also the LCST of the PNIPAAM block. Higher loading led to increased cytotoxicity but also to increased LCST values since the host-guest complex mainly buries the hydrophobic part of the drug while the hydrophilic part is exposed. The cytotoxicity results can potentially be correlated to the loading capacity but more studies are needed to fully understand how the structure of the polymer affects drug release and cellular uptake.

Chapter 6: Shell Crosslinking of Cyclodextrin-based Micelles via Supramolecular Chemistry for the Delivery of Drugs

A polymer with a block based on poly(*N*-isopropyl acrylamide) (PNIPAAm) and a block with a statistical distribution of 2-hydroxyethyl acrylate (HEA) and trimethylsilylpropargyl methacrylate **(**TMSPA) was prepared via reversible addition fragmentation chain transfer (RAFT) polymerization leading to PNIPAAm$_{80}$-*b*-P(HEA$_{12}$-*s*-TMSPMA$_{18}$). Subsequent deprotection and click reaction with 6I-azido-6I-deoxy-*β*-cyclodextrin resulted in polymers with pendant *β*-cyclodextrin groups. The block copolymer underwent reversible micelle formation above the lower critical solution temperature (LCST). Loading of albendazole (ABZ) into the cyclodextrin cavity slightly increased the LCST to 42 °C. Addition of poly(2-hydroxyethyl acrylate-*s*-adamantylmethyl acrylate) P(HEA$_{17}$-*s*-AdMA$_{7}$) above the LCST of the block copolymer led to capture of the micelle structure and nanoparticles of 36 nm, that were stable at ambient temperature against disassembly, were obtained. The drug loaded supramolecular assembly, which was fixed via host-guest complexation between *β*-cyclodextrin and adamantane, was then tested as drug carrier. Cell viability studies using OVCAR-3 cell lines show a higher toxicity of the shell-crosslinked micelle compared to the free block copolymer.

6.1 Introduction

Drugs molecules are commonly hydrophobic and their poor pharmacokinetics resulted in the failure of clinical trial.[272] In order to improve their water solubility, thermodynamic, and kinetics stability, nanoscale materials including liposomes, polymer/drug conjugates, polymer-DNA complexes (polyplexes) and polymeric micelles are utilized.[273] Polymeric micelles are promising drug carriers due to their ability to encapsulate hydrophobic drugs while big enough in size to prevent fast clearance from the kidney.[274] They can also exert the enhanced permeation and retention (EPR) effect in solid tumors.[275] The importance of polymeric micelles in drug delivery has frequently been highlighted in various reviews.[272-273, 276-282]

Drugs are frequently physically encapsulated into micelles albeit this pathway is not always suitable and the loading capacity can be difficult to control. Alternatively, conjugation of the drug to the polymer backbone can be a mean to increase loading, but this technique is only suitable when the drug can be cleaved from the polymer.[283] A different pathway is the encapsulation of the drug via host-guest chemistry such as the formation of inclusion complexes between cyclodextrins and drugs.[223] Although cyclodextrin can enhance water-solubility, it cannot display the EPR effect to the same extend nano-sized carrier can. The need for nano-sized drug carriers with cyclodextrin building blocks were recognized earlier and structures such as nano-sponges were created.[284-285] One way of achieving this aim is by combining cyclodextrins with micelles, which are based on block copolymers with cyclodextrin pendant groups.[286]

Polymeric micelles[287] are formed when the block copolymers self-assemble in the aqueous environment above critical micelle concentration and temperature, with the hydrophilic (water-loving) block forming the shell/corona, whilst the hydrophobic (lypophilic) block build up the core. Once assembled, dissociation into unimers is prevented by strong interaction between the core forming blocks.[276] Due to the high dissolution in the blood circulation system, high kinetic stability can be important for

polymeric micelles. Micelles were frequently crosslinked to prevent disintegration at low concentrations or upon environmental changes, which could in addition have the effect that cellular uptake is enhanced.[288] Hence, cross-linking is a convenient approach to develop a more robust delivery system. Crosslinking can be done at the core of the micelles,[289-291] along the interface between hydrophobic and hydrophilic blocks,[292] and at the shell.[293-298] The scope of crosslinking chemistry is extensive and has been reviewed elsewhere.[299] The most popular approach to cross-link micelle is through covalent bond formation,[300] but also interpolymer complexation via electrostatic interactions or hydrogen bonding become increasingly popular.[301] Polyion complex micelles have the advantage that crosslinking is reversible. Trigger can be ionic strength,[132] temperature and pH.[302-303] Covalently crosslinked micelles in contrast require degradable groups such as ketals/acetals[304-306] and disulfide[292, 307-308] to achieve the same.

Cyclodextrin host-guest chemistry is a powerful tool to introduce dynamic cross linking points to a polymer system.[252, 309] Very recently it became a popular tool to design hydrogels,[252, 310-314] but also graft copolymers[315] and block copolymers were created.[316] Also nano-assemblies were described, that were simply held together via supramolecular forces.[317-319] Many of these examples employ adamantane as the guest of *β*-cyclodextrins. The complex with a 1:1 ratio has a high equilibrium constant, which is driven by hydrophobic and van der Waals forces[320] and is comparable in strength to protein-ligand system.[321]

In this work, we describe the first example of a shell-cross linked micelle that owes their stability to supramolecular forces between *β*-cyclodextrin and adamantane. A block copolymer composed of poly(*N*-isopropylacrylamide) (PNIPAAm) for the core and a water-soluble statistical copolymer of poly(*N*-hydroxyethylacrylate) (PHEA) and a building block with pendant *β*-cyclodextrin were prepared by a combination of RAFT (reversible addition fragmentation chain transfer) polymerization and *click* chemistry. Cross-linking using an adamantyl containing polymer can then capture the micelle, which are formed when the aqueous block copolymer solution has been heated above the LCST

of NIPAAm. The dual functionality of cyclodextrin as crosslinking point and as drug carrier is then demonstrated by loading albendazole (ABZ) as guest (**Scheme 6.1**).

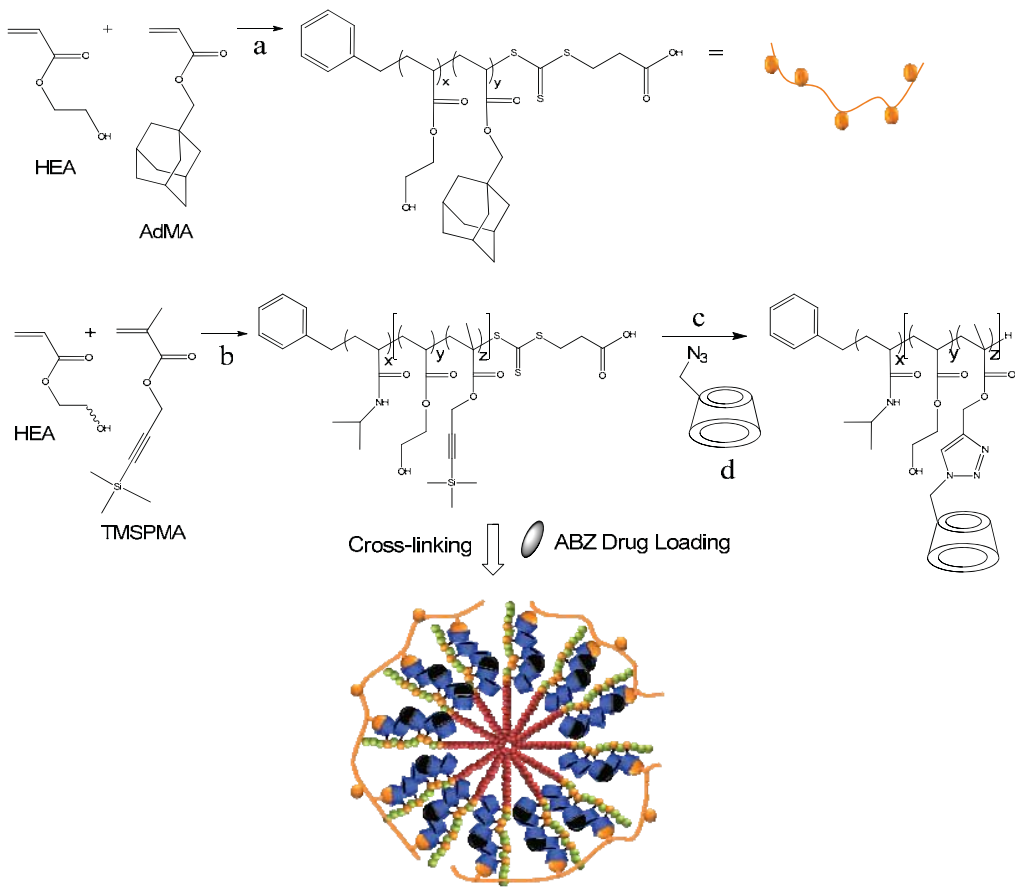

Scheme 6.1 *Schematic approach to thermo-responsive cross-linked micelles based on block copolymers with pendant β-cyclodextrin. (a): 3-BSPA, AIBN, toluene, 60 °C; (b): 3-BSPA, AIBN, DMAc, 60 °C; (c): TBAF, AcOH, THF; (d): CuAAC, DMF, 100 °C for 96 h.*

6.2 Experimental part

6.2.1 Materials

The synthesis of RAFT agent, 3-benzylsulfanylthiocarbonylsulfanyl propionic acid (3-BSPA), is described elsewhere.[235-236] 3-BSPA is a trithiocarbonate more suitable for polymerizing acrylates (TMSPMA, HEA, and AdMA) and acrylamide such as NIPAAM. 3-Mercaptopropionic acid, carbon disulphide, benzyl bromide, *N*-isopropyl acrylamide (NIPAAm), propargyl alcohol, acryloyl chloride, methacryloyl chloride, 2-hydroxyethyl acrylate (HEA), chlorotrimethylsilane (CTMS), silver chloride, anhydrous magnesium sulfate, 1,8-diazabicyclo[5.4.0]undec-7-ene (DBU), *p*-toluenesulfonyl chloride (PTSC), sodium azide, tetrabutylammonium fluoride (TBAF), silica gel, sodium azide, 1-adamantane methanol, potassium carbonate, sodium hydrogen carbonate, sodium hydroxide, zinc, hydrochloric acid, ammonia solution, pentaerythritol tetrakis(3-mercaptopropionate), and albendazole (ABZ) were purchased from Sigma-Aldrich and used as received. 2,2'-azobisisobutyronitrile (AIBN) was purified by recrystallization twice in methanol. Triethylamine was dried using molecular sieves overnight prior to use and *β*-cyclodextrin was recrystallized from water. All solvents used were of analytical grade, except acetone and ethanol. Distilled water from Ultrapure was used throughout this work. All chemicals were used as received unless stated otherwise.

6.3 Synthesis and Methods

6.3.1 Synthesis of trimethylsilylpropargyl methacrylate (TMSPMA)

The synthesis of TMSPMA was carried out in a two-stage process. Propargyl methacrylate [237] was synthesized first and later reacted with chlorotrimethylsilane to obtain TMSPMA.[238] Initially, methacryloyl chloride (10.06 mL, 1.03×10^{-1} mol) was added dropwise to a stirred solution of propargyl alcohol (5 mL, 8.60×10^{-2} mol) and

triethylamine (14.4 mL, 1.03×10^{-1} mol) in dichloromethane (400 mL) at 0 °C. The clear solution turned yellow. The reaction mixture was allowed to reach room temperature resulting in darkening of the solution. The mixture was stirred overnight and then quenched with saturated sodium hydrogen carbonate solution. The organic layer was extracted with 10% hydrochloric acid (3 x 30 mL), saturated sodium hydrogen carbonate solution (1 x 30 mL), and water (1 x 30 mL), dried over magnesium sulphate, filtered through neutral alumina, concentrated *in vacuo* to obtain green/yellow propargyl acrylate (87% yield). In the second stage, silver chloride (1.56 g, 1.06×10^{-2} mol) was suspended in 154 mL of dry dichloromethane. Propargyl methacrylate (13.90 g, 1.12×10^{-1} mol) and DBU (21.4 mL, 1.43×10^{-2} mol) were added to this suspension. A dark red color was observed. The reaction mixture was then heated to 40 °C and chlorotrimethylsilane (21.2 mL, 1.59×10^{-1} mol) was added dropwise and continued to be stirred for the next 24 h. The dark solution obtained was diluted with *n*-hexane (400 mL) and the organic phase was washed successively with saturated aqueous sodium hydrogen carbonate, hydrochloric acid (1%) and water, dried over magnesium sulfate, filtered, and concentrated *in vacuo*. The crude product obtained was purified by column chromatography eluting with a 25:1 mixture of *n*-hexane and diethyl ether to obtain colorless trimethylsilylpropargyl methacrylate liquid (74.1% yield).

6.3.2 Synthesis of PNIPAAm macro-RAFT agent

NIPAAm was recrystallized from *n*-hexane and 2,2'-azobisisobutyronitrile (AIBN) was recrystallized twice from methanol. NIPAAm (3.39 g, 3.00×10^{-2} mol) was mixed with RAFT agent (3-BSPA) (32.6 mg, 1.20×10^{-4} mol) inside a 25 mL round-bottomed flask. A stock solution of 1.20×10^{-5} mol L^{-1} of AIBN with *N*,*N*-dimethylacetamide (DMAc) was prepared and 10 mL of this solution was added to the flask. The molar ratio used was [NIPAAm]:[RAFT agent 3-BSPA]:[AIBN] = 2500:10:1. The solution was then placed into a 1 cm quartz cuvette, sealed with rubber septum, and degassed by purging nitrogen through the solution for 1 h. The polymerization was run at 60 ^{o}C in the FT-IR and the progress of polymerization was monitored on-line. The polymerization was stopped after 4 h when 32% conversion was obtained. After polymerization, the solid yellow polymer

was recovered by precipitation in diethyl ether and dried under reduced pressure. The polymer was analyzed using NMR and SEC to confirm the monomer conversion and to determine molecular weight, respectively. Theoretical M_n of $PNIPAAm_{80}$ macro-RAFT agent calculated to be $M_{n\ (NMR)}$= $M_{n\ (SEC)}$= 9 300 g mol^{-1}. Size exclusion chromatography (SEC) determined number-average molecular weight $M_{n\ (SEC)}$= 23 000 g mol^{-1}, PDI= 1.18 (polystyrene standards).

6.3.3 Synthesis of PNIPAAm-*b*-P(HEA-*s*-TMSPMA) block copolymer

The molar ratio [HEA]:[TMSPMA] = 50:50 was employed. HEA (7.26 x 10^{-2} g, 6.25 × 10^{-4} mol), TMSPMA (1.23 x 10^{-1} g, 6.25 × 10^{-4} mol) and PNIPAAm macro-RAFT agent (2.33 x 10^{-1} g, 2.50 × 10^{-5} mol) were dissolved in 625 μL of AIBN stock solution in *N*,*N*-dimethylacetamide (DMAc) (6.50 × 10^{-1} mol L^{-1}). The final ratio was [HEA + TMPSA]:[PNIPAAm macro-RAFT agent]:[AIBN] = 500:10:1, with a total monomer concentration of 2M. The 1 cm quartz cuvette was sealed and the solution was degassed using nitrogen for 1 h. The polymerization was carried out at 60 ^{o}C using FT-NIR and the progress of polymerization was monitored on-line. The polymerization was stopped after 10 h when 75% of conversion was obtained. The polymers were analyzed using NMR and SEC analyses to confirm monomer conversion and to determine molecular weight, respectively. The block copolymers were purified by dialysis (12 000 molecular weight cut-off) for 48 h in ethanol and then 48 h in water followed by freeze-drying to obtain $PNIPAAm_{80}$-*b*-P(HEA_{12}-*s*-$TMSPMA_{18}$). Theoretical number-average molecular weight calculated using conversion was $M_{n\ (theo)}$= 14 200 g mol^{-1}. The number-average molecular weight $M_{n\ (SEC)}$= 29 000 g $mol^{-1,}$ PDI= 1.38 (polystyrene standards) was determined by SEC.

6.3.4 Deprotection of block copolymer

The deprotection was done according to the method reported previously.[286] The trimethylsilyl protecting group from 174 mg of PNIPAAm$_{80}$-*b*-P(HEA$_{12}$-*s*-TMSPMA$_{18}$) block polymer was cleaved using acetic acid, tetrabutylammonium fluoride (TBAF·3H$_2$O), and THF for 48 h. PNIPAAm$_{80}$-*b*-P(HEA$_{12}$-*s*-PMA$_{18}$) was obtained after deprotection, dialysis, and freeze drying.

6.3.5 Synthesis of 6I-azido-6I-deoxy-*β*-cyclodextrin

β-cyclodextrin was monotosylated before azidification to obtain 6I-azido-6I-deoxy-*β*-cyclodextrin (*β*-cyclodextrin azide).[240, 286] Mass spectrometry results confirmed the purity of mono-6-*p*-toluenesulfonyl-*β*-cyclodextrin (*m/z* = 1311.4 [M+Na$^+$]) and 6I-azido-6I-deoxy-*β*-cyclodextrin (*β*-cyclodextrin azide) (*m/z* = 1182.6 [M+Na$^+$]). Yield = 81.0%.

6.3.6 Huisgen azide-alkyne 1,3-dipolar cycloaddition reaction between *β*-cyclodextrin azide and block copolymer

Prior to reaction of *β*-cyclodextrin azide, the PNIPAAm$_{80}$-*b*-P(HEA$_{12}$-*s*-TMSPMA$_{18}$) block copolymer was deprotected using tetrabutylammonium fluoride. The polymer lost its color due to the cleavage of the RAFT group during the procedure, probably replaced by a hydrogen as earlier as mass spectroscopy analysis indicated.[246] NMR analysis confirmed the efficient removal of the protective group and the loss of the RAFT end group yielding PNIPAAm$_{80}$-*b*-P(HEA$_{12}$-*s*-PMA$_{18}$). A procedure from literature has initially been adopted for the Huisgen azide-alkyne 1,3-dipolar cycloaddition using a copper-catalyzed *click* system using copper(II) sulfate pentahydrate/ascorbic acid at 140 °C.[26] However, from ^{1}H NMR analysis it was found that the clicking efficiency was only 11%. The procedure was used with modifications; the temperature was reduced to 100 ^{o}C while the reaction time was increased to 96 h ensuring 100% clicking efficiency. The

polymer was purified by dialysis against water in MWCO 3500 dialysis bag for 4 days with frequent changes of water before being freeze-dried to obtain PNIPAAm$_{80}$-*b*-P(HEA$_{12}$-*s*-PMA-*β*-CD$_{18}$) amphiphilic block copolymer. Mn$_{(NMR)}$ = 33 548 g mol^{-1}, Mn$_{(SEC)}$ = 47 000 g mol^{-1}, PDI = 1.77.

6.3.7 Copper removal from block copolymer

The residual copper in the polymer must be removed prior to the ABZ drug loading and cell tests. The polymers were purified until the solution did not absorb within the visible spectrum. There were 3 major steps used. In the first step, the block copolymer was dissolved in water and filtered through neutral alumina. In the second step, the 4-arm thiol pentaerythritol tetrakis(3-mercaptopropionate) was added drop wise to the filtered solution,[322] and stirred for 2 h at room temperature until an emulsion was formed. This emulsion was then centrifuged until the white precipitate of copper-thiol complex settled at the bottom. The remaining solution was almost colorless. In the final step, the aqueous solution was filtered, dialyzed in ammonia solution for 24 h and water for another 48 h before freeze-drying.

6.3.8 Synthesis of 1-adamantylmethyl acrylate (AdMA) monomer

The synthesis was carried out according to a procedure described in literature[323] but with slight modifications. A three times molar excess of acryloyl chloride and triethylamine was used to ensure the completion of the reaction. The monomer can be used directly without purification by column chromatography. A yellow viscous liquid was obtained which turned to a colourless solid upon refrigeration. Yield = 70.0%.

6.3.9 Synthesis of P(HEA-*s*-AdMA) cross-linker

2-hydroxyethylacrylate (HEA, 1.3934 g, 1.20 x 10^{-2} mol), 1-adamantylmethyl acrylate (AdMA, 0.6609 g, 3.00 x 10^{-3} mol), 3-BSPA RAFT agent (0.1360 g, 5.00 x 10^{-4} mol) and

AIBN (0.0246 g, 1.50 x 10^{-4} mol) were dissolved with 5.00 mL of toluene. The ratio used was [monomers]:[RAFT]:[AIBN] = 30:1:0.3 with an initial monomer concentration of 3M. The solution was degassed for 75 min, then polymerized at 60 ^{o}C using online FT-NIR and stopped when the conversion was 80%. Total polymerization time was eight hours. The crude polymer solution was initially dialyzed in water : ethanol = 1:1 and then in water only. After freeze-drying, the water-soluble yellow polymer was analyzed by ^{1}H NMR and SEC (polystyrene standard) to obtain P(HEA$_{17}$-*s*-AdMA$_{7}$). $Mn_{(theo)}$ = 3 788 g mol^{-1}, $Mn_{(SEC)}$ = 14 000 g mol^{-1}, PDI = 1.46.

6.3.10 Micelles cross-linking

2 mg of PNIPAAM$_{80}$-*b*-P(HEA$_{12}$-*s*-PMA-*β*-CD$_{18}$) block copolymer containing 1.08 x 10^{-6} mol of cyclodextrin moieties was dissolved in 2 mL of water at 50°C before adding P(HEA$_{17}$-*s*-AdMA$_{7}$) (cyclodextrin : adamantyl = 10:1), followed by stirring for 6 h at 50 ^{o}C. The solution was analyzed by DLS. The solution for ^{1}H NMR ROESY was prepared by using deuterium oxide instead of water.

6.3.11 Addition of competing ligand to the cross-linked micelles

β-cyclodextrin (1.5 mol times of the *β*-cyclodextrin moieties in block copolymer) was added to the aforementioned crosslinked micelle solution as a competing ligand and the solution was stirred at room temperature for 6 h prior to DLS analysis.

6.3.12 Albendazole loading in micelles

20 mg of PNIPAAm$_{80}$-*b*-P(HEA$_{12}$-*s*-PMA-*β*-CD$_{18}$) copolymer was dissolved in 4 mL of water while albendazole (ABZ) was dissolved in 4 mL of THF. The molar ratio between ABZ and cyclodextrin were 10:1, but also 7:1 and 3:1 were investigated. The ABZ solution was then added dropwise to the polymer solution while stirring until a clear solution was formed. The temperature was raised to 40 ^{o}C and the solution was stirred for an hour. Water was added slowly until the solution became cloudy. Stirring was then

continued for another 24 h while the reaction vessel was kept closed. Subsequently, THF was evaporated by opening the flask, which was accompanied by visible precipitation of albendazole. The unloaded drug was removed filtering the solution through a 0.45 μm filter, followed by freeze-drying of the solution. For crosslinking purposes, the P(HEA$_{17}$-*s*-AdMA$_{7}$) crosslinker was added after filtration and the solution was stirred again at 50 ^{o}C for another 4 h before freeze-drying. For ABZ loading analysis via ^{1}H NMR, the dried solid together with 0.50 μL of styrene as internal standard were dissolved in deuterated DMSO. Meanwhile, for DLS analysis, the dried solid was dissolved in water at concentration of 0.5 g mL^{-1}.

6.3.13 2D ROESY NMR characterization of complex between *β*-cyclodextrin and ABZ

40 mg of *β*-CD was dissolved in 6 mL of water while 93.6 mg of ABZ (*β*-CD:ABZ = 1:10) was dissolved in 12 mL of THF. The THF was added and stirred until the ABZ solution turned clear. Both clear solution was mixed together and stirred for 1 h at room temperature. The water was added dropwise slowly until the solution turned turbid. The solution was then stirred at high speed at 40 ^{o}C for 24 h. Next, THF was evaporated slowly under reduced pressure at 40 ^{o}C for 48 h. After the THF has been removed, the remaining dispersion was filtered using 0.45 μm filter to remove the unloaded drug. The clear solution was freeze-dried for 72 h to remove water and traces of THF. Only 20.5 mg of dried solid was dissolved in 400 μL of D_2O for ROESY analysis.

6.3.14 Drug release studies

After drug loading and freeze-drying, 20 mg of ABZ-loaded polymer was dissolved in 2 mL of water at a total concentration of 10 mg mL^{-1}. The 2 mL solution was then placed into a dialysis bag and dialyzed for 48 h in 100 mL of water with slow stirring at 37 ^{o}C. 4 mL of samples (outside the dialysis bag) were taken at each interval; 0, 2, 4, 6, 8, 24, 32, and 48 h. The sampled solutions were then subject to HPLC analysis.

6.3.15 In vitro cytotoxicity tests

Human ovarian cancer OVCAR-3 cells were seeded in 96-well plates (3 000 cells per well) with culture medium 10% RPMI-1640 [2 x 10^{-3} M L-glutamine, 1.5 g L^{-1} sodium bicarbonate, 0.010 M of 2-hydroxyethylpiperazinesulfonic acid (HEPES), 4.5 g L^{-1} glucose, 1.00 × 10^{-3} M sodium pyruvate at 37 ^{o}C in 5% CO_2 environment for 24 h. The medium was refreshed with 0.2 mL of a solution consisting of 0.1 mL medium and 0.1 mL of micelle solution of PNIPAAm$_{80}$-*b*-P(HEA$_{12}$-*s*-PMA-β-CD$_{18}$) cross-linked without copper removal, PNIPAAm$_{80}$-*b*-P(HEA$_{12}$-*s*-PMA-β-CD$_{18}$) cross-linked after copper removal, ABZ loaded PNIPAAm$_{80}$-*b*-P(HEA$_{12}$-*s*-PMA-β-CD$_{18}$) uncross-linked after copper removal, and ABZ loaded PNIPAAm$_{80}$-*b*-P(HEA$_{12}$-*s*-PMA-β-CD$_{18}$) cross-linked after copper removal to reach a final micelle concentration of 25, 75, 125, and 250 μg ml^{-1}, respectively, followed by incubation at 37 ^{o}C in the incubator for 72 h. Subsequently, the medium was removed and washed 5 times with tap water and 5 times with 1% acetic acid. After drying overnight, 100 μg of 0.010 M Tris (pH = 10.5) was added to solubilise the dye. Absorbance was measured at 570 nm using Σ960 platereader (Metertech, Taiwan). Non-treated cells were used as controls. The absorbance was measured at 570 nm and the optical density (OD) was used to calculate cell viability [cell viability = (test – blank) / (control – blank) x 100]:

Cell viability (%) = $[(OD_{570,sample} - OD_{570,blank}) / OD_{570,control} - OD_{570,blank})] \times 100$

6.3.16 Preparation of buffer solutions

For acetate buffer pH 5.5, the concentration was 20 mM. 181 mg acetic acid and 2.31 g sodium acetate were dissolved in 1L of water. For phosphate buffer pH 7.4, 250.7 mg of sodium dihydrogen orthophosphate (monobasic) and 1.68 g di-sodium hydrogen orthophosphate (dibasic) were dissolved in 400 mL of water. The buffer solutions were used for size measurement of micelles in acidic or slightly basic conditions.

6.3.17 Self-assembly and thermal properties of micelles

Solution of both ABZ loaded and unloaded copolymers were prepared at the concentration of 1 mg mL^{-1} in water. The solution was filled into a quartz cuvette after passing through 0.45 μm filter to remove dust. The cuvette was placed in a dynamic light scattering (DLS) particle size analyzer. The temperature was increased slowly from 20 to 50 ^{o}C, with 20 min stabilization period before measurement at each temperature. The change of the average particles diameters or mean count rate vs. temperature was then observed.

6.4 Analysis

6.4.1 NMR spectroscopy

NMR spectra were recorded using a Bruker 300 MHz spectrometer; samples were analyzed in $CDCl_3$ and d_6-DMSO at 25 ^{o}C.

6.4.2 Fourier transform- near infrared (FT-NIR) spectroscopy

The rate of the polymerization was monitored on-line for the synthesis of the $PNIPAAm_{80}$ macro-RAFT agent and $P(HEA_{17}$-*s*-$AdMA_7)$ polymer crosslinker syntheses. The spectra were recorded on a Perkin-Elmer FT-NIR spectrometer. The scanning range was 400-8000 cm^{-1} and the resolution was 1 cm^{-1}. The temperature used for both polymerizations was 60 ^{o}C and the conversion was calculated based on the peak assigned to the vinylic double bond between 6100 and 6250 cm^{-1}.

6.4.3 Size exclusion chromatography (SEC)

Molecular weight distributions of the copolymer systems were determined by means of SEC using a Shimadzu modular system, comprising an autoinjector , a Polymer Laboratories (PL) 5.0 μm bead-size guard column (50 x7.5 mm^2), followed by three linear PL columns (10^5, 10^4, 10^3) and a differential-refractive-index detector. The eluent was DMAc (0.05% w/v LiBr, 0.05% 2,6-di-butyl-4-methylphenol) at 50 ^oC with a flow rate of 1 mL min^{-1}. The system was calibrated using narrowly dispersed polystyrene standards ranging from 500 to 10^6 g mol^{-1}. The polymer (5 mg) was dissolved in 2 mL DMAc, followed by filtration using a filter with a pore size of 0.45 μm.

6.4.4 Dynamic light scattering (DLS)

Hydrodynamic diameters and scattering intensity of copolymers in water were obtained using a Malvern Zetasizer Nanoseries Nano ZS particle size analyzer. The temperature range used was from 20-50 ^oC.

6.4.5 High pressure liquid chromatography (HPLC)

A gradient reverse HPLC was used to investigate the ABZ release from the $PNIPAAM_{80}$-*b*-P(HEA_{12}-*s*-PMA-β-CD_{18}) micelles. A Polymer Laboratories Jupiter C-18 analytical column 5 μm, 3.9 x 300 mm^2 was used. Gradient elution was performed at a flow rate of 1 mL min^{-1} with a mobile phase consisting of solution A = 100% acetonitrile, buffer solution solution B = 30% acetonitrile (volume), 70% water (volume), 0.01M phosphoric acid (weight), 5mM tetrabutylammonium hydrogen sulphate (weight). The buffer solution was filtered with a 0.45 μm filter before use. The mobile phase was programmed to run a mixture of 30:70 of Solution A and Solution B. ABZ retention time was found to be 10.6 min.

6.4.6 Transmission electron microscopy (TEM)

The TEM micrographs were obtained using a JEOL 1400 transmission electron microscope. The instrument operates at an accelerating voltage of 100 kV. Samples were negative stained with phosphotungstic acid (2 wt.-%). A Formvar-coated grid was coated by casting a polymer aqueous solution for 1 min. Excess solution was removed using filter paper. For staining, a drop of phosphotungstic acid was gently applied onto the surface of the grid for 30 s. The stained grid was dried under air.

6.5 Results and Discussion

RAFT polymerization was chosen to construct the copolymers due to its simplicity and ability to control polymer architectures.[324] PNIPAAm was identified as a suitable core-forming block: It does not encapsulate albendazole by physical interaction and therefore drug loading can only take place via host-guest chemistry; in addition, the block copolymer is fully water soluble, which facilitates clearance of the polymer from the body; furthermore, the thermo-responsive nature of the polymer signals immediately successful crosslinking. Therefore, NIPAAm was polymerized in *N*,*N*-dimethylacetamide (DMAc) using 3-benzylsulfanylthiocarbonylsulfanyl propionic acid (3-BSPA) as RAFT agent to afforded the $P(NIPAAm)_{80}$ macro-RAFT ($M_{n\ (SEC)}$= 23 000 g $mol^{-1,}$ PDI= 1.18). The polymer was then chain-extended with 2-hydroxyethyl acrylate (HEA) and trimethylsilylpropargyl methacrylate (TMSPMA) at a molar ratio of 1:1. Copolymerization with HEA was deemed necessary because the reaction with *β*-cyclodextrin azide may be otherwise subject to steric congestion.[315] The $PNIPAAm_{80}$-*b*-$P(HEA_{12}$-*s*-$TMSPMA_{18})$ ($M_{n\ (SEC)}$= 29 000 g mol^{-1}, PDI= 1.38, **Figure 6.1 and Table 6.1**) was subsequently deprotected to yield the acetylenyl groups for click reaction. The disappearance of signal at 0.10 ppm in the ^{1}H-NMR (**Figure 6.2**) shows the complete removal of the protecting group while SEC shows a small decline of the molecular weight ($M_{n\ (SEC)}$= 25 000 g mol^{-1}, PDI= 1.38, **Figure 6.1 and Table 6.1**). The signal for the alkyne group at around 3.50 ppm was hidden under the water peak. In a subsequent

step, *β*-cyclodextrin azide was clicked using procedures reported in literature with either employs Cu(I)-catalyzed click reaction at 140°C [26] or the copper-free Huisgen cycloaddition.[286] Both protocols led to incomplete reaction. Finally, conditions at 100 °C at 96 hours in the presence of Cu(I)-catalyst were chosen, which resulted in complete conversion of all acetylenyl groups (**Figure 6.2**). The catalyst was removed via a short alumina column, followed by stirring of the product with tetrakis(3-mercaptopropionate). The polymer was then purified via dialysis against water to remove unreacted *β*-cyclodextrin azide. Complete removal was confirmed *via* SEC, which showed only the final polymer product, but any traces of *β*-cyclodextrin azide were absent ($M_{n\ (SEC)}$= 47 000 g mol^{-1}, PDI= 1.77, **Figure 6.1 and Table 6.1**). The final polymer, PNIPAAm$_{80}$-*b*-P(HEA$_{12}$-*s*-PMA-*β*-CD$_{18}$), was analyzed using ^{1}H-NMR. The anomeric H-1 signal of the seven glucose units in β-cyclodextrin were clearly visible in the final polymer spectra. The glucose unit that serves as attachment point to the polymer via the 1,2,3-triazole functionality has a slight downfield shift.

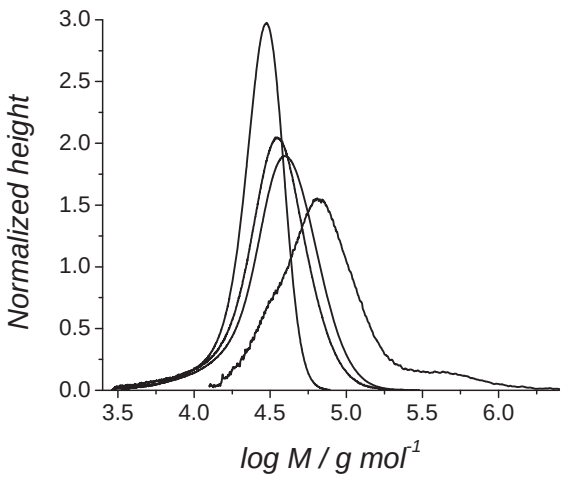

Figure 6.1 *SEC traces of (from left to right) for PNIPAAm$_{80}$ macro-RAFT agent, PNIPAAm$_{80}$-b-P(HEA$_{12}$-s-TMSPMA$_{18}$) block copolymer after deprotection, PNIPAAm$_{80}$-b-P(HEA$_{12}$-s-TMSPMA$_{18}$ before deprotection, and PNIPAAm$_{80}$-b-P(HEA$_{12}$-s-PMA-β-CD$_{18}$). All samples were run in DMAc against polystyrene standard.*

Table 6.1 *Summary of Block Copolymers Synthesized in this Chapter.*

Polymer	$M_{n,theoretical}$/g mol^{-1}	$M_{n,SEC}$/g mol^{-1}	PDI
PNIPAAm$_{80}$ macro-RAFT agent	9 312	23 000	1.18
PNIPAAm$_{80}$-*b*-P(HEA$_{12}$-*s*-TMSPMA$_{18}$)	14 239	29 000	1.38
PNIPAAm$_{80}$-*b*-P(HEA$_{12}$-*s*-TMSPMA$_{18}$ after deprotection	12 668	25 000	1.38
PNIPAAm$_{80}$-*b*-P(HEA$_{12}$-*s*-PMA$_{18}$) after *β*-cyclodextrin attachment	33 548	47 000	1.77
P(HEA$_{17}$-*s*-AdMA$_{7}$)	3 788	14 000	1.46

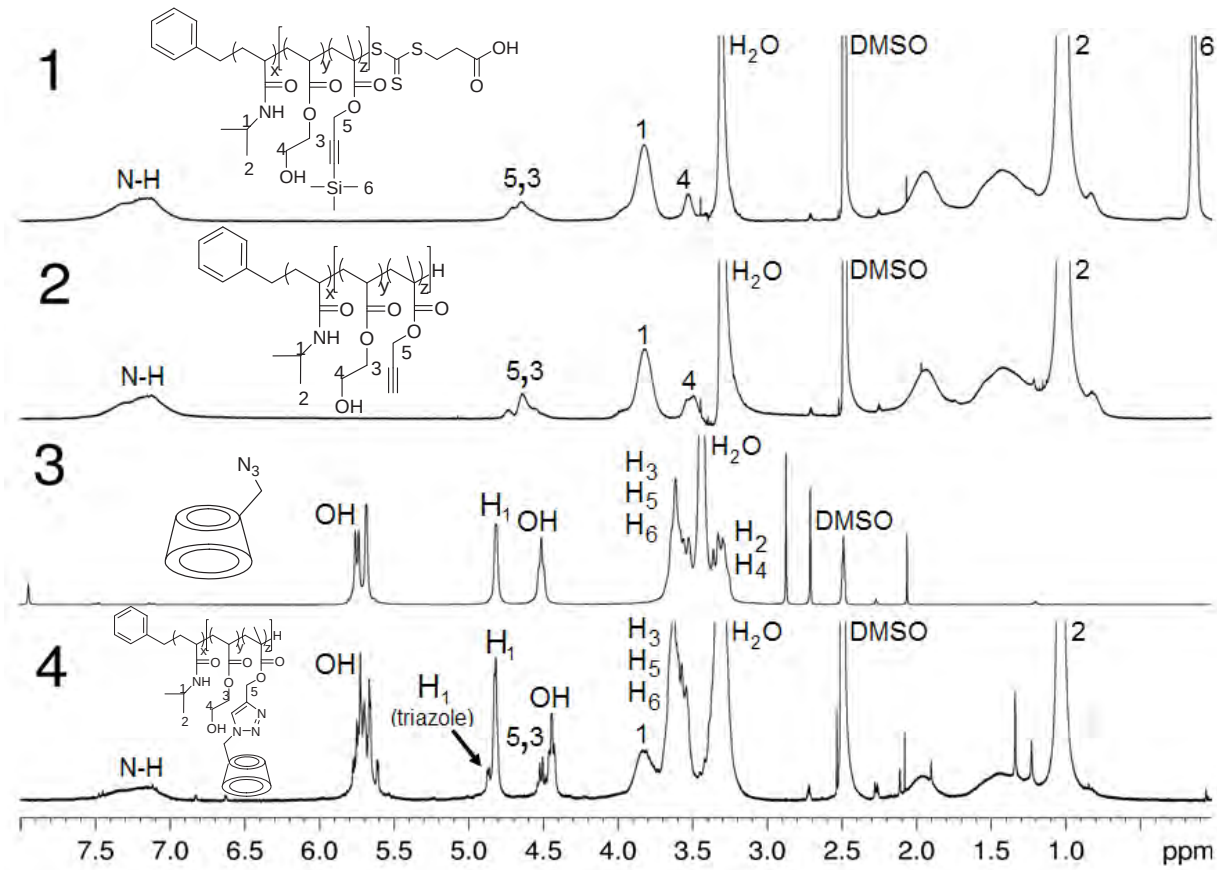

Figure 6.2 *^{1}H NMR analysis (d-DMSO) of (1) PNIPAAm$_{80}$-b-P(HEA$_{12}$-s-TMSPMA$_{18}$), (2) PNIPAAm$_{80}$-b-P(HEA$_{12}$-s-PMA$_{18}$), (3) 6I-azido-6I-deoxy-β-cyclodextrin (β-cyclodextrin azide), (4) PNIPAAm$_{80}$-b-P(HEA$_{12}$-s-PMA-β-CD$_{18}$).*

The repeated heating and cooling cycle monitored by DLS measurement showed that the PNIPAAm$_{80}$-*b*-P(HEA$_{12}$-*s*-PMA-*β*-CD$_{18}$) exhibits a lower critical solution temperature (LCST) at 37 ^{o}C (**Table 6.1**). Above the LCST, micelles of around 40 nm in size were observed while below the LCST the measured hydrodynamic diameter was less than 10 nm, which indicates the presence of free, non-associated block copolymers (**Figure 6.3**). Subsequently, the micelles were loaded with albendazole at various cyclodextrin-albendazole ratios. The aqueous polymer solution was mixed with albendazole in tetrahydrofuran (THF), which is the only solvent that dissolves a reasonable amount of albendazole. THF was then slowly evaporated to ensure that albendazole is given sufficient time to form a host-guest inclusion complex with *β*-CD. A high THF evaporation rate in contrast leads to significant albendazole precipitation in water. The amount of encapsulated albendazole was measured using HPLC after removing insoluble albendazole by filtration. Encapsulation of albendazole into the *β*-cyclodextrin cavity was confirmed using 2D-ROESY (Rotating Frame Overhauser Effect Spectroscopy) NMR in D_2O. The appearance of cross-peaks between the propyl group of albendazole (0.96, 1.69–2.12, and 3.80 ppm) and the *β*-CD cavity protons (H_3, H_5, and H_6 at 3.63–4.06 ppm) and the increase in the multiplicity of the signals for the propyl protons confirm the complex formation (**Figure 6.4**).[93] In addition, the cross peaks between the aromatic ring and the *β*-CD cavity protons (**Figure 6.4**) suggest an inclusion complex similar to the structure depicted in **Figure 6.4**. The amount of loaded albendazole increased with the amount of the drug which has been used for incubation. While overall loading efficiency seems rather low, the solubility of albendazole increased significantly compared to albendazole alone. The amount of loading had a direct effect on the LCST value, which is equivalent to unimers-micelle transition. With increasing albendazole amount, the LCST increases as evidence using the scattering intensity of the solution *vs* the temperature (**Figure 6.5**). Interestingly, the LCST seems to increase with increasing amount of albendazole (**Figure 6.6**). In earlier studies, it has shown that the albendazole-*β*-cyclodextrin complex is more hydrophilic than *β*-cyclodextrin alone.[286] This increased hydrophilicity may contribute to the increase of the LCST of PNIPAAm suggesting some interactions between the core and the shell.

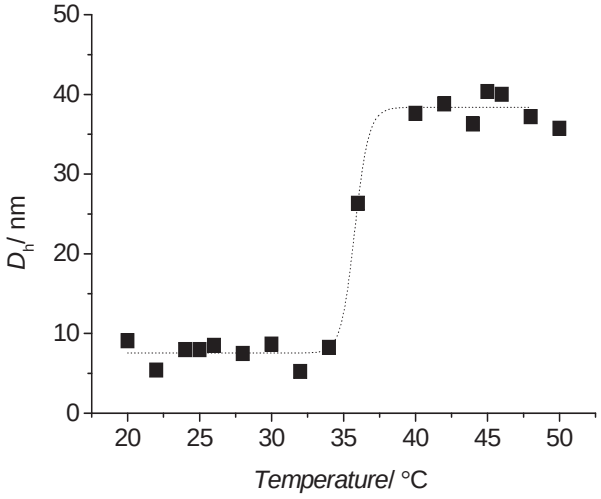

Figure 6.3 *Hydrodynamic diameter of NIPAAm$_{80}$-b-P(HEA$_{12}$-s-PMA-β-CD$_{18}$) in water vs temperature.*

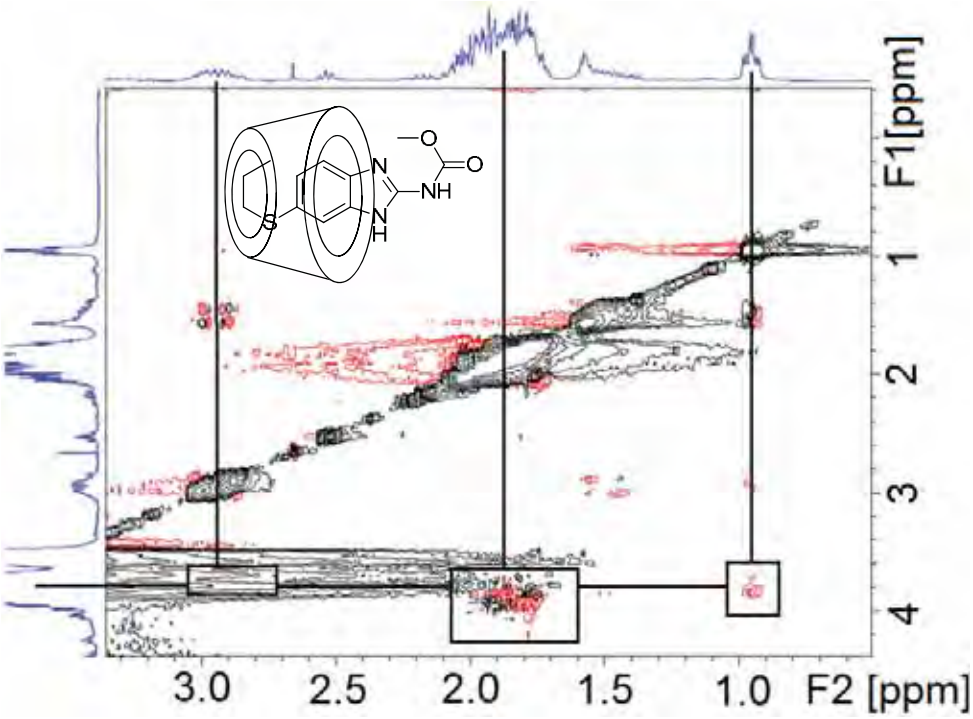

Figure 6.4 (a) *2D ROESY spectra of β-CD/ABZ mixture in D_2O (concentration = 50 g L^{-1}) at 25 °C. The cross-peaks have shown the interaction between propyl group of ABZ and H_3, H_5, and H_6 inside the cavity of β-CD.*

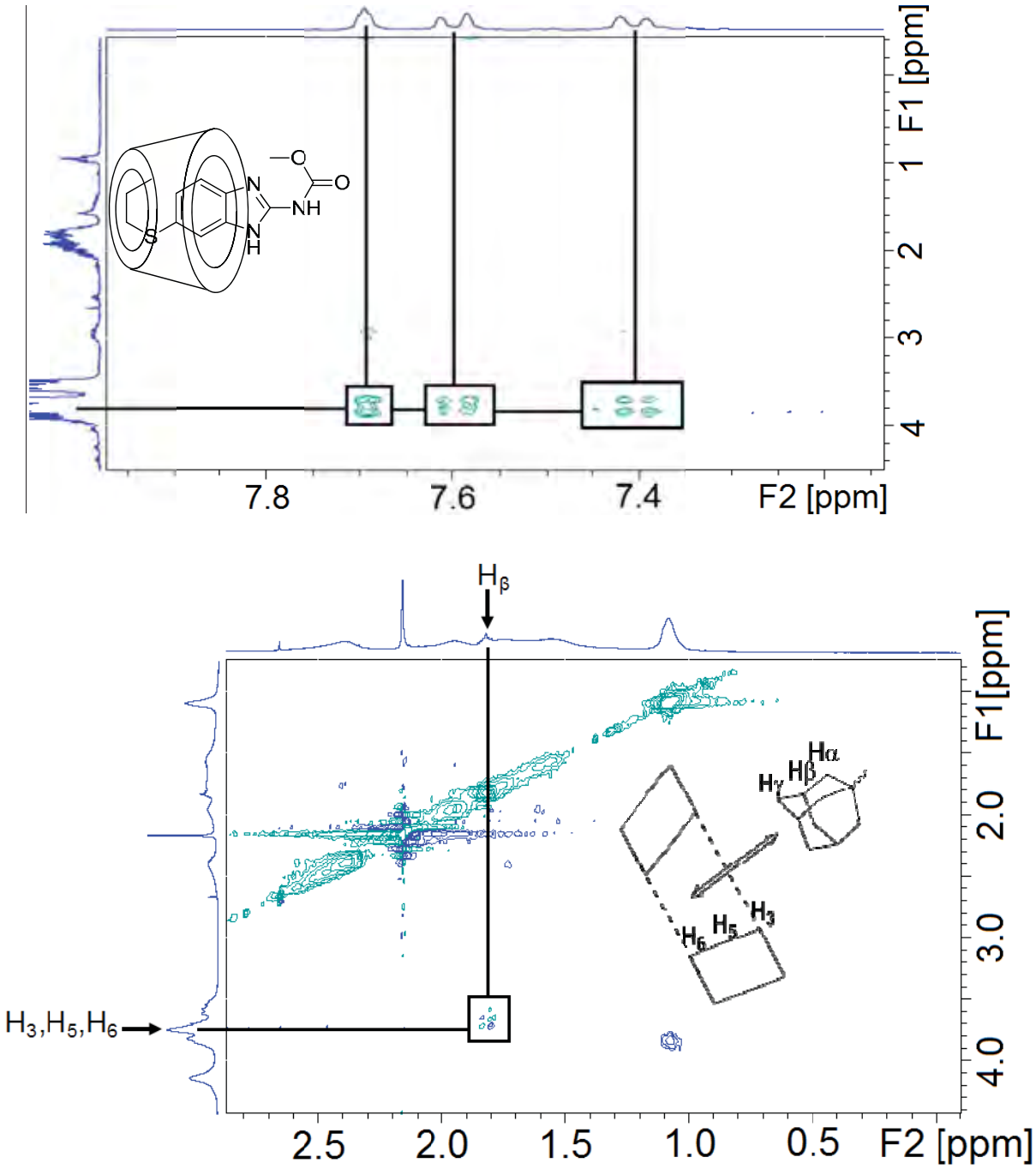

Figure 6.4(b) *Top: 2D ROESY spectra of β-CD/ABZ mixture in D_2O (concentration = 50 g L^{-1}) at 25 °C. The cross-peaks have shown the interaction between phenylic group of ABZ and H_3, H_5, and H_6 inside the cavity of β-CD. Bottom: 2D ROESY spectra of PNIPAAm$_{80}$-b-P(HEA$_{12}$-s-PMA-β-CD$_{18}$) / P(HEA$_{17}$-s-AdMA$_7$) mixture (11.75 g L^{-1}; β-CD : Ada = 10 : 1) in D_2O at 25 °C. H_β is from the adamantyl moieties while H_3, H_5, H_6 are from β-CD moieties.*

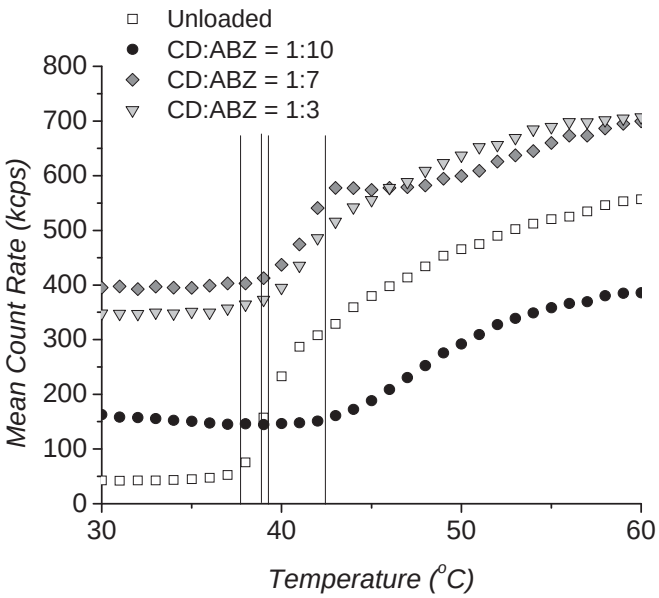

Figure 6.5 *Scattering intensity of NIPAAm$_{80}$-b-P(HEA$_{12}$-s-PMA-β-CD$_{18}$) loaded with various amounts of albendazole in water vs temperature.*

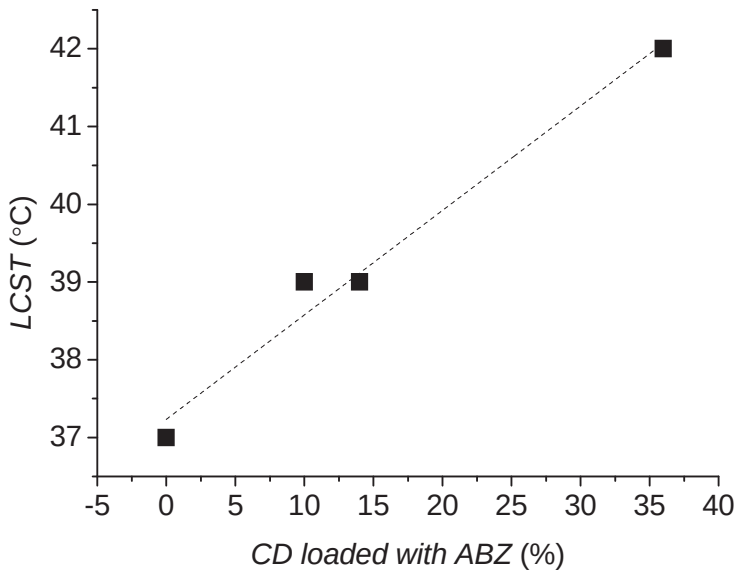

Figure 6.6 *Correlation between NIPAAm$_{80}$-b-P(HEA$_{12}$-s-PMA-β-CD$_{18}$) loaded with various amounts of albendazole (as expressed as the percentage of CD pendant groups that host one albendazole molecule) vs the measured LCST.*

Table 6.2 *Solubility of albendazole using a polymer solution with a concentration of 5 g L^{-1} with various amounts of drug (molar ratio between albendazole and β-cyclodextrin) initially added to the polymer (at different ratios between cyclodextrin and ABZ) and the resulting LCST of the drug-loaded polymer.*

[ABZ]/[CD]	ABZ concentration (g L^{-1})	%CD with ABZ as guest	LCST/ °C	D_h/ nm Above LCST
ABZ only	0.0002		-	-
0	0	0	35	40±5
3	0.069	10%	39	n.m
7	0.099	14%	39	n.m
10	0.255	36%	42	30±8
0-crosslinked	0	0	*	35±6
10-crosslinked	0.255	36%	*	36±3

* LCST cannot be measured due to insufficient changes of the D_h; n.m.: not measured.

Supramolecular chemistry was utilized for cross-linking of the PNIPAAm$_{80}$-*b*-P(HEA$_{12}$-*s*-PMA-*β*-CD$_{18}$) micelles. 2-Hydroxyethyl acrylate (HEA) was copolymerized with 1-adamantylmethyl acrylate (AdMA) in the presence of a RAFT agent (**Scheme 6.1**) to obtain P(HEA$_{17}$-*s*-AdMA$_7$). The polymer was not fully water-soluble and formed a slightly cloudy solution in water. The cross linker P(HEA$_{17}$-*s*-AdMA$_7$) was then added to the aqueous micelle solution of PNIPAAm$_{80}$-*b*-P(HEA$_{12}$-*s*-PMA-*β*-CD$_{18}$) at 40°C (above the LCST) at a ratio between adamantyl groups and *β*-cyclodextrin of 1:10. The solution turned initially slightly cloudy because of the low water-solubility of P(HEA$_{17}$-*s*-AdMA$_7$) but then cleared up with no precipitation or gel formation being visible. The low polymer concentration during this process prevented inter-micellar cross linking. The hydrophobic adamantyl groups were engaged in the inclusion complex with the cyclodextrin moieties leaving only the hydrophilic HEA units exposed. The changes between in the 1H-NMR spectra of PNIPAAm$_{80}$-*b*-P(HEA$_{12}$-*s*-PMA-*β*-CD$_{18}$) and the final product, which was cross linked with P(HEA$_{17}$-*s*-AdMa$_7$), are not significant and could almost be a simple overlay of the spectra of both polymers (**Figure 6.7**). More conclusive is the ^{1}H NMR

ROESY spectra (**Figure 6.4**). The appearance of cross-peaks between protons H_β of the adamantyl group at 1.80 ppm with the *β*-CD cavity protons (H_3, H_5, and H_6 at 3.60 and 3.90 ppm) were observed.

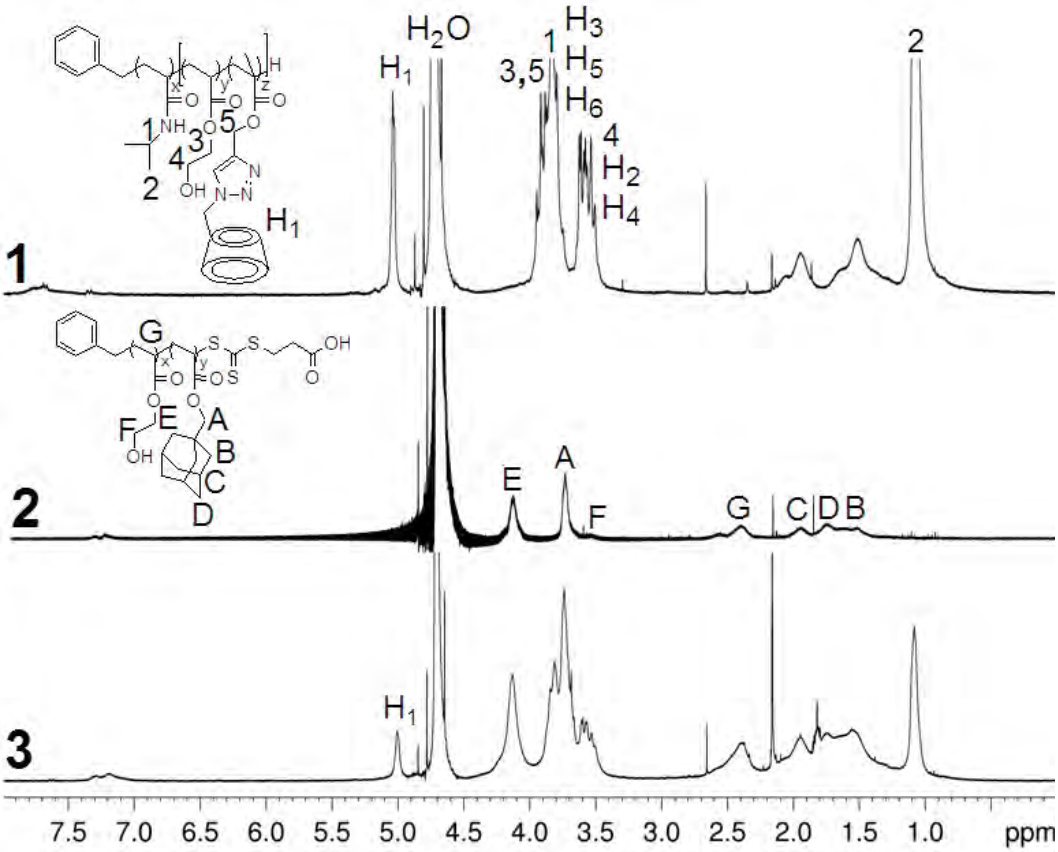

Figure 6.7 *^{1}H NMR analysis of (1) PNIPAAm$_{80}$-b-P(HEA$_{12}$-s-PMA-β-CD$_{18}$), (2) P(HEA$_{17}$-s-AdA$_7$), (3) (1) + (2) after cross-linking. All spectra were run in D_2O.*

Further evidence for crosslinking was provided by DLS analysis. The block copolymer underwent reversible unimers-micelle transformation in the uncrosslinked state. With the addition of P(HEA$_{17}$-*s*-AdMA$_7$), the formation of unimers is absent and the micelle is stable independent from the temperature. The hydrodynamic diameter is with 35±6 nm barely affected by the temperature. The different stabilities can also be observed using TEM (**Figure 6.8**). The micrographs of the block copolymer PNIPAAm$_{80}$-*b*-P(HEA$_{12}$-*s*-PMA-*β*-CD$_{18}$) below the LCST did not show any features that may resemble aggregates (**Figure 6.8**). Above the LCST however, micelles are visible as white spheres against the

dark, negatively stained background. Similar observations were made for the cross linked micelles prepared from a solution of 50 °C. Spherical micelles with diameters of around 30 nm were observed, which is in the same order of magnitude to the DLS results. At room temperature, the same features of around 30 nm remained visible contrasting the micrographs of the uncrosslinked block copolymer (**Figure 6.8**). Cross linking via supramolecular chemistry therefore help maintaining the structural integrity even at ambient temperature.

Addition of excess *β*-cyclodextrin (1.5 mol times of cyclodextrin moieties in the polymer) to the solution leads to competition between the polymer-bound *β*-cyclodextrin and the free *β*-cyclodextrin for the adamantyl groups.[315] As a consequence, the crosslinking of the copolymer was reversed and the micelles re-exhibit a visible LCST again with a transition between unimers and micelles. The measured sizes are now smaller, which is probably the result of the presence of free *β*-cyclodextrin and P(HEA$_{17}$-*s*-AdMA$_{7}$), which was now complexed by *β*-cyclodextrin.

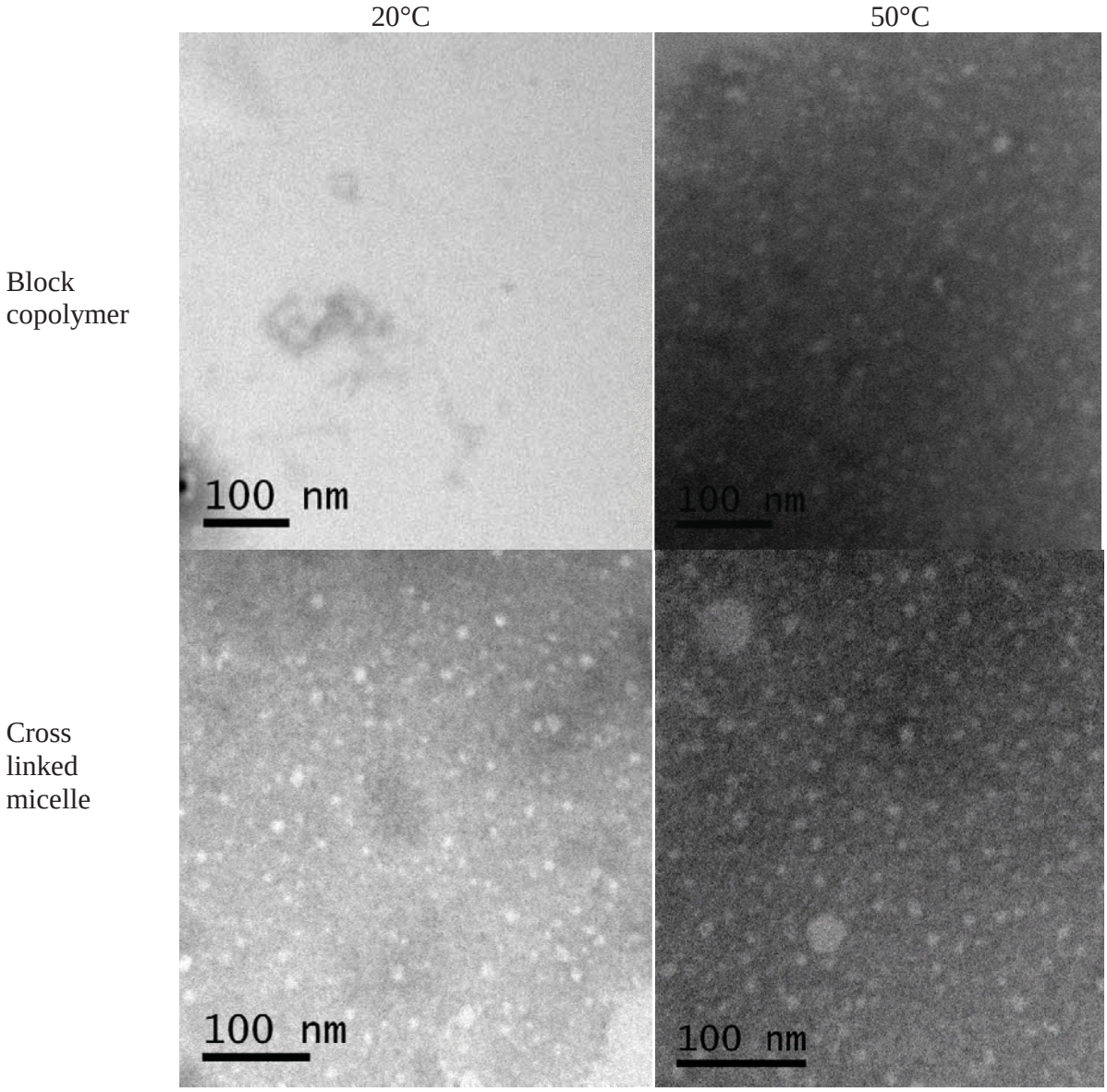

Figure. 6.8 *TEM analysis (negative staining) of the block copolymer PNIPAAm$_{80}$-b-P(HEA$_{12}$-s-PMA-β-CD$_{18}$) (top row) below the LCST (25°C) and above the LCST (50°C) and after crosslinking with P(HEA$_{17}$-s-AdA$_{7}$ (bottom row) where spheres were visible below the LCST.*

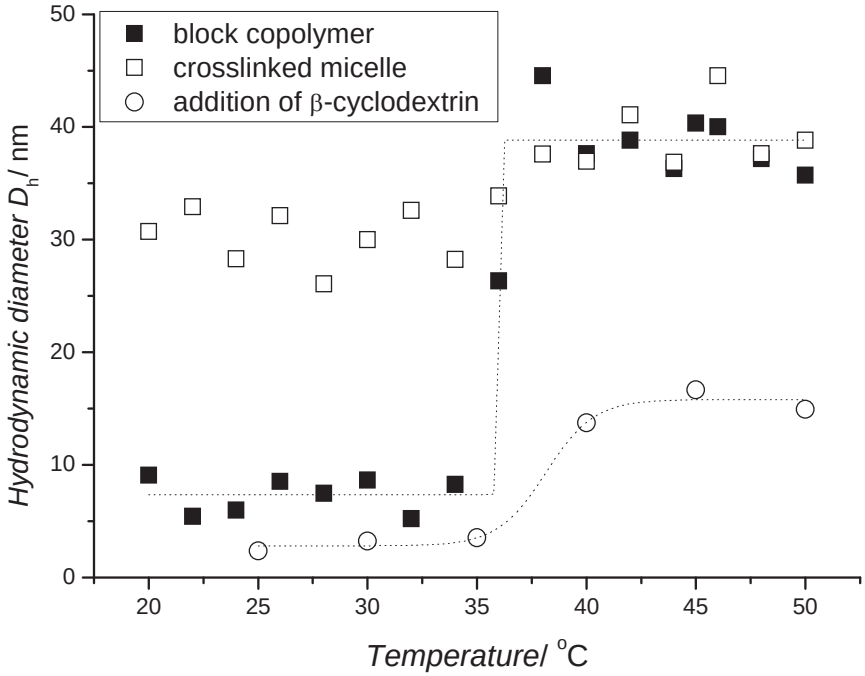

Figure 6.9 *Hydrodynamic diameter (water) vs temperature for PNIPAAm$_{80}$-b-P(HEA$_{12}$-s-PMA-β-CD$_{18}$) (closed square), cross-linked with P(HEA$_{17}$-s-AdMA$_7$ (open square), and after the addition of β-CD (as a competing species) to the cross-linked micelles (circle).*

The stability of these crosslinked micelles was further tested in buffer solution at pH 7.4 (phosphate buffer) and 5.5 (acetate buffer). Salts can form inclusion complexes with *β*-cyclodextrin although it has been suggested that the phosphate anion is too hydrophilic to do so.[325] Acetic acid in contrast is capable of forming inclusion complexes,[326] which may act as a competitor. The results observed in both buffer solutions were similar to the ones in water (**Figure 6.9**). Upon complexation with P(HEA$_{17}$-*s*-AdMA$_7$), the micelles were stable across the whole temperature range. In fact, the expected contraction of the crosslinked micelle at higher temperature was now visible.[305] The micelles were slightly smaller above the LCST due to the dehydration of the core. Addition of excess *β*-cyclodextrin led again to the disassembly of the micelle (**Figure 6.10**), which was similar to the behavior in pure water (**Figure 6.9**).

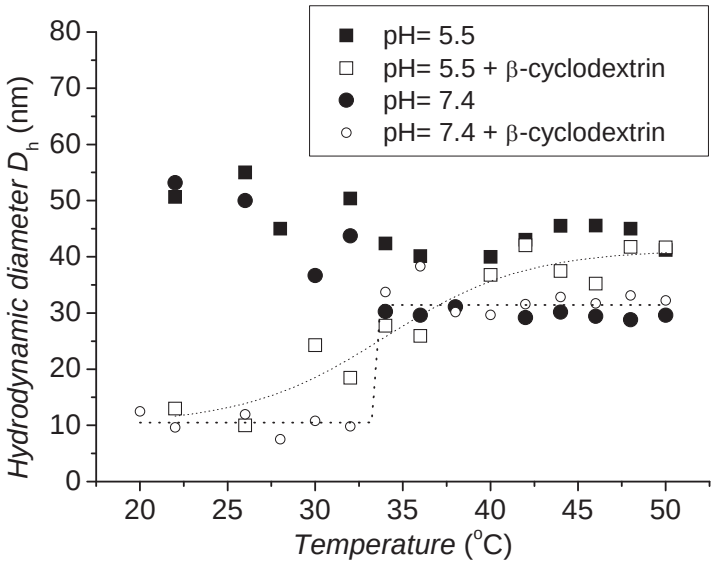

Figure 6.10 *Hydrodynamic diameter vs temperature for cross-linked, and cross linked micelles with addition of β-CD in buffer solution of pH 5.5 (square) and pH 7.4 (circle).*

Drug loading and cross-linking were now combined to generate a drug carrier for albendazole. The block copolymer was loaded with albendazole with a ten-time excess of albendazole (**Table 6.2**). The hydrodynamic diameter after loading was within similar range above the LCST to the albendazole-free micelle (**Table 6.2**). Below the LCST, where only unimers are expected, aggregates of around 150 nm were observed, which are indicative some interaction between the albendazole loaded polymer chains. The solution was subsequently cross linked at 50 °C with P(HEA_{17}-*s*-$AdMA_7$) (ratio *β*-cyclodextrin to adamantyl groups = 10:1). The drug loaded and crosslinked micelles were again stable at various temperatures although below the LCST the formation of selected bigger aggregates was observed. These aggregates were clearly absent above the LCST and DLS intensity distribution and volume distribution of the product were similar indicating a narrow particle distribution (**Table 6.2**).

The drug release experiment was performed against distilled water at 37 °C. Within 8 hours all albendazole was released. This rate of release is similar to most cyclodextrin-based drug delivery systems.[317, 319] The effect of these polymers on cell viability was then tested using ovarian cancer OVCAR-3 cells. The copper(I)-catalyzed azide-alkyne

cycloaddition (CuACC) is well-known and the most utilized type of 'click chemistry'. However, the downside of this approach is that copper traces may remain in the final product, often ligated by the triazole rings.[73, 327] Cell deaths of 90% was observed at all polymer concentrations before thorough copper removal (**Figure 6.11**). This polymer was purified by filtering the solution over a column with neutral alumina. The resulting greenish-brown color of the polymer clearly indicated traces of copper. Therefore, a more thorough purification scheme had to be implemented. The cell viability was almost 100% after full copper removal showing that the PNIPAAm$_{80}$-*b*-P(HEA$_{12}$-*s*-PMA-β-CD$_{18}$) and the P(HEA$_{17}$-*s*-AdMA$_{7}$) crosslinker were non-toxic. As expected, the crosslinked polymer became more toxic after drug loading. Interestingly, the ABZ-loaded cross-linked polymer was more toxic than the uncrosslinked one. Both nanoparticles had the same drug loading. However, in the absence of crosslinker the unimers-micelle transition was observed at an LCST of 42°C. It is therefore possible that only free block copolymers are present in the cell growth media. It has recently been shown that crosslinked micelles can be taken up by the cell much more efficiently, which could potentially translate into higher toxicity.[288]

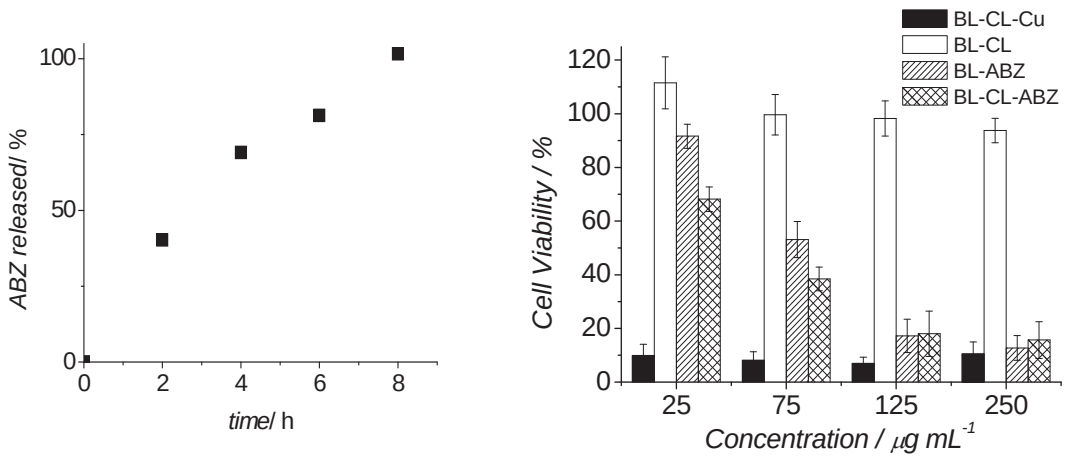

Figure 6.11 left: *ABZ drug release rate for uncross linked PNIPAAm$_{80}$-b-P(HEA$_{12}$-s-PMA-β-CD$_{18}$) micelles at 37 ^{o}C.* ***right****: Cell viability test using OVCAR-3 cancer cell lines for cross linked PNIPAAm$_{80}$-b-P(HEA$_{12}$-s-PMA-β-CD$_{18}$) with traces of copper catalyst (BL-CL-Cu), cross-linked NIPAAm$_{80}$-b-P(HEA$_{12}$-s-PMA-β-CD$_{18}$) with copper removed (BL-CL), uncrosslinked PNIPAAm$_{80}$-b-P(HEA$_{12}$-s-PMA-β-CD$_{18}$) with copper removed and ABZ loaded, and cross-linked PNIPAAm$_{80}$-b-P(HEA$_{12}$-s-PMA-β-CD$_{18}$) with copper removed and ABZ loaded (BL-CL-ABZ).*

6.6 Conclusion

A well-defined, biocompatible drug delivery system has been created by combining host-guest complexation of β-CD and micelles. Shell- crosslinking of the micelles through supramolecular chemistry has been presented as a novel and efficient way of stabilizing the micelles. The benefit of shell crosslinking has been shown in the cell viability studies, where the shell-crosslinked system was slightly superior to the uncrosslinked block copolymer, which – under the circumstances- did probably not form micelle. There is still a range of questions that need to be addressed such as the crosslinking density. At the moment, it has been shown that the current conditions are sufficient for crosslinking, but it is not known what percentage of adamantyl groups actually takes place in the process. For further applications in a biological environment, the stability of these micelles in a surrounding of different active biomolecules are of interest.

Chapter 7: One-pot end group-modification of hydrophobic RAFT polymers with cyclodextrin using thiol-ene chemistry and the subsequent formation of dynamic core-shell nanoparticles using supramolecular host-guest chemistry

Poly(methyl methacrylate) PMMA, synthesized using reversible addition fragmentation chain transfer (RAFT) polymerization, was heated in solvent at 100 °C for 24 hour leading to the loss of the RAFT end functionality and complete conversion to a vinyl group. Mono(6-Deoxy-6-Mercapto)-*β*-Cyclodextrin (*β*-CD-SH) was subsequently clicked onto the polymer via thiol-ene reaction leading to PMMA with one *β*-CD as terminal group ($PMMA_{70}$-*β*-CD). Meanwhile, a RAFT agent with an adamantyl group has been prepared for the polymerization of 2-hydroxyethyl acrylate (HEA) leading to $PHEA_{95}$-Ada. Two processes were employed to generate core-shell nanoparticles from these two polymers: a one-step approach that employs a solution of both polymers at stoichiometric amounts in DMF, followed by the addition of water and a two step process that uses PMMA solid particles with surface enriched *β*-CD in water, which have a strong tendency to aggregate, followed by the addition of $PHEA_{95}$-Ada in water. Both pathways lead to stable core-shell nanoparticles with approximately 150 nm in size. Addition of free *β*-CD competes with the polymer bound *β*-CD releasing the PHEA hairs from the particle surface. As a result, the PMMA particles start agglomerating resulting in a cloudy solution. A similar effect was observed when heating the solution. Since the equilibrium constant between *β*-CD and adamantane decreases with increasing temperature, the stabilizing PHEA chains cleave from the surface and the solution turns cloudy due to the aggregation of the naked PMMA chain. This process is reversible and with decreasing temperature the core-shell nanoparticle forms again leading to a clear solution.

7.1 Introduction

Self-sorting/molecular recognition at supramolecular level plays an important role in biological systems.[328] Self-sorting is the ability to distinguish between different molecules in a mixture. Common in nature, it can be simulated in the lab, where experiments show that a mixture of hosts, including cyclodextrin, can find their guests in the multi-component blend with high level of confidence.[329] Metallosupramolecular architectures based on self-sorting, which are the recognition of a metal ion and its ligand in combination with a templating effect, have been frequently described in the literature.[330-333] In contrast, synthetic macromolecular recognition is still in its infancy, but significant advances were made in the last decade.[334] Recently, some excellent reports emerged that explore host-guest complexation as a mean to self-sorting materials. The by far most popular route utilizes host-guest complexation between β-cyclodextrins and an adamantyl group.[309, 329, 335-352] The formed complex with its 1:1 ratio has a high equilibrium constant, which is comparable to protein-ligand system.[321] Cyclodextrin based host guest chemistry has been applied for surface modification,[343, 347-348] and tissue engineering,[342] but also to build up complex polymer architectures such as graft copolymers[315] and block copolymers.[345, 349-352] Especially the latter has recently inspired researchers due to the ability of block copolymers to form self-assembled structures such as micelles. Block copolymers with cyclodextrin end functionality were mixed with polymers with an adamantyl end functional polymer at stoichiometric amounts. Most block copolymers described by this technique were water-soluble and only an environmental change such as temperature or pH value led to amphiphilic structures, thus micelle formation. Examples are poly(2-methyl-2-oxazoline) and poly(*N*-isopropylacrylamide) (PNIPAAm),[352] poly(4-vinylpyridine) (P4VP) and PNIPAAm,[349] and a block copolymer based on poly(2-(diethylamino)ethyl methacrylate) (PDEA) and PNIPAAm.[345] Also pom-pom-type block copolymers were created by combing star polymers with cyclodextrin cores with linear adamantyl-terminated polymers.[350] The choice of these polymers is not surprising. The water-solubility allows direct dissolution of the polymer in water where host-guest complexation will almost instantaneously take

place. Adjustment of temperature or pH value converts one of the blocks into water-insoluble block, thus micelle formation occurs. Amphiphilic block copolymers in contrast, where one block is insoluble in water, require the use of common solvents such as *N*,*N*-Dimethyl formamide (DMF). The equilibrium constant of the cyclodextrin-guest system in these solvents is however too low to ensure block copolymer formation.

In this work, the strength of these host-guest systems was put to test. Aim is the preparation of micelles from amphiphilic block copolymers with one water-insoluble block. The two blocks are held together by a β-cyclodextrin (β-CD)-adamantane host guest system. Considering the usual technique of micelles preparation, which involves the dissolution in a common solvent such as DMF first, followed by the addition of water, the central question is if the host-guest complex can form during water addition allowing the formation of stable micelles before the water-insoluble block will precipitate out of solution. For this purpose, CD-terminated poly (methyl methacrylate) (PMMA) and adamantyl end functionalized poly(2-hydroxyethylacrylate) (PHEA) were synthesized and their formation of block copolymers were investigated (**Scheme 7.1**).

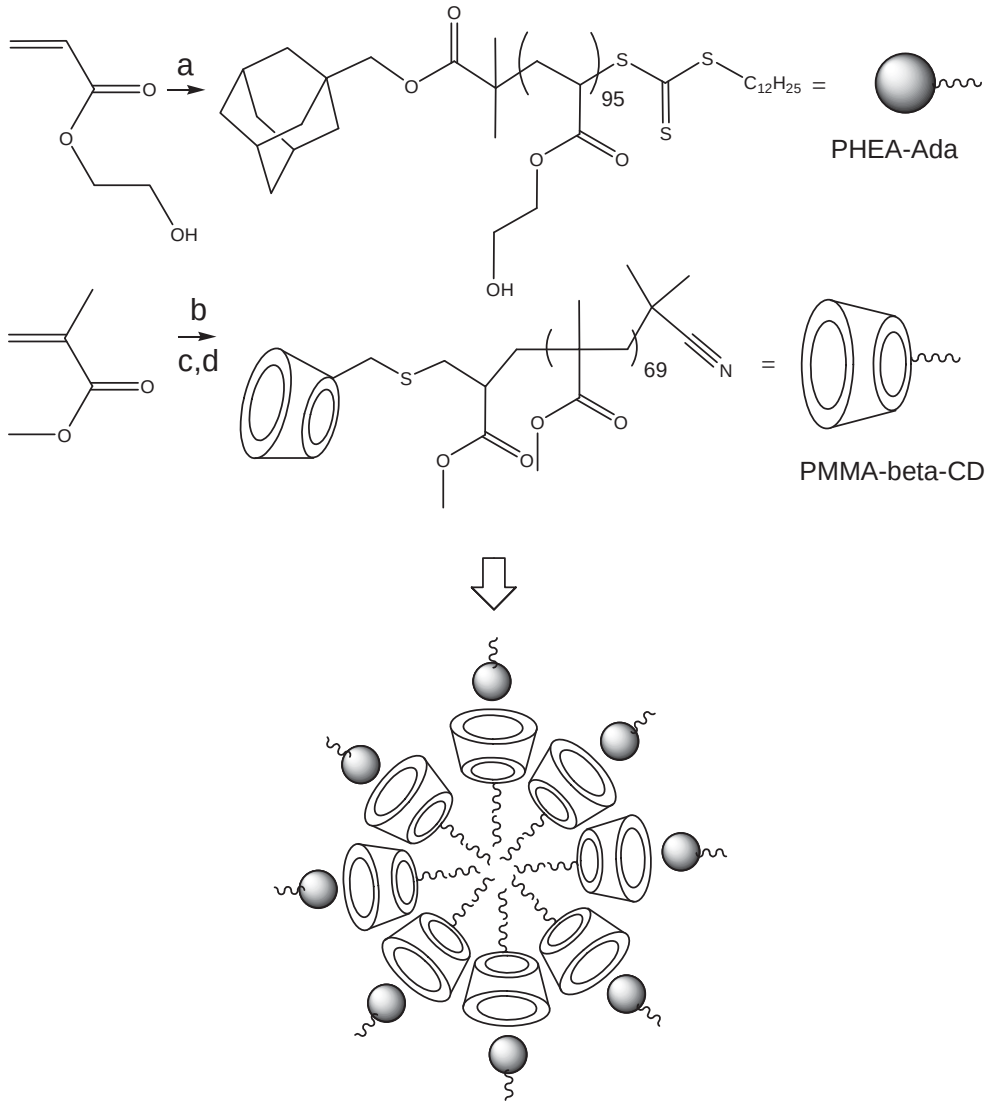

Scheme 7.1 *Synthetic pathway for PHEA-Ada and PMMA-β-CD building blocks, and schematic representation of the resulting molecular recognition.; (a) Ada-RAFT, AIBN, toluene, 60 °C, 1 h ; (b) CPDB, AIBN, acetonitrile, 70 °C, 16 h ; (c) 100 °C, 24 h ; (d) β-CD-SH, DMPP, n-hexylamine, 25 °C, 48 h.*

7.2 Materials

Ada-RAFT (a trithiocarbonate) and CPDB (a dithiobenzoate) are suitable for polymerizing acrylate (HEA) and methacrylate (MMA) respectively. 1-Adamantane methanol, 2,2'-Azobis(2-methylpropionitrile), azobisisobutyronitrile (AIBN), bis(thiobenzoyl) disulfide, *β*-cyclodextrin, 2-cyanopropyl dithiobenzoate (CPDB), dicyclohexylcarbodiimide (DCC), 4-dimethylaminopyridine (DMAP),

dimethylphenylphosphine (DMPP), *S*-1-Dodecyl-*S'*-(α,α'dimethyl-α"-acetic acid)trithiocarbonate, *n*-hexylamine, 2-hydroxyethyl acrylate (HEA), methyl methacrylate (MMA), sodium hydroxide, sodium sulphate, thiourea, *p*-toluenesulfonyl chloride, trichloroethylene were all purchased from Sigma-Aldrich, Hydrochloric acid and solvents were purchased from Ajax Chemicals. Deuterated solvents for ^{1}H NMR analyses were purchased from Cambridge Isotope Laboratories. All chemicals were used as received unless stated otherwise. Reverse Osmosis (RO) water (17.6 M Ω x cm) of 99.0% purity from Sartorius Arium 61316/611VF was used throughout this work.

7.3 Synthesis and Methods

7.3.1 Synthesis of mono(6-Deoxy-6-Mercapto)-*β*-Cyclodextrin (*β*-CD-SH)

Synthesis of *β*-CD-SH was done in two major steps, firstly the synthesis of monotosylated *β*-cyclodextrin (*β*-CD-Tos)[44] followed by monothiolation to obtain *β*-CD-SH.[210] Mass spectroscopy analyses confirmed the monofunctionalization. *β*-CD-Tos: (*m/z* = 1311.4 [M+Na^{+}]), *β*-CD-SH: (*m/z* = 1173.5 [M+Na^{+}]). Yield = 88.7%.

7.3.2 Synthesis of poly(methyl methacrylate) ($PMMA_{70}$) macro-RAFT agent

The purpled-colored RAFT agent 2-cyanopropyl dithiobenzoate (CPDB) was synthesized according to the procedures described elsewhere.[209] MMA (5.00 mL, 4.67 × 10^{-2} mol) was placed in a Schlenk tube along with CPDB (1.03 × 10^{-1} g, 4.68 × 10^{-4} mol) and AIBN (7.68 × 10^{-3} g, 4.68 × 10^{-5} mol) with the ratio used was [MMA]:[CPDB]:[AIBN] = 1000 : 10 : 1. The reagents were dissolved in acetonitrile (9.36 mL) and the Schlenk tube was sealed and subjected to four freeze-pump-thaw cycles. After the last cycle the tube was refilled with dry nitrogen and the Schlenk tube was placed in a preheated oil bath (70 °C) for 16 h. The polymer was collected by precipitation into a cold mixture of methanol and water (75:25) and dried under vacuum. The traces of monomers were removed by Soxhlet extraction for 4 h in methanol to obtain a pink solid of $PMMA_{70}$. (conversion = 70%, $M_{n(NMR)}$ = 7 228 g mol^{-1}, $M_{n(SEC)}$ = 12 000 g mol^{-1}, PDI = 1.09).

7.3.3 Thermolysis of poly(methyl methacrylate) ($PMMA_{70}$) macro-RAFT agent

20 mg of $PMMA_{70}$ was dissolved in 100 μL of DMF and then put in an NMR tube before another 300 μL of deuterated DMSO was added. The tube was then heated at 100 ^{o}C for 24 h to obtain a clear solution before ^{1}H NMR analysis.

7.3.4 Synthesis of *β*-CD terminated PMMA ($PMMA_{70}$-*β*-CD) micelles and preparation of $PMMA_{70}$-*β*-CD nanospheres.

After ^{1}H NMR analysis, the tube was taken back for the next step. By using the mol ratio of PMMA : *β*-CD-SH : hexylamine : DMPP = 1 : 4 : 2 : 0.05, *β*-CD-SH (0.0131 g, 1.14 x 10^{-5} mol) was added into the tube together with 1.51 μL of hexylamine and 0.041 μL of DMPP. The thiol-ene reaction was then allowed to proceed at room temperature (25 ^{o}C) for 48 h prior to ^{1}H NMR analysis. Subsequently, 200 μL of the clear solution was dialyzed in water with a dialysis membrane (MWCO=3500) for 48 h and freeze-dried for purification. The remaining 200 μL of solution was diluted with DMF until the total volume was 2 mL (polymer concentration = 5 mg/mL). 8 mL of water was added very slowly to the 2 mL solution, and then the resulting 10 mL of solution was dialyzed against water for 24 h. The cloudy solution was used directly for molecular recognition experiments and DLS analysis.

7.3.5 Synthesis of adamantyl-terminated poly(2-hydroxyethyl acrylate) ($PHEA_{95}$-Ada)

The synthesis of adamantylmethyl 2-(dodecylthiocarbonothioylthio)-2-methylpropanoate (Ada-RAFT) was carried out according to the literature.[315] 2-hydroxyethyl acrylate (HEA, 10 mL, 11.0760 g, 9.54 x 10^{-2} mol), Ada-RAFT (0.1957 g, 3.816 x 10^{-4} mol), and AIBN (6.27 x 10^{-3}, 3.816 x 10^{-5} mol) were dissolved in 20 mL of *N*, *N*-dimethylacetamide (DMAc). The molar ratio was [HEA : Ada-RAFT: AIBN] = 2500 : 10 : 1. The solution was sealed and degassed for 1 h. The polymerization was carried out

at 60 ^{o}C for 1 h. The polymer was purified by dialysis against water with 3500 MWCO membrane for 48 h. The yellow solution was freeze-dried and analyzed by SEC (DMAc) and ^{1}H NMR in $CDCl_3$. ($PHEA_{95}$-Ada, conversion = 38%, $M_{n(NMR)}$ = 11 544 g mol^{-1}, PDI = 1.43).

7.3.6 Preparation of core-shell nanoparticles

The $PMMA_{70}$-β-CD micelle solution obtained after the dialysis was 14.5 mL (polymer concentration = 0.69 g L^{-1}).

Two step procedure: 3 mL of the $PMMA_{70}$-β-CD solution was taken and filled in a quartz cuvette and the size was measured by DLS at 25 ^{o}C. A solution of 2.9 mg of $PHEA_{95}$-Ada in 100 μL of water (concentration = 29 g L^{-1}, molar ratio between CD : Ada = 1:1) was then dropped into the $PMMA_{70}$-β-CD solution and analyzed by DLS. The solution was heated slowly from 25 to 60 ^{o}C with 1 h relaxation time before each measurement.

One-step procedure: The remaining 11.5 mL of $PMMA_{70}$-β-CD solution was then freeze-dried. After drying, 4.60 mg of the white/colorless solid was redissolved again in 1.11 mL DMF together with 6.51 mg of $PHEA_{95}$-Ada while keeping the molar ratio of CD : Ada = 1 : 1 (total polymer concentration = 1 mg mL^{-1}). 9.99 mL of water was added very slowly at a rate of 1.11 mL / h for the first 4 h, while the remaining 5.55 mL was added in just 1h to a total of 11.1 mL. DMF was removed by dialysis. The solutions were analyzed by DLS for several days and at different temperatures (The solution was heated slowly from 25 to 60 ^{o}C with 1 h relaxation time before each measurement).

7.4 Analysis

7.4.1 NMR spectroscopy

NMR spectra were recorded using a Bruker 300 MHz spectrometer; samples were analyzed in $CDCl_3$ and d_6-DMSO at 25 ^oC. The solvent d_6-DMSO and an ^1H-NMR relaxation time of 1 s were deemed suitable.

7.4.2 Electrospray Ionisation Mass Spectrometry (ESI-MS)

ESI-MS was used to confirm the existence of mono-6-*p*-toluenesulfonyl-*β*-cyclodextrin (*β*-CD-Tos) and mono(6-Deoxy-6-Mercapto)-*β*-Cyclodextrin (*β*-CD-SH). Each sample was freshly prepared before analysis by dissolving the product in a 1:1 solution of water: methanol with concentration of 1 mg/mL and filtered with 0.45 μm filter. Mass spectrometry analyses were undertaken with a Thermo Finnegan LCQ Decca quadruple ion trap mass spectrometer (Thermo Finnegan, San Jose, CA), equipped with an atmospheric pressure ionization source operating in the nebulizer assisted electrospray mode and were used in positive ion mode. Mass calibration was performed using caffeine, MRFA and Ultramark 1621 (Aldrich) in the m/z range of 195-1 822 Da. All spectra was acquired within the m/z range of 150-2 000 Da, and typical instrumental parameters were a spray voltage of 4.5 kV, a capillary voltage of 44 V, a capillary temperature of 275 ^oC and flow rate of 5 μL/min. Nitrogen was used as sheath gas (flow: 50% maximum) and helium was used as auxiliary gas (flow: 5% maximum). 30 microscans, with maximum inject time of 10 ms per microscan. For each respective scan, approximately 35 scans were averaged to obtain the final spectrum. The solvent used was a 3:1 mixture of dichloromethane: methanol with sodium acetate concentration of 0.3 μM. Sodium acetate was added to the solvent prior to analyses to ensure ionization and to suppress potassium salt peaks. All theoretical molecular weights were calculated using the exact mass for the first peak in any given isotopic pattern. The molecular weights of the most abundant isotopes were calculated using the following values: c^{12} = 12.000000; H^1 = 1.007825; O^{16} = 15.994915; Na^{23} = 22.989768.

7.4.3 Size exclusion chromatography (SEC)

Molecular weight distributions of the copolymer systems were determined by means of SEC using a Shimadzu modular system, comprising an auto injector , a Polymer Laboratories (PL) 5.0 μm bead-size guard column (50 x7.5 mm^2), followed by three linear PL columns (10^5, 10^4, 10^3) and a differential-refractive-index detector. The eluent was DMAc (0.05% w/v LiBr, 0.05% 2,6-di-butyl-4-methylphenol) at 50 ^oC with a flow rate of 1 mL min^{-1}. The system was calibrated using narrowly dispersed polystyrene standards ranging from 500 to 10^6 g mol^{-1}. The polymer (5 mg) was dissolved in 2 mL DMAc, followed by filtration using a filter with a pore size of 0.45 μm.

7.4.4 Dynamic light scattering (DLS)

Hydrodynamic diameter and scattering intensity values in this work were obtained using a Malvern Zetasizer Nanoseries Nano ZS particle size analyzer. The temperature range used was from 25 to 60 ^oC.

7.4.5 Transmission electron microscopy (TEM)

The TEM micrographs were obtained using a JEOL 1400 transmission electron microscope. The instrument operates at an accelerating voltage of 100 kV. Samples were negative stained with phosphotungstic acid (2 wt.-%). A Formvar-coated grid was coated by casting a polymer aqueous solution for 1 min. Excess solution was removed using filter paper. For staining, a drop of phosphotungstic acid was gently applied onto the surface of the grid for 30 s. The stained grid was dried under air.

7.5 Results and Discussions

The preparation of block copolymer requires the synthesis of polymers with a single cyclodextrin endfunctionality.[353] Typically, cyclodextrin was monofunctionalized with an ATRP initiator[345, 352] or a RAFT agent,[349] followed by living radical polymerization.

Here, an efficient postfunctionalization step was employed, which uses thiol-ene *click* chemistry as an efficient tool for macromolecular design.[354] Polymers made via reversible addition fragmentation chain transfer (RAFT) polymerization[324] carry a potentially labile thiocarbonylthio end functionality that can be converted into a selection of other functional groups.[355-357] It is therefore envisaged to use this reactivity to functionalize RAFT-made polymers with *β*-CD in one pot.

Methyl methacrylate (MMA) was polymerized with 2-cyanopropyl dithiobenzoate (CPDB) RAFT agent to obtain PMMA with 70 repeating units. The dithiobenzoate endfunctionality is clearly visible in ^{1}H-NMR with a relative intensity between the methyl signal of the MMA repeating unit at 3.55 ppm and the aromatic signals of 70 indicating good agreement between the theoretical molecular weight obtain from conversion determination using gravimetry and NMR (**Figure 7.1**). RAFT end group removal via thermolysis is well known and results in the formation of vinyl endfunctionalities.[358-361] PMMA synthesized via the RAFT process shows an earlier weight loss onset compared to PMMA prepared by free radical polymerization. Significant weight loss was often observed at around 150°C although the onset of the decomposition seems to vary between publications.[358, 362-363] Depending on the polymer and the RAFT agent, the weight loss as measured using TGA, was either equivalent to the loss of RAFT end group only or was significantly higher suggesting unzipping of the polymer chain. A more detailed study on PMMA synthesized by RAFT was carried out by Moad and co-workers who proposed that heating of PMMA prepared with trithiocarbonates leads to hemolytic cleavage of the C-S bond, followed by unzipping, while PMMA prepared with dithiobenzoates are dominated by Chugaev elimination.[358]

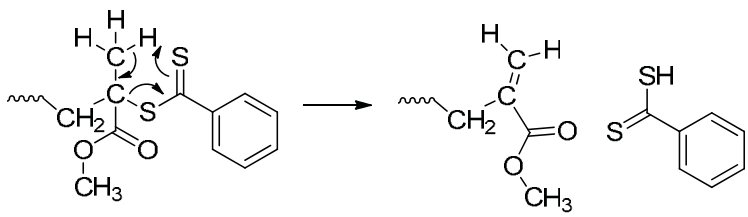

Scheme 7.2 *Proposed mechanism of the Chugaev reaction.*

Elimination was usually achieved in solid state. Here, we attempt the same process in solution at lower temperatures to generate a process that is softer and therefore more suitable for other, potentially more sensitive polymers. The polymer $PMMA_{70}$ was dissolved in DMSO and heated at 100°C. The proceeding reaction was monitored by the disappearance of the pink color. After 24 hours, a colorless solution was obtained. Subsequent ^{1}H-NMR analysis of a purified sample revealed the appearance of signals between 5.5 and 6 ppm corresponding to the expected vinyl functionality (**Figure 7.1**). The integrals were in good agreement with the intensity of the methyl ester functionality at 3.55 ppm suggesting that the number of repeating unit of 70 has not changed. This was confirmed by SEC analysis, where the polymer almost overlapped with the original $PMMA_{70}$ (**Figure 7.2**). The removal of RAFT end group at the end of $PMMA_{70}$ chain has created a double bond available for thiol-ene reaction. Therefore, *β*-CD was monofunctionalized with thiol via a tosylation step to obtain mono(6-deoxy-6-mercapto)-*β*-cyclodextrin (*β*-CD-SH) using a procedure described in literature.[210] The thiol *β*-CD-SH was subsequently added to the PMMA solution, which has been has been heated prior for 24 hours. The Michael addition at ambient temperatures between the vinyl group and an excess of thiol was initiated by the addition of DMPP and hexylamine.[364] It was observed that the conjugation took slightly longer than expected to complete, probably due to the bulkiness of *β*-CD-SH. After a generous reaction time of 48 hours, the double bond has fully disappeared (**Figure 7.1**). Purification of the polymer to remove excess *β*-CD-SH leads to pure $PMMA_{70}$ terminated with *β*-CD. Comparison of the signal intensity of the anomeric proton of CD at 4.8 ppm and the PMMA signal at 3.55 ppm confirm the 1:70 ratio (**Figure 7.1**). The final polymer dissolved easily in DMSO while PMMA without the CD end group was difficult to dissolve.

Meanwhile, an adamantyl-modified RAFT agent (Ada-RAFT) was employed to mediate the polymerization of 2-hydroxyethylacrylate (HEA) to obtain adamantyl-terminated PHEA (PHEA-Ada) resulting in $PHEA_{95}$-Ada.

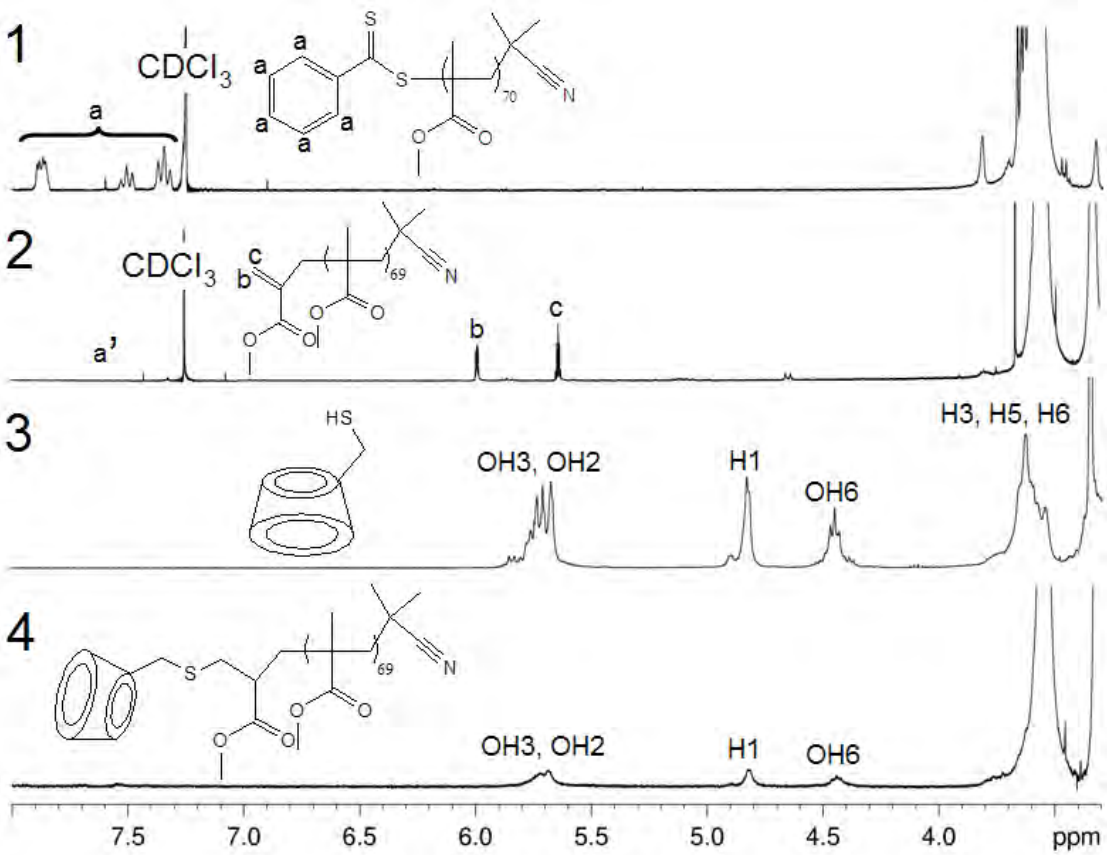

Figure 7.1 *^{1}H NMR spectra of (1) $PMMA_{70}$, (2) $PMMA_{70}$ after thermolysis, (3) β-cyclodextrin thiol, and (4) $PMMA_{70}$ after conjugation with β-cyclodextrin ($PMMA_{70}$-β-CD). Spectra (1) and (2) were run in CDCl3, while spectra (3) and (4) were run in DMSO-d_6.*

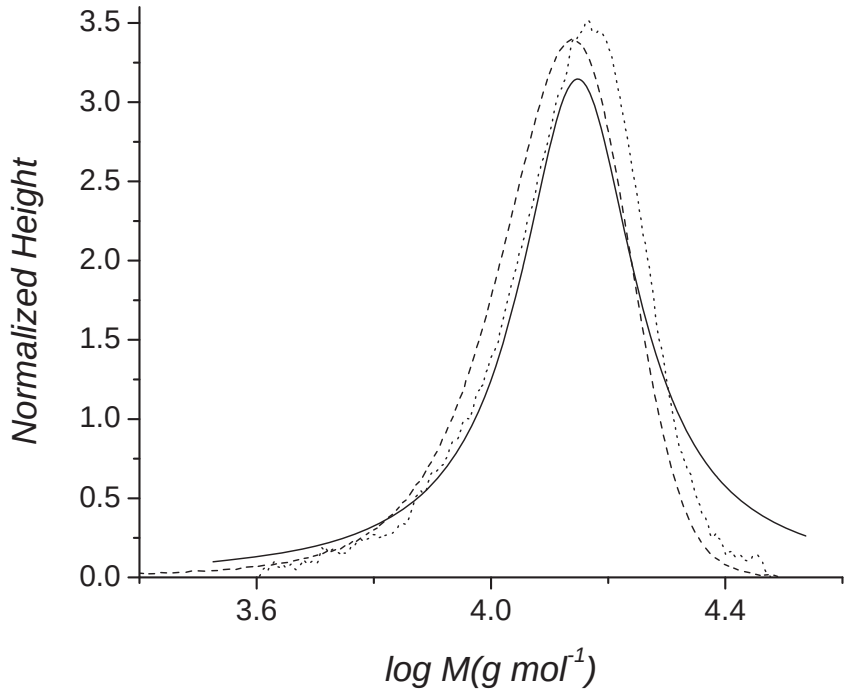

Figure 7.2 *SEC curves of $PMMA_{70}$, M_n= 11 600 g mol^{-1}, PDI=1.11 (dashed); $PMMA_{70}$ after thermolysis M_n= 11 400 g mol^{-1}, PDI=1.16 (solid); $PMMA_{70}$ after conjugation with β-cyclodextrin ($PMMA_{70}$-β-CD) M_n= 13 000 g mol^{-1}, PDI=1.08 (dotted).*

Both polymers, $PHEA_{95}$-Ada and $PMMA_{70}$-*β*-CD, were first investigated separately prior to mixing. Although PHEA is a highly water-soluble polymer, the presence of the adamantane end group led to strong aggregate formation. The solution is milky and DLS confirms the presence of large aggregates of 200 nm and more (**Figure 7.3 and 7.4**). $PMMA_{70}$-*β*-CD in contrast, is not directly soluble in water. After dissolving the polymer in DMF, water was added slowly, which was followed by a dialysis step to remove DMF. The resulting milky solution is similar in appearance to the aqueous solution of $PHEA_{95}$-Ada. The hydrophilic *β*-CD was probably enriched on the surface leading to stable dispersions, which did not change over time. The measured size was 1000 nm (**Figure 7.4**), but TEM analysis shows particles of only 150 nm in size suggesting a strong tendency of these particles to aggregate. It is unlikely that the observed spherical aggregates are micelles. The radius of the measured particle would exceed the size of the

fully extended $PMMA_{70}$ chain. It is more likely a compact polymer sphere decorated with CD on the surface (**Scheme 7.3**).

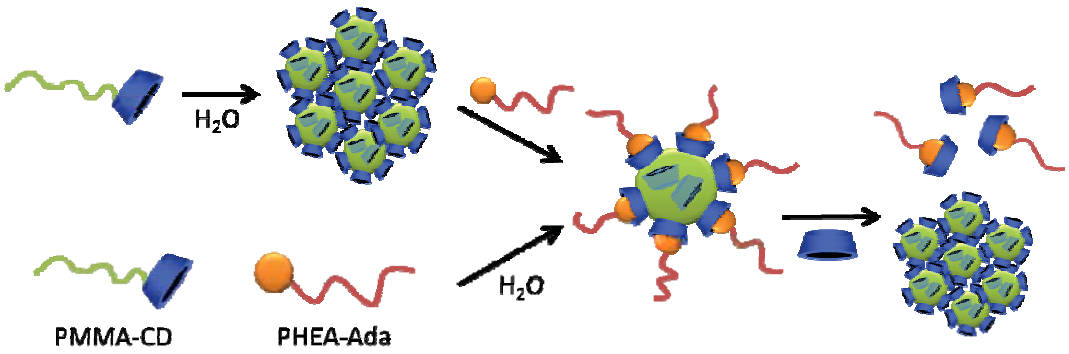

Scheme 7.3 *Schematic representation of the preparation of core-shell nanoparticles using host-guest chemistry prepared via two routes: (top) two-step process: preparation of $PMMA_{70}$-β-CD spheres in water, followed by addition of $PHEA_{95}$-Ada in water (bottom) one-step process: preparation of a solution of $PMMA_{70}$-β-CD and $PHEA_{95}$-Ada in DMF, followed by the slow addition of water and subsequent dialysis against water.*

Figure 7.3 *Polymer solutions (from left to right); (a) $PHEA_{95}$-Ada in water; (b) shortly after addition of $PHEA_{95}$-Ada to a solution with $PMMA_{70}$-β-CD spheres at 25 ^{o}C; (c) solution (b) after 5 hours (d) stoichiometric mixture of $PHEA_{95}$-Ada and $PMMA_{70}$-β-CD, first dissolved in DMF, followed by the addition of water leading to a final solvent ratio 90:10 water : DMF (v/v); (e) 1:1 mixture of $PHEA_{95}$-Ada and $PMMA_{70}$-β-CD solution (d) in 100% water (after removal of DMF via dialysis); (f) addition of excess free β-CD to solution (c).*

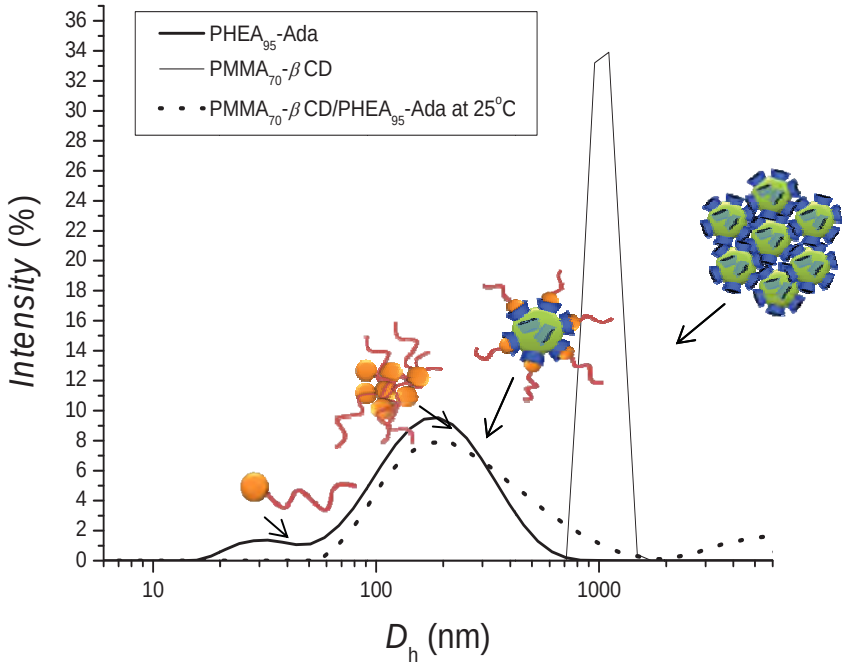

Figure 7.4 *Hydrodynamic diameter of PHEA$_{95}$-Ada and PMMA$_{70}$-β-CD measured in water before mixing (solid curves) and after being mixed with each other in stoichiometric amounts (dashed curve).*

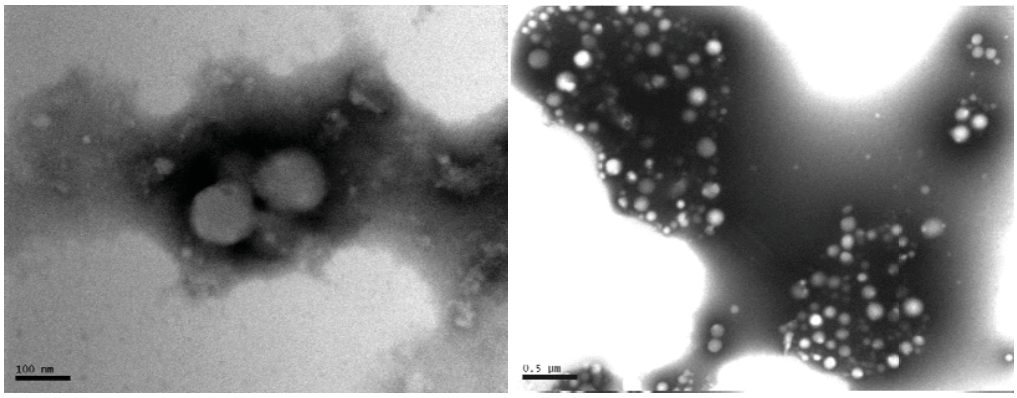

Figure 7.5 *TEM images of PMMA$_{70}$-β-CD nanospheres (left) and PMMA$_{70}$-β-CD/ PHEA$_{95}$-Ada prepared by adding water to a DMF solution, followed by dialysis (right).*

Addition of PHEA-Ada solution in water to the PMMA-β-CD micelles led to the molecular recognition of adamantyl group by β-CD. The formation of host-guest complexation between adamantyl and β-CD cavities can be monitored real-time via dynamic light scattering (DLS). Within a short period of time, the two cloudy solutions turned almost clear. The water-soluble PHEA chains anchor themselves to the surface of the CD-decorated PMMA sphere resulting in the stabilization of the sphere against aggregation. The size of the sphere as determined using TEM is similar, but the stabilization is evident from the DLS data where the measured hydrodynamic diameter D_h= 200 nm complements the TEM data. The interaction between adamantane and the β-CD cavity could unfortunately not be detected using ROESY experiments[315] due to the low concentration of these functional groups in the sample. Indirect evidence for the occurring complex formation can be collected by reversing the process. Addition of excess β-CD leads to competition for the adamantane end group. Removal of the stabilizing PHEA hairs from the surface of the PMMA sphere leads to immediate cloudiness (**Scheme 7.3**). Within seconds, particles with a hydrodynamic volume of more than 3000 nm were measured whose intensity increases significantly over time. In the absence of added β-CD the solution remains stable and clear for several days.

Instead of using a two step procedure, the direct preparation of core-shell nanoparticles was attempted. Earlier work usually employed two water-soluble polymers, which were directly mixed together leading to the formation of block copolymers[349-352] or graft copolymers.[315] The challenge in the current work is the insolubility of PMMA in water, which required the use of DMF as a common solvent for both blocks. However, the equilibrium constant in such a solvent is rather low. Two processes will take place with the addition of water: Water will promote the interaction between β-CD and adamantane, but will also cause precipitation of PMMA, which may restrict further host-guest formation. The water was therefore added at a very low speed leading to a slight cloudy solution (**Figure 7.3d**). Excess DMF was then finally removed by dialysis, but the appearance of the solution remained similar (**Figure 7.3e**). The hydrodynamic diameter of the aqueous solution was measured using DLS, which reveals a bimodal distribution. The main population at around 150 nm was the core-shell particles observed using the

two-step process (**Figure 7.6**). TEM analysis revealed indeed particle sizes of approximately 120 nm (**Figure 7.5**). Of concern is the second distribution in the product (**Figure 7.6**). When comparing the measured size with $PHEA_{95}$-Ada alone it seems that it is the result of free polymer that has not had the opportunity to form a host-guest complex (Note: the distribution of $PHEA_{95}$-Ada in **Figure 7.6** is the volume distribution, which suppresses the aggregates formed by the polymer and highlights the size of the single polymer chain).

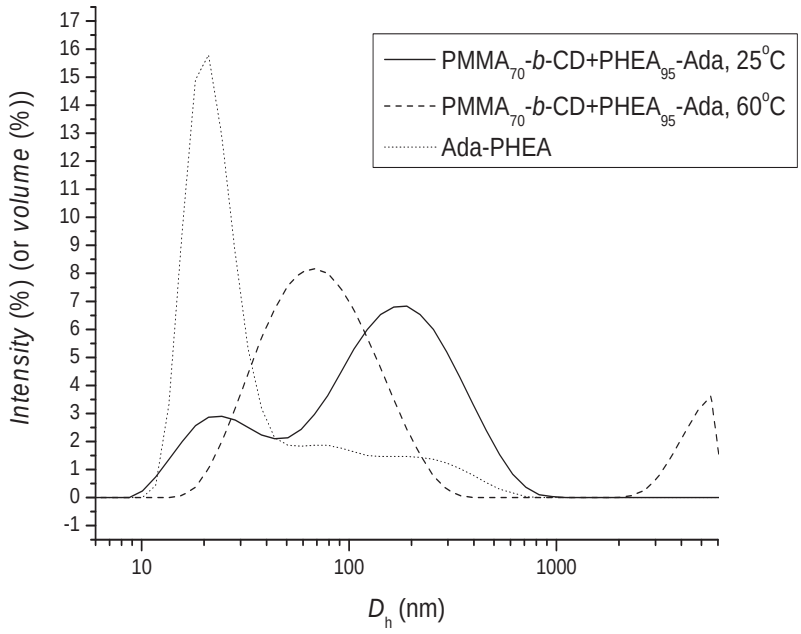

Figure 7.6 *DLS analyses (intensity distribution) of $PMMA_{70}$-β-CD/$PHEA_{95}$-Ada in 100% water (prepared by addition of water to DMF, followed by dialysis) at 25 °C (solid line) and 60 °C (dashed line) and $PHEA_{95}$-Ada only (volume distribution). All measurements were done after 10 h; the curves at 25°C and 60°C are reversible.*

Heating of the sample did not improve the outcome. A population at D_h>3000 nm appears resulting in increased cloudiness. The supramolecular recognition between $PMMA_{70}$-β-CD and $PHEA_{95}$-Ada should not have any thermoresponsivity like PNIPAAm-based micelles. However, some changes in overall size distribution can be observed at the temperature ranges between 25 to 60 °C (**Figure 7.7**). With increasing temperature the amount of free $PHEA_{95}$-Ada increases while the particle size at 150 nm

decreases and is replaced by products with a large hydrodynamic diameter (>3000 nm). The increase in cloudiness is reflected by the increasing scattering intensity (**Figure 7.8**). It needs to be considered that the equilibrium constant of the complex formation between *β*-CD and adamantane declines with temperature.[365] At high temperatures, free $PHEA_{95}$-Ada is present while the PMMA spheres starts precipitating due to the absence of stabilizing PHEA hairs. Interesting is that this behavior is reversible and with decreasing temperature the original distribution reappears while the cloudiness of the solution disappears. A schematic presentation of this process is depicted in **Figure 7.8**. The resulting core-shell nanoparticles can therefore acts as a thermo-responsive sensor turning an almost clear solution into a milky solution at higher temperature, which will clear again once the temperature decreases.

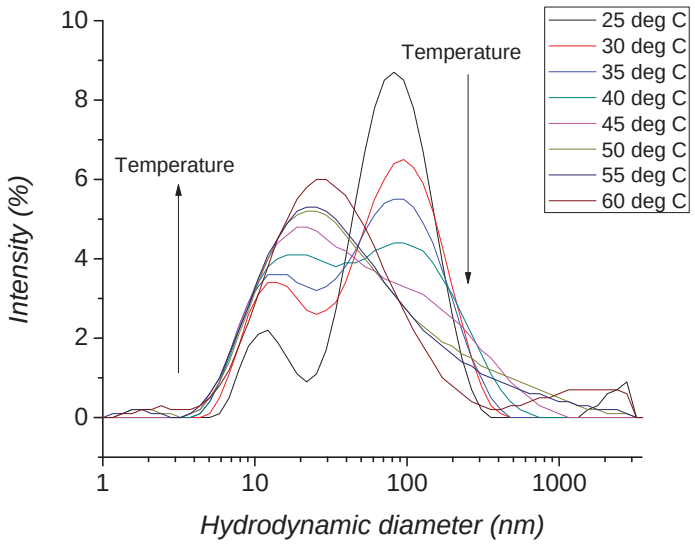

Figure 7.7 *Intensity distribution of the hydrodynamic diameter of* $PMMA_{70}$*-β-CD/*$PHEA_{95}$*-Ada in water, prepared in a one-step process at different temperatures.*

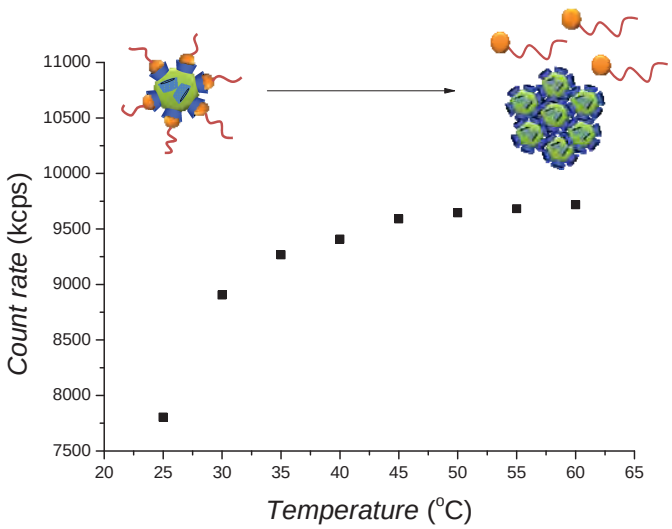

Figure 7.8 *Scattering intensity of PMMA$_{70}$-β-CD/PHEA$_{95}$-Ada in 100% water at different temperatures from the distribution in Figure 7.7.*

7.6 Conclusion

A dynamic core-shell nanoparticle system based on a *β*-CD-adamantane host-guest complex with a hydrophobic PMMA core and water-soluble hydrophilic shell was prepared. The underlying PMMA polymer with *β*-CD was prepared by simply heating the RAFT made polymer leading to the elimination of the end group. The subsequent thiol-ene reaction with *β*-CD-SH was found to be highly efficient. Meanwhile adamantyl-terminated PHEA was prepared using RAFT polymerization. The core shell particles were obtained either by generating PMMA sphere in water, followed by the addition of an aqueous solution of PHEA-Ada or by mixing both polymers in stoichiometric amounts in DMF, followed by water addition. Both pathways lead to nanoparticles similar in appearance according to TEM and DLS results. It seems that some PHEA does not attach to the surface, which may be the dynamic of the system, but also the possibility that not all *β*-CD is available for reaction. The equilibrium constant between *β*-CD and adamantane declines with temperature, therefore the nanospheres loose their stabilizing hairs. This process is reversed at lower temperatures. As a result, a system that can respond to temperature changes by turning the solution from cloudy to almost clear has been created.

Chapter 8: Conclusion and Recommendations

The inability to conjugate thiols onto inactive vinyloxy groups by both nucleophilic and radical thiol-ene required a solution. Enzymatic thiol-ene click is a novel way of conjugating thiols onto polymers with inactive pendant/side vinyl groups. A high clicking/conjugation efficiency for small molecular weight thiols is achievable. However, the azide alkyne 'click chemistry' performs better than the thiol-ene click reaction, with respect to the conjugation efficiency of β-CD. Post-modification of polymer side groups with β-CD by click chemistry has been shown as an effective way to impart functionality to the polymers. The dual functionality of β-CD as drug loading cavities and cross linking point has been demonstrated. In addition, the modification of the end-group of polymer with β-CD is a novel and simple way to construct an amphiphilic polymer. Together with an adamantyl-terminated polymer, a dynamic molecular recognition system can be realized. All these have demonstrated that the modifications of polymers with β-CD can be tailored for specific applications.

There exist areas of research in this topic that require further investigation. In the work presented in Chapter 4, thiols and amines with different functional groups can be tested for the suitability for conjugation through enzymatic pathway. Thiol-functionalized α and γ-cyclodextrins can be synthesized to study the effect of cyclodextrins size to the conjugation efficiency. For Chapter 5, the cyclodextrin cavities are inside the micelle core when the block copolymer began to self-assemble. More studies are needed to fully understand how the structure of the polymer affects drug release and cellular uptake. Regarding the work presented in Chapter 6, the cyclodextrin cavities are on the outer shell when the block copolymer started forming micelles. The given conditions are sufficient for cross linking, but it is not known what percentage of adamantyl functional groups actually participate in the process. For further applications in biologically relevant conditions , the stability of these micelles in the presence of different active biomolecules is of interest. Additionally, the molecular recognition system developed in Chapter 7 may be tested as a temperature sensor in real-world conditions.

References

1. Szejtli, J., Utilization of cyclodextrins in industrial products and processes. *Journal of Materials Chemistry* **1997,** 7, (4), 575-587.

2. Szejtli, J., Past, present, and future of cyclodextrin research. *Pure and Applied Chemistry* **2004,** 76, (10), 1825-1845.

3. Del Valle, E. M. M., Cyclodextrins and their uses: a review. *Process Biochemistry (Oxford, United Kingdom)* **2004,** 39, (9), 1033-1046.

4. Badr, T.; Hanna, K.; de Brauer, C., Enhanced solubilization and removal of naphthalene and phenanthrene by cyclodextrins from two contaminated soils. *Journal of Hazardous Materials* **2004,** 112, (3), 215-223.

5. Cooper, A. D.; Jefferies, T. M.; Gaskell, R. M., Resolution of racemic pharmaceuticals by high-performance liquid chromatography using beta -cyclodextrin in the mobile phase. *Analytical Proceedings* **1992,** 29, (6), 258-9.

6. Szejtli, J., Introduction and General Overview of Cyclodextrin Chemistry. *Chemical Reviews (Washington, D. C.)* **1998,** 98, (5), 1743-1753.

7. Wenz, G.; Han, B.-H.; Mueller, A., Cyclodextrin rotaxanes and polyrotaxanes. *Chemical Reviews (Washington, DC, United States)* **2006,** 106, (3), 782-817.

8. Harada, A.; Takashima, Y.; Yamaguchi, H., Cyclodextrin-based supramolecular polymers. *Chemical Society Reviews* **2009,** 38, (4), 875-882.

9. Liu, Y.-y.; Fan, X.-d.; Gao, L., Synthesis and characterization of beta -cyclodextrin based functional monomers and its copolymers with N-isopropylacrylamide. *Macromolecular Bioscience* **2003,** 3, (12), 715-719.

10. Furue, M.; Harada, A.; Nozakura, S., Preparation of cyclodextrin-containing polymers and their catalysis in ester-hydrolysis. *Journal of Polymer Science, Polymer Letters Edition* **1975,** 13, (6), 357-60.

11. Harada, A.; Furue, M.; Nozakura, S., Cyclodextrin-containing polymers. 1. Preparation of polymers. *Macromolecules* **1976,** 9, (5), 701-4.

12. Harada, A.; Furue, M.; Nozakura, S., Cyclodextrin-containing polymers. 2. Cooperative effects in catalysis and binding. *Macromolecules* **1976,** 9, (5), 705-10.

13. Seo, T.; Kajihara, T.; Iijima, T., The synthesis of poly(allylamine) containing covalently bound cyclodextrin and its catalytic effect in the hydrolysis of phenyl esters. *Makromolekulare Chemie* **1987,** 188, (9), 2071-82.

14. Seo, T.; Kajihara, T.; Miwa, K.; Iijima, T., Catalytic hydrolysis of phenyl esters in cyclodextrin/poly(allylamine) systems. *Makromolekulare Chemie* **1991,** 192, (10), 2357-69.

15. Martin, R.; Sanchez, I.; Cao, R.; Rieumont, J., Solubility and kinetic release studies of Naproxen and Ibuprofen in soluble epichlorohydrin-beta -cyclodextrin polymer. *Supramolecular Chemistry* **2006,** 18, (8), 627-631.

16. Velaz, I.; Isasi, J. R.; Sanchez, M.; Uzqueda, M.; Ponchel, G., Structural characteristics of some soluble and insoluble β-cyclodextrin polymers. *Journal of Inclusion Phenomena and Macrocyclic Chemistry* **2007,** 57, (1-4), 65-68.

17. Nielsen, T. T.; Wintgens, V.; Larsen, K. L.; Amiel, C., Synthesis and characterization of poly(ethylene glycol) based β-cyclodextrin polymers. *Journal of Inclusion Phenomena and Macrocyclic Chemistry* **2009,** 65, (3-4), 341-348.

18. Crini, G.; Bertini, S.; Torri, G.; Naggi, A.; Sforzini, D.; Vecchi, C.; Janus, L.; Lekchiri, Y.; Morcellet, M., Sorption of aromatic compounds in water using insoluble cyclodextrin polymers. *Journal of Applied Polymer Science* **1998,** 68, (12), 1973-1978.

19. Romo, A.; Penas, F. J.; Isasi, J. R., Sorption of dibenzofuran derivatives from aqueous solutions by beta -cyclodextrin polymers: an isosteric heat approach. *Journal of Colloid and Interface Science* **2004,** 279, (1), 55-60.

20. Renard, E.; Deratani, A.; Volet, G.; Sebille, B., Preparation and characterization of water soluble high molecular weight Î²-cyclodextrin-epichlorohydrin polymers. *European Polymer Journal* **1997,** 33, (1), 49-57.

21. Liu, Y.-Y.; Fan, X.-D., Preparation and characterization of a novel responsive hydrogel with a β-cyclodextrin-based macromonomer. *Journal of Applied Polymer Science* **2003,** 89, (2), 361-367.

22. Liu, Y.-Y.; Fan, X.-D., Synthesis and characterization of pH- and temperature-sensitive hydrogel of N-isopropylacrylamide/cyclodextrin based copolymer. *Polymer* **2002,** 43, (18), 4997-5003.

23. Janus, L.; Crini, G.; El-Rezzi, V.; Morcellet, M.; Cambiaghi, A.; Torri, G.; Naggi, A.; Vecchi, C., New sorbents containing beta-cyclodextrin. Synthesis, characterization, and sorption properties. *Reactive & Functional Polymers* **1999,** 42, (3), 173-180.

24. Carbonnier, B.; Janus, L.; Deratani, A.; Morcellet, M., Methacryloylpropyl-beta -cyclodextrin and vinylpyrrolidone copolymers: Synthesis and characterization as potential chiral selector. *Journal of Applied Polymer Science* **2005,** 97, (6), 2364-2374.

25. Wang, J.; Jiang, M., Polymeric self-assembly into micelles and hollow spheres with multiscale cavities driven by inclusion complexation. *Journal of the American Chemical Society* **2006,** 128, (11), 3703-3708.

26. Munteanu, M.; Choi, S.; Ritter, H., Cyclodextrin Methacrylate via Microwave-Assisted Click Reaction. *Macromolecules (Washington, DC, U. S.)* **2008,** 41, (24), 9619-9623.

27. Gonzalez, H.; Hwang, S. J.; Davis, M. E., New Class of Polymers for the Delivery of Macromolecular Therapeutics. *Bioconjugate Chemistry* **1999,** 10, (6), 1068-1074.

28. Maeda, K.; Mochizuki, H.; Watanabe, M.; Yashima, E., Switching of macromolecular helicity of optically active poly(phenylacetylene)s bearing cyclodextrin pendants induced by various external stimuli. *Journal of the American Chemical Society* **2006,** 128, (23), 7639-7650.

29. Cheng, J.; Khin, K. T.; Jensen, G. S.; Liu, A.; Davis, M. E., Synthesis of Linear, β-Cyclodextrin-Based Polymers and Their Camptothecin Conjugates. *Bioconjugate Chemistry* **2003,** 14, (5), 1007-1017.

30. Weickenmeier, M.; Wenz, G., Cyclodextrin side chain polyesters. Synthesis and inclusion of adamantane derivatives. *Macromol. Rapid Commun.* **1996,** 17, (10), 731-736.

31. Weickenmeier, M.; Wenz, G.; Huff, J., Association thickener by host guest interaction of a β-cyclodextrin polymer and polymer with hydrophobic side-groups. *Macromol. Rapid Commun.* **1997,** 18, (12), 1117-1123.

32. Renard, E.; Volet, G.; Amiel, C., Synthesis of a novel linear water-soluble β-cyclodextrin polymer. *Polym. Int.* **2005,** 54, (3), 594-599.

33. Martel, B.; Leckchiri, Y.; Pollet, A.; Morcellet, M., Cyclodextrin-poly(vinylamine) systems. I. Synthesis, characterization and conformational properties. *European Polymer Journal* **1995,** 31, (11), 1083-8.

34. Crini, G.; Torri, G.; Guerrini, M.; Martel, B.; Lekchiri, Y.; Morcellet, M., Linear cyclodextrin-poly(vinylamine): synthesis and NMR characterization. *European Polymer Journal* **1997,** 33, (7), 1143-1151.

35. Suh, J.; Lee, S. H.; Zoh, K. D., A novel host containing both binding site and nucleophile prepared by attachment of β-cyclodextrin to poly(ethylenimine). *Journal of the American Chemical Society* **1992,** 114, (20), 7916-17.

36. Pun, S. H.; Bellocq, N. C.; Liu, A.; Jensen, G.; Machemer, T.; Quijano, E.; Schluep, T.; Wen, S.; Engler, H.; Heidel, J.; Davis, M. E., Cyclodextrin-Modified Polyethylenimine Polymers for Gene Delivery. *Bioconjugate Chemistry* **2004,** 15, (4), 831-840.

37. Guo, X.; Abdala, A. A.; May, B. L.; Lincoln, S. F.; Khan, S. A.; Prud'homme, R. K., Novel associative polymer networks based on cyclodextrin inclusion compounds. *Macromolecules* **2005,** 38, (7), 3037-3040.

38. Li, L.; Guo, X.; Wang, J.; Liu, P.; Prud'homme, R. K.; May, B. L.; Lincoln, S. F., Polymer Networks Assembled by Host-Guest Inclusion between Adamantyl and beta -Cyclodextrin Substituents on Poly(acrylic acid) in Aqueous Solution. *Macromolecules (Washington, DC, United States)* **2008,** 41, (22), 8677-8681.

39. Ramirez, H. L.; Valdivia, A.; Cao, R.; Torres-Labandeira, J. J.; Fragoso, A.; Villalonga, R., Cyclodextrin-grafted polysaccharides as supramolecular carrier systems for naproxen. *Bioorganic & Medicinal Chemistry Letters* **2006,** 16, (6), 1499-1501.

40. Giammona, G.; Cavallaro, G.; Maniscalco, L.; Craparo, E. F.; Pitarresi, G., Synthesis and characterization of novel chemical conjugates based on alpha ,beta -polyaspartylhydrazide and beta -cyclodextrins. *European Polymer Journal* **2006,** 42, (10), 2715-2729.

41. Liu, Y.-Y.; Fan, X.-D.; Zhao, Y.-B., Synthesis and characterization of a poly(N-isopropylacrylamide) with beta-cyclodextrin as pendant groups. *Journal of Polymer Science, Part A: Polymer Chemistry* **2005,** 43, (16), 3516-3524.

42. Hollas, M.; Chung, M.-A.; Adams, J., Complexation of Pyrene by Poly(allylamine) with Pendant β-Cyclodextrin Side Groups. *Journal of Physical Chemistry B* **1998,** 102, (16), 2947-2953.

43. Takashima, Y.; Nakayama, T.; Miyauchi, M.; Kawaguchi, Y.; Yamaguchi, H.; Harada, A., Complex formation and gelation between copolymers containing pendant azobenzene groups and cyclodextrin polymers. *Chemistry Letters* **2004,** 33, (7), 890-891.

44. Petter, R. C.; Salek, J. S.; Sikorski, C. T.; Kumaravel, G.; Lin, F. T., Cooperative binding by aggregated mono-6-(alkylamino)-β-cyclodextrins. *Journal of the American Chemical Society* **1990,** 112, (10), 3860-8.

45. Brown, S. E.; Coates, J. H.; Coghlan, D. R.; Easton, C. J.; van Eyk, S. J.; Janowski, W.; Lepore, A.; Lincoln, S. F.; Luo, Y.; et al., Synthesis and properties of 6A-amino-6A-deoxy-α- and β-cyclodextrin. *Aust. J. Chem.* **1993,** 46, (6), 953-8.

46. Ohga, K.; Takashima, Y.; Takahashi, H.; Kawaguchi, Y.; Yamaguchi, H.; Harada, A., Preparation of supramolecular polymers from a cyclodextrin dimer and ditopic guest molecules: control of structure by linker flexibility. *Macromolecules* **2005,** 38, (14), 5897-5904.

47. Cornwell, M. J.; Huff, J. B.; Bieniarz, C., A one-step synthesis of cyclodextrin monoaldehydes. *Tetrahedron Letters* **1995,** 36, (46), 8371-4.

48. Li, J.; Xiao, H.; Kim, Y. S.; Lowe, T. L., Synthesis of water-soluble cationic polymers with star-like structure based on cyclodextrin core via ATRP. *Journal of Polymer Science, Part A: Polymer Chemistry* **2005,** 43, (24), 6345-6354.

49. Xu, J.; Liu, S., Synthesis of well-defined 7-arm and 21-arm poly(N-isopropylacrylamide) star polymers with beta -cyclodextrin cores via click chemistry and their thermal phase transition behavior in aqueous solution. *Journal of Polymer Science, Part A: Polymer Chemistry* **2009,** 47, (2), 404-419.

50. Topchieva, I. N.; Polyakov, V. A.; Elezkaya, S. V.; Bystryzky, G. I.; Karezin, K. I., One-pot synthesis of cyclodextrins, modified with poly(ethylene oxide). *Polymer Bulletin (Berlin, Germany)* **1997,** 38, (4), 359-364.

51. Karaky, K.; Reynaud, S.; Billon, L.; Francois, J.; Chreim, Y., Organosoluble star polymers from a cyclodextrin core. *Journal of Polymer Science, Part A: Polymer Chemistry* **2005,** 43, (21), 5186-5194.

52. Hadjichristidis, N.; Pitsikalis, M.; Pispas, S.; Iatrou, H., Polymers with complex architecture by living anionic polymerization. *Chemical reviews* **2001,** 101, (12), 3747-92.

53. Matyjaszewski, K.; Xia, J., Atom Transfer Radical Polymerization. *Chemical Reviews (Washington, D. C.)* **2001,** 101, (9), 2921-2990.

54. Ohno, K.; Wong, B.; Haddleton, D. M., Synthesis of well-defined cyclodextrin-core star polymers. *Journal of Polymer Science, Part A: Polymer Chemistry* **2001,** 39, (13), 2206-2214.

55. Stenzel-Rosenbaum, M. H.; Davis, T. P.; Chen, V.; Fane, A. G., Synthesis of Poly(styrene) Star Polymers Grown from Sucrose, Glucose, and Cyclodextrin Cores via Living Radical Polymerization Mediated by a Half-Metallocene Iron Carbonyl Complex. *Macromolecules* **2001,** 34, (16), 5433-5438.

56. Plamper, F. A.; Becker, H.; Lanzendoerfer, M.; Patel, M.; Wittemann, A.; Ballauff, M.; Mueller, A. H. E., Synthesis, characterization and behavior in aqueous solution of star-shaped poly(acrylic acid). *Macromolecular Chemistry and Physics* **2005,** 206, (18), 1813-1825.

57. Zhang, Z.-X.; Liu, X.; Xu, F. J.; Loh, X. J.; Kang, E.-T.; Neoh, K.-G.; Li, J., Pseudo-Block Copolymer Based on Star-Shaped Poly(N-isopropylacrylamide) with a beta-Cyclodextrin Core and Guest-Bearing PEG: Controlling Thermoresponsivity through Supramolecular Self-Assembly. *Macromolecules (Washington, DC, United States)* **2008,** 41, (16), 5967-5970.

58. Xu, F. J.; Zhang, Z. X.; Ping, Y.; Li, J.; Kang, E. T.; Neoh, K. G., Star-Shaped Cationic Polymers by Atom Transfer Radical Polymerization from beta -Cyclodextrin Cores for Nonviral Gene Delivery. *Biomacromolecules* **2009,** 10, (2), 285-293.

59. Miura, Y.; Narumi, A.; Matsuya, S.; Satoh, T.; Duan, Q.; Kaga, H.; Kakuchi, T., Synthesis of well-defined AB20-type star polymers with cyclodextrin-core by combination of NMP and ATRP. *Journal of Polymer Science, Part A: Polymer Chemistry* **2005,** 43, (18), 4271-4279.

60. He, T.; Hu, T.; Zhang, X.; Zhong, G.; Zhang, H., Synthesis and characterization of a novel liquid crystalline star-shaped polymer based on β-CD core via ATRP. *Journal of Applied Polymer Science* **2009,** 112, (4), 2120-2126.

61. Xiao, Q.; Li, Z.; Gao, D.; He, T.; Zhang, H., Preparation and electrochemical performance of gel polymer electrolytes with a novel star network. *Journal of Applied Electrochemistry* **2009,** 39, (2), 247-251.

62. Badi, N.; Auvray, L.; Guegan, P., Synthesis of half-channels by the anionic polymn. of ethylene oxide initiated by modified cyclodextrin. *Advanced Materials (Weinheim, Germany)* **2009,** 21, (40), 4054-4057.

63. Adeli, M.; Zarnegar, Z.; Kabiri, R., Amphiphilic star copolymers containing cyclodextrin core and their application as nanocarrier. *European Polymer Journal* **2008,** 44, (7), 1921-1930.

64. Guo, Y.; Yu, C.; Gu, Z., Synthesis and characterization of novel beta -cyclodextrin cored poly(.vepsiln.-caprolactone)s by anionic ring opening polymerization. *e-Polymers* **2008**, No pp given.

65. Gou, P.-F.; Zhu, W.-P.; Xu, N.; Shen, Z.-Q., Synthesis and characterization of well-defined cyclodextrin-centered seven-arm star poly(e-caprolactone)s and amphiphilic star poly(e-caprolactone-b-ethylene glycol)s. *Journal of Polymer Science, Part A: Polymer Chemistry* **2008,** 46, (19), 6455-6465.

66. Jiang, Y.; Zhang, H.; Du, L.; Zhang, K.; Wang, J., Synthesis and characterization of novel star polymer with beta -cyclodextrin core and its metal complexes. *Journal of Applied Polymer Science* **2007,** 106, (1), 28-33.

67. Yang, C.; Li, H.; Goh, S. H.; Li, J., Cationic star polymers consisting of alpha -cyclodextrin core and oligoethylenimine arms as nonviral gene delivery vectors. *Biomaterials* **2007,** 28, (21), 3245-3254.

68. Kakuchi, T.; Narumi, A.; Matsuda, T.; Miura, Y.; Sugimoto, N.; Satoh, T.; Kaga, H., Glycoconjugated Polymer. 5. Synthesis and Characterization of a Seven-Arm Star Polystyrene with a beta -Cyclodextrin Core Based on TEMPO-Mediated Living Radical Polymerization. *Macromolecules* **2003,** 36, (11), 3914-3920.

69. Chiefari, J.; Chong, Y. K.; Ercole, F.; Krstina, J.; Jeffery, J.; Le, T. P. T.; Mayadunne, R. T. A.; Meijs, G. F.; Moad, C. L.; Moad, G.; Rizzardo, E.; Thang, S. H., Living Free-Radical Polymerization by Reversible Addition-Fragmentation Chain Transfer: The RAFT Process. *Macromolecules* **1998,** 31, (16), 5559-5562.

70. Barner, L., Davis. T.P., Stenzel, M.H., Kowollik, C.B., Complex Macromolecular Architectures by Reversible Addition Fragmentation Chain Transfer Chemistry: Theory and Practice. *Macromolecular Rapid Communications* **2007,** 28, 539-559.

71. Stenzel, M. H.; Davis, T. P., Star polymer synthesis using trithiocarbonate functional beta-cyclodextrin cores (reversible addition-fragmentation chain-transfer polymerization). *Journal of Polymer Science, Part A: Polymer Chemistry* **2002,** 40, (24), 4498-4512.

72. Zhang, L.; Stenzel, M. H., Spherical Glycopolymer Architectures using RAFT: From Stars with a β-Cyclodextrin Core to Thermoresponsive Core-Shell Particles. *Aust. J. Chem.* **2009,** 62, (8), 813-822.

73. Binder, W. H.; Sachsenhofer, R., 'Click' chemistry in polymer and materials science. *Macromol. Rapid Commun.* **2007,** 28, (1), 15-54.

74. Hoogenboom, R.; Moore, B. C.; Schubert, U. S., Synthesis of star-shaped poly(ε-caprolactone) via 'click' chemistry and 'supramolecular click' chemistry. *Chemical Communications (Cambridge, United Kingdom)* **2006**, (38), 4010-4012.

75. Kurganov, B. I.; Topchieva, I. N.; Efremova, N. V., Protein Conjugates with Water-Soluble Poly(alkylene oxide)s Entrapped in Hydrated Reversed Micelles. *Bioconjugate Chemistry* **1997,** 8, (5), 637-642.

76. Kakuchi, T.; Narumi, A.; Miura, Y.; Matsuya, S.; Sugimoto, N.; Satoh, T.; Kaga, H., Glycoconjugated Polymer. 4. Synthesis and Aggregation Property of Well-Defined End-Functionalized Polystyrene with beta -Cyclodextrin. *Macromolecules* **2003,** 36, (11), 3909-3913.

77. Giacomelli, C.; Schmidt, V.; Putaux, J.-L.; Narumi, A.; Kakuchi, T.; Borsali, R., Aqueous Self-Assembly of Polystyrene Chains End-Functionalized with beta -Cyclodextrin. *Biomacromolecules* **2009,** 10, (2), 449-453.

78. Zeng, J.; Shi, K.; Zhang, Y.; Sun, X.; Zhang, B., Construction and micellization of a noncovalent double hydrophilic block copolymer. *Chemical Communications (Cambridge, United Kingdom)* **2008**, (32), 3753-3755.

79. Barbosa, M. E. M.; Bouteiller, L.; Cammas-Marion, S.; Montembault, V.; Fontaine, L.; Ponchel, G., Synthesis and ITC characterization of novel nanoparticles constituted by poly(γ-benzyl L-glutamate)- β-cyclodextrin. *Journal of Molecular Recognition* **2008,** 21, (3), 169-178.

80. Guo, M.; Jiang, M.; Zhang, G., Surface Modification of Polymeric Vesicles via Host-Guest Inclusion Complexation. *Langmuir* **2008,** 24, (19), 10583-10586.

81. van de Manakker, F.; van der Pot, M.; Vermonden, T.; van Nostrum, C. F.; Hennink, W. E., Self-Assembling Hydrogels Based on β-Cyclodextrin/Cholesterol Inclusion Complexes. *Macromolecules (Washington, DC, United States)* **2008,** 41, (5), 1766-1773.

82. van de Manakker, F.; Vermonden, T.; El Morabit, N.; van Nostrum, C. F.; Hennink, W. E., Rheological behavior of self-assembling PEG-beta -cyclodextrin/PEG-cholesterol hydrogels. *Langmuir* **2008,** 24, (21), 12559-12567.

83. Chun, I. K.; Park, I. S., Solubilization and dissolution enhancement of benzimidazole anthelmintic drugs by cyclodextrin complexation. *Yakhak Hoechi* **1993,** 37, (3), 216-27.

84. Bassini, V. L.; Krieger, D.; Duchene, D.; Wouessidjewe, D., Enhanced water-solubility of albendazole by hydroxypropyl-β-cyclodextrin complexation. *Journal of Inclusion Phenomena and Molecular Recognition in Chemistry* **1996,** 25, (1-3), 149-152.

85. Diaz, D.; Bernad, J. B.; Mora, J. G.; Llanos, C. M. E., Complexation and solubility behavior of albendazole with some cyclodextrins. *Pharmaceutical Development and Technology* **1998,** 3, (3), 395-403.

86. Castillo, J. A.; Palomo-Canales, J.; Garcia, J. J.; Lastres, J. L.; Bolas, F.; Torrado, J. J., Preparation and characterization of albendazole-β-cyclodextrin complexes. *Drug Development and Industrial Pharmacy* **1999,** 25, (12), 1241-1248.

87. Evrard, B.; Chiap, P.; DeTullio, P.; Ghalmi, F.; Piel, G.; Van Hees, T.; Crommen, J.; Losson, B.; Delattre, L., Oral bioavailability in sheep of albendazole from a suspension and from a solution containing hydroxypropyl-β-cyclodextrin. *Journal of Controlled Release* **2002,** 85, (1-3), 45-50.

88. Shyale, S.; Chowdhary, K. P. R.; Krishnaiah, Y. S. R., Development of colon-targeted albendazole-β-cyclodextrin-complex drug delivery systems. *Drug Development Research* **2005,** 65, (2), 76-83.

89. Casulli, A.; Gomez Morales, M. A.; Gallinella, B.; Turchetto, L.; Pozio, E., 2-Hydroxypropyl-β-cyclodextrin improves the effectiveness of albendazole against encapsulated larvae of Trichinella spiralis in a murine model. *Journal of Antimicrobial Chemotherapy* **2006,** 58, (4), 886-890.

90. Moriwaki, C.; Costa, G. L.; Ferracini, C. N.; de Moraes, F. F.; Zanin, G. M.; Pineda, E. A. G.; Matioli, G., Enhancement of solubility of albendazole by complexation with β-cyclodextrin. *Brazilian Journal of Chemical Engineering* **2008,** 25, (2), 255-267.

91. Pourgholami, M. H.; Akhter, J.; Wang, L.; Lu, Y.; Morris, D. L., Antitumor activity of albendazole against the human colorectal cancer cell line HT-29: in vitro and in a xenograft model of peritoneal carcinomatosis. *Cancer Chemotherapy and Pharmacology* **2005,** 55, (5), 425-432.

92. Pourgholami, M. H.; Wangoo, K. T.; Morris, D. L., Albendazole-cyclodextrin complex: enhanced cytotoxicity in ovarian cancer cells. *Anticancer Research* **2008,** 28, (5A), 2775-2779.

93. Joudieh, S.; Bon, P.; Martel, B.; Skiba, M.; Lahiani-Skiba, M., Cyclodextrin polymers as efficient solubilizers of albendazole: complexation and physico-chemical characterization. *Journal of Nanoscience and Nanotechnology* **2009,** 9, (1), 132-140.

94. Patel, V. P.; Parikh, R. K.; Gohel, M. C.; Desai, T. R.; Bhimani, D. R.; Tirgar, P. R., In vitro dissolution enhancement of albendazole by preparation of inclusion complexs with HP-β cyclodextrin. *Pharma Science Monitor* **2011,** 2, (1), 161-173.

95. Hawker, C. J.; Bosman, A. W.; Harth, E., New Polymer Synthesis by Nitroxide Mediated Living Radical Polymerizations. *Chemical Reviews (Washington, D. C.)* **2001,** 101, (12), 3661-3688.

96. Matyjaszewski, K.; Patten, T. E.; Xia, J., Controlled/"Living" Radical Polymerization. Kinetics of the Homogeneous Atom Transfer Radical Polymerization of Styrene. *Journal of the American Chemical Society* **1997,** 119, (4), 674-680.

97. Barner-Kowollik, C.; Editor, *Handbook of RAFT Polymerization*. 2008; p 543 pp.

98. Odian, G., *Principles of Polymerization, 4th Edition*. 2004; p 768 pp.

99. Schilli, C. M.; Zhang, M.; Rizzardo, E.; Thang, S. H.; Chong, Y. K.; Edwards, K.; Karlsson, G.; Mueller, A. H. E., A New Double-Responsive Block Copolymer Synthesized via RAFT Polymerization: Poly(N-isopropylacrylamide)-block-poly(acrylic acid). *Macromolecules* **2004,** 37, (21), 7861-7866.

100. Barner-Kowollik, C.; Quinn, J. F.; Morsley, D. R.; Davis, T. P., Modeling the reversible addition-fragmentation chain transfer process in cumyl dithiobenzoate-mediated styrene homopolymerizations: Assessing rate coefficients for the addition-fragmentation equilibrium. *Journal of Polymer Science Part A: Polymer Chemistry* **2001,** 39, (9), 1353-1365.

101. Barner, L.; Barner-Kowollik, C.; Davis, T. P.; Stenzel, M. H., Complex Molecular Architecture Polymers via RAFT. *Aust. J. Chem.* **2004,** 57, (1), 19-24.

102. Vana, P.; Davis, T. P.; Barner-Kowollik, C., Kinetic analysis of reversible addition fragmentation chain transfer (RAFT) polymerizations: conditions for inhibition, retardation, and optimum living polymerization. *Macromolecular Theory and Simulations* **2002,** 11, (8), 823-835.

103. Convertine, A. J.; Ayres, N.; Scales, C. W.; Lowe, A. B.; McCormick, C. L., Facile, Controlled, Room-Temperature RAFT Polymerization of N-Isopropylacrylamide. *Biomacromolecules* **2004,** 5, (4), 1177-1180.

104. Vana, P.; Albertin, L.; Barner, L.; Davis, T. P.; Barner-Kowollik, C., Reversible addition-fragmentation chain-transfer polymerization: Unambiguous end-group assignment via electrospray ionization mass spectrometry. *J. Polym. Sci., Part A Polym. Chem.* **2002,** 40, (22), 4032-4037.

105. Barner-Kowollik, C.; Quinn, J. F.; Nguyen, T. L. U.; Heuts, J. P. A.; Davis, T. P., Kinetic Investigations of Reversible Addition Fragmentation Chain Transfer Polymerizations: Cumyl Phenyldithioacetate Mediated Homopolymerizations of Styrene and Methyl Methacrylate. *Macromolecules* **2001,** 34, (22), 7849-7857.

106. Barner, L.; Davis, T. P.; Stenzel, M. H.; Barner-Kowollik, C., Complex macromolecular architectures by reversible addition fragmentation chain transfer chemistry: theory and practice. *Macromol. Rapid Commun.* **2007,** 28, (5), 539-559.

107. Perrier, S.; Takolpuckdee, P.; Mars, C. A., Reversible Addition-Fragmentation Chain Transfer Polymerization: End Group Modification for Functionalized Polymers and Chain Transfer Agent Recovery. *Macromolecules* **2005,** 38, (6), 2033-2036.

108. Such, G. K.; Evans, R. A.; Davis, T. P., The Use of Block Copolymers to Systematically Modify Photochromic Behavior. *Macromolecules* **2006,** 39, (26), 9562-9570.

109. Save, M.; Manguian, M.; Chassenieux, C.; Charleux, B., Synthesis by RAFT of Amphiphilic Block and Comblike Cationic Copolymers and Their Use in Emulsion Polymerization for the Electrosteric Stabilization of Latexes. *Macromolecules* **2005,** 38, (2), 280-289.

110. Sumerlin, B. S.; Donovan, M. S.; Mitsukami, Y.; Lowe, A. B.; McCormick, C. L., Water-Soluble Polymers. 84. Controlled Polymerization in Aqueous Media of Anionic Acrylamido Monomers via RAFT. *Macromolecules* **2001,** 34, (19), 6561-6564.

111. Szablan, Z.; Toy, A. A.; Davis, T. P.; Hao, X.; Stenzel, M. H.; Barner-Kowollik, C., Reversible addition fragmentation chain transfer polymerization of sterically hindered monomers: Toward well-defined rod/coil architectures. *J. Polym. Sci., Part A Polym. Chem.* **2004,** 42, (10), 2432-2443.

112. Xu, J.; He, J.; Fan, D.; Tang, W.; Yang, Y., Thermal Decomposition of Dithioesters and Its Effect on RAFT Polymerization. *Macromolecules* **2006,** 39, (11), 3753-3759.

113. Quinn, J. F.; Barner, L.; Barner-Kowollik, C.; Rizzardo, E.; Davis, T. P., Reversible Addition-Fragmentation Chain Transfer Polymerization Initiated with Ultraviolet Radiation. *Macromolecules* **2002,** 35, (20), 7620-7627.

114. Albertin, L.; Stenzel, M. H.; Barner-Kowollik, C.; Davis, T. P., Effect of an added base on (4-cyanopentanoic acid)-4-dithiobenzoate mediated RAFT polymerization in water. *Polymer* **2006,** 47, (4), 1011-1019.

115. Vasilieva, Y. A.; Thomas, D. B.; Scales, C. W.; McCormick, C. L., Direct Controlled Polymerization of a Cationic Methacrylamido Monomer in Aqueous Media via the RAFT Process. *Macromolecules* **2004,** 37, (8), 2728-2737.

116. Thomas, D. B.; Convertine, A. J.; Hester, R. D.; Lowe, A. B.; McCormick, C. L., Hydrolytic Susceptibility of Dithioester Chain Transfer Agents and Implications in Aqueous RAFT Polymerizations. *Macromolecules* **2004,** 37, (5), 1735-1741.

117. Hao, X.; Stenzel, M. H.; Barner-Kowollik, C.; Davis, T. P.; Evans, E., Molecular composite materials formed from block copolymers containing a side-chain liquid crystalline segment and an amorphous styrene/maleic anhydride segment. *Polymer* **2004,** 45, (22), 7401-7415.

118. Relogio, P.; Charreyre, M.-T.; Farinha, J. P. S.; Martinho, J. M. G.; Pichot, C., Well-defined polymer precursors synthesized by RAFT polymerization of N,N-dimethylacrylamide/N-acryloxysuccinimide: random and block copolymers. *Polymer* **2004,** 45, (26), 8639-8649.

119. Wong, K. H.; Davis, T. P.; Barner-Kowollik, C.; Stenzel, M. H., Gold-Loaded Organic/Inorganic Nanocomposite Honeycomb Membranes. *Aust. J. Chem.* **2006,** 59, (8), 539-543.

120. Laschewsky, A.; Mertoglu, M.; Kubowicz, S.; Thuenemann, A. F., Lamellar Structured Nanoparticles Formed by Complexes of a Cationic Block Copolymer and Perfluorodecanoic Acid. *Macromolecules* **2006,** 39, (26), 9337-9345.

121. Krasia, T.; Soula, R.; Boerner, H. G.; Schlaad, H., Controlled synthesis of homopolymers and block copolymers based on 2-(acetoacetoxy)ethyl methacrylate via RAFT radical polymerisation. *Chemical Communications (Cambridge, United Kingdom)* **2003**, (4), 538-539.

122. Hu, Y.-C.; Liu, Y.; Pan, C.-Y., Reversible addition-fragmentation transfer polymerization of p-nitrophenyl acrylate and synthesis of diblock copolymers poly(p-nitrophenyl acrylate)-b-polystyrene. *J. Polym. Sci., Part A Polym. Chem.* **2004,** 42, (19), 4862-4872.

123. Donovan, M. S.; Lowe, A. B.; Sanford, T. A.; McCormick, C. L., Sulfobetaine-containing diblock and triblock copolymers via reversible addition-fragmentation chain transfer polymerization in aqueous media. *Journal of Polymer Science Part A: Polymer Chemistry* **2003,** 41, (9), 1262-1281.

124. Hoogenboom, R.; Schubert, U. S.; Van Camp, W.; Du Prez, F. E., RAFT Polymerization of 1-Ethoxyethyl Acrylate: A Novel Route toward Near-Monodisperse Poly(acrylic acid) and Derived Block Copolymer Structures. *Macromolecules* **2005,** 38, (18), 7653-7659.

125. Beattie, D.; Wong Kok, H.; Williams, C.; Poole-Warren Laura, A.; Davis Thomas, P.; Barner-Kowollik, C.; Stenzel Martina, H., Honeycomb-structured porous films from polypyrrole-containing block copolymers prepared via RAFT polymerization as a scaffold for cell growth. *Biomacromolecules* **2006,** 7, (4), 1072-82.

126. Zhang, B.-Q.; Chen, G.-D.; Pan, C.-Y.; Luan, B.; Hong, C.-Y., Preparation, characterization, and thermal properties of polystyrene-block-quaternized poly(4-vinylpyridine)/montmorillonite nanocomposites. *Journal of Applied Polymer Science* **2006,** 102, (2), 1950-1958.

127. Kanagasabapathy, S.; Sudalai, A.; Benicewicz, B. C., Reversible addition-fragmentation chain-transfer polymerization for the synthesis of poly(4-acetoxystyrene) and poly(4-acetoxystyrene)-block-polystyrene by bulk, solution and emulsion techniques. *Macromol. Rapid Commun.* **2001,** 22, (13), 1076-1080.

128. Garnier, S.; Laschewsky, A., Synthesis of New Amphiphilic Diblock Copolymers and Their Self-Assembly in Aqueous Solution. *Macromolecules* **2005,** 38, (18), 7580-7592.

129. Stenzel, M. H.; Barner-Kowollik, C.; Davis, T. P.; Dalton, H. M., Amphiphilic block copolymers based on poly(2-acryloyloxyethyl phosphorylcholine) prepared via RAFT polymerisation as biocompatible nanocontainers. *Macromolecular Bioscience* **2004,** 4, (4), 445-453.

130. de Lambert, B.; Charreyre, M.-T.; Chaix, C.; Pichot, C., Poly(N-tert-butyl acrylamide-b-N-acryloylmorpholine) amphiphilic block copolymers via RAFT polymerization: Synthesis, purification and characterization. *Polymer* **2007,** 48, (2), 437-447.

131. Wong, K. H.; Davis, T. P.; Barner-Kowollik, C.; Stenzel, M. H., Honeycomb structured porous films from amphiphilic block copolymers prepared via RAFT polymerization. *Polymer* **2007,** 48, (17), 4950-4965.

132. Lokitz, B. S.; Convertine, A. J.; Ezell, R. G.; Heidenreich, A.; Li, Y.; McCormick, C. L., Responsive Nanoassemblies via Interpolyelectrolyte Complexation of Amphiphilic Block Copolymer Micelles. *Macromolecules* **2006,** 39, (25), 8594-8602.

133. Mertoglu, M.; Garnier, S.; Laschewsky, A.; Skrabania, K.; Storsberg, J., Stimuli responsive amphiphilic block copolymers for aqueous media synthesised via reversible addition fragmentation chain transfer polymerization (RAFT). *Polymer* **2005,** 46, (18), 7726-7740.

134. Yang, C.; Cheng, Y.-L., RAFT synthesis of poly(N-isopropylacrylamide) and poly(methacrylic acid) homopolymers and block copolymers: kinetics and characterization. *Journal of Applied Polymer Science* **2006,** 102, (2), 1191-1201.

135. Chong, Y. K.; Le, T. P. T.; Moad, G.; Rizzardo, E.; Thang, S. H., A more versatile route to block copolymers and other polymers of complex architecture by living radical polymerization: the RAFT process. *Macromolecules* **1999,** 32, (6), 2071-2074.

136. Mayadunne, R. T. A.; Rizzardo, E.; Chiefari, J.; Krstina, J.; Moad, G.; Postma, A.; Thang, S. H., Living polymers by the use of trithiocarbonates as reversible addition-fragmentation chain transfer (RAFT) agents. ABA triblock copolymers by radical polymerization in two steps. *Macromolecules* **2000,** 33, (2), 243-245.

137. Yuan, J.-J.; Ma, R.; Gao, Q.; Wang, Y.-F.; Cheng, S.-Y.; Feng, L.-X.; Fan, Z.-Q.; Jiang, L., Synthesis and characterization of polystyrene/poly(4-vinylpyridine) triblock copolymers by reversible addition-fragmentation chain transfer polymerization and their self-assembled aggregates in water. *Journal of Applied Polymer Science* **2003,** 89, (4), 1017-1025.

138. Harrisson, S.; Wooley, K. L., Shell-crosslinked nanostructures from amphiphilic AB and ABA block copolymers of styrene-alt-(maleic anhydride) and styrene: polymerization, assembly and stabilization in one pot. *Chemical Communications (Cambridge, United Kingdom)* **2005**, (26), 3259-3261.

139. Han, D.-H.; Pan, C.-Y., A novel strategy to synthesize double comb-shaped water soluble copolymer by RAFT polymerization. *Macromolecular Chemistry and Physics* **2006,** 207, (9), 836-843.

140. Lopez, R. G.; Boisson, C.; D'Agosto, F.; Spitz, R.; Boisson, F.; Gigmes, D.; Bertin, D., New functional polyolefins: towards a bridge between catalytic and RAFT polymerizations? *Macromol. Rapid Commun.* **2006,** 27, (3), 173-181.

141. Xu, X.; Jia, Z.; Sun, R.; Huang, J., Synthesis of well-defined, brush-type, amphiphilic [poly(styrene-co-2-hydroxyethyl methacrylate)-graft-poly(-caprolactone)]-b-poly(ethylene oxide)-b-[poly(styrene-co-2-hydroxyethyl methacrylate)-graft-poly(-caprolactone)] and its aggregation behavior inaqueous media. *Journal of Polymer Science Part A: Polymer Chemistry* **2006,** 44, (15), 4396-4408.

142. Brouwer, H. D.; Schellekens, M. A. J.; Klumperman, B.; Monteiro, M. J.; German, A. L., Controlled radical copolymerization of styrene and maleic anhydride and the synthesis of novel polyolefin-based block copolymers by reversible addition-fragmentation chain-transfer (RAFT) polymerization. *Journal of Polymer Science Part A: Polymer Chemistry* **2000,** 38, (19), 3596-3603.

143. Shi, L.; Chapman, T. M.; Beckman, E. J., Poly(ethylene glycol)-block-poly(N-vinylformamide) Copolymers Synthesized by the RAFT Methodology. *Macromolecules* **2003,** 36, (7), 2563-2567.

144. Ma, Z.; Lacroix-Desmazes, P., Synthesis of hydrophilic/CO2-philic poly(ethylene oxide)-b-poly (1,1,2,2-tetrahydroperfluorodecyl acrylate) block copolymers via controlled/living radical polymerizations and their properties in liquid and supercritical CO_2. *Journal of Polymer Science Part A: Polymer Chemistry* **2004,** 42, (10), 2405-2415.

145. Ma, Z.; Lacroix-Desmazes, P., Dispersion polymerization of 2-hydroxyethyl methacrylate stabilized by a hydrophilic/CO_2-philic poly(ethylene oxide)-b-poly(1,1,2,2-tetrahydroperfluorodecyl acrylate) (PEO-b-PFDA) diblock copolymer in supercritical carbon dioxide. *Polymer* **2004,** 45, (20), 6789-6797.

146. Hong, C.-Y.; You, Y.-Z.; Pan, C.-Y., Synthesis and characterization of well-defined diblock and triblock copolymers of poly(*N*-isopropylacrylamide) and poly(ethylene oxide). *Journal of Polymer Science Part A: Polymer Chemistry* **2004,** 42, (19), 4873-4881.

147. Li, Y.; Lokitz, B. S.; McCormick, C. L., RAFT Synthesis of a Thermally Responsive ABC Triblock Copolymer Incorporating N-Acryloxysuccinimide for Facile in Situ Formation of Shell Cross-Linked Micelles in Aqueous Media. *Macromolecules* **2006,** 39, (1), 81-89.

148. Kawahara, N.; Kojoh, S.-i.; Matsuo, S.; Kaneko, H.; Matsugi, T.; Saito, J.; Kashiwa, N., Synthetic method of polyethylene-poly(methyl methacrylate) (PE-PMMA) polymer hybrid via reversible addition-fragmentation chain transfer (RAFT) polymerization with functionalized polyethylene. *Polymer Bulletin (Heidelberg, Germany)* **2006,** 57, (6), 805-812.

149. Pai, T. S. C.; Barner-Kowollik, C.; Davis, T. P.; Stenzel, M. H., Synthesis of amphiphilic block copolymers based on poly(dimethylsiloxane) via fragmentation chain transfer (RAFT) polymerization. *Polymer* **2004,** 45, (13), 4383-4389.

150. Hales, M.; Barner-Kowollik, C.; Davis, T. P.; Stenzel, M. H., Shell-Cross-Linked Vesicles Synthesized from Block Copolymers of Poly(D,L-lactide) and Poly(N-isopropyl acrylamide) as Thermoresponsive Nanocontainers. *Langmuir* **2004,** 20, (25), 10809-10817.

151. You, Y.; Hong, C.; Wang, W.; Lu, W.; Pan, C., Preparation and Characterization of Thermally Responsive and Biodegradable Block Copolymer Comprised of PNIPAAM and PLA by Combination of ROP and RAFT Methods. *Macromolecules* **2004,** 37, (26), 9761-9767.

152. Mahanthappa, M. K.; Bates, F. S.; Hillmyer, M. A., Synthesis of ABA Triblock Copolymers by a Tandem ROMP-RAFT Strategy. *Macromolecules* **2005,** 38, (19), 7890-7894.

153. Thurecht, K. J.; Gregory, A. M.; Villarroya, S.; Zhou, J.; Heise, A.; Howdle, S. M., Simultaneous enzymatic ring opening polymerization and RAFT-mediated polymerization in supercritical CO_2. *Chemical Communications (Cambridge, United Kingdom)* **2006**, (42), 4383-4385.

154. Jia, Z.; Xu, X.; Fu, Q.; Huang, J., S Synthesis and self-assembly morphologies of amphiphilic multiblock copolymers [poly(ethylene oxide)-b-polystyrene]n via trithiocarbonate- embedded PEO macro-RAFT agent. *Journal of Polymer Science Part A: Polymer Chemistry* **2006,** 44, (20), 6071-6082.

155. Motokucho, S.; Sudo, A.; Sanda, F.; Endo, T., Controlled monomer insertion into polymer main chain: synthesis of sequence ordered polystyrene containing thiourethane and trithiocarbonate units by the RAFT process. *Chemical Communications (Cambridge, United Kingdom)* **2002**, (17), 1946-1947.

156. Stenzel, M. H.; Cummins, L.; Roberts, G. E.; Davis, T. P.; Vana, P.; Barner-Kowollik, C., Xanthate mediated living polymerization of vinyl acetate: A systematic variation in MADIX/RAFT agent structure. *Macromolecular Chemistry and Physics* **2003,** 204, (9), 1160-1168.

157. Theis, A.; Stenzel, M. H.; Davis, T. P.; Coote, M. L.; Barner-Kowollik, C., A Synthetic Approach to a Novel Class of Fluorine-Bearing Reversible Addition-Fragmentation Chain Transfer (RAFT) Agents: F-RAFT. *Aust. J. Chem.* **2005,** 58, (6), 437-441.

158. Kolb, H. C.; Finn, M. G.; Sharpless, K. B., Click chemistry: diverse chemical function from a few good reactions. *Angewandte Chemie, International Edition* **2001,** 40, (11), 2004-2021.

159. Quemener, D.; Davis, T. P.; Barner-Kowollik, C.; Stenzel, M. H., RAFT and click chemistry: a versatile approach to well-defined block copolymers. *Chemical Communications (Cambridge, United Kingdom)* **2006**, (48), 5051-5053.

160. Ting, S. R. S.; Granville, A. M.; Quemener, D.; Davis, T. P.; Stenzel, M. H.; Barner-Kowollik, C., RAFT Chemistry and Huisgen 1,3-Dipolar Cycloaddition: A Route to Block Copolymers of Vinyl Acetate and 6-O-Methacryloyl Mannose? *Aust. J. Chem.* **2007,** 60, (6), 405-409.

161. Gondi, S. R.; Vogt, A. P.; Sumerlin, B. S., Versatile pathway to functional telechelics via RAFT polymerization and click chemistry. *Macromolecules* **2007,** 40, (3), 474-481.

162. O'Reilly, R. K.; Joralemon, M. J.; Hawker, C. J.; Wooley, K. L., Facile syntheses of surface-functionalized micelles and shell cross-linked nanoparticles. *Journal of Polymer Science Part A: Polymer Chemistry* **2006,** 44, (17), 5203-5217.

163. O'Reilly, R. K.; Joralemon, M. J.; Hawker, C. J.; Wooley, K. L., Fluorogenic 1,3-dipolar cycloaddition within the hydrophobic core of a shell cross-linked nanoparticle. *Chemistry--A European Journal* **2006,** 12, (26), 6776-6786.

164. Skoog, D. A., *Principles of Instrumental Analysis. 3rd Ed*. 1985; p 879 pp.

165. Field, L. D.; Sternhell, S.; Kalman, J. R.; Editors, *Organic Structures from Spectra, Fourth Edition*. 2008; p 453 pp.

166. Silverstein, R. M.; Webster, F. X.; Kiemie, D., *Spectrometric Identification of Organic Compounds, 7th Edition*. 2002; p 490 pp.

167. Skoog, D. A.; West, D. M.; Holler, F. J., *Fundamentals of Analytical Chemistry. 5th Ed*. 1988; p 894 pp.

168. Patrick, G. L., *Organic Chemistry, Second Edition*. 2004; p 357 pp.

169. Thomas, G.; Goringe, M. J., *Transmission Electron Microscopy of Materials*. 1979; p 388 pp.

170. Posner, T., Contributions for the knowledge of the unsaturated compounds. [machine translation]. *Berichte der Deutschen Chemischen Gesellschaft* **1905,** 38, 646-57.

171. Dondoni, A., The emergence of thiol-ene coupling as a click process for materials and bioorganic chemistry. *Angewandte Chemie, International Edition* **2008,** 47, (47), 8995-8997.

172. Shen, Y.; Tang, H.; Ding, S., Catalyst separation in atom transfer radical polymerization. *Progress in Polymer Science* **2004,** 29, (10), 1053-1078.

173. Hoyle, C. E.; Lowe, A. B.; Bowman, C. N., Thiol-click chemistry: a multifaceted toolbox for small molecule and polymer synthesis. *Chemical Society Reviews* **2010,** 39, (4), 1355-1387.

174. Scales, C. W.; Convertine, A. J.; McCormick, C. L., Fluorescent Labeling of RAFT-Generated Poly(N-isopropylacrylamide) via a Facile Maleimide-Thiol Coupling Reaction. *Biomacromolecules* **2006,** 7, (5), 1389-1392.

175. Lowe, A. B.; Harvison, M. A., Thiol-Based 'Click' Chemistries in Polymer: Synthesis and Modification. *Australian Journal of Chemistry* **2010,** 63, (8), 1251-1266.

176. Lowe, A. B., Thiol-ene "click" reactions and recent applications in polymer and materials synthesis. *Polymer Chemistry* **2010,** 1, (1), 17-36.

177. Chan, J. W.; Yu, B.; Hoyle, C. E.; Lowe, A. B., Convergent synthesis of 3-arm star polymers from RAFT-prepared poly(N,N-diethylacrylamide) via a thiol-ene click reaction. *Chemical Communications (Cambridge, United Kingdom)* **2008**, (40), 4959-4961.

178. Chan, J. W.; Yu, B.; Hoyle, C. E.; Lowe, A. B., The nucleophilic, phosphine-catalyzed thiol-ene click reaction and convergent star synthesis with RAFT-prepared homopolymers. *Polymer* **2009,** 50, (14), 3158-3168.

179. Singha, N. K.; Gibson, M. I.; Koiry, B. P.; Danial, M.; Klok, H.-A., Side-Chain Peptide-Synthetic Polymer Conjugates via Tandem "Ester-Amide/Thiol–Ene" Post-Polymerization Modification of Poly(pentafluorophenyl methacrylate) Obtained Using ATRP. *Biomacromolecules* **2011,** 12, (8), 2908-2913.

180. Chen, G.; Amajjahe, S.; Stenzel, M. H., Synthesis of thiol-linked neoglycopolymers and thermo-responsive glycomicelles as potential drug carrier. *Chemical Communications (Cambridge, United Kingdom)* **2009**, (10), 1198-1200.

181. Sun, J.; Schlaad, H., Thiol−Ene Clickable Polypeptides. *Macromolecules* **2010,** 43, (10), 4445-4448.

182. Huynh, V. T.; Chen, G.; Souza, P. d.; Stenzel, M. H., Thiol-yne and Thiol-ene "Click" Chemistry as a Tool for a Variety of Platinum Drug Delivery Carriers, from Statistical Copolymers to Crosslinked Micelles. *Biomacromolecules* **2011,** 12, (5), 1738-1751.

183. Espeel, P.; Goethals, F.; Du Prez, F. E., One-Pot Multistep Reactions Based on Thiolactones: Extending the Realm of Thiol−Ene Chemistry in Polymer Synthesis. *Journal of the American Chemical Society* **2011,** 133, (6), 1678-1681.

184. Bousquet, A.; Barner-Kowollik, C.; Stenzel, M. H., Synthesis of Comb Polymers via Grafting-Onto Macromolecules Bearing Pendant Diene Groups via the Hetero-Diels-Alder-RAFT Click Concept. *Journal of Polymer Science Part a-Polymer Chemistry* **2010,** 48, (8), 1773-1781.

185. Valade, D.; Boyer, C.; Davis, T. P.; Bulmus, V., Synthesis of siRNA Polyplexes Adopting a Combination of RAFT Polymerization and Thiol-ene Chemistry. *Australian Journal of Chemistry* **2009,** 62, (10), 1344-1350.

186. Jia, Z.; Liu, J.; Davis, T. P.; Bulmus, V., RAFT polymerization and thiol-ene modification of 2-vinyloxyethyl methacrylate: Towards functional branched polymers. *Polymer* **2009,** 50, (25), 5928-5932.

187. Ma, J.; Cheng, C.; Sun, G.; Wooley, K. L., Well-Defined Polymers Bearing Pendent Alkene Functionalities via Selective RAFT Polymerization. *Macromolecules (Washington, DC, United States)* **2008,** 41, (23), 9080-9089.

188. Ma, J.; Bartels, J. W.; Li, Z.; Zhang, K.; Cheng, C.; Wooley, K. L., Synthesis and Solution-state Assembly or Bulk State Thiol-ene Crosslinking of Pyrrolidinone- and Alkene-functionalized Amphiphilic Block Fluorocopolymers: From Functional Nanoparticles to Anti-fouling Coatings. *Australian Journal of Chemistry* **2010,** 63, (8), 1159-1163.

189. Dong, Z. M.; Liu, X. H.; Tang, X. L.; Li, Y. S., Synthesis of Hyperbranched Polymers with Pendent Norbornene Functionalities via RAFT Polymerization of a Novel Asymmetrical Divinyl Monomer. *Macromolecules* **2009,** 42, (13), 4596-4603.

190. Sugiyama, F.; Satoh, K.; Kamigaito, M., Regiospecific Radical Polymerization of Vinyl Methacrylate in the Presence of Lewis Acids into Soluble Polymers with Pendent Vinyl Ester Substituents. *Macromolecules (Washington, DC, United States)* **2008,** 41, (9), 3042-3048.

191. Nishikubo, T.; Kishida, M.; Ichijyo, T.; Takaoka, T., Photopolymers. 10. Cationic polymerization of vinyloxyethyl acrylate. *Makromolekulare Chemie* **1974,** 175, (12), 3357-66.

192. Yasuda, H.; Morita, Y.; Noda, I.; Sugi, K.; Nakamura, A., Organometallic polymers containing tricarbonyl(η4-diene)ruthenium(0) and -iron(0) as pendant groups. *Journal of Organometallic Chemistry* **1981,** 205, (2), C9-C13.

193. Yokota, K.; Matsumura, M.; Yamaguchi, K.; Takada, Y., Synthesis of polymers with benzo-19-crown-6 units via cyclopolymerization of divinyl ethers. *Makromolekulare Chemie, Rapid Communications* **1983,** 4, (11), 721-4.

194. Hashimoto, T.; Ibuki, H.; Sawamoto, M.; Higashimura, T., Living cationic polymerization of 2-vinyloxyethylphthalimide: synthesis of poly(vinyl ether) with pendant primary amino functions. *Journal of Polymer Science, Part A: Polymer Chemistry* **1988,** 26, (12), 3361-74.

195. Kakuchi, T.; Aoki, K.; Haba, O.; Yokata, K., Polymeric chiral crown ethers. 9. Synthesis and chiral recognition ability of copolymers with (S)-binaphtho-21-crown-6 and D-manno-21-crown-6-units by cyclocopolymerizations of α,ω-divinylethers with monovinyl ether. *Polymer Bulletin (Berlin, Germany)* **1993,** 31, (1), 37-42.

196. Nishikubo, T.; Kameyama, A.; Sasano, M., Synthesis of functional polymers bearing cyclic carbonate groups from (2-oxo-1,3-dioxolan-4-yl)methyl vinyl ether. *Journal of Polymer Science, Part A: Polymer Chemistry* **1994,** 32, (2), 301-8.

197. Yamada, K.; Minoda, M.; Miyamoto, T., Controlled synthesis of glycopolymers with pendant D-glucosamine residues by living cationic polymerization. *Journal of Polymer Science, Part A: Polymer Chemistry* **1997,** 35, (4), 751-757.

198. Maddess, M. L.; Lautens, M., Preparation of Homoallylic Homopropargylic Alcohols from 2-Vinyloxiranes. *Organic Letters* **2005,** 7, (16), 3557-3560.

199. Wu, Q.; Liu, B.-K.; Lin, X.-F., Enzymatic promiscuity for organic synthesis and cascade process. *Current Organic Chemistry* **2010,** 14, (17), 1966-1988.

200. Busto, E.; Gotor-Fernandez, V.; Gotor, V., Hydrolases: catalytically promiscuous enzymes for non-conventional reactions in organic synthesis. *Chemical Society Reviews* **2010,** 39, (11), 4504-4523.

201. Dhake, K. P.; Tambade, P. J.; Singhal, R. S.; Bhanage, B. M., Promiscuous Candida antarctica lipase B-catalyzed synthesis of β-amino esters via aza-Michael addition of amines to acrylates. *Tetrahedron Letters* **2010,** 51, (33), 4455-4458.

202. Humble, M. S.; Berglund, P., Biocatalytic Promiscuity. *European Journal of Organic Chemistry* **2011,** 2011, (19), 3391-3401.

203. Heise, A.; Palmans, A. R. A., Hydrolases in polymer chemistry: chemoenzymatic approaches to polymeric materials. *Advances in Polymer Science* **2010,** 237, (Enzymatic Polymerisation), 79-113.

204. Kobayashi, S.; Morino, K.; Yashima, E., Macromolecular helicity inversion of an optically active helical poly(phenylacetylene) by chemical modification of the side groups. *Chemical Communications (Cambridge, United Kingdom)* **2007**, (23), 2351-2353.

205. Duxbury, C. J.; Hilker, I.; de Wildeman, S. M. A.; Heise, A., Enzyme-responsive materials: chirality to program polymer reactivity. *Angewandte Chemie, International Edition* **2007,** 46, (44), 8452-8454.

206. Padovani, M.; Hilker, I.; Duxbury, C. J.; Heise, A., Functionalization of Polymers with High Precision by Dual Regio- and Stereoselective Enzymatic Reactions. *Macromolecules (Washington, DC, United States)* **2008,** 41, (7), 2439-2444.

207. Lou, F.-W.; Liu, B.-K.; Wu, Q.; Lv, D.-S.; Lin, X.-F., Candida antarctica lipase B (CAL-B)-catalyzed carbon-sulfur bond addition and controllable selectivity in organic media. *Advanced Synthesis & Catalysis* **2008,** 350, (13), 1959-1962.

208. Lou, F.-W.; Liu, B.-K.; Wang, J.-L.; Pan, Q.; Lin, X.-F., Controllable enzymatic Markovnikov addition and acylation of thiols to vinyl esters. *Journal of Molecular Catalysis B: Enzymatic* **2009,** 60, (1-2), 64-68.

209. Thang, S. H.; Chong, Y. K.; Mayadunne, R. T. A.; Moad, G.; Rizzardo, E., A novel synthesis of functional dithioesters, dithiocarbamates, xanthates and trithiocarbonates. *Tetrahedron Letters* **1999,** 40, (12), 2435-2438.

210. Kuzuya, A.; Ohnishi, T.; Wasano, T.; Nagaoka, S.; Sumaoka, J.; Ihara, T.; Jyo, A.; Komiyama, M., Efficient Guest Inclusion by β-Cyclodextrin Attached to the Ends of DNA Oligomers upon Hybridization to Various DNA Conjugates. *Bioconjugate Chemistry* **2009,** 20, (8), 1643-1649.

211. Petter, R. C.; Salek, J. S.; Sikorski, C. T.; Kumaravel, G.; Lin, F. T., Cooperative binding by aggregated mono-6-(alkylamino)-β-cyclodextrins. *Journal of the American Chemical Society* **1990,** 112, (10), 3860-8.

212. Kawai, W., Polymerizations of some diene monomers. Preparations and polymerizations of vinyl methacrylate, allyl methacrylate, N-allylacrylamide, and N-allylmethacrylamide. *Journal of Polymer Science Part A-1: Polymer Chemistry* **1966,** 4, (5), 1191-1201.

213. Guaita, M.; Camino, G.; Trossarelli, L., Free radical polymerization of unconjugated dienes. XI. Vinylmethacrylate in benzene at 60°C. *Die Makromolekulare Chemie* **1971,** 146, (1), 133-140.

214. Lu, Z.; Lee, S. Y.; Goh, S. H., Group transfer copolymerisation of vinyl methacrylate and methyl methacrylate. *Polymer* **1997,** 38, (23), 5893-5895.

215. Destarac, M., On the Critical Role of RAFT Agent Design in Reversible Addition-Fragmentation Chain Transfer (RAFT) Polymerization. *Polymer Reviews* **2011,** 51, (2), 163-187.

216. Dong, Z.-m.; Liu, X.-h.; Tang, X.-l.; Li, Y.-s., Synthesis of Hyperbranched Polymers with Pendent Norbornene Functionalities via RAFT Polymerization of a Novel Asymmetrical Divinyl Monomer. *Macromolecules (Washington, DC, United States)* **2009,** 42, (13), 4596-4603.

217. Uwe Theo Bornscheuer; Kazlauskas, R. J., *Hydrolases in Organic Synthesis: Regio- and Stereoselective Biotransformations* Second Edition ed.; Wiley-VCH Verlag GmbH& Co. KGaA, Weinheim: 2006; p 27.

218. Hoyle, C. E.; Lee, T. Y.; Roper, T., Thiol-enes: Chemistry of the past with promise for the future. *Journal of Polymer Science, Part A: Polymer Chemistry* **2004,** 42, (21), 5301-5338.

219. Uekama, K.; Hirayama, F.; Irie, T., Cyclodextrin Drug Carrier Systems. *Chemical Reviews (Washington, D. C.)* **1998,** 98, (5), 2045-2076.

220. Cheng, J.; Khin, K. T.; Davis, M. E., Antitumor activity of β-cyclodextrin polymer-camptothecin conjugates. *Mol. Pharm.* **2004,** 1, (3), 183-193.

221. Skiba, M.; Bounoure, F.; Barbot, C.; Arnaud, P.; Skiba, M., Development of cyclodextrin microspheres for pulmonary drug delivery. *Journal of Pharmacy & Pharmaceutical Sciences* **2005,** 8, (3), 409-418.

222. Zhang, J.-T.; Huang, S.-W.; Zhuo, R.-X., Preparation and characterization of novel temperature sensitive poly(N-isopropylacrylamide-co-acryloyl beta-cyclodextrin) hydrogels with fast shrinking kinetics. *Macromolecular Chemistry and Physics* **2004,** 205, (1), 107-113.

223. Maciollek, A.; Munteanu, M.; Ritter, H., New Generation of Polymeric Drugs: Copolymer from NIPAAM and Cyclodextrin Methacrylate Containing Supramolecular-Attached Antitumor Derivative. *Macromol. Chem. Phys.* **2010,** 211, (2), 245-249.

224. Yhaya, F.; Gregory, A. M.; Stenzel, M. H., Polymers with Sugar Buckets The Attachment of Cyclodextrins onto Polymer Chains. *Australian Journal of Chemistry* **2010,** 63, (2), 195-210.

225. Amajjahe, S.; Choi, S.; Munteanu, M.; Ritter, H., Pseudopolyanions based on poly(NIPAAM-co-beta-cyclodextrin methacrylate) and ionic liquids. *Angewandte Chemie-International Edition* **2008,** 47, (18), 3435-3437.

226. Amajjahe, S.; Munteanu, M.; Ritter, H., Switching the Solubility of PMMA Bearing Attached Cyclodextrin-Moieties by Supramolecular Interactions with Ionic Liquids. *Macromolecular Rapid Communications* **2009,** 30, (11), 904-908.

227. Perrier, S.; Takolpuckdee, P., Macromolecular design via reversible addition-fragmentation chain transfer (RAFT)/xanthates (MADIX) polymerization. *Journal of Polymer Science Part A: Polymer Chemistry* **2005,** 43, (22), 5347-5393.

228. Favier, A.; Charreyre, M. T., Experimental requirements for an efficient control of free-radical polymerizations via the reversible addition-fragmentation chain transfer (RAFT) process. *Macromolecular Rapid Communications* **2006,** 27, (9), 653-692.

229. Moad, G.; Rizzardo, E.; Thang, S. H., Living Radical Polymerization by the RAFT Process – A Second Update. *Australian Journal of Chemistry* **2009,** 62, (11), 1402-1472.

230. Moad, G.; Thang, S. H., RAFT Polymerization: Materials of The Future, Science of Today: Radical Polymerization - The Next Stage Foreword. *Australian Journal of Chemistry* **2009,** 62, (11), 1379-1381.

231. Stenzel, M. H., RAFT polymerization: an avenue to functional polymeric micelles for drug delivery. *Chemical Communications* **2008**, (30), 3486-3503.

232. Stenzel, M. H., Hairy Core-Shell Nanoparticles via RAFT: Where are the Opportunities and Where are the Problems and Challenges? *Macromolecular Rapid Communications* **2009,** 30, (19), 1603-1624.

233. Gregory, A.; Stenzel, M. H., The use of reversible addition fragmentation chain transfer polymerization for drug delivery systems. *Expert Opinion on Drug Delivery* **2011,** 8, (2), 237-269.

234. Kim, S.; Shi, Y. Z.; Kim, J. Y.; Park, K.; Cheng, J. X., Overcoming the barriers in micellar drug delivery: loading efficiency, in vivo stability, and micelle-cell interaction. *Expert Opinion on Drug Delivery* **2010,** 7, (1), 49-62.

235. Stenzel, M. H.; Davis, T. P., Star polymer synthesis using trithiocarbonate functional β-cyclodextrin cores (reversible addition-fragmentation chain-transfer polymerization). *J. Polym. Sci., Part A Polym. Chem.* **2002,** 40, (24), 4498-4512.

236. Stenzel, M. H.; Davis, T. P.; Fane, A. G., Honeycomb structured porous films prepared from carbohydrate based polymers synthesized via the RAFT process. *Journal of Materials Chemistry* **2003,** 13, (9), 2090-2097.

237. Harvey, D. F.; Lund, K. P.; Neil, D. A., Cyclization reactions of molybdenum and chromium carbene complexes with 1,6- and 1,7-enynes: effect of tether length and composition. *Journal of the American Chemical Society* **1992,** 114, (22), 8424-34.

238. Malkoch, M.; Thibault, R. J.; Drockenmuller, E.; Messerschmidt, M.; Voit, B.; Russell, T. P.; Hawker, C. J., Orthogonal Approaches to the Simultaneous and Cascade Functionalization of Macromolecules Using Click Chemistry. *Journal of the American Chemical Society* **2005,** 127, (42), 14942-14949.

239. Ladmiral, V.; Mantovani, G.; Clarkson, G. J.; Cauet, S.; Irwin, J. L.; Haddleton, D. M., Synthesis of Neoglycopolymers by a Combination of "Click Chemistry" and Living Radical Polymerization. *Journal of the American Chemical Society* **2006,** 128, (14), 4823-4830.

240. Khan, A. R.; Forgo, P.; Stine, K. J.; D'Souza, V. T., Methods for Selective Modifications of Cyclodextrins. *Chemical Reviews (Washington, D. C.)* **1998,** 98, (5), 1977-1996.

241. Zhang, L.; Bernard, J.; Davis, T. P.; Barner-Kowollik, C.; Stenzel, M. H., Acid-degradable core-crosslinked micelles prepared from thermosensitive glycopolymers synthesized via RAFT polymerization. *Macromolecular Rapid Communications* **2008,** 29, (2), 123-129.

242. vanHerk, A. M., *CONTOUR (v1.8).*

243. vanHerk, A. M.; Droge, T., Nonlinear least squares fitting applied to copolymerization modeling. *Macromol. Theory Simul.* **1997,** 6, (6), 1263-1276.

244. Feldermann, A.; Toy, A. A.; Phan, H.; Stenzel, M. H.; Davis, T. P.; Barner-Kowollik, C., Reversible addition fragmentation chain transfer copolymerization: influence of the RAFT process on the copolymer composition. *Polymer* **2004,** 45, (12), 3997-4007.

245. Pai, T. S. C.; Barner-Kowollik, C.; Davis, T. P.; Stenzel, M. H., Synthesis of amphiphilic block copolymers based on poly (dimethyl siloxane) via fragmentation chain transfer (RAFT) polymerization. *Polymer* **2004,** 45, (13), 4383-4389.

246. Quemener, D.; Le Hellaye, M.; Bissett, C.; Davis, T. P.; Barner-Kowollik, C.; Stenzel, M. H., Graft block copolymers of propargyl methacrylate and vinyl acetate via a combination of RAFT/MADIX and click chemistry: Reaction analysis. *Journal of Polymer Science Part a-Polymer Chemistry* **2008,** 46, (1), 155-173.

247. Schild, H. G., POLY (N-ISOPROPYLACRYLAMIDE) - EXPERIMENT, THEORY AND APPLICATION. *Progress in Polymer Science* **1992,** 17, (2), 163-249.

248. Choi, S.; Munteanu, M.; Ritter, H., Monoacrylated cyclodextrin via "click" reaction and copolymerization with N-isopropylacrylamide: guest controlled solution properties. *Journal of Polymer Research* **2009,** 16, (4), 389-394.

249. Tonelli, A. E., Soluble PEG-alpha-CD-rotaxanes: Where on the PEG chains are the permanently threaded alpha-CDs located and are they mobile? *Macromolecules* **2008,** 41, (11), 4058-4060.

250. Tonelli, A. E., Nanostructuring and functionalizing polymers with cyclodextrins. *Polymer* **2008,** 49, (7), 1725-1736.

251. Harada, A.; Kamachi, M., Complex formation between poly(ethylene glycol) and α-cyclodextrin. *Macromolecules* **1990,** 23, (10), 2821-2823.

252. van de Manakker, F.; Vermonden, T.; van Nostrum, C. F.; Hennink, W. E., Cyclodextrin-Based Polymeric Materials: Synthesis, Properties, and Pharmaceutical/Biomedical Applications. *Biomacromolecules* **2009,** 10, (12), 3157-3175.

253. Zhu, W.; Li, Y.; Liu, L.; Chen, Y.; Wang, C.; Xi, F., Supramolecular Hydrogels from Cisplatin-Loaded Block Copolymer Nanoparticles and α-Cyclodextrins with a Stepwise Delivery Property. *Biomacromolecules* **2010,** 11, (11), 3086-3092.

254. Pourgholami, M. H.; Woon, L.; Almajd, R.; Akhter, J.; Bowery, P.; Morris, D. L., In vitro and in vivo suppression of growth of hepatocellular carcinoma cells by albendazole. *Cancer Letters (Shannon, Ireland)* **2001,** 165, (1), 43-49.

255. Morris, D. L.; Jourdan, J.-L.; Pourgholami, M. H., Pilot study of albendazole in patients with advanced malignancy: effect on serum tumor markers/high incidence of neutropenia. *Oncology* **2001,** 61, (1), 42-46.

256. Hossein Pourgholami, M.; Cai, Z. Y.; Lu, Y.; Wang, L.; Lawson Morris, D., Albendazole: a Potent Inhibitor of Vascular Endothelial Growth Factor and Malignant Ascites Formation in OVCAR-3 Tumor-Bearing Nude Mice. *Clinical Cancer Research* **2006,** 12, (6), 1928-1935.

257. Khalilzadeh, A.; Wangoo, K. T.; Morris, D. L.; Pourgholami, M. H., Epothilone-paclitaxel resistant leukemic cells CEM/dEpoB300 are sensitive to albendazole: Involvement of apoptotic pathways. *Biochemical Pharmacology* **2007,** 74, (3), 407-414.

258. Jung, H.; Medina, L.; Garcia, L.; Fuentes, I.; Moreno-Esparza, R., Absorption studies of albendazole and some physicochemical properties of the drug and its metabolite albendazole sulfoxide. *Journal of Pharmacy and Pharmacology* **1998,** 50, (1), 43-48.

259. Kim, Y.; Pourgholami, M. H.; Morris, D. L.; Stenzel, M. H., An Optimized RGD-Decorated Micellar Drug Delivery System for Albendazole for the Treatment of Ovarian Cancer: From RAFT Polymer Synthesis to Cellular Uptake. *Macromolecular Bioscience* **2011,** 11, (2), 219-233.

260. Evrard, B.; Chiap, P.; DeTullio, P.; Ghalmi, F.; Piel, G.; Van Hees, T.; Crommen, J.; Losson, B.; Delattre, L., Oral bioavailability in sheep of albendazole from a suspension and from a solution containing hydroxypropyl-[beta]-cyclodextrin. *Journal of Controlled Release* **2002,** 85, (1-3), 45-50.

261. Kata M, Shauer M,, Increasing the solubility characteristics of albendazole by dimethyl-β-cyclodextrin. *Acta Pharm Hung* **1991,** 61, 23.

262. Moriwaki, C.; Costa, G. L.; Ferracini, C. N.; de Moraes, F. F.; Zanin, G. M.; Pineda, E. A. G.; Matioli, G., Enhancement of solubility of albendazole by complexation with beta-cyclodextrin. *Brazilian Journal of Chemical Engineering* **2008,** 25, (2), 255-267.

263. Rojas-Aguirre, Y.; Yépez-Mulia, L.; Castillo, I.; López-Vallejo, F.; Soria-Arteche, O.; Hernández-Campos, A.; Castillo, R.; Hernández-Luis, F., Studies on 6-chloro-5-(1-naphthyloxy)-2-(trifluoromethyl)-1H-benzimidazole/2-hydroxypropyl-β-cyclodextrin association: Characterization, molecular modeling studies, and in vivo anthelminthic activity. *Bioorganic & Medicinal Chemistry* **2011,** 19, (2), 789-797.

264. Weickenmeier, M.; Wenz, G., Cyclodextrin sidechain polyesters - Synthesis and inclusion of adamantan derivatives. *Macromolecular Rapid Communications* **1996,** 17, (10), 731-736.

265. Gelb, R. I.; Schwartz, L. M., COMPLEXATION OF ADAMANTANE-AMMONIUM SUBSTRATES BY BETA-CYCLODEXTRIN AND ITS O-METHYLATED DERIVATIVES. *Journal of Inclusion Phenomena* **1989,** 7, (5), 537-543.

266. Zhang, B. L.; Breslow, R., ENTHALPIC DOMINATION OF THE CHELATE EFFECT IN CYCLODEXTRIN DIMERS. *Journal of the American Chemical Society* **1993,** 115, (20), 9353-9354.

267. Rekharsky, M. V.; Inoue, Y., Complexation thermodynamics of cyclodextrins. *Chemical Reviews* **1998,** 98, (5), 1875-1917.

268. Irie, T.; Uekama, K., Pharmaceutical applications of cyclodextrins. III. Toxicological issues and safety evaluation. *Journal of Pharmaceutical Sciences* **1997,** 86, (2), 147-162.

269. Stella, V. J.; Rajewski, R. A., Cyclodextrins: their future in drug formulation and delivery. *Pharmaceutical Research* **1997,** 14, (5), 556-567.

270. Brewster, M. E.; Loftsson, T., Cyclodextrins as pharmaceutical solubilizers. *Advanced Drug Delivery Reviews* **2007,** 59, (7), 645-666.

271. Loftsson, T.; Brewster, M. E., Pharmaceutical applications of cyclodextrins: basic science and product development. *Journal of Pharmacy and Pharmacology* **2010,** 62, (11), 1607-1621.

272. Savic, R.; Eisenberg, A.; Maysinger, D., Block copolymer micelles as delivery vehicles of hydrophobic drugs: micelle-cell interactions. *J. Drug Targeting* **2006,** 14, (6), 343-355.

273. Rapoport, N., Physical stimuli-responsive polymeric micelles for anti-cancer drug delivery. *Prog. Polym. Sci.* **2007,** 32, (8-9), 962-990.

274. Seymour, L. W.; Duncan, R.; Strohalm, J.; Kopecek, J., Effect of molecular weight (.hivin.Mw) of N-(2-hydroxypropyl)methacrylamide copolymers on body distribution and rate of excretion after subcutaneous, intraperitoneal, and intravenous administration to rats. *J. Biomed. Mater. Res.* **1987,** 21, (11), 1341-58.

275. Matsumura, Y.; Maeda, H., A new concept for macromolecular therapeutics in cancer chemotherapy: mechanism of tumoritropic accumulation of proteins and the ntitumor agent smancs. *Cancer Res.* **1986,** 46, (12, Pt. 1), 6387-92.

276. Stenzel, M. H., RAFT polymerization: an avenue to functional polymeric micelles for drug delivery. *Chem. Commun. (Cambridge, U. K.)* **2008**, (30), 3486-3503.

277. Nishiyama, N.; Kataoka, K., Current state, achievements, and future prospects of polymeric micelles as nanocarriers for drug and gene delivery. *Pharmacol. Ther.* **2006,** 112, (3), 630-648.

278. Allen, C.; Maysinger, D.; Eisenberg, A., Nano-engineering block copolymer aggregates for drug delivery. *Colloids Surf., B* **1999,** 16, (1-4), 3-27.

279. Savic, R.; Luo, L.; Eisenberg, A.; Maysinger, D., Micellar Nanocontainers Distribute to Defined Cytoplasmic Organelles. *Science (Washington, DC, U. S.)* **2003,** 300, (5619), 615-618.

280. Lavasanifar, A.; Samuel, J.; Kwon, G. S., Poly(ethylene oxide)-block-poly(L-amino acid) micelles for drug delivery. *Adv. Drug Delivery Rev.* **2002,** 54, (2), 169-190.

281. Kakizawa, Y.; Kataoka, K., Block copolymer micelles for delivery of gene and related compounds. *Adv. Drug Delivery Rev.* **2002,** 54, (2), 203-222.

282. Kabanov, A. V.; Alakhov, V. Y., Pluronic block copolymers in drug delivery: from micellar nanocontainers to biological response modifiers. *Crit. Rev. Ther. Drug Carrier Syst.* **2002,** 19, (1), 1-72.

283. Huynh, V. T.; de Souza, P.; Stenzel, M. H., Polymeric Micelles with Pendant Dicarboxylato Chelating Ligands Prepared via a Michael Addition for cis-Platinum Drug Delivery. *Macromolecules* **2011,** 44, (20), 7888-7900.

284. Cavalli, R.; Trotta, F.; Tumiatti, W., Cyclodextrin-based Nanosponges for Drug Delivery. *Journal of Inclusion Phenomena and Macrocyclic Chemistry* **2006,** 56, (1), 209-213.

285. Vyas, A.; Saraf, S.; Saraf, S., Cyclodextrin based novel drug delivery systems. *Journal of Inclusion Phenomena and Macrocyclic Chemistry* **2008,** 62, (1), 23-42.

286. Yhaya, F.; Lim, J.; Kim, Y.; Liang, M.; Gregory, A. M.; Stenzel, M. H., Development of Micellar Novel Drug Carrier Utilizing Temperature-Sensitive Block Copolymers Containing Cyclodextrin Moieties. *Macromolecules (Washington, DC, U. S.)* **2011,** 44, (21), 8433-8445.

287. Riess, G., Micellization of block copolymers. *Prog. Polym. Sci.* **2003,** 28, (7), 1107-1170.

288. Kim, Y.; Pourgholami, M. H.; Morris, D. L.; Stenzel, M. H., Effect of crosslinking on the performance of micelles as drug delivery carriers: A cell uptake study. *Biomacromolecules* **2012**.

289. Iijima, M.; Nagasaki, Y.; Okada, T.; Kato, M.; Kataoka, K., Core-Polymerized Reactive Micelles from Heterotelechelic Amphiphilic Block Copolymers. *Macromolecules* **1999,** 32, (4), 1140-1146.

290. Emoto, K.; Nagasaki, Y.; Kataoka, K., Coating of Surfaces with Stabilized Reactive Micelles from Poly(ethylene glycol)-Poly(DL-lactic acid) Block Copolymer. *Langmuir* **1999,** 15, (16), 5212-5218.

291. Won, Y.-Y.; Davis, H. T.; Bates, F. S., Giant wormlike rubber micelles. *Science (Washington, D. C.)* **1999,** 283, (5404), 960-963.

292. Li, Y.; Lokitz, B. S.; Armes, S. P.; McCormick, C. L., Synthesis of Reversible Shell Cross-Linked Micelles for Controlled Release of Bioactive Agents. *Macromolecules* **2006,** 39, (8), 2726-2728.

293. Ma, Q.; Remsen, E. E.; Kowalewski, T.; Schaefer, J.; Wooley, K. L., Environmentally-Responsive, Entirely Hydrophilic, Shell Cross-linked (SCK) Nanoparticles. *Nano Lett.* **2001,** 1, (11), 651-655.

294. Wooley, K. L., Shell crosslinked polymer assemblies: nanoscale constructs inspired from biological systems. *J. Polym. Sci., Part A Polym. Chem.* **2000,** 38, (9), 1397-1407.

295. Thurmond, K. B., II; Kowalewski, T.; Wooley, K. L., Water-Soluble Knedel-like Structures: The Preparation of Shell-Cross-Linked Small Particles. *J. Am. Chem. Soc.* **1996,** 118, (30), 7239-7240.

296. Huang, H.; Remsen, E. E.; Kowalewski, T.; Wooley, K. L., Nanocages Derived from Shell Cross-Linked Micelle Templates. *J. Am. Chem. Soc.* **1999,** 121, (15), 3805-3806.

297. O'Reilly, R. K.; Hawker, C. J.; Wooley, K. L., Crosslinked block copolymer micelles: functional nanostructures of great potential and versatility. *Chem. Soc. Rev.* **2006,** 35, (11), 1068-1083.

298. O'Reilly, R. K.; Joralemon, M. J.; Hawker, C. J.; Wooley, K. L., Facile syntheses of surface-functionalized micelles and shell cross-linked nanoparticles. *J. Polym. Sci., Part A Polym. Chem.* **2006,** 44, (17), 5203-5217.

299. Read, E. S.; Armes, S. P., Recent advances in shell cross-linked micelles. *Chem. Commun. (Cambridge, U. K.)* **2007**, (29), 3021-3035.

300. van Nostrum, C. F., Covalently cross-linked amphiphilic block copolymer micelles. *Soft Matter* **2011,** 7, (7), 3246-3259.

301. Lefevre, N.; Fustin, C.-A.; Gohy, J.-F., Polymeric Micelles Induced by Interpolymer Complexation. *Macromol. Rapid Commun.* **2009,** 30, (22), 1871-1888.

302. Lokitz, B. S.; York, A. W.; Stempka, J. E.; Treat, N. D.; Li, Y.; Jarrett, W. L.; McCormick, C. L., Aqueous RAFT Synthesis of Micelle-Forming Amphiphilic Block Copolymers Containing N-Acryloylvaline. Dual Mode, Temperature/pH Responsiveness, and "Locking" of Micelle Structure through Interpolyelectrolyte Complexation. *Macromolecules (Washington, DC, U. S.)* **2007,** 40, (18), 6473-6480.

303. Li, Y.; Lokitz, B. S.; McCormick, C. L., Thermally Responsive Vesicles and Their Structural ldquoLockingrdquo through Polyelectrolyte Complex Formation13. *Angewandte Chemie International Edition* **2006,** 45, (35), 5792-5795.

304. Lee, S. J.; Min, K. H.; Lee, H. J.; Koo, A. N.; Rim, H. P.; Jeon, B. J.; Jeong, S. Y.; Heo, J. S.; Lee, S. C., Ketal Cross-Linked Poly(ethylene glycol)-Poly(amino acid)s Copolymer Micelles for Efficient Intracellular Delivery of Doxorubicin. *Biomacromolecules* **2011,** 12, (4), 1224-1233.

305. Zhang, L.; Bernard, J.; Davis, T. P.; Barner-Kowollik, C.; Stenzel, M. H., Acid-degradable core-crosslinked micelles prepared from thermosensitive glycopolymers synthesized via RAFT polymerization. *Macromol. Rapid Commun.* **2008,** 29, (2), 123-129.

306. Li, Y.; Du, W.; Sun, G.; Wooley, K. L., pH-Responsive Shell Cross-Linked Nanoparticles with Hydrolytically Labile Cross-Links. *Macromolecules* **2008,** 41, (18), 6605-6607.

307. Zhang, J.; Jiang, X.; Zhang, Y.; Li, Y.; Liu, S., Facile Fabrication of Reversible Core Cross-Linked Micelles Possessing Thermosensitive Swellability. *Macromolecules (Washington, DC, U. S.)* **2007,** 40, (25), 9125-9132.

308. Zhang, L.; Liu, W.; Lin, L.; Chen, D.; Stenzel, M. H., Degradable Disulfide Core-Cross-Linked Micelles as a Drug Delivery System Prepared from Vinyl Functionalized Nucleosides via the RAFT Process. *Biomacromolecules* **2008,** 9, (11), 3321-3331.

309. Harada, A.; Hashidzume, A., Supramolecular Polymers Based on Cyclodextrins and Their Derivatives. *Aust. J. Chem.* **2010,** 63, (4), 599-610.

310. Guo, X. H.; Wang, J.; Li, L.; Pham, D. T.; Clements, P.; Lincoln, S. F.; May, B. L.; Chen, Q. C.; Zheng, L.; Prud'homme, R. K., Tailoring Polymeric Hydrogels through Cyclodextrin Host-Guest Complexation. *Macromol. Rapid Commun.* **2010,** 31, (3), 300-304.

311. Wang, J.; Main, D. T.; Guo, X. H.; Li, L.; Lincoln, S. F.; Luo, Z. F.; Ke, H. L.; Zheng, L.; Prud'homme, R. K., Polymeric Networks Assembled by Adamantyl and beta-Cyclodextrin Substituted Poly(acrylate)s: Host-Guest Interactions, and the Effects of Ionic Strength and Extent of Substitution. *Industrial & Engineering Chemistry Research* **2010,** 49, (2), 609-612.

312. Wang, J.; Pham, D. C.; Kee, T. W.; Clafton, S. N.; Guo, X. H.; Clements, P.; Lincoln, S. F.; Prud'homme, R. K.; Easton, C. J., Aggregation and Host-Guest Interactions in Dansyl-Substituted Poly(acrylate)s in the Presence of beta-Cyclodextrin and a beta-Cyclodextrin Dimer in Aqueous Solution: A UV-Vis, Fluorescence, (1)H NMR, and Rheological Study. *Macromolecules* **2011,** 44, (24), 9782-9791.

313. Harada, A.; Kobayashi, R.; Takashima, Y.; Hashidzume, A.; Yamaguchi, H., Macroscopic self-assembly through molecular recognition. *Nature Chemistry* **2011,** 3, (1), 34-37.

314. Tamesue, S.; Takashima, Y.; Yamaguchi, H.; Shinkai, S.; Harada, A., Photoswitchable Supramolecular Hydrogels Formed by Cyclodextrins and Azobenzene Polymers. *Angewandte Chemie-International Edition* **2010,** 49, (41), 7461-7464.

315. Bertrand, A.; Stenzel, M.; Fleury, E.; Bernard, J., Host-guest driven supramolecular assembly of reversible comb-shaped polymers in aqueous solution. *Polym. Chem.* **2012,** 3, (2), 377-383.

316. Stadermann, J.; Komber, H.; Erber, M.; Daebritz, F.; Ritter, H.; Voit, B., Diblock Copolymer Formation via Self-Assembly of Cyclodextrin and Adamantyl End-

Functionalized Polymers. *Macromolecules (Washington, DC, U. S.)* **2011,** 44, (9), 3250-3259.

317. Zhang, J.; Ma, P. X., Polymeric core-shell assemblies mediated by host-guest interactions: versatile nanocarriers for drug delivery. *Angew. Chem., Int. Ed.* **2009,** 48, (5), 964-968.

318. Wang, H.; Wang, S.; Su, H.; Chen, K.-J.; Armijo, A. L.; Lin, W.-Y.; Wang, Y.; Sun, J.; Kamei, K.-i.; Czernin, J.; Radu, C. G.; Tseng, H.-R., A Supramolecular Approach for Preparation of Size-Controlled Nanoparticles. *Angew. Chem., Int. Ed.* **2009,** 48, (24), 4344-4348.

319. Zhang, J.; Sun, H.; Ma, P. X., Host−Guest Interaction Mediated Polymeric Assemblies: Multifunctional Nanoparticles for Drug and Gene Delivery. *ACS Nano* **2010,** 4, (2), 1049-1059.

320. Harrison, J. C.; Eftink, M. R., Cyclodextrin-adamantanecarboxylate inclusion complexes: a model system for the hydrophobic effect. *Biopolymers* **1982,** 21, (6), 1153-66.

321. Eftink, M. R.; Andy, M. L.; Bystrom, K.; Perlmutter, H. D.; Kristol, D. S., Cyclodextrin inclusion complexes: studies of the variation in the size of alicyclic guests. *J. Am. Chem. Soc.* **1989,** 111, (17), 6765-72.

322. Kumar, J.; McDowall, L.; Chen, G.; Stenzel, M. H., Synthesis of thermo-responsive glycopolymers via copper catalysed azide-alkyne "click" chemistry for inhibition of ricin: the effect of spacer between polymer backbone and galactose. *Polymer Chemistry* **2011,** 2, (8), 1879-1886.

323. Kavitha, A. A.; Singha, N. K., High temperature resistant tailor-made poly(meth)acrylates bearing adamantyl group via atom transfer radical polymerization. *J. Polym. Sci., Part A Polym. Chem.* **2008,** 46, (21), 7101-7113.

324. Gregory, A.; Stenzel, M. H., Complex polymer architectures via RAFT polymerization: From fundamental process to extending the scope using click chemistry and nature's building blocks. *Progress in Polymer Science* **2012,** 37, (1), 38-105.

325. Yi, Z.; Zhao, C.; Huang, Z.; Chen, H.; Yu, J., Investigation of buffer-cyclodextrin systems. *Physical Chemistry Chemical Physics* **1999,** 1, (3).

326. Aree, T.; Schulz, B.; Reck, G., Crystal Structures of beta-Cyclodextrin Complexes with Formic Acid and Acetic Acid. *Journal of Inclusion Phenomena and Macrocyclic Chemistry* 47, (1-2), 39-45.

327. Chan, T. R.; Hilgraf, R.; Sharpless, K. B.; Fokin, V. V., Polytriazoles as copper(I)-stabilizing ligands in catalysis. *Org. Lett.* **2004,** 6, (17), 2853-2855.

328. Harada, A.; Li, J.; Kamachi, M., Double-stranded inclusion complexes of cyclodextrin threaded on poly(ethylene glycol). *Nature (London)* **1994,** 370, (6485), 126-8.

329. Mukhopadhyay, P.; Wu, A.; Isaacs, L., Social Self-Sorting in Aqueous Solution. *J. Org. Chem.* **2004,** 69, (19), 6157-6164.

330. Nitschke, J. R.; Lehn, J.-M., Self-organization by selection: Generation of a metallosupramolecular grid architecture by selection of components in a dynamic library of ligands. *Proc. Natl. Acad. Sci. U. S. A.* **2003,** 100, (21), 11970-11974.

331. Bureekaew, S.; Shimomura, S.; Kitagawa, S., Chemistry and application of flexible porous coordination polymers. *Sci. Technol. Adv. Mater.* **2008,** 9, 014108.

332. Friese, V. A.; Kurth, D. G., Soluble dynamic coordination polymers as a paradigm for materials science. *Coord. Chem. Rev.* **2008,** 252, (1+2), 199-211.

333. Kurth, D. G., Metallo-supramolecular modules as a paradigm for materials science. *Sci. Technol. Adv. Mater.* **2008,** 9, 014103.

334. Fox, J. D.; Rowan, S. J., Supramolecular Polymerizations and Main-Chain Supramolecular Polymers. *Macromolecules* **2009,** 42, (18), 6823-6835.

335. Miyauchi, M.; Takashima, Y.; Yamaguchi, H.; Harada, A., Chiral Supramolecular Polymers Formed by Host-Guest Interactions. *J. Am. Chem. Soc.* **2005,** 127, (9), 2984-2989.

336. Chelli, S.; Majdoub, M.; Jouini, M.; Aeiyach, S.; Maurel, F.; Chane-Ching, K. I.; Lacaze, P.-C., Host-guest complexes of phenol derivatives with β-cyclodextrin: an experimental and theoretical investigation. *J. Phys. Org. Chem.* **2007,** 20, (1), 30-43.

337. Yamauchi, K.; Takashima, Y.; Hashidzume, A.; Yamaguchi, H.; Harada, A., Switching between Supramolecular Dimer and Nonthreaded Supramolecular Self-Assembly of Stilbene Amide-α-Cyclodextrin by Photoirradiation. *J. Am. Chem. Soc.* **2008,** 130, (15), 5024-5025.

338. Tomimasu, N.; Kanaya, A.; Takashima, Y.; Yamaguchi, H.; Harada, A., Social Self-Sorting: Alternating Supramolecular Oligomer Consisting of Isomers. *J. Am. Chem. Soc.* **2009,** 131, (34), 12339-12343.

339. Harada, A.; Kobayashi, R.; Takashima, Y.; Hashidzume, A.; Yamaguchi, H., Macroscopic self-assembly through molecular recognition. *Nat. Chem.* **2010,** 3, (1), 34-37.

340. Yamaguchi, H.; Kobayashi, R.; Takashima, Y.; Hashidzume, A.; Harada, A., Self-Assembly of Gels through Molecular Recognition of Cyclodextrins: Shape Selectivity for Linear and Cyclic Guest Molecules. *Macromolecules* **2011,** 44, (8), 2395-2399.

341. Bertrand, A.; Stenzel, M.; Fleury, E.; Bernard, J., Well-defined graft copolymers assembled by host-guest inclusion between adamantane-functionalized poly(acrylic acid) and β-cyclodextrin-grafted polymer. *PMSE Prepr.* **2011**, No pp given.

342. Jin, H.; Liu, Y.; Zheng, Y.; Huang, W.; Zhou, Y.; Yan, D., Cytomimetic Large-Scale Vesicle Aggregation and Fusion Based on Host-Guest Interaction. *Langmuir* **2012,** 28, 2066-2072.

343. Kaftan, O.; Tumbiolo, S.; Dubreuil, F.; Auzely-Velty, R.; Fery, A.; Papastavrou, G., Probing Multivalent Host-Guest Interactions between Modified Polymer Layers by Direct Force Measurement. *J. Phys. Chem. B* **2011,** 115, (24), 7726-7735.

344. Karaky, K.; Brochon, C.; Schlatter, G.; Hadziioannou, G., pH-Switchable supramolecular "sliding" gels based on polyrotaxanes of polyethyleneimine-block-poly(ethylene oxide)-block-polyethyleneimine block copolymer and α-cyclodextrin: synthesis and swelling behaviour. *Soft Matter* **2008,** 4, (6), 1165-1168.

345. Liu, H.; Zhang, Y.; Hu, J.; Li, C.; Liu, S., Multi-Responsive Supramolecular Double Hydrophilic Diblock Copolymer Driven by Host-Guest Inclusion Complexation between β-Cyclodextrin and Adamantyl Moieties. *Macromol. Chem. Phys.* **2009,** 210, (24), 2125-2137.

346. Osaki, M.; Takashima, Y.; Yamaguchi, H.; Harada, A., An Artificial Molecular Chaperone: Poly-pseudo-rotaxane with an Extensible Axle. *J. Am. Chem. Soc.* **2007,** 129, (46), 14452-14457.

347. Rydzek, G.; Parat, A.; Polavarapu, P.; Baehr, C.; Voegel, J.-C.; Hemmerle, J.; Senger, B.; Frisch, B.; Schaaf, P.; Jierry, L.; Boulmedais, F., One-pot morphogen driven self-constructing films based on non-covalent host-guest interactions. *Soft Matter* **2012,** 8, (2), 446-453.

348. Wu, J.; He, H.; Gao, C., β-Cyclodextrin-Capped Polyrotaxanes: One-Pot Facile Synthesis via Click Chemistry and Use as Templates for Platinum Nanowires. *Macromolecules* **2010,** 43, (5), 2252-2260.

349. Zeng, J.; Shi, K.; Zhang, Y.; Sun, X.; Zhang, B., Construction and micellization of a noncovalent double hydrophilic block copolymer. *Chem. Commun.* **2008**, (32), 3753-5.

350. Zhang, Z.-X.; Liu, K. L.; Li, J., Self-assembly and micellization of a dual thermoresponsive supramolecular pseudo-block copolymer. *Macromolecules* **2011,** 44, (5), 1182-1193.

351. Zhang, Z.-X.; Liu, X.; Xu, F. J.; Loh, X. J.; Kang, E.-T.; Neoh, K.-G.; Li, J., Pseudo-Block Copolymer Based on Star-Shaped Poly(N-isopropylacrylamide) with a β-Cyclodextrin Core and Guest-Bearing PEG: Controlling Thermoresponsivity through Supramolecular Self-Assembly. *Macromolecules* **2008,** 41, (16), 5967-5970.

352. Stadermann, J.; Komber, H.; Erber, M.; Däbritz, F.; Ritter, H.; Voit, B., Diblock Copolymer Formation via Self-Assembly of Cyclodextrin and Adamantyl End-Functionalized Polymers. *Macromolecules* **2011,** 44, (9), 3250-3259.

353. Yhaya, F.; Lim, J.; Kim, Y.; Liang, M. T.; Gregory, A. M.; Stenzel, M. H., Development of Micellar Novel Drug Carrier Utilizing Temperature-Sensitive Block Copolymers Containing Cyclodextrin Moieties. *Macromolecules* **2011,** 44, (21), 8433-8445.

354. Lowe, A. B.; Harvison, M. A., Thiol-Based 'Click' Chemistries in Polymer Synthesis and Modification. *Aust. J. Chem.* **2010,** 63, (8), 1251-1266.

355. Chen, M.; Moad, G.; Rizzardo, E., A Potential New RAFT–Click Reaction or a Cautionary Note on the Use of Diazomethane to Methylate RAFT-synthesized Polymers†. *Aust. J. Chem.* **2011,** 64, (4), 433-437.

356. Harvison, M. A.; Roth, P. J.; Davis, T. P.; Lowe, A. B., End Group Reactions of RAFT-Prepared (Co)Polymers. *Aust. J. Chem.* **2011,** 64, (8), 992-1006.

357. Moad, G.; Rizzardo, E.; Thang, S. H., End-functional polymers, thiocarbonylthio group removal/transformation and reversible addition-fragmentation-chain transfer (RAFT) polymerization. *Polymer International* **2011,** 60, (1), 9-25.

358. Chong, B.; Moad, G.; Rizzardo, E.; Skidmore, M.; Thang, S. H., Thermolysis of RAFT-synthesized poly(methyl methacrylate). *Australian Journal of Chemistry* **2006,** 59, (10), 755-762.

359. Moad, G.; Chong, Y. K.; Postma, A.; Rizzardo, E.; Thang, S. H., Advances in RAFT polymerization: the synthesis of polymers with defined end-groups. *Polymer* **2005,** 46, (19), 8458-8468.

360. Postma, A.; Davis, T. P.; Moad, G.; O'Shea, M. S., Thermolysis of RAFT-Synthesized Polymers. A Convenient Method for Trithiocarbonate Group Elimination. *Macromolecules* **2005,** 38, (13), 5371-5374.

361. Postma, A.; Davis, T. P.; Evans, R. A.; Li, G.; Moad, G.; O'Shea, M. S., Synthesis of Well-Defined Polystyrene with Primary Amine End Groups through the Use of Phthalimido-Functional RAFT Agents. *Macromolecules* **2006,** 39, (16), 5293-5306.

362. Lima, V.; Jiang, X. L.; Brokken-Zijp, J.; Schoenmakers, P. J.; Klumperman, B.; Van Der Linde, R., Synthesis and characterization of telechelic polymethacrylates via RAFT polymerization. *J. Polym. Sci. Pol. Chem.* **2005,** 43, (5), 959-973.

363. Xu, J. T.; He, J. P.; Fan, D. Q.; Tang, W.; Yang, Y. L., Thermal decomposition of dithioesters and its effect on RAFT polymerization. *Macromolecules* **2006,** 39, (11), 3753-3759.

364. Li, G.-Z.; Randev, R. K.; Soeriyadi, A. H.; Rees, G.; Boyer, C.; Tong, Z.; Davis, T. P.; Becer, C. R.; Haddleton, D. M., Investigation into thiol-(meth)acrylate Michael addition reactions using amine and phosphine catalysts. *Polym. Chem.* **2010,** 1, (8), 1196-1204.

365. Kaya, E.; Mathias, L. J., Synthesis and characterization of physical crosslinking systems based on cyclodextrin inclusion/host-guest complexation. *J. Polym. Sci. Part A: Polym. Chem.* **2010,** 48, (3), 581-592.